Universitat Autònoma de Barcelona

Estudio sobre la expresión y localización de la guanilil ciclasa sensible a NO (GC_{NO}) en células nerviosas.

Memoria presentada por María Paula Pifarré para obtener el grado de Doctor en Bioquímica y Biología Molecular

Trabajo realizado bajo la dirección de la Dra. Agustina García y la Dra. María Antonia Baltrons, en el Institut de Biotecnologia i Biomedicina V. Villar Palasí y en el Departament de Bioquimica i Biologia Molecular.

María Paula Pifarré

Dra. Agustina García

Dra. María Antonia Baltrons

Bellaterra, Mayo 2007

A mi familia,
mis padres, mi hermana
y mis sobrinas

Yo adivino el parpadeo
de las luces que a lo lejos,
van marcando mi retorno.
Son las mismas que alumbraron,
con sus pálidos reflejos
hondas horas de dolor.
Y aunque no quise el regreso,
siempre se vuelve al primer amor.
La quieta calle, donde un eco dijo:
"tuya es su vida, tuyo es su querer",
bajo el burlón mirar de las estrellas
que con indiferencia hoy me ven volver.

Tango Volver 1935
Carlos Garcel y Alfredo Lepera

ÍNDICE

RESUMEN GENERAL

La guanilil ciclasa sensible a NO (GC_{NO}) es la principal diana del NO en el SNC. Esta enzima cataliza la formación del segundo mensajero GMPc a partir de GTP. El GMPc es el mediador de las importantes acciones neuro-reguladoras del NO. La GC_{NO} está presente en la mayoría de las células de mamíferos como un heterodímero compuesto por una subunidad α y una β. Dos isoformas de cada subunidad, α1-2 y β1-2, han sido clonadas. Durante el desarrollo de esta tesis hemos estudiado la distribución anatómica detallada de los mRNAs de las subunidades de la GC_{NO} en cerebro de rata y mono. Nuestros resultados revelan que en ambas especies el mRNA de la subunidad β1 es el más abundante en cerebro, siendo máxima su expresión en caudado-putamen, núcleo accumbens, tubérculo olfatorio, corteza, giro dentado e hipocampo, así como también en varios núcleos talámicos e hipotalámicos, amígdala y cerebelo. Por el contrario, el mRNA de la subunidad β2 no pudo ser detectado en ninguna de las dos especies estudiadas. La distribución de las subunidades α presentó similitudes en el sistema límbico y en el caudado-putamen de ambas especies. Sin embargo, existen pequeñas diferencias en la distribución laminar de la corteza cerebral. Mientras que en la rata la expresión de la subunidad α1 es elevada en las capas externas corticales, en el mono lo es en las capas internas. Por otro lado, el mRNA de α1 es más ubicuo en el cerebro de mono y el mRNA de la α2 en el de rata.

Una elevada expresión de las tres subunidades estudiadas se observó en los ganglios basales, el sistema olfatorio, el hipocampo y la corteza cerebral. Sin embargo, también encotramos regiones del cerebro donde la expresión de la subunidad β1 era muy alta y por el contrario la expresión de ambas subunidades α era muy baja o indetectable. En la rata, esta situación se apreció en las islas de Calleja, la mayoría de los núcleos talámicos estudiados y el colículo superior, y en cerebro de mono en los núcleos talámicos y en el claustrum. Teniendo en cuenta que el sistema NO-GMPc ha sido implicado en plasticidad sináptica, el procesamiento sensorial y el comportamiento en la rata, los niveles elevados de los mRNA de las tres subunidades en regiones como los ganglios basales, el hipocampo y el cerebelo en el mono sugieren que este sistema estaría también involucrado en la regulación de estos importantes procesos cerebrales en primates.

Estudios previos del laboratorio habían demostrado que los agentes inflamatorios que inducen la NOS-2, entre ellos el LPS y los péptidos β-amiloides, eran capaces de disminuir la actividad GC_{NO} como consecuencia de la disminución en los niveles de la subunidad β1 en astrocitos en cultivo y en cerebro de ratas adultas. En este trabajo nos propusimos estudiar si la

actividad de la enzima GC_{NO} también estaba alterada en cerebro de pacientes con enfermedades neurodegenerativas con un componente inflamatorio como son el Alzheimer (AD), Creytzfeldt-Jakob (CJ) y la esclerosis múltiple (MS). Los resultados que obtuvimos en homogenados de corteza de cerebro de enfermos AD demuestran que no existen diferencias significativas entre los individuos control y los enfermos de AD con distinto grado de afectación en la actividad basal GC_{NO} o estimulada con donadores de NO, ni en los niveles de expresión de las subunidades β1 y α1 medidos por WB. Mediante inmunocitoquímica demostramos que las neuronas corticales y de hipocampo y los astrocitos fibrilares de la sustancia blanca subcortical presentaban un nivel de expresión elevado para la subunidad β1 mientras que en los astrocitos de sustancia gris era difícil detectar por inmunocitoquímica la presencia de esta subunidad. En pacientes con AD, los niveles de expresión no se vieron alterados en neuronas y astrocitos fibrilares mientras que se detectó una disminución en los niveles de β1 en los astrocitos reactivos ubicados alrededor de las placas amiloides. El marcaje se ve también disminuido en astrocitos reactivos de sustancia blanca en cerebro de pacientes con CJ y MS. Así, la inducción de la reactividad glial está asociada a una disminución en la capacidad de generar GMPc en respuesta a NO tanto in vitro como in vivo y en diferentes especies. Este mecanismo de disminución de la GC_{NO} podría constituir una adaptación de las células astrogliales para prevenir la señalización mediada por GMPc en condiciones de elevada formación de NO.

Estudios previos de nuestro laboratorio habían demostrado que el tratamiento de cultivos de astrocitos con LPS producía una disminución en la vida media de la subunidad β1 de la GC_{NO} por un mecanismo dependiente de transcripción y síntesis de proteínas, pero independiente de la formación de NO. En esta tesis hemos estudiado el mecanismo involucrado en la degradación de esta subunidad en astrocitos, siendo la vía que involucra al proteosoma y la ubiquitina la responsable de la disminución en los niveles de la β1. Por otro lado, hemos demostrado que en estas células el tratamiento con LPS produce la acumulación en forma de agregados de la subunidad β1 en el núcleo celular, en estructuras ricas en proteosoma 20S y ubiquitina con caracterísiticas de clastosomas. De acuerdo con esto, la formación de estos cuerpos nucleares es inhibida por el tratamiento con inhibidores específicos del proteosoma.

En el transcurso de los estudios sobre la degradación de la subunidad β1 de la GC_{NO} hemos observado por inmunocitoquímica la presencia de esta subunidad en células que presentan actividad GC_{NO} (neuronas y astrocitos), así como en células incapaces de generar GMPc en respuesta a NO (microglía). En ambos casos la localización intracelular era mayoritariamente citosólica pero también aparecía inmunoreactividad para la β1 en el núcleo

celular. Además, la intensidad de marcaje era mayor en células en división. A mayor aumento observamos que la subunidad β1 se encontraba asociada periféricamente a los cromosomas durante todas las fases de la mitosis. Debido a que las proteínas que intervienen en la condensación de la cromatina tienen una localización pericromosomal, nos propusimos estudiar si la β1 ejercía alguna función sobre la condensación de la cromatina. Mediante un ensayo de condensación *in vitro* demostramos que la inmunodepleción tanto de la proteína nuclear como de la citoplasmática provocaban un mayor número de núcleos en los que la cromatina aparecía condensada. En el mismo sentido, pudimos demostrar que el silenciamiento de la proteína por siRNA producía un aumento del número de células que ingresaban en el ciclo celular y un aumento de la proliferación. Todos estos efectos sobre la condensación de la cromatina y el control del ciclo celular fueron independientes de la actividad enzimática ya que el tratamiento de las células con un inhibidor especifico de la GC_{NO} (ODQ) no mimetizaba los efectos del siRNA ni el de la inmunodepleción. Todos estos resultados nos llevan a proponer que probablemente la subunidad β1 de la GC_{NO} pueda tener una función independiente de su actividad enzimática.

1 INTRODUCCIÓN

El segundo mensajero guanosin-5'-monofosfato cíclico (GMPc) es formado a partir de guanosin-5'-trifosfato (GTP) mediante una reacción catalizada por una familia de enzimas las guanilil ciclasas (GC). La actividad enzimática GC fue descubierta en la década de los 60 y ha sido detectada en todos los tejidos de mamíferos. Se han descrito dos familias de GC, una mayoritariamente citosólica (GC soluble, GC_{NO}) y otra que está asociada a la membrana (GC particulada, GCp). Ambos tipos de GC presentan similitudes en sus secuencias de aminoácidos y comparten características estructurales pero difieren en el mecanismo de activación y regulación (Lucas et al., 2000; Mittal and Murad, 1977; Schulz et al., 1991). La GC_{NO} es el receptor del oxido nítrico (NO), mientras que la GCp es activada por una familia de péptidos entre los que se encuentran los péptidos natriuréticos. La activación de las GC por péptidos natriuréticos (GCp) o por NO (GC_{NO}) permite la transmisión de la señal a otros componentes de la cascada de señalización, como son las quinasas dependientes de GMPc (PKG), los canales iónicos activados por GMPc o las fosfodiesterasas (PDE) reguladas por GMPc (Schmidt et al., 1993; Wang and Robinson, 1995).

Los niveles de GMPc se regulan también mediante la degradación llevada a cabo a través de las PDEs, responsables de la hidrólisis del GMPc y del AMPc a sus correspondientes nucleósidos-5'-monofosfato. Las PDEs conocidas hasta la fecha pueden ser clasificadas en tres grandes grupos: 1- PDEs que hidrolizan tanto GMPc como AMPc (PDE1, 2, 3, 10 y 11); 2- PDEs que hidrolizan AMPc (PDE4, 7 y 8); y 3- PDEs que hidrolizan GMPc (PDE5, 6 y 9). La PDE9 es la enzima con mayor afinidad por el GMPc estudiada hasta el momento, así como la más abundante y ubicua en el sistema nervioso central (SNC) (Andreeva et al., 2001; Bender and Beavo, 2006; van Staveren et al., 2002).

El NO fue considerado durante muchos años como un gas tóxico sin aplicaciones terapéuticas conocidas. En la década de los 70, sin embargo, se descubrió que era un potente activador de la GC_{NO}. Este descubrimiento permitió relacionar la estimulación de la formación de GMPc en células de músculo liso vascular por compuestos vasodilatadores que contenían nitrógeno y oxígeno con un mecanismo que involucraba la liberación de NO (Murad et al., 1978). En esos momentos se pensaba que la biosíntesis de NO estaba restringida a bacterias nitrificantes y desnitrificantes, por lo que el significado de estos descubrimientos en relación con las células animales no fue apreciado, a pesar de conocerse la capacidad de los macrófagos activados de secretar nitritos y nitratos como respuesta a infecciones a través de un proceso que requería L-arginina (Furchgott, 1999; Moncada et al., 1991). El descubrimiento del factor relajante derivado de endotelio (EDRF) (Furchgott and Zawadzki, 1980) y su posterior

identificación como NO en el sistema vascular (Ignarro et al., 1987; Palmer et al., 1987), no sólo puso de manifiesto que otras células animales eran capaces de sintetizar NO y que éste era un mensajero intercelular, sino que sirvió para identificar un activador endógeno de las GC_{NO} y una nueva vía de señalización que involucra al NO, la GC_{NO} y el GMPc (Furchgott, 1999). Poco después, Garthwaite y col. (1988) demostraron que el NO también podía ser un mensajero intercelular en el SNC. Estudios sobre la formación de GMPc en células cerebelares tras la estimulación de receptores de glutamato de tipo N-metil-D-aspartato (NMDA) revelaron que el intermediario intercelular que estimulaba la formación del nucleótido era el NO.

Desde esos descubrimientos hasta la fecha se ha podido identificar un gran número de procesos fisiológicos en los que se encuentra involucrada la vía NO-GC_{NO}-GMPc, incluyendo la relajación del músculo liso vascular y no vascular, la agregación de las plaquetas y la neurotransmisión periférica y central. En el SNC, el NO está implicado en procesos de regulación de la plasticidad sináptica relacionados con la memoria y el aprendizaje, en diversos aspectos del desarrollo cerebral, en la secreción neuroendocrina y en el control del flujo sanguíneo (Garthwaite and Boulton, 1995). En el sistema nervioso periférico (SNP) el NO parece ser el neurotransmisor liberado por las terminales no-adrenérgicas-no-colinérgicas que regulan la relajación del músculo liso del sistema gastrointestinal y la erección del pene (Lefebvre, 1995).

El NO revolucionó el concepto de neurotransmisor ya que este compuesto es una molécula no cargada de carácter altamente hidrofóbico, es un gas, radical libre, que no se almacena en vesículas. Al contrario de los neurotransmisores convencionales no es liberado por exocitosis, su actividad no está regulada por procesos de recaptación, no necesita receptores específicos en la superficie celular (ya que es capaz de difundir libremente a través de las membranas celulares) y puede unirse a diversas dianas, de la que la principal parece ser la GC_{NO}. Por otro lado, el NO puede ser neurotóxico cuando es generado en exceso como consecuencia de la hiperestimulación de receptores NMDA o tras la inducción de la NO sintasa tipo 2 (NOS-2, ver más abajo) en procesos neuroinflamatorios (Bredt, 1999; Dawson and Dawson, 1996; Szabo, 1996).

Formación de NO

El NO es generado en las células mediante la oxidación de uno de los nitrógenos del grupo guanidino del aminoácido L-arginina por una familia de enzimas llamadas NO sintasas (NOS) (EC 1.14.13.39). Estas enzimas utilizan como co-sustratos el oxígeno y el NADPH. El resultado de la reacción oxidativa de estequiometría impar que implica 5 electrones y que ocurre en dos etapas, es la formación del radical libre NO y la L-citrulina. Existen tres isoformas de la NOS

producto de tres genes distintos, que se distinguen por la dependencia de calcio-calmodulina y por la inducibilidad (Forstermann et al., 1994; Schmidt et al., 1993). Las isoformas constitutivas y dependientes de calcio, NOS-1 y NOS-3, que fueron originalmente identificadas en neuronas y células endoteliales respectivamente, son estimuladas por agonistas que hacen aumentar la concentración intracelular de calcio y generan niveles moderados de NO (picomoles) que modulan procesos rápidos como la neurotransmisión y la dilatación de vasos sanguíneos (Bredt, 1999). Aunque se expresan constitutivamente, sus niveles pueden ser regulados a largo plazo en respuesta a diferentes estímulos.

Se ha podido identificar la presencia de NOS-1 en diversas regiones del SNC mayoritariamente en poblaciones neuronales discretas del cerebelo, el bulbo olfatorio accesorio, el núcleo tegmental pedúnculo-pontino y, en menor medida, en el giro dentado del hipocampo, el bulbo olfatorio principal, el colículo superior y el colículo inferior, el núcleo supraóptico, la corteza cerebral y el caudado-putamen (Bredt et al., 1991; Bredt et al., 1990). También se ha descrito la presencia de NOS-1 en astrocitos del hipocampo y de cerebelo (Baltrons and García, 1999). En estudios inmunohistoquímicos, algunos autores han observado la expresión de la NOS-3 en algunas poblaciones neuronales (células piramidales del hipocampo, neuronas granulares internas del bulbo olfatorio, (Dinerman et al., 1994) y en astrocitos corticales (Wiencken and Casagrande, 1999). La microglía y los oligodendrocitos no parecen expresar actividad NOS constitutiva ni *in vivo* ni *in vitro* (Agullo et al., 1995; Murphy et al., 1995).

La isoforma inducible a nivel transcripcional de la NOS (NOS-2) se identificó en macrófagos. Ésta se expresa sólo en células estimuladas inmunológicamente y genera cantidades superiores de NO (nanomoles). Sus principales estímulos son el lipopolisacárido bacteriano (LPS) y algunas citoquinas como el interferón-γ (INF-γ), la interleuquina–1β (IL-1β) y el factor de necrosis tumoral α (TNF-α). Sin embargo, la regulación de la expresión de la NOS-2 depende de la especie y del tipo de células. Se ha descrito la inducción de NOS-2 en SNC, epitelio pulmonar, células beta del páncreas, mácula densa del riñón, músculo esquelético y en otros tipos celulares (Schmidt et al., 1992). En el SNC, el LPS y combinaciones de citoquinas pro-inflamatorias (INFγ, IL-1β y TNFα) inducen la expresión de NOS-2 en astrocitos y microglía de roedores en cultivo (Murphy et al., 1993). La inducción de NOS-2 en estas células también ha sido determinada en modelos animales con lesiones cerebrales, infecciones víricas, isquemia cerebral y tras la inducción de encefalitis alérgica experimental (Endoh et al., 1994; Grzybicki et al., 1998; Okuda et al., 1997; Wallace and Bisland, 1994). La expresión de NOS-2 en oligodendrocitos de roedores sólo se ha demostrado en células en cultivo (Merrill et al., 1997; Molina-Holgado et al., 2001).

En humanos, la expresión de NOS-2 se ha detectado principalmente en astroglia, tanto en tejido post-mortem de pacientes con Esclerosis múltiple (MS) (Bo et al., 1994), como en las enfermedades de Alzheimer (AD) (Wallace et al., 1997), Parkinson (Hunot et al., 1996) y Esclerosis lateral amiotrófica (Almer et al., 1999). También se ha encontrado expresión de NOS-2 en cerebro de pacientes con SIDA (Bukrinsky et al., 1995). Existen datos sobre la expresión de la NOS-2 en microglía humana en cultivo en respuesta a la combinación de citoquinas (Colasanti et al., 1995; Ding et al., 1997) aunque otros autores niegan la expresión de esta enzima en estas células en humanos (Liu et al., 1996).

Las isoformas de la NOS difieren en su localización subcelular. La NOS-1 es una enzima soluble, pero puede aparecer asociada a la membrana. Esta asociación se debe a la presencia de un dominio PDZ en el extremo N-terminal que le confiere capacidad para interaccionar con proteínas de anclaje a membrana como la proteína de densidad post-sináptica PSD-95 en neuronas, o con otras proteínas como la distrofina en células musculares. Esta asociación permite la proximidad con el receptor de glutamato de tipo NMDA, principal activador de esta isoforma en neuronas, y a canales de Ca^{2+} en músculo, favoreciendo así su rápida activación (Brenman et al., 1996a; Brenman et al., 1996b). Por el contrario, la NOS-3 es una enzima particulada que se asocia a la membrana a través de residuos miristoilados (Forstermann et al., 1991), mientras que la NOS-2 es una proteína citosólica.

Las Guanilil Ciclasas.

1.1.1 Guanilil ciclasa particulada.

Actualmente se han purificado y clonado siete isoformas de GCp (desde GC-A, hasta GC-G) que presentan una estructura altamente conservada entre sí. Todas ellas cuando están activas parecen ser proteínas homodiméricas u homotetraméricas. Cada subunidad está compuesta por un solo dominio hidrofóbico transmembrana, un dominio extracelular variable de unión para los diferentes ligandos, un dominio intracelular conservado que posee gran similitud con tirosina quinasas y un dominio catalítico (Lucas et al., 2000; Wedel and Garbers, 2001). Las isoformas GC-C, -D, -E y -F poseen una cola C-terminal adicional. En base a la especificidad del ligando, las GCp se han clasificado en tres grupos: receptores de péptidos natriuréticos (GC-A y GC-B), receptores de péptidos intestinales (GC-C) y receptores huérfanos (sin ningún ligando específico). Dos de ellas, la GC-A y la GC-B, son activadas por péptidos natriuréticos de tipo A, B y C (ANP, BNP y CNP, respectivamente). La isoforma GC-C se activa por enterotoxinas bacterianas y por péptidos endógenos como la guanilina, la uroguanilina y la

linfoguanilina (Currie et al., 1992; Forte et al., 1999a; Forte et al., 1999b). La activación de esta enzima es un proceso complejo que requiere la unión del ligando al dominio extracelular, la oligomerización y la unión de ATP y autofosforilación por el dominio quinasa (Labrecque et al., 1999; Tremblay et al., 2002).

En el SNC, estudios inmunohistoquímicos utilizando anticuerpos frente al GMPc han detectado la acumulación de este nucleótido en respuesta a los péptidos natriuréticos mayoritariamente en astrocitos y en pocas estructuras neuronales (de Vente et al., 1989). Estudios recientes de nuestro grupo han demostrado que las células microgliales también responden al tratamiento con péptidos natriuréticos generando GMPc (Boran and Garcia, 2005).

1.1.2 Guanilil ciclasa sensible a NO.

1.2.2.1 Estructura y mecanismos de activación

La GC_{NO} es una enzima que se expresa de forma ubicua en los tejidos animales y participa en un gran número de importantes procesos fisiológicos, tales como la inhibición de la agregación plaquetaria, la vasodilatación y la neurotransmisión (Garthwaite and Boulton, 1995; Zhang and Snyder, 1995). En las células de mamíferos, la GC_{NO} es un heterodímero, compuesto por una subunidad α y una β y contiene ferroprotoporfirina IX como grupo prostético (grupo hemo), el cual constituye el sitio de unión del NO. Hasta la fecha, se han clonado y secuenciado dos tipos de cada una de las subunidades (α1-2, β1-2), pero sólo se han encontrado dos combinaciones de proteínas funcionalmente activas: la $\alpha1\beta1$ que parece ser la isoforma más ubicua y la $\alpha2\beta1$ que se ha encontrado en placenta humana y en SNC (Denninger and Marletta, 1999; Hobbs, 1997; Mergia et al., 2003). Cada subunidad posee: (1) un dominio regulador de unión al grupo prostético hemo en el extremo N-terminal, que es la región menos conservada entre las distintas subunidades, (2) un dominio catalítico ciclasa en el extremo C-terminal cuya secuencia presenta un alto grado de similitud con la de las subunidades de las formas particuladas de la enzima y con las adenilil ciclasas (AC), y (3) un dominio central de dimerización (Foster et al., 1999; Schulz et al., 1991) (Figura 1).

Técnicas moleculares han permitido identificar los residuos involucrados en la unión del grupo hemo. Se ha identificado un residuo de histidina (His 105) involucrado en la unión al Fe^{2+} del grupo hemo, y la deleción de 131 aminoácidos del N-terminal de la subunidad α y de 62 aminoácidos del N-terminal de la subunidad β da lugar a una enzima insensible al NO (Fan et al., 1998; Wedel et al., 1995). La presencia del grupo hemo no es necesaria para mantener la estructura de la proteína, sin embargo el equilibrio entre las formas de la enzima con o sin el

grupo hemo constituye un mecanismo potencial de regulación de la sensibilidad de la enzima al NO (Foerster et al., 1996).

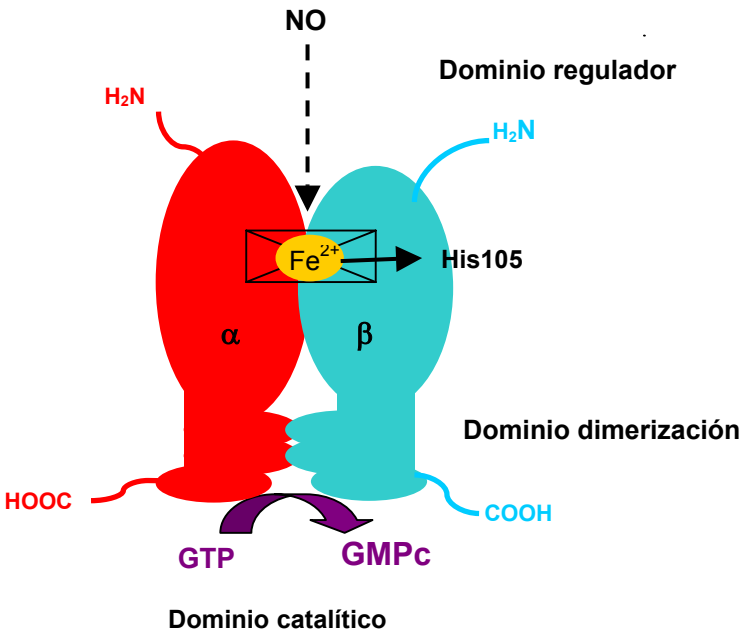

Figura 1: Estructura heterodimérica de la GC_{NO}.

Las dos isoformas de cada subunidad conocidas están codificadas por genes diferentes (Koesling et al., 1991; Koesling and Friebe, 1999). Las subunidades α1 y β1 se purificaron como un heterodímero a partir de pulmón bovino y de rata obteniéndose una proteína de 70 kDa para la β1 y de 82 KDa o de 73 KDa para la α1 (rata y bovina respectivamente). Las subunidades α2 (82 KDa) y β2 (76 KDa) se clonaron a partir de cerebro fetal humano y de riñón de rata, respectivamente (Koesling and Friebe, 1999; Koesling et al., 1990; Nakane et al., 1990). La subunidad β2 posee en el extremo C-terminal 86 aminoácidos adicionales en comparación con la β1, en ellos se encuentra una secuencia consenso que permite las modificaciones postraduccionales de isoprenilación o carboximetilación y de asociación a membrana. Sin embargo, todavía no existen evidencias de que esta subunidad se encuentre asociada a la membrana ni que sea funcional (Yuen et al., 1990).

Aunque cada subunidad de la enzima posee su propio dominio catalítico, es necesaria la expresión de ambas para obtener actividad. La enzima posee un solo sitio de unión al sustrato y un único sitio catalítico. La dimerización está mediada por una región específica que se encuentra próxima al dominio catalítico en ambas subunidades (Liu et al., 1997b).

Los intentos fallidos por obtener un animal experimental homocigoto negativo para el gen de la subunidad β1 (knockout), sugieren que la pérdida de esta subunidad es letal,

pudiéndose concluir que no solo la GC_{NO} es fundamental para el crecimiento y desarrollo, sino que parece no haber una subunidad alternativa que sustituya a la subunidad β1 (Hobbs, 1997).

1.2.2.2 Regulación de la actividad GC_{NO}

Teniendo en cuenta la importancia de las acciones del GMPc en el organismo, es importante controlar sus niveles, tanto en estados fisiológicos como fisiopatológicos. Existen diferentes mecanismos que regulan la actividad GC_{NO} a diferentes niveles: modulando directamente la actividad enzimática, modificando los niveles de expresión de la proteína o variando el patrón de expresión de las diferentes isoformas en distintos momentos del desarrollo.

La GC_{NO} requiere cationes divalentes como cofactores para alcanzar la máxima activación. Las especies que probablemente actúan como cofactores fisiológicos son el Mn^{2+} y el Mg^{2+} (este último presenta concentraciones intracelulares mayores) (Waldman and Murad, 1987). Por el contrario, el Ca^{2+} inhibe la actividad GC_{NO}, al parecer mediante la interacción con la región catalítica de la enzima disminuyendo su afinidad por el sustrato (Parkinson et al., 1999; Serfass et al., 2001).

En estudios con la proteína GC_{NO} purificada se ha descrito un aumento de la actividad enzimática por fosforilación con PKC y PKA (Zwiller et al., 1981; Zwiller et al., 1985). Estos resultados fueron corroborados en cultivos de células de pituitaria de rata, donde se demostró que el sitio de fosforilación por PKA se encuentra en la subunidad α1 (Kostic et al., 2004). Por el contrario, en células cromafines bovinas se ha demostrado una relación inversa entre el grado de fosforilación de la subunidad β1 y la actividad GC_{NO}. La desfosforilación de la proteína mediada indirectamente por PKG produce la inhibición de la GC_{NO} (Ferrero et al., 2000).

La regulación de la actividad GC_{NO} ha sido más intensamente estudiada en células del sistema vascular. Los primeros estudios sobre el desarrollo de tolerancia durante el tratamiento con compuestos nitrovasodilatadores demostraron que su propio activador, el NO, era capaz de regular negativamente a la GC_{NO}. Papapetropoulos y col. (1996b) observaron en células de músculo liso de aorta de rata una disminución en la acumulación de GMPc en respuesta a nitroprusiato sódico (SNP) en células pretratadas con el donador por periodos no excesivamente largos (2 horas). Este efecto se debía aparentemente a la oxidación de grupos tioles en la proteína ya que podía ser prevenido por la acción de agentes reductores con grupos tiol. Sin embargo, el tratamiento a tiempos largos implicaba una reducción en los niveles de proteína y de mRNA de la GC_{NO} producida por un mecanismo sensible a GMPc y PKA. Estos mismos autores habían demostrado previamente que agentes que aumentan la

concentración intracelular de adenosina-5-monofosfato cícliclo (AMPc) son capaces de disminuir la expresión de la GC_{NO} mediante un mecanismo que implica la activación de PKA (Papapetropoulos et al., 1995). Además, se ha demostrado en células de músculo liso de vasos sanguíneos una disminución en los niveles de mRNA de las subunidades α1 y β1 inducida por la exposición prolongada a NO que es debida a pérdida de estabilidad y que ocurre de manera dependiente de la trascripción y síntesis de proteínas (Filippov et al., 1997). Este tipo de efecto también fue observado cuando las células eran expuestas a agentes que generaban el NO de manera endógena como el LPS o citoquinas proinflamatorias (Papapetropoulos et al., 1996b; Takata et al., 2001).

Recientemente, se ha descrito en células endoteliales y de músculo liso la formación de un complejo proteico integrado por la chaperona HSP90, la subunidad β1 de la GC_{NO} y la NOS-3 (Venema et al., 2003). Estos autores sugieren que la HSP90 interacciona directamente con la GC_{NO} e indirectamente con la NOS-3, generando un complejo estable que facilita la interacción NOS-3-GC_{NO} y, por lo tanto, la estimulación directa por el NO de su diana. También se ha estudiado la interacción con la HSP70. Balashova y col. (2005) han sugerido que la interacción con esta chaperona podría regular la actividad GC_{NO} facilitando o estabilizando la inserción del grupo hemo, confiriéndole una mayor sensibilidad al NO.

La capacidad de interaccionar con otras proteínas puede conferir a la GC_{NO} un mecanismo de estabilización. Papapetropoulos y col. (2005) han descrito que en células de músculo liso, la inhibición farmacológica de la HSP90 durante periodos largos (24-48hs) produce una gran disminución en los niveles proteicos de las subunidades α1 y β1 y de la actividad GC_{NO}. Además, sugieren que esta disminución está mediada por el proteosoma ya que inhibidores específicos de éste impiden estos efectos.

A diferencia de lo que ocurre en células de músculo liso donde el tratamiento con agentes que generan NO endógeno disminuyen la GC_{NO} de manera dependiente de NO, estudios realizados en el laboratorio donde se llevó a cabo esta tesis, en cultivos primarios de células astrogliales de rata, demostraron que el tratamiento con LPS, citoquinas proinflamatorias (IL-1β) y péptidos β-amiloides (todos ellos agentes que inducen la NOS-2) disminuyen la GC_{NO} de una manera independiente de NO (Baltrons and Garcia, 1999; Baltrons et al., 2003; Baltrons et al., 2002; Pedraza et al., 2003). La disminución en los niveles de la subunidad β1 luego del tratamiento crónico con LPS o IL-1β, es más rápido que el que se produce en células tratadas durante el mismo período de tiempo con un inhibidor de la síntesis de proteínas como la cicloheximida, indicando que este efecto es debido a una disminución de la vida media de la proteína. Además, se ha demostrado que el efecto es prevenido por

inhibidores de la síntesis proteica y de la transcripción, sugiriendo que los agentes inflamatorios podrían estar induciendo la expresión de una proteína que estaría involucrada directa o indirectamente en la degradación de la GC_{NO} (Baltrons and Garcia, 1999; Pedraza et al., 2003). Una disminución en la expresión de GC_{NO} independiente de NO también ha sido descrita en células PC12 expuestas al factor de crecimiento neural (NGF) (Liu et al., 1997b).

A pesar de que los efectos de agentes inflamatorios en células astrogliales son independientes de NO, tal como ocurre en células de músculo liso, la GC_{NO} astroglial también puede ser desensibilizada y regulada negativamente por la exposición al NO. Estudios en células cerebelares disociadas demostraron que en astrocitos la desensibilización ocurre a los pocos segundos del tratamiento con NO (Bellamy et al., 2000). Estudios previos en nuestro laboratorio, en cultivos de astrocitos cerebelares de rata, demuestran que la exposición a un donador de NO (SNP) da lugar a una disminución dependiente del tiempo en la formación de GMPc. La máxima disminución tiene lugar a las 2 hs y se mantiene en ese nivel al menos en un periodo de 20 hs, no reestableciéndose los niveles normales por lo menos durante 48 hs. Este efecto se debe a una disminución en los niveles de la proteína a tiempos largos y a tiempos cortos es debido a la oxidación de grupos SH (Sardon et al., 2004). Durante este período también fue posible detectar una bajada en los niveles del mRNA de la subunidad β1. De la misma manera, la generación endógena de NO por el tratamiento prolongado con citoquinas y LPS afecta los niveles de mRNA de las subunidades α1 y β1 (Baltrons and Garcia, 1999; Pedraza et al., 2003). Teniendo en cuenta estos resultados, dos mecanismos podrían intervenir en la regulación de los niveles de GC_{NO} en condiciones de reactividad glial e inducción de NOS-2: una disminución inicial de la vida media de la enzima independiente de NO, y una disminución posterior de los niveles del mRNA que es dependiente de NO.

Además de la regulación fisiológica, agentes citotóxicos también pueden modificar la capacidad de generar GMPc. Por ejemplo, la exposición crónica al aluminio o la hiperamonémia crónica disminuyen la expresión de la GC_{NO} y su actividad en cerebro de ratas (Llansola et al., 1999; Minana et al., 1999).

Además de la regulación de la actividad GC_{NO} y de la síntesis de GMPc, existen evidencias de que los niveles de expresión de las distintas subunidades de la GC_{NO} se ven alterados durante el desarrollo y la diferenciación celular. Un estudio reciente demuestra que tanto el mRNA de la subunidad β1 como la proteína se expresan en células madre embrionarias de ratón indiferenciadas, donde no es posible detectar niveles de expresión para ninguna de las dos subunidades α conocidas, ni es posible detectar la producción de GMPc en respuesta a NO. Durante la diferenciación a cardiomiocitos, la expresión de la subunidad β1 y

de la subunidad α1 aumenta dramáticamente de la misma manera que lo hace la formación de GMPc dependiente de NO. Sin embargo, los niveles de β1 siguen siendo mayores que los de la α1 (Krumenacker and Murad, 2006). Mujoo y col. (2006) también han demostrado una expresión dependiente del desarrollo en células madres embrionarias de humanos. Describieron que la expresión de las subunidades α1 y β1 se veía aumentada con la diferenciación a nivel de mRNA y de proteína. Este mismo comportamiento fue descrito para el mRNA de la subunidad α2. Por el contrario, el mRNA de la subunidad β2 disminuía con la diferenciación de las células.

En el SNC, diferencias en el contenido de GMPc y el grado de estimulación de la GC_{NO} fueron descritas en cerebro durante la maduración y el envejecimiento (de Vente and Steinbusch, 1992). Los niveles de expresión de las distintas subunidades de la GC_{NO} determinados por PCR en cerebro de rata recién nacida y en adultas difieren, en estas últimas los niveles de la señal parecen ser más débiles (Gibb and Garthwaite, 2001). Bidmon y col. (2004), demostraron que la expresión de la subunidad α2 en el cerebro de rata está asociada al desarrollo cerebral. También se ha descrito que la expresión de esta subunidad está regulada por la activación de los receptores NMDA en células granulares del cerebelo *in vitro* durante la maduración (Jurado et al., 2003).

En humanos, se ha descrito una disminución de los niveles de expresión de las distintas subunidades de la GC_{NO} de manera dependiente de la edad (Ibarra et al., 2001). Esta disminución podría estar relacionada con los aumentos de las citoquina IL-1β observados en cerebro durante el envejecimiento (Mrak and Griffin, 2001). Tal como se ha indicado previamente, esta citoquina regula negativamente los niveles de la subunidad β1 en cerebro de rata (Ibarra et al., 2001; Pedraza et al., 2003).

A raíz de las diferencias en los niveles de expresión de las tres subunidades sumado a la expresión de la β1 en ausencia de α en algunas células durante el desarrollo, y teniendo en cuenta que los homodimeros β1/β1, α1/α1 y α2/α2 son catalíticamente inactivos, algunos autores han sugerido que estas subunidades podrían tener una función independiente de la actividad guanilil ciclasa (Bidmon et al., 2004; Zabel et al., 1999).

1.2.2.3 Localización de la GC_{NO} en el SNC.

Los primeros estudios inmunohistoquímicos sobre la GC_{NO} llevados a cabo en regiones del SNC datan de los años 80. Ariano y Nakane describieron por primera vez la distribución en cortes de cerebro de rata de la GC_{NO} utilizando anticuerpos frente a la enzima purificada. Sin

embargo, estos estudios no aportaban información sobre la distribución de las distintas subunidades, que aún no habían sido totalmente identificadas (Ariano et al., 1982; Nakane et al., 1983). Posteriormente, distintos grupos han utilizado técnicas de hibridación *in situ* para describir la distribución de las subunidades de la GC_{NO} en cerebro de rata. Matsuoka y col. (1992) fueron los primeros en describir la localización del mRNA de la subunidad β1 en cortes sagitales. Determinaron que la distribución estaba restringida a áreas discretas del cerebro y establecieron que las áreas de mayor intensidad de marcaje eran el estriado, el núcleo accumbens, el subiculum, el cortex piriforme, el tubérculo olfatorio, el núcleo habenular medial, el locus coeruleus, los colículos superior e inferior del cerebro medio y las células granulares del cerebelo, mientras que las áreas del hipocampo correspondientes a las capas de células piramidales y la capa de células granulares del giro dentado, los núcleos amigdaloides basolaterales y la capa de células de Purkinje cerebelares presentaban un marcaje moderado. No detectaron hibridación en el bulbo olfatorio de ratas. Posteriormente, Furuyama y col. (1993) confirmaron estos resultados sobre la abundante distribución de la subunidad β1 y describieron por primera vez en rata mediante hibridación *in situ* la presencia de la subunidad α1 en bulbo olfatorio, neocórtex, hipocampo, amígdala, diencéfalo, puente y médula oblonga, cerebro medio, hipotálamo, caudado-putamen y fundus estriati, siendo los tres últimos los lugares de máxima expresión de esta subunidad.

Recientemente, Gibb y Garthwaite (2001) han confirmado estos resultados y han descrito, además, que en cerebro de rata inmadura la subunidad α2 se encuentra concentrada en la capa de células piramidales del hipocampo y en células granulares de cerebelo, donde la expresión de la subunidad β1 es abundante y la expresión de α1 es baja, sugiriendo una localización diferencial de los heterodímeros. Pese a detectar la expresión de la subunidad β2 mediante RT-PCR, no pudieron detectar su mRNA por hibridación *in situ*, probablemente debido a los bajos niveles de expresión de esta subunidad en cerebro de rata (Gibb and Garthwaite, 2001). Estudios de RT-PCR cuantitativa permitieron describir la presencia del mRNA de todas las subunidades (α1-2, β1-2) en el SNC de ratón. Estos estudios demostraron que en cortex cerebral, cerebelo, bulbo olfatorio, médula, hipocampo y nervio óptico se expresan los mRNAs de ambas isoformas de la subunidad α y el de la subunidad β1 y que la proporción es similar (Mergia et al., 2003). Sin embargo, estos autores no fueron capaces de detectar mediante Northern Blot la presencia de la subunidad β2. En un estudio reciente, Ding y col. (2004), utilizando un anticuerpo frente a la subunidad β1 y otro que no distingue entre los dos tipos de subunidades αs, han descrito la presencia de células positivas para los dos tipos de subunidades en distintas regiones del cerebro de rata, como el cortex cerebral, hipocampo,

neoestriatum, tubérculo olfatorio y colículo superior e inferior. En cortex cerebelar la mayoría de las células de Purkinje presentaban marcaje para ambas subunidades, pero existían además células de Purkinje que no presentaban marcaje para ninguna de las 2 subunidades y que tendían a localizarse en grupos. Por el contrario, las células granulares eran positivas para β1 pero presentaban un marcaje muy débil para las α y lo mismo ocurría con pequeñas neuronas de la capa molecular.

Actualmente, son pocos los estudios que describen la expresión de las diferentes subunidades de la GC_{NO} en cerebro de primates. En humanos, Budworth y col. (1999) demostraron utilizando la técnica de dot blot que en todas las regiones estudiadas los niveles de la subunidad β1 eran mayores que los de la subunidad α1. Este mismo resultado fue obtenido a nivel de proteína por Ibarra y col. (2001). El mensajero de la subunidad α2 fue detectado en cerebro de humanos pero no se ha descrito ninguna distribución regional de esta subunidad (Budworth et al., 1999).

1.2.2.4 Localización intracelular de la GC_{NO}

Estudios estructurales llevados a cabo sobre la subunidad α2 han demostrado que posee una región próxima al C-terminal que le permite interaccionar con un dominio PDZ de la proteína de densidad post-sináptica PSD-95 (Mergia et al., 2003). Esta proteína posee otros dos dominios PDZ a través de los cuales puede interaccionar con la NOS neuronal (NOS-1) y con el receptor de tipo NMDA del glutamato (Bredt, 1996). Esta proximidad de los elementos del sistema de señalización (Figura 2), sugiere una explicación para el hecho de que la entrada de calcio resultante de la estimulación de los receptores de NMDA sea el mecanismo más eficaz para activar la formación de NO y de GMPc en cerebro (Tomita et al., 2001). Ya que el dominio PDZ confiere a la isoforma α2β1 la capacidad de ser reclutada a la fracción de membrana, la denominación GC soluble no parece ser totalmente apropiada, prefiriéndose en la actualidad la de “GC sensible a NO” (Koesling et al., 2004).

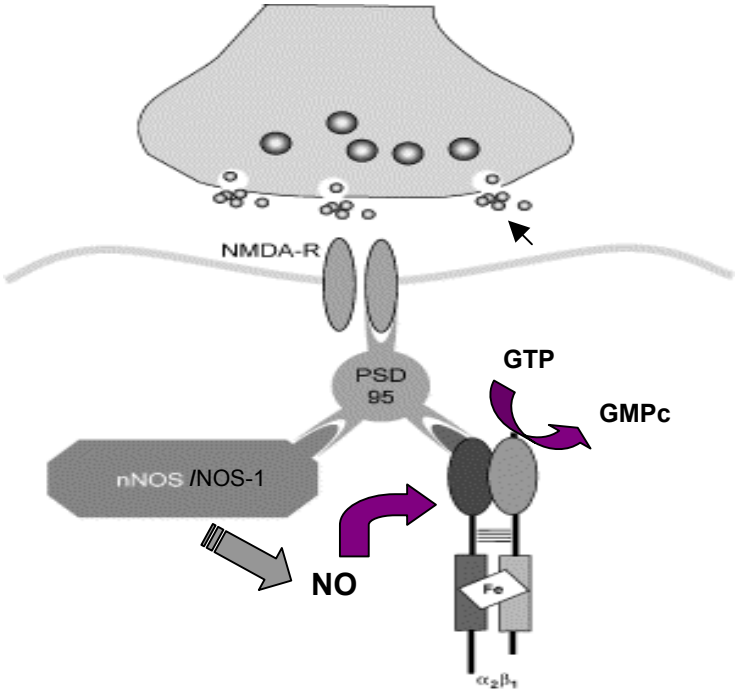

Figura 2: Dominios de interacción de la GC_{NO}, nNOS y receptor NMDA. Adaptado de Koesling et al. 2004.

Este dominio PDZ de interacción entre proteínas no se encuentra en la secuencia de aminoácidos de la subunidad α1, sin embargo se han descrito mecanismos de asociación a la membrana de esta subunidad relacionados con la regulación de la enzima y con la sensibilidad de la misma a la activación por NO (Zabel et al., 2002). Mediante técnicas histoquímicas se ha podido detectar la presencia del heterodímero $\alpha1\beta1$ en el sarcolema del músculo esquelético (Feussner et al., 2001). Esta asociación a la membrana de las subunidades α1 y β1 ha sido demostrada también en músculo cardíaco, células endoteliales y plaquetas, y existen evidencias de que es dependiente de Ca^{2+} (Agullo et al., 2005; Zabel et al., 2002). Un estudio reciente propone que la interacción entre la chaperona HSP70 y la subunidad β1 está implicado en la asociación de la isoforma $\alpha1\beta1$ de la GC_{NO} con la membrana celular (Balashova et al., 2005).

A pesar de que utilizando métodos inmunocitoquímicos y bioquímicos se ha localizado la GC_{NO} y el GMPc predominantemente en el citoplasma, algunos autores han descrito una localización perinuclear y nuclear (Earp et al., 1977; Heinrich et al., 2000). Muy recientemente, Krumenacker y Murad (2006) describieron mediante inmunocitoquímica la presencia de GMPc en el núcleo de células madres precursoras de cardiomiocitos mientras que Gobeil y col. (2006) han descrito la presencia de GMPc y de la subunidad β1 en fracciones nucleares de hepatocitos bovinos. Esta localización nuclear de la subunidad β1 y su producto hace pensar en una posible función nuclear de la GC_{NO}.

2 OBJETIVOS

- En ninguno de los estudios previos disponibles en la literatura sobre la expresión de las subunidades de la GC_{NO} en SNC de roedores se había realizado un mapeo completo en cortes coronales de cerebro adulto. Por otro lado, no existía ninguna información sobre la localización de las subunidades de la GC_{NO} en cerebro de primates. Así pues, el primer objetivo de este trabajo fue realizar un **estudio comparativo de la localización de los mRNAs de las cuatro subunidades de la GC_{NO} en cortes coronales de cerebro de rata y de mono mediante hibridación *in situ*.**

- Datos previos obtenidos en el laboratorio habían demostrado que diversos agentes inflamatorios, entre ellos los péptidos β-amiloides, producían una disminución de la expresión de la GC_{NO} en astrocitos de rata en cultivo, así como en cerebro de animales adultos. Teniendo en cuenta estos datos nos propusimos **estudiar si este mismo fenómeno tenía lugar en cerebro de pacientes con enfermedades neurodegenerativas que llevan asociada neuroinflamación.**

- En los estudios sobre la disminución de los niveles de la GC_{NO} en astrocitos tratados con el agente inflamatorio LPS realizados previamente en el laboratorio, se había demostrado que se producía una disminución de la vida media de la subunidad β1 de la enzima. Otro objetivo de este trabajo fue **estudiar el mecanismo a través del cual el LPS provoca la degradación de la subunidad β1 de la GC_{NO}.**

- A lo largo de los estudios sobre la degradación de la subunidad β1 en astrocitos tratados con LPS, observamos que esta subunidad de la GC_{NO} tenía una localización parcialmente nuclear y que estaba asociada a los cromosomas durante la mitosis. Así nos propusimos caracterizar la **localización nuclear de la subunidad β1 de la GC_{NO} y su posible función.**

3 MATERIALES

Animales

Para la preparación de los cultivos primarios, en este trabajo se han utilizado ratas albinas de una semana de edad, de la cepa Sprague-Dawley criadas en el estabulario de la Universidad Autónoma de Barcelona. Los animales fueron mantenidos con la madre hasta el momento de ser sacrificados, en condiciones constantes de luz (ciclos de 12 hs luz-oscuridad) y temperatura (21-24ºC), con acceso libre a comida y bebida.

Para la hibridación in situ las especies utilizadas para los distintos estudios fueron rata (Wistar), y mono (*Macaca fascicularis*, edad de entre 3-7 años, rango de peso entre 2.4-2.7 kg, tiempo post mortem 1h). Las ratas estuvieron estabuladas en la Universidad de Barcelona y mantenidas en régimen de alternancia de 12 hs de luz y oscuridad con libre acceso a comida y bebida. Los monos fueron sacrificados por la administración de una sobredosis de sodio-pentobarbital.

Las muestras de tejido humano fueron cedidas por el Dr. I. Ferrer del Instituto de Neuropatología, Hospital del Bellvitge, Barcelona.

Material de cultivo

El medio de cultivo Dulbecco's modified Eagle's (DMEM), arabinósido de citosina (cit-ara), poli-L-α-ornitina, sulfato de estreptomicina, penicilina G, nigrosina y tripsina fueron proporcionados por SIGMA. El suero fetal bovino (FCS) de Ingelheim Diagnóstica y el colcemid fue proporcionado por GIBCO. Los medios y soluciones se prepararon con agua Milli-Q (Millipore) y fueron esterilizados por filtración utilizando filtros de acetato de celulosa de 0,2 μm de tamaño de poro.

Reactivos

Los compuestos 3-isobutil-1-metilxantina (IBMX), ATP, lipopolisacárido bacteriano (LPS), nitroprusiato de sodio (SNP), cicloheximida (CHX), HEPES, 1H-[1,2,4]oxadiazolo[4,3-a]quinoxalin-1-one (ODQ), dibutiril-cGMP (dbGMP), cloroformo, isopropanol, Tris-base, Tris-HCl, albúmina bovina (BSA) y forbol-12-miristate13-acetato (PMA) fueron proporcionados por SIGMA. Los compuestos ácido etilen diaminotetraacético (EDTA), dodecilsulfato sódico (SDS), β-2-mercaptoetanol, glicerol, p-formaldehído, tritón X-100, persulfato amónico, nitrito sódico, sacarosa, glucosa, NaCl, KCl, KH_2PO_4, Na_2HPO_4, $CaCl_2$, NaOH, glicina, sulfanilamida y anhídrido acético, por Fluka; la acrilamida, bisacrilamida, el TEMED y la agarosa por BioRad; las membranas de PDVF por Millipore, el film fotográfico por Kodak. El [^{3}H] cGMP (33 ó 34.5

Ci/mmol) fue obtenido de New England Nuclear. El líquido de centelleo BCS fue proporcionado por Amersham.

El plásmidos pEGFP-C1 (Clonotech) fue donado por el Dr. Saura (Instituto de Neurociencias, UAB); el plásmido conteniendo la secuencia de la β1-GC_{NO} (pEYFP-β1) y los plásmidos pEYFP-C1 conteniendo las secuencias codificantes de las subunidades α1 y α2 de la GC_{NO} fueron donados por el Dr. J. Garthwaite (Wolfsoin Inst. Biomed. Res., UK).

Como marcadores de DNA se emplearon el 4',6-diamidino-2-phenylindole (DAPI) y el Hoesch 33342. La lipoproteína de baja densidad acetilada marcada con 1,1´ dioctadecil-3,3,3´,3´-tetrametil-indocarbocianina-perclorato (DIL-Ac-LDL) de Biomedical Technologies se utilizó como marcador de microglía. El anticuerpo policlonal purificado de conejo anti-subunidad β1 de la GC_{NO} y el anticuerpo los anticuerpos monoclonales de ratón contra la proteína acida fibrilar de la glia (GFAP), el anticuerpo anti-γ-actina y anti-gliceraldehido-3-fosfato deshidrogenada (GAPDH) fueron adquiridos de SIGMA; el anticuerpo de conejo anti-GFAP de DAKO; el anticuerpo anti-laminin-B y anti-SUMO-1 de Zymed, el anticuerpo anti 2,2,7-trimetilcuanosina cap de Oncogene, el anticuerpo monoclonal anti-pan-histona de Roche, el policlonal anti-ubiquitina conjugada a proteína y el anticuerpo anti proteosoma 20 S de Biomol International, el monoclonal anti-ubiquitina (P4D1) de Santa Cruz, el anticuerpo anti HSP90 de Transduction Laboratorios, el péptido antigénico de la subunidad β1 de la GC_{NO} de Cayman; el antisuero anti-GMPc empleado para RIA fue preparado en nuestro laboratorio según Brooker et al. (1979); el anticuerpo policlonal anti-cGMP-para-formaldehydo-tiroglobuline fue gentilmente cedido por el Dr. J. de Vente (Universidad de Maastricht, Netherlands); los anticuerpos secundarios conjugados con Alexa 488 y Alexa 555 fueron proporcionados por Molecular Probes; las IgG de conejos conjugados a FITC de DAKO; los anticuerpos secundarios acoplados a fosfatasa alcalina fueron adquiridos en Bio-Rad y los secundarios con HRP fueron proporcionados por Amersham.

El inhibidor del proteosoma I (PSI), lactasistin, MG-132, inhibidor de calpaina II, inhibidor ICE II fueron adquiridos en Calbiochem. El 17-AGG fue gentilmente cedido por Conforma Therapeutics Corporation.

4 MÉTODOS

Cultivos Celulares

4.1.1 Líneas celulares

En esta tesis se han utilizado líneas células de glioma de rata (C6) obtenidas de la American type Culture Collection (ATCC) y la línea celular de microglía de rata (HAPI) cedidas gentilmente por el Dr. James R. Connor (Hershey Medical Center, Hershey, PA). Ambas han sido crecidas en DMEM suplementado con L-glutamina (2mM), 20 U/ml de penicilina y 20 µg/ml de estreptomicina y el 10% de FCS para las C6 o el 5 % de FCS para las HAPI. Las células fueron mantenidas en una atmósfera de 90% aire-10% CO_2 a 37°C. Estas fueron subcultivadas cada 3-4 días a una densidad de 1×10^5 células/cm^2 y utilizadas entre un 50-80% de confluencia. En algunos experimentos las células fueron sincronizadas privándolas de suero durante 48 hs para poder obtener mayor número de células en interfase. Para los estudios del ciclo celular se arrestaron en metafase agregándoles nuevamente suero y tratándolas con colcemid (GIBC0; 0.1 µg/ml) durante 18 hs.

Otras líneas celulares como las COS-7, Hela, Ditanc1, SW1040 y A7R5 obtenidas de la ATCC fueron utilizadas en esta tesis para realizar controles en algunos experimentos; fueron mantenidas en las mismas condiciones que las C6.

4.1.2 Cultivos primarios enriquecidos en astrocitos de cerebelo

Los cultivos primarios enriquecidos en astrocitos se prepararon a partir de cerebelos de ratas de siete días de edad por el método rutinariamente utilizado en el laboratorio (Agulló y col., 1995). Las ratas se sacrificaron por decapitación y se diseccionó el cerebro mantenido en un medio salino (medio D_1: NaCl 137 mM; KCl 5,5 mM; KH_2PO4 2,22 mM; Na_2HPO_4 0,17 mM; glucosa 5 mM y sacarosa 58,5 mM) a pH 7,4. La disgregación del tejido se realizó por pasos sucesivos a través de dos mallas de nylon de 210 y 135 µm de poro en el medio D_1. La suspensión celular obtenida se centrifugó a 500 g durante 5 min a 20ºC y las células se resuspendieron en medio de cultivo (90 % DMEN, 10 % FCS, 20 unidades de penicilina y 20 µg/ml de estreptomicina) a 37ºC. En esta suspensión se realizó un recuento de células utilizando un hemocitómetro, determinando la viabilidad por exclusión del colorante vital nigrosina (concentración final 0,25 % p/v). Las células se sembraron a una concentración de 0,6 x 10^5 células viables/ml en placas de cultivo de 35 mm, 60 mm ó 100 mm de diámetro, o placas de 12 ó 24 pocillos, y se incubaron a 37ºC en atmósfera de 90 % aire-10 % CO_2 con una humedad del 95 %. El medio fue remplazado una vez a la semana y las células fueron

utilizadas cuando llegaban a la confluencia que fue para los distintos experimentos entre los 14 y 21 días. Estudios previos del laboratorio en cultivos obtenidos por este método, describen que la mayoría de las células presentes en cultivos confluentes de 14 días son GFAP positivas. La contaminación por neuronas y oligodendrocitos es escasa, y la presencia de células de microglía puede variar considerablemente de una preparación a otra, pudiendo alcanzar un 30 % del total de células (Agulló y col., 1995).

4.1.3 Cultivos primarios enriquecidos en microglía de cerebelo

Los cultivos primarios de microglía se obtuvieron a partir del método descrito por Saura y col. (2003), a partir de cultivos primarios de astrocitos de 2-3 semanas de edad, las células se lavaron con DMEM 2 veces para retirar el exceso de suero y se sometieron a una tripsinización suave (tripsina 0,0625%) durante 30 min a 37ºC, de esta manera se levanta la monocapa de astrocitos mientras que las células de microglía quedan adheridas a la placa. Éstas se lavaron a continuación con DMEM en presencia de suero para detener el efecto de la tripsina y se utilizaron en las siguientes 24 hs.

Tinciones celulares

La identificación de los distintos tipos celulares en cultivos primarios se realizó por inmunofluorescencia indirecta utilizando como marcador celular la GFAP (dilución 1:300) para astrocitos y el caso de la microglía la proteína Dil-Ac-LDL (Simmons y Murphy, 1993). Los núcleos fueron teñidos en todos los casos utilizando DAPI (dilución 1:1000) o Hoesch 33342.

4.1.4 Inmunofluorescencia de cultivos celulares

Para realizar las tinciones las células fueron crecidas en cubreobjetos y se procedió a realizar la tinción según el siguiente protocolo:

- *Fijación*: Después de aspirar el medio y lavar las monocapas con PBS a 37ºC, las células se fijaron con paraformaldehído 4% (p/v) en PBS, durante 30 min a temperatura ambiente o con metanol durante 2 min a -20ºC.

- *Permeabilización y bloqueo de uniones inespecíficas* : Tras lavados (3 x 2 min) con tampón PBS a temperatura ambiente, las células se incubaron primero con tritón X-100 al 0,5 % (v/v) en PBS durante 20 min, y a continuación con PBS-glicina 0.1 M o BSA 1% (v/v).

- *Incubación con el primer anticuerpo*: Las células se incubaron durante 16-20 hs a 4ºC y en cámara húmeda con 100 μl del primer anticuerpo a las siguientes diluciones: anti-GFAP de ratón 1:300, GC_{NO} β1 de conejo 1:300 en PBS.

- *Incubación con el segundo anticuerpo*: Tras varios lavados (3 x 10 min) con PBS y un lavado con PBS-tween 0.05% (v/v), las células se incubaron 1 h a temperatura ambiente en cámara húmeda con IgG de conejo anti-ratón conjugada con diferentes fluoróforos (Alexa 555 o 488 dilución 1:1000 en PBS). Éste y los sucesivos pasos se realizaron en la oscuridad. Como control de inespecificidad de los segundos anticuerpos se utilizaron placas que fueron procesadas en ausencia del primer anticuerpo.

- *Lavados y montaje*: A continuación, las células se lavaron (3 x 10 min) con PBS (un lavado con el DAPI 1:1000) y 5 min con agua destilada. Luego de lavarlas las células fueron montadas en Fluoprep (Biomérieux SA, France).

- *Fotografías:* Las fotos fueron tomadas utilizando un microscopio confocal (confocal láser scanning microscope Leica TCS SP2 AOBS equipado con lasers de argón 488 y He ne 561 nm) o en un microscopio de fluorescencia (Nikon). Las imágenes de las muestras marcadas con más de un fluoróforo fueron tomadas de manera secuencial.

4.1.5 Marcaje de células microgliales

Las células microgliales fueron incubadas con DIL-Ac-LDL (10 µg/ml) por 4 hs a 37ºC antes de ser fijadas con PFA durante 30 min a temperatura ambiente. Luego se procedió de la misma manera que con el resto de las células para completar las tinciones.

Tinciones Histológicas

Para examinar la localización anatómica precisa de las diferentes poblaciones neuronales, las mismas secciones histológicas o secciones consecutivas a las utilizadas en la hibridación *in situ* (ver apartado 4.4) se tiñeron con los siguientes métodos de tinción histológica:

4.1.6 Tinción de violeta de cresilo o Nissl

Las secciones de tejido se incubaron durante 10 min a temperatura ambiente en una solución al 0.25% de violeta de cresilo (SIGMA). Se lavaron en agua destilada y se deshidrataron en concentraciones crecientes de etanol; posteriormente se incubaron en Histoclear (National Diagnostics) 2 veces, 5 min cada vez y se montaron en Entellan (Merck).

4.1.7 Actividad acetilcolinesterasa

Mediante esta técnica se tiñen núcleos celulares y tractos fibrilares que son difíciles de identificar con la tinción de Nissl o violeta de cresilo. Se utilizó el método descrito por Karnovsky

y Root (1964). 50 ml de medio A que contiene 1.9 mM de ioduro de acetil-tiocolina, 0.06 M acetato sódico (pH 5.5), 0.1 M citrato sódico, 30 nM $CuSO_4 \cdot 5H_2O$, 4 mM tetraisopropilo de pirofosforamida, se mezclaron con 5.5 ml de medio B (5mM $K_3Fe(CN)_6$). Las secciones de tejido se incubaron en esta mezcla durante 2 hs a 37ºC. Seguidamente, se lavaron con agua destilada y posteriormente se deshidrataron en concentraciones crecientes de etanol. Se sumergieron en Histoclear y se montaron en Entellan.

Hibridación *in situ*

La técnica histoquímica de la hibridación *in situ* permite conocer en detalle la distribución anatómica y celular del mRNA que codifica para una determinada proteína presente en secciones de tejido. Para poder detectar una cadena simple de mRNA en una sección de tejido, es necesario preparar y marcar convenientemente una sonda apropiada, es decir, una cadena de ácido nucleico complementaria al mRNA que se quiere detectar.

Las condiciones experimentales para cada uno de los estudios realizados se encuentran detalladas en el capítulo de resultados. En la figura 3, se presentan de forma esquemática aquellos elementos que intervienen en la técnica de hibridación *in situ*, así como los pasos a seguir para su realización.

4.1.8 Obtención y preparación de tejidos

Para ambos animales (rata y mono), el cerebro se extrajo de la cavidad craneal después de la decapitación del animal, procediéndose a su congelación y almacenamiento (-20ºC) hasta su uso. Todos los procesos de manipulación de animales se realizaron respetando la legislación española de protección de animales usados en experimentación y otros propósitos científicos (L358/1 de 18/12/1986 del DOCE), y de acuerdo con las normas europeas de bienestar animal, directiva europea del 24 de Noviembre de 1986, 86/609/EEC.

La preparación del tejido se realizó de manera que pudieran utilizarse secciones histológicas próximas o consecutivas para las distintas técnicas autoradiográficas (hibridación *in situ*), así como diferentes métodos de tinción (violeta de cresilo, tinción de acetilcolinesterasa). Las secciones histológicas de 14 y 20 μm de espesor (rata y mono respectivamente), se obtuvieron a partir de las muestras congeladas (-20ºC) mediante un crióstato (Leitz 1720 o Microm HM 500 OM) y fueron montadas por congelación/descongelación en portaobjetos previamente tratados con APTS (3-aminopropiltrietoxisilano, SIGMA) para evitar el desprendimiento del tejido en procesos posteriores. Una vez montadas sobre los

portaobjetos, estas secciones histológicas se almacenaron congeladas a -20ºC hasta su utilización.

Todos los experimentos de hibridación *in situ* fueron realizados en el Departamento de Neuroquímica, IIBB-CSIC, IDIBAPS.

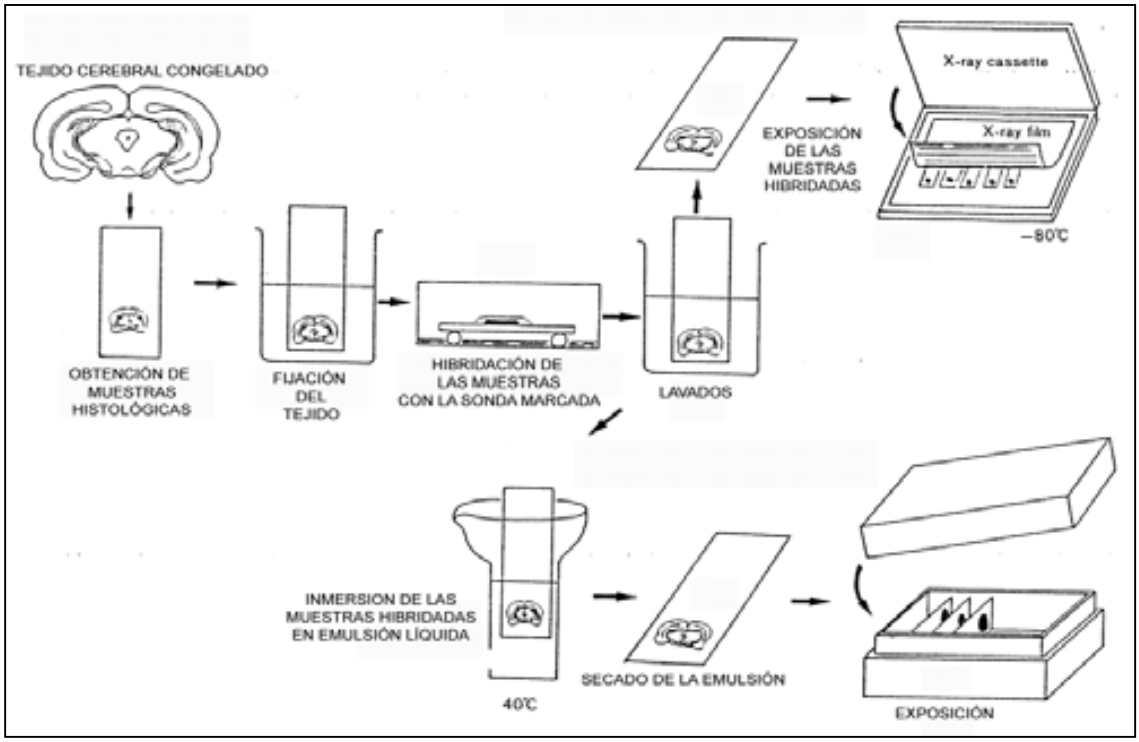

Figura 3. Representación esquemática del proceso de la técnica histoquímica de hibridación *in situ*.

4.1.9 Sondas de hibridación

Las sondas complementarias que se utilizan para la hibridación *in situ* pueden ser cadenas de RNA o de DNA de longitud variable (desde 30 bases hasta varios cientos de bases) y de distintos tipos, como por ejemplo cDNA (ácido desoxirribonucléico complementario), cRNA, DNA de cadena simple o de doble cadena, así como oligonucleótidos sintéticos. Los oligonucleótidos son cadenas cortas de cDNA (de unas 45 bases, en nuestro caso) que se preparan con sintetizadores de DNA automáticos, lo que permite su obtención de manera comercial (Pharmacia Biotech).

El uso de oligonucleótidos presenta una serie de ventajas. En primer lugar son de fácil obtención; para diseñar la secuencia de un oligonucleótido basta con conocer la secuencia del DNA ya publicada en la literatura o en bases de datos sin necesidad de disponer del clon del gen en cuestión que se pretende estudiar. Además, debido a su pequeño tamaño, los oligonucleótidos pueden penetrar fácilmente en las células así como marcarse radiactivamente

con alta actividad específica. Otra gran ventaja que presentan debido a su reducido tamaño es su gran especificidad por el mRNA que se quiere detectar, ya que permite disponer de sondas capaces de discriminar un mRNA de otros miembros de una misma familia de genes e incluso con los productos generados por *splicing* alternativo de un mismo mRNA. Este aspecto fue especialmente importante para nosotros, ya que nos permitió trabajar con distintas subunidades de la misma proteína que presentaban entre ellas un alto grado de similitud de secuencia.

Las sondas se diseñaron de manera que fueran complementarias a aquellas regiones del mRNA donde se encontraron mayores diferencias en la secuencia nucleotídica de las distintas subunidades. Se utilizaron un total de 13 oligonucleótidos diferentes. Las principales características de las sondas utilizadas están especificadas en la Tabla 1. Los experimentos de hibridación *in situ* se llevaron a cabo en ambas especies con dos oligos diferentes para cada subunidad (resaltados en negro).

Tabla1: Características de las sondas de hibridación.

Oligonucleótido	mRNAs, clave identificación	Subunidad	Límites
rGCα1/1	**+ M57405**	**subunidad α1**	**NH_2 term bp 556-600**
rGCα1/2	**+** M57405	subunidad α1	NH_2 term bp 642-692
rGCα1/3	**+ M57405**	**subunidad α1**	**Bp 738-755 (Gibb & Garthwaite)**
rGCα1/4	**+** M57405	subunidad α1	Bp 796-840
rGCα2/1	+ NM_023956	subunidad α2	NH_2 term bp 494-538
rGCα2/2	**+** NM_023956	subunidad α2	NH_2 term bp 464-508
rGCα2/3	**+ NM_023956**	**subunidad α2**	**Bp 675-711 (Gibb & Garthwaite)**
rGCα2/4	**+ NM_023956**	**subunidad α2**	**Bp: 713-757**
rGCβ1/1	**+ M22562**	**subunidad β1**	**NH_2 term bp 70-114**
rGCβ1/2	**+ M22562**	**subunidad β1**	**NH_2 term bp 196-240**
rGCβ2/1	**+** AY004153 **-** NM_012770	subunidad β2	NH_2 term bp 61-105

rGCβ2/3	**+ AY004153** **+ NM_012770**	**subunidad β2**	**COOH bp 2271-2315** **COOH bp 2154-2198**
rGCβ2/4	**+ AY004153** **+ NM_012770**	**subunidad β2**	**NH_2 term bp 423-467** **NH_2 term bp 306-350**

4.1.10 Marcaje de las sondas de hibridación

Las sondas que se utilizaron para la detección de mRNA por hibridación se marcaron radiactivamente utilizando ^{33}P, que por su alta energía permite una detección rápida de la señal de hibridación con gran sensibilidad. El marcaje de las sondas se realizó en su extremo 3' con [^{33}P]α-dATP. El oligonucleótido (2 pmoles) se hizo reaccionar con 25 unidades de la enzima desoxinucleotidiltransferasa terminal (TdT) (Roche Molecular Biochemicals) y 17 pmoles de [^{33}P]α-dATP (3000Ci/mmol, DuPont-NEN) en un tampón consistente en 200 mM cacodilato de potasio, 25 mM Tris-HCl (pH 6.6), 1.25 mg/ml de albúmina de suero bovina (BSA) y 2.5 mM de cloruro de cobalto. La reacción se efectuó a 37ºC durante 2 hs, y después se detuvo a 65ºC durante 5 min. La purificación de la sonda así marcada radiactivamente se realizó mediante cromatografía empleando columnas QIAquick Nucleotide Removal Kit (QIAGEN) siguiendo las instrucciones del proveedor.

4.1.11 Fijación del tejido e hibridación

La técnica de hibridación *in situ* puede aplicarse tanto en tejido congelado (fresco o perfundido) como en tejido incluidos en parafina. En el presente trabajo se utilizó únicamente tejido congelado fresco. Las secciones se descongelaron bajo corriente de aire frío, y se fijaron por inmersión en PFA al 4% en tampón fosfato salino (PBS: 2.6 mM KCl, 1.4 mM KH_2PO_4, 136 mM NaCl, 8mM Na_2HPO_4) a 4ºC durante 20 min. Seguidamente se lavaron una vez en PBS tres veces concentrado (3x) y dos veces en PBS (1x), 5 min cada lavado.

Posteriormente, las secciones se incubaron con pronaza predigerida (24 U/ml, Calbiochem) diluida en 50 mM Tris-HCl pH 7.5, 5mM EDTA durante 2 min a 20ºC. La actividad proteolítica se detuvo por inmersión durante 30 seg en una solución de glicina (2 mg/ml en PBS), seguidamente se lavaron de forma rápida dos veces en PBS y se deshidrataron en etanol (70% y 100%). Una vez secas, las secciones se hibridaron con la sonda marcada, previamente diluida a una concentración final entre 1.5-2 x 10^7 cpm/ml en tampón que contiene 50% formamida, SSC cuatro veces concentrado (SSC: 150mM NaCl; 15mM citrato sódico), solución Denhardt (0.02% ficoll, 0.02% polivinilpirrolidona, 0.02% BSA fracción V), 1% de

sarcosil, 20 mM tampón fosfato pH 7.0, 10% de sulfato de dextrano, 250 μg/ml de tRNA de levadura (BRL) y 500 μg/ml de DNA de esperma de salmón (SIGMA).

Para la hibridación, el tejido se cubrió con unos 100 μl de la solución de hibridación y con un cubreobjetos (NESCOFILM). Se hibridó durante una noche (18-20 hs) a 42ºC en cajas húmedas.

4.1.12 Lavados y generación de la señal autorradiográfica

Finalizada la hibridación, las secciones de tejido se lavaron cuatro veces durante 45 min cada vez, en un tampón compuesto por 0.6 M NaCl, 10 mM Tris-HCl (pH 7.5) y 1 mM EDTA (pH 8.0), a 50ºC o 60ºC, dependiendo de la sonda (ver resultados). Posteriormente las secciones se deshidrataron en etanol (70% y 100%).

Las imágenes autorradiográficas se obtuvieron por exposición de las secciones de tejido hibridadas en film Hyperfilm ß-max (Amersham) o Kodak Biomax MR. Los films se expusieron a -70ºC, temperatura necesaria para que tengan efecto las pantallas intensificadoras de la emisión radioactiva del ^{33}P, durante un tiempo variable (4-5 semanas) dependiendo de la intensidad de la señal generada por la sonda radioactiva. Al finalizar la exposición, se revelaron con revelador D-19 (Kodak) 5 min. Para realizar detalles a mayor aumento, las secciones fueron sumergidas rápidamente en etanol al 70% y al 100%, secados con aire y sumergidos en la emulsión nuclear Ilford K5 (Ilford, Mobberly, Chesire, el Reino Unido) diluido 1:1 con agua destilada. Los portaobjetos fueron expuestos en la oscuridad en 4°C durante 6 semanas, y finalmente revelados en Kodak D19 (Kodak, Rochester, Nueva York, EE. UU) durante 5 min y fijados con Ilford Hypam (Ilford). Algunas de estas secciones una vez reveladas se tiñeron débilmente con violeta de cresilo, para poder observar los cuerpos celulares por microscopía de campo claro a la vez que la señal autorradiográfica.

4.1.13 Estudios de control de especificidad de la señal de hibridación de oligonucleótidos

Como en cualquier técnica histoquímica, no toda señal observada por hibridación *in situ* tiene que ser específica, ya que las sondas utilizadas pueden unirse inespecíficamente a otros componentes del tejido como lípidos o RNAs no homólogos. Así, un paso importante a realizar cuando se optimizan las condiciones experimentales en las que vamos a utilizar una determinada sonda en experimentos de hibridación *in situ* es asegurarse de que la señal de hibridación obtenida sea específica. Para ello y debido a que no existe un método único para determinar de manera infalible la especificidad de la señal de hibridación, se realizan diferentes controles de especificidad:

1.Co-hibridación del oligonucleótido marcado con un exceso del mismo sin marcar (exceso de 20 a 50 veces). La señal autorradiográfica específica desaparece y nos da una idea de los niveles del ruido de fondo.

2.Análisis de la estabilidad térmica de los híbridos formados. Se realiza lavando las secciones hibridadas, a temperaturas crecientes en intervalos de 10-20ºC. Si la interacción es específica, se observa un descenso brusco de la intensidad de la señal de hibridación a temperaturas cercanas a la Tm (temperatura en la que se disocian el 50% de los híbridos). Este control a su vez también permite encontrar la temperatura óptima de lavado para cada sonda, siempre inferior a la Tm, y que para las sondas utilizadas en este trabajo varía entre 50-60ºC (ver resultados).

3.El uso por separado de dos oligonucleótidos marcados, complementarios a distintas regiones del mismo mRNA, ha de resultar en un patrón de hibridación similar para cada uno de ellos.

4.Utilización de emulsiones líquidas (técnica del *dipping*) o de métodos de hibridación *in situ* no isotópicos para verificar que la señal de hibridación obtenida proviene de cuerpos celulares.

Determinación de los niveles de proteína de las subunidades de la GC_{NO} por Western blot

La determinación de la expresión de las distintas subunidades de la GC_{NO} en las células y en los tejidos, se realizó por ensayos de inmunotransferencia (Western Blot) a partir de extractos celulares y de homogenados de tejido. Los pasos seguidos fueron:

4.1.14 Preparación de fracciones citosólicas

Los lisados celulares se obtuvieron a partir de células en cultivo sembradas en placas individuales de 90 o 60 mm, o bien a partir de homogenados de tejidos de cerebro humano post-mortem (dilución 10% p/v).

En las placas tras aspirar el medio, se lavaron dos veces con un tampón salino (PBS) a 4ºC. Las células fueron despegadas de la placa de cultivo con la ayuda de una espátula y se homogenizaron en un tampón 50 mM Tris-HCl (pH 7,4) (1 ml/placa de 100 mm) que contenía 0,1 mM EDTA, inhibidores de proteasas (Roche) e inhibidores de fosfatasas (SIGMA). Todas las homogenizaciones se realizaron mediante 15 subidas y bajadas en un homogenizador tipo Patter-Elvehjeim vidrio-teflón a 800 rpm. Las fracciones citosólicas se obtuvieron por una centrifugación a 100,000g durante 1 h (Centrifuga Beckham). Los homogenados se

mantuvieron en alícuotas a -80ºC hasta su utilización. La concentración de proteína se determinó mediante los métodos de Lowry y Bradford (ver apartado 5.10.2).

Para las muestras de tejido los cerebros fueron troceados y pesados. Se añadió el tampón de homogenización (Tris-HCl 50 mM, EDTA 1mM, pH 7,4) en una relación 1/10 (p/v). Las muestras se procesaron en un mortero en presencia de nitrógeno líquido. Las suspensiones resultantes se centrifugaron a baja velocidad (1000 rpm en centrífuga sorvall) para eliminar los restos de tejido mal disgregados. Luego se procedió de la misma manera que en los cultivos celulares para obtener la fracción citosólica.

En ambos casos, una vez terminadas las centrifugaciones se obtienen una fracción citoplasmática o "fracción soluble" y un "pellet" que constituyó la "fracción de membrana". Las fracciones nucleares se obtuvieron según el método descrito para aislar núcleos interfásicos (ver más adelante)

4.1.15 Inmunoblots (Western Blot)

La técnica de Western blot se utiliza para identificar y localizar proteínas en base a su capacidad para migrar y de unirse a anticuerpos específicos. Se realizó según el siguiente protocolo:

- Preparación del gel de poliacrilamida (7,5%):

a) *Preparación de soluciones*:

- Solución A: 29,2% acrilamida, 0,8% bisacrilamida.

- Solución B: Tris 1,5 M, SDS 0,4%, pH 8,8.

- Solución C: Tris 0,5 M, SDS 0,4%, pH 6,8.

b) *Gel separador (10%)*: Sobre 6 ml de agua se añadieron 3 ml de solución B y 3 ml de solución A. Después de mezcla durante 10 min, se añadieron 6 μl de TEMED y 48 μl de persulfato amónico (15%), y se dejó polimerizar el gel.

c) *Gel apilador (3%)*: El gel apilador se preparó mezclando en estricto orden 2 ml de agua, 0,75 ml de solución C, 0,225 ml de solución A, 3 μl de TEMED y 30 μl de persulfato amónico (15%).

- Electroforesis en gel de poliacrilamida (SDS-PAGE): Las muestras (15-80 μg de proteína de los homegenados) se cargaron en el gel apilador, y seguidamente las proteínas se

separaron mediante electroforesis en tampón Tris-glicina (Tris 25 mM, glicina 192 mM, SDS 0,1%). Estándares premarcados (Invitrogen) se usaron como marcadores de peso molecular.

- *Electrotransferencia*: Las proteínas se transfirieron a membranas de PDVF (Millipore) por medio de una exposición a 100 V durante 1,5 hs a 4ºC en tampón Tris-glicina-metanol (Tris 25 mM, glicina 192 mM, metanol 20%).

- *Bloqueo de uniones inespecíficas*: Para evitar las uniones inespecíficas de los anticuerpos, las membranas se incubaron en tampón PBS-5% leche desnatada (5% (p/v) leche desnatada en polvo en PBS) durante 16-24 hs a 4ºC.

- *Incubación con el primer anticuerpo*: Las membranas se incubaron con los anticuerpos primarios anti-GC_{NO} β1 (1:2000), αs (1:4000), Actina (1:100000), Lamin-B (1:2000), GAPDH (1:40000) diluidos en PBS-1% leche desnatada durante 2 hs a temperatura ambiente o toda la noche a 4ºC.

- *Incubación con el segundo anticuerpo*: Después de varios lavados (3 x 15 min) con el tampón de lavado (0,05% Tween 20 en PBS), las membranas se incubaron con IgGs anti-conejo/ratón conjugadas con peroxidasa o conjugados a fosfatasa alcalina (dilución 1:4000 en PBS) durante 1 h a temperatura ambiente.

- *Visualización del segundo anticuerpo*: Tras varios lavados (3 x 15 min) con tampón de lavado, el segundo anticuerpo se visualizó mediante dos métodos:

a) Método quimioluminiscente: empleando el compuesto ECL, la membrana se incubó 1 min con la solución de revelado (Immobilon Western Chemiluminescent HRP sustrate, Millipore) según especificaciones del fabricante. Se secaron del exceso de solución y se expusieron a papel fotográfico el tiempo necesario (habitualmente entre 20 seg y 5 min) en un *cassete* en una habitación oscura. Se revelan con reactivos comerciales de fotografía (revelador y fijador Fujifilm).

b) Método calorimétrico: se utilizó un anticuerpo secundario acoplado a fosfastasa alcalina. Luego de los lavados del anticuerpo secundario las membranas se equilibraron con tampón T3 (NaCl 100mM, Tris-HCl 100 mM, $MgCl_2$ 50mM, pH 9,5) durante 10 min. Se preparó el sustrato agregando 35 μl de NBT (Roche) y 35 μl de BCIP (Roche) a 10 ml de tampón T3. Se incubó las membranas en oscuridad durante al menos 5 min. Al visualizar las bandas la reacción se finalizó lavando las membranas con agua destilada.

Determinación de los niveles de mRNA de las subunidades de la GC_{NO} en líneas celulares.

4.1.16 Análisis mediante la técnica de la transcripción reversa y reacción en cadena de la polimerasa (RT-PCR)

4.6.1.1 Extracción de RNA

El RNA total de células C6 y HAPI (sembradas en placas de 60 mm de diámetro) se extrajo con el reactivo Trizol (Gibco, BRL), siguiendo el protocolo sugerido por el fabricante. Tras aspirar el medio de cultivo, se añadió 1 ml del reactivo Trizol sobre la monocapa de células. El lisado celular se agitó varias veces con la pipeta, se recogió en un tubo eppendorf y se incubó a temperatura ambiente 5 min para completar la disociación de complejos núcleo-proteicos. Sobre el lisado se añadieron 200 μl de cloroformo, se agitaron los tubos vigorosamente 15 seg, se incubaron a temperatura ambiente 5 min y se centrifugaron a 12000 g durante 15 min a 4ºC. Tras la centrifugación se recogió la fase acuosa y se precipitó el RNA añadiendo 0,5 ml de isopropanol. Los tubos se centrifugaron a 12000g durante 10 min a 4ºC, el precipitado formado se lavó con 1 ml de etanol 75% y se dejó secar al aire. Una vez evaporado el etanol, el RNA se redisolvió en 30-50 μl de agua estéril libre de RNAsas. La concentración resultante de RNA se determinó por espectrofotometría o por fluorometría utilizando un kit comercial de Invitrogen y un nanoflorímetro (Qubit, Invitrogen), y su calidad se analizó mediante electroforesis en gel de agarosa (1%).

4.6.1.2 RT-PCR

- *Retrotranscripción del RNA*: La reacción de retrotranscripción se llevó a cabo usando la transcriptasa inversa Superscript-II y hexámeros random (ambos de Invitrogen). En un volumen final de 20 μl de tampón de reacción 1x, se añadieron 1 μg de RNA total, 1 U de Superscript-II, la mezcla de dATP/dCTP/dGTP/dUTP (200 mM cada uno), DTT 20 mM y cebadores random 0,3 μg/μl. La reacción de retrotranscripción se llevó a cabo a 42ºC durante 1 h, y se finalizó calentando la mezcla 5 min a 95ºC.

- *PCR*: Mediante PCR se amplificaron las subunidades α_1, $\alpha 2$ y β_1 de la GC_{NO} y la GAPDH (control). La reacción se llevó a cabo en un volumen final de 50 μl que contenía 5 μl de solución de cDNA (producto de la RT), 10 mM Tris-HCl pH 8,3, 50 mM KCl, 1,75 mM $MgCl_2$, 200 mM de cada dNTP, 0,5 U de *taq* DNA polimerasa (Invitrogen) y 400 ng de cebador específico, y se desarrolló como muestra el siguiente esquema:

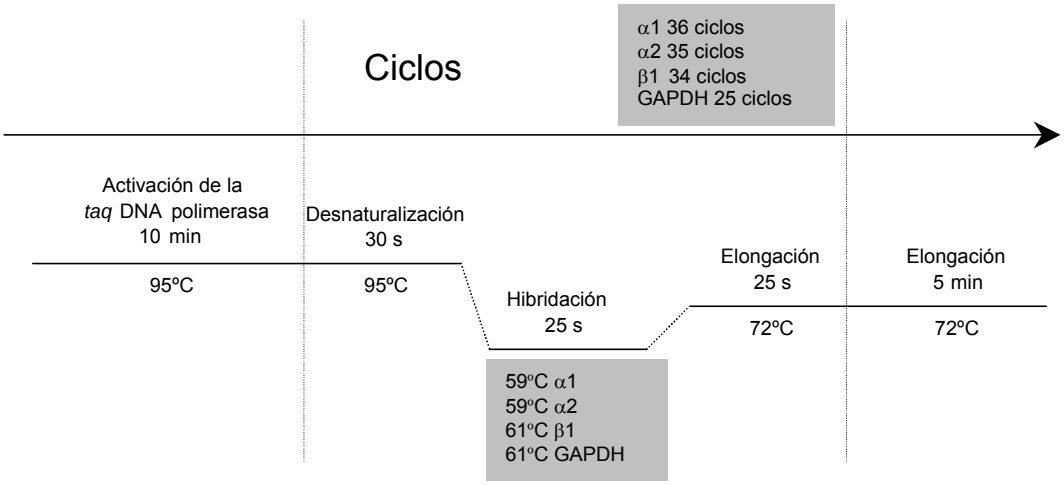

Figura 4: Representación esquemática de los tiempos y temperaturas empleados en la PCR. Los ciclos empleados para la amplificación del cDNA estaban compuestos por 30 s a 95ºC, 25 s a la temperatura de hibridación (59ºC para GC_{NO} $\alpha_{1,2}$ y 61ºC para GC_{NO} β_1 y GAPDH) y 25 s a 72ºC. El número de ciclos fue 25, 34, 36 ó 35 para la GAPDH, la β_1 GC_{NO}, α_1 y α_2 respectivamente.

Los cebadores usados para la amplificación de GC_{NO} α_1 fueron: F1495 (5´-ATAC GGGTGAGGAGATGGGATAACT-3´) correspondiente a las bases 1495-1520 y R1869 (5´-CCTCATTGAACTTCTTGGCTTGC-3´) complementario a las bases 1844-1869. Para amplificar la GC_{NO} β_1 los cebadores usados fueron: F1281 (5´-GCCAAAAGATACGACAATGTGACCA-3´) correspondiente a las bases 1281-1306 y R1561 (5´-TTGCCATCTACTTGAACTTGACCAG-3´) complementaria a las bases 1536-1561. Los cebadores para amplificar la GC_{NO} α_2 fueron, D1 (5'- ACTGCAAATGTACTCGGACTGAAG-3') y el R1 (5' CAGCTCGAAGGACTCGC TCATTCT-3'). La amplificación de la GAPDH se uso para controlar la diferencia de eficiencia en la síntesis de cDNA entre distintas muestras. Los cebadores empleados fueron: *forward* 5´-GCCAAGTATGATGACATCAAGAAG-3´, y *reverse* 5´-TCCAG GGGTTTCTTACTCCTTGGA-3´.

Los productos de la PCR se sometieron a electroforesis en gel de agarosa (agarosa 2%-bromuro de etídio 0,5 mg/ml) y se visualizaron con luz ultravioleta. Según estudios previos del laboratorio, la amplificación del cDNA resultó lineal entre 33-37 ciclos para la GC_{NO} α_1, entre 32 y 36 ciclos para la GC_{NO} β_1, entre 30 y 35 ciclos para la GC_{NO} α_2 y entre 20 y 26 ciclos en el caso de la GAPDH.

4.1.17 Análisis por Real–Time PCR (cuantitativa) de los niveles de GC_{NO} β1

La técnica de PCR a tiempo real permite cuantificar el contenido de un RNA o DNA determinado dentro de una muestra. En este trabajo se ha empleado esta técnica para comprobar el silenciamiento del mensajero de la GC_{NO} β1 (ver apartado 4.8).

El RNA total y la reacción de trascripción reversa de las células transfectadas se realizó tal como se ha descrito previamente en los apartados 4.7.1.1 y 4.7.1.2. La real-time PCR se llevó a cabo empleando el kit comercial de Roche LightCycler FastStart DNA Master Plus SYBR Green I según las indicaciones del proveedor con mínimas modificaciones. Este fluoróforo se une a DNA doble cadena a medida que se va sintetizando, así pues la incorporación del SYBR green se puede cuantificar a cada momento de la reacción pudiéndose calcular una curva de concentración del DNA estudiado. La reacción se llevó a cabo en un volumen final de 10 μl, conteniendo 2,5 μl de cDNA, 1 μl de la mezcla de primers, 2 μl de la mezcla de reacción 5x del kit y el resto de H_2O. Previamente, se realizó una recta patrón de la GC_{NO} β1 en C6 que fue utilizada para interpolar las muestras y calcular los valores exactos de moléculas de cDNA. Los primers empleados para la GC_{NO} β1 son los mismos que se utilizaron para realizar la PCR convencional y los ciclos fueron un precalentamiento a 10 min a 95ºC, 45 ciclos de 10 seg a 95ºC, 10 seg a 61ºC y 20 seg a 70ºC, seguido de un ciclo de 15 seg a 70ºC y un ciclo final de 30 seg a 40ºC. El equipo utilizado fue un termociclador LightCycler 2.0 de Roche.

Los datos obtenidos para cada muestra fueron normalizados respecto de la amplificación de la GAPDH. Los primers empleados para le GAPDH fueron: foward, 5'-GCCAAGTAGAC ATCAAGAAG-3', y reverse, 5'-TCCAGGGGTTTCTTACTCCTTGGA-3'. Se consideró aceptable un error no superior al 5 % y una diferencia de no más de medio ciclo entre los duplicados de las muestras analizadas por real-time-PCR.

Transfecciones de células de glioma (C6) con las subunidades de la GC_{NO}

4.1.18 Construcciones plasmídicas.

El plásmido p-β1 cedido por el Dr. Garthwaite conteniendo la secuencia del mRNA de la subunidad β1 de la GC_{NO} fue utilizado como molde para amplificar el cDNA mediante PCR para así clonarlo dentro de un plásmido pEGFP que contiene el gen que codifica para una proteína verde fluorescente y así poder visualizar su localización celular por fluorescencia dentro de las células transfectadas. Los cebadores utilizados para la clonación fueron diseñados de manera tal que contuvieran dentro de su secuencia un sitio de corte para dos enzimas de restricción (*MroI y XbaI*). Los cebadores fueron: GC_{NO} β1-directo (5′-TCCGGAATGTACGGTTTTGTG-3′) y GC_{NO} β1-reverso (5′-TCTAGACATTCAGTTTCATCCT G-3′).

La reacción para realizar la clonación fue preparada conteniendo 5 μl del tampón de reacción (Roche), 4 μl de una mezcla de dNTPs (2.5 mM, Roche), 1 μl de cada primer (50 μM),

5 μl del pEYFP-β1 y 1,5 unidades de Taq polimerasa (high expand, Roche) y se ajustó hasta un volumen final de 50 μl con agua MilliQ estéril. La reacción de PCR fue realizada en un equipominicycler ^{tm} PCR, de acuerdo al siguiente protocolo: 1-desnaturalización a 94ºC 3 min; 2- 94ºC 30 seg; 3- 50ºC 30 seg y 4- 68ºC 2 min, los pasos del 2 al 4 se repitieron 35 veces; finalmente ser realizó un ciclo a 68ºC por 7 min. Los productos de PCR fueron corridos electroforéticamente en un gel de agarosa y las bandas recuperados mediante un kit de extracción del DNA de los geles de Qiagen. El DNA extraído fue clonado dentro de un plásmido pEGFP-C1 (Clontech) predigerido con las mismas enzimas de restricción *Mro*I y *Xba*I.

Una vez cortados tanto el plásmido como la secuencia clonada se ligaron utilizando 1 μl de ligasa (Roche) durante 1,5 hs. Una vez terminada la ligación se procedió a amplificar el plásmido utilizando bacterias *E. coli* competentes (que permiten la incorporación de plásmidos extraños), y se cultivaron en placas conteniendo medio LB con antibióticos (el plásmido confiere resistencia a kanamicina). Las placas se incubaron durante 18-24 hs en un incubador a 37ºC. Paralelamente, se transformaron bacterias competentes con los plásmidos de las otras subunidades de la GC_{NO} (pEYPF-α1 y pEYFP-α2) y con el plásmido pEGFP sin inserto que posteriormente será empleado como control de transfección. Se seleccionaron varios clones de cada transformación y se subcultivaron en placas con antibiótico y en medio líquido para disponer de una buena concentración del DNA plasmídico. En el caso de la subunidad β1 varios de estos clones se enviaron al Servicio Veterinario de Genética Molecular (Fac. de Veterinaria, UAB) para determinar si la secuencia del DNA era correcta y se encontraba correctamente insertada y orientada para garantizar la expresión de la proteína en las células.

4.1.19 Transfecciones

Con el fin de determinar la localización subcelular de las diferentes subunidades de la GC_{NO}, se llevó a cabo la transfección de los plásmidos conteniendo las secuencias codificantes de las tres subunidades en cultivo de células C6 crecidas sobre cubreobjetos de 24x24 mm en de placas de 35 mm. Las células entre el 60-80% de confluencia se transfectaron con polietilenimida (PEI) lineal de 25 KDa (Polysciences) y 1 μg de DNA correspondiente a los plásmidos pEGFP-β1 GC_{NO}, pEGFP como control de transfección, o con pEYFP-α1 GC_{NO} y pEYFP-α2 GC_{NO} para las subunidades α en una relación entre el DNA y el PEI de 1:10 (μg de DNA/ μl de PEI).

-Protocolo:

Cuando las células se encontraban entre el 60-80% de confluencia, se incubaron con DMEN-10% FCS fresco por lo menos durante 2 hs antes de agregar el DNA. El DNA (1 µg) se diluyó en un volumen de DMEM sin suero de 10 µl y el PEI en una relación 1:10, en un volumen final de 100 µl en DMEM sin suero. La mezcla se agitó rápidamente durante 5 min y se incubó durante 10 min a temperatura ambiente. Finalmente, se agregó a las células de manera circular generando un espiral sobre la monocapa. A continuación, las células fueron incubadas durante 24 hs a 37ºC en una atmósfera húmeda de 90% aire-10% CO_2. La eficiencia de transfección fue de entre un 25 y un 40% para las tres subunidades. Tras este período, las células fueron fijadas con 4% PFA y analizada la localización celular en un microscopio de fluorescencia (Nikon) o por microscopía confocal (confocal láser scanning microscope Leica TCS SP2 AOBS). En el caso de ser utilizadas para realizar observaciones *in vivo* por "time lapse" con microscopio confocal, el inóculo se mantuvo por 24 hs y se observaron al microscopio otras 18 hs manteniendo las condiciones de temperatura, humedad y CO_2. En estos casos como marcador de DNA se utilizó Hoechst 33342 que no resulta tóxico para las células sin fijar.

Silenciamiento de la subunidad β1 de la GC_{NO} en células C6 por RNA de interferencia (siRNA)

4.1.20 Preparación de los híbridos doble cadena de los siRNA (ds-siRNA)

El diseño de las secuencias de los siRNA para las subunidad β1 de la GC_{NO} fue realizado por la empresa Dharmacon y obtenidos en Invitrogen. Las secuencias para la subunidad β1 fueron: Marco de lectura 1098- sentido siRNA: 5' CCUGGACGACCUAACAAGA-dTdT-Fluoresceína y el complementario antisentido siRNA: 5' UCUUGUUAGGUCGUCCAGG-dTdT. Las secuencias controles utilizadas para transfectar las células fueron: sentido siRNA: 5' CCUG GACGACCUAAGUAGA-dTdT-Fluoresceína y la complementaria anti- sentido siRNA: 5' UCUA CUUAGGUCGUCCAGG-dTdT.

Las secuencias fueron hibridadas según el protocolo descrito por Vickers y col (Vickers et al., 2003). Se incubaron 30 µl de la solución patrón 50 µM de cada siRNA (sentido y antisentido) y 15 µl de una solución de hibridación 5X (100 mM acetato de potasio, 30 mM Hepes-KOH, pH 7,4 y 2 mM de acetato de magnesio). La mezcla se calentó durante 1 min a 90ºC y luego se incubó 1 h a 37ºC utilizando el termociclador de PCR. Los híbridos doble cadena de siRNA (ds-siRNA) fueron almacenados a -20ºC hasta su utilización. La confirmación

de la presencia de los híbridos se realizo a través de una electroforesis en gel de agarosa al 2%, utilizando como control los siRNA de cadena simple.

4.1.21 Transfección de los ds-siRNA

Los ds-siRNA se transfectaron en células C6 que se habían sembrado el día anterior a una densidad de $2x10^5$ células por pocillo en placas de 12 pocillos y se utilizaron cuando se encontraban entre un 50 y 70% de confluencia. Para transfectar se utilizó la oligofectamina (Invitrogen 12252-001) siguiendo las especificaciones del fabricante. Para la solución de tranfección se preparó una solución (A) conteniendo 5 μl del stock 20 μM del duplex de siRNA y 85 μl de medio sin suero y sin antibióticos mezclados vigorosamente y una solución (B) que contenía entre 1-3 μl de oligofectamina en un volumen final de 10 μl con un medio sin suero ni antibióticos. Finalmente, las soluciones A y B se mezclaron y se incubaron durante 20 min a temperatura ambiente antes de ser añadidas a las células.

Tras aspirar el medio, se añadieron 400 μl de medio sin suero por pocillo, se adicionaron 100 μl de la mezcla de A y B y se incubaron durante 4 hs a 37ºC, 10%-CO_2. Pasado este período, se añadieron 250 μl de medio completo (con suero y antibiótico concentrado 3 veces) sin quitar el medio de transfección y se incubaron entre 24 y 48 hs. Tras la transfección, algunos pocillos fueron procesados por real-time PCR para confirmar la disminución del mRNA. El estudio de la función producida por el silenciamiento fue realizado mediante estudios de proliferación celular (EZ4U) y analizando el ciclo celular por citometría de flujo (ver apartados 4.10 y 4.11)

Análisis de proliferación celular (EZ4U).

Para estudiar los cambios en la proliferación celular y la muerte celular producidos por el silenciamiento de la β1 en C6 se empleó un kit comercial no radioactivo (EZ4U, Biomédica Gruppe) según las indicaciones del fabricante adaptándolo a placas de 12 pocillos. La absorbancia fue medida durante 2 hs a intervalos de 30 min, a una longitud de onda de 492 nm y también de 620 nm como valor de referencia del ruido de fondo, paralelamente en las células transfectadas con los siRNA y sin transfectar.

Análisis del ciclo celular mediante citometría de flujo

La cuantificación del contenido de DNA permite determinar la distribución de una población celular a lo largo de las distintas fases del ciclo celular. La distribución celular de una población se analiza por citometría de flujo utilizando colorantes de DNA que incrementan su

fluorescencia tras su unión al ácido nucleico. Una representación esquemática del análisis del ciclo celular en una población de linfocitos T se aprecia en la figura 5

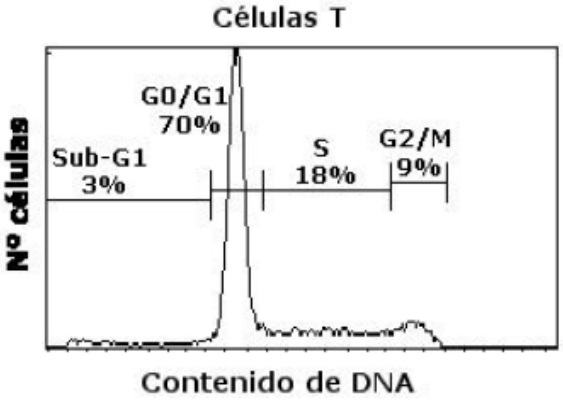

Figura 5: Análisis esquematico del ciclo celular por citometría de flujo de una población de linfocitos T.

En este trabajo se utilizó el ioduro de propídio como colorante de DNA. Para cuantificar la proporción de células en cada una de las fases del ciclo celular utilizamos el software ModFit LT. Las muestras para citometría de flujo se prepararon de la siguiente manera:

- Protocolo:

Se utilizaron células transfectadas con los siRNA durante 48 hs. Tras lavar las monocapas con DMEM sin suero se levantaron por tripsinización suave (0,25%) y se fijaron con metanol 80% durante al menos 2 hs a -20ºC. Las células se tiñeron con ioduro de propidio (50 mg/ml) durante 30 min a 4ºC. Se pasaron a través del citómetro (FACSCalibur-Beckton Dickinson) y se analizaron con el software CellQUEST-Pro y se ajustaron los porcentajes con el modelo de análisis del ModFit LT. Los resultados se graficaron con el programa SigmaPlot y el análisis estadístico se realizó aplicando un ANOVA de un factor (no paramétrico).

Estudio morfológico de los núcleos de células C6 mediante el análisis de estado de condensación de la cromatina

Con el fin analizar la posible función de la localización nuclear de la subunidad β1 de GC_{NO} se llevó a cabo un estudio sobre la condensación de la cromatina en la línea celular C6 según el método descrito por Collas y col. (1999).

4.1.22 Obtención de extracto mitótico de células C6

Para obtener los extractos mitóticos se utilizó el método descrito por Collas y col. (1999). Las células fueron sincronizadas manteniéndolas durantes 48 hs en ausencia de suero y posteriormente se estimuló la proliferación añadiendo suero y se arrestaron en mitosis con colcemid (0,005%v/v) (desestabilizador de microtúbulos) durante 18 hs. Las células arrestadas en mitosis se lavaron una vez en PBS frío y una vez en 20 volúmenes de tampón de lisis frío (20 mM Hepes, pH. 8.2; 5 mM $MgCl_2$, 10 mM EDTA, 1mM DTT) conteniendo 20 µg/ml citocalasina B , inhibidores de proteasas y fosfatasas (Roche, SA). Las células se centrifugaron a 800 g durante 10 min y el pellet celular fue resuspendido en 1 volumen de tampón de lisis he incubado durante 30 min en hielo. Las células fueron homogenizadas por sonicación 2 veces durante 2 min en hielo y el lisado se centrifugó a 10000 g durante 15 min a 4ºC. El sobrenadante fue aclarado por centrifugación a 100000g durante 1h a 4ºC. La fracción soluble es lo que llamamos “extracto mitótico” que se alicuotó y almacenó a -80ºC hasta su uso.

4.1.23 Preparación de núcleos interfásicos

Células C6 confluentes sincronizadas fueron cosechadas, lavadas con PBS, sedimentadas a 400 g y resuspendidas en 20 volúmenes de tampón N (10 mM Hepes, pH. 7,5, 2 mM $MgCl_2$, 250 mM sacarosa, 25 mM KCl, 1 mM DTT e inhibidores de proteasas) conteniendo 10 µg/ml citocalasina B. Tras 30 min de incubación en hielo, las células fueron homogenizadas en frío manualmente en un homogenizador de vidrio de 5 ml entre 140 y 170 veces. Los núcleos fueron sedimentados a 400 g por 10 min a 4ºC, lavados 2 veces con tampón N y finalmente resuspendidos en este tampón y centrifugados a 400 g. Todos los núcleos recolectados se encontraban morfológicamente intactos según lo observado en un microscopio de contraste de fase y mediante fluorescencia tiñéndolos con DAPI. Los núcleos fueron conservados a -80ºC hasta su posterior uso en tampón N conteniendo 70% de glicerol.

4.1.24 Tratamiento de los núcleos con el anticuerpo anti-GC_{NO} β1

Los núcleos purificados de C6 (2000 núcleos/µl) fueron permeabilizados con 500 µl del tampón N conteniendo 0.75 µg/ml de L-A-liso-fosfatidilcolina de tipo I (SIGMA) durante 15 min a temperatura ambiente. El exceso de fosfatidilcolina fue eliminado añadiendo a la preparación 1 ml de BSA al 3% en tampón N he incubándolo durante 5 min en hielo antes de sedimentarla y lavarla con tampón N. Los núcleos fueron resuspendidos a una concentración de 2000 núcleos/µl en 100 µl de tampón N conteniendo 2.5 µg del anticuerpo anti-GC_{NO} β1 o 2.5 µg de un suero pre-inmune de conejo (IgGs). Luego de 1 h de incubación en hielo en agitación fuerte,

los núcleos fueron sedimentados a 500 g en una solución de sacarosa 1 M por 20 min y dejados en tampón N en hielo hasta que fueron utilizados. La entrada del anticuerpo al núcleo fue corroborada mediante técnicas de inmunofluorescencia.

4.1.25 Análisis del estado de condensación de la cromatina en núcleos inmunodepletados de la subunidad β1

El método de condensación de la cromatina fue llevado a cabo según describen Collas y colaboradores (1999) con algunas modificaciones.

La reacción de condensación de la cromatina se llevó a cabo mezclando 25 μl del extracto mitótico, 5 μl de la suspensión de núcleos (~2000 núcleos) y 2 μl de un sistema generador de ATP (1 mM ATP, 10 mM creatina fosfato, 25 μg/ml creatina quinasa). La reacción se inició con la adición del sistema generador de ATP y se incubó durante 1:30 h a 30ºC. El estado de condensación de la cromatina fue analizada tiñendo los núcleos con 1 μl de Hoechst 33342 (0.1 μg/ml) y observándolo al microscopio. La cromatina se consideró condensada cuando los núcleos presentaban una forma irregular o una morfología compacta, distinguiéndose en algunos casos cromosomas diferenciados o fragmentos de cromosomas. En algunos casos el extracto mitótico fue preincubado con el anticuerpo de la $GC_{NO}\beta 1$ durante 1 h antes de comenzar la reacción para eliminar la proteína del extracto, o tratado con un inhibidor específico de la GC_{NO} (ODQ 1mM, SIGMA) para analizar si los efectos eran debidos a una perdida de la actividad enzimática. El porcentaje de condensación de la cromatina fue calculado como la relación entre la masa de cromatina condensada por número de núcleos examinados (100 núcleos por tratamiento).

Otros métodos

4.1.26 Determinación de la concentración de nitritos

Como medida de la formación de NO se determinó la concentración de nitritos en los medios de cultivos utilizando la reacción de Griess (Baltrons and García 1999). Después de los correspondientes tratamientos o días en cultivo, 150 μl del medio de cultivo se pasaron a una placa de 96 pocillos, donde se mezclaron con el mismo volumen de solución de reacción: sulfanilamida 0,5% (p/v), acido fosfórico 2,5% (v/v) y NEDA 0,05% (p/v). Tras 30 min de incubación a temperatura ambiente se leyó la absorbancia a 540 nm. La concentración de nitritos acumulados se calculó utilizando soluciones de nitrito sódico de concentraciones conocidas (0 – 100 μM) procesadas en paralelo como estándares.

4.1.27 Valoración de la concentración de proteínas.

Para determinar la concentración de proteínas de los homogenados de cultivos celulares o de tejido se utilizó el método de Bradford (1976) utilizando el reactivo comercial de “Bio-Rad protein Assay” (Bio-Rad) según indicaciones del fabricante. Las muestras de fracciones de membrana fueron analizadas mediante la técnica de Lowry y col. (1951). Para ello, los cultivos celulares se lavaron 2 veces con 1 ml del tampón de incubación y se dejaron durante 18-20 hs con NaOH 1 N. Después de verificar que la monocapa de células se había levantado y disgregado, se determinó la cantidad de proteína. En ambos casos se utilizó como patrón la albúmina bovina.

5 Resumen Trabajo 1

La guanilil ciclasa soluble (GC_{NO}) es la principal diana del NO en el SNC y el GMPc el mediador de sus importantes acciones neuroreguladoras. La GC_{NO} está presente en la mayoría de las células de mamíferos como un heterodímero compuesto por una subunidad α y una β. Dos isoformas de cada subunidad, α1-2 y β1-2, han sido clonadas. En este trabajo, hemos estudiado la distribución anatómica de las células que expresan el mRNA de estas subunidades en cerebro de rata y mono mediante hibridación *in situ*, utilizando como sondas oligonucleótidos marcados con ^{33}P complementarios al mRNA de las distintas subunidades. Hemos encontrado que el mRNA de la subunidad β1 es el más abundante en ambas especies y su expresión es máxima en caudado-putamen, núcleo accumbens, tubérculo olfatorio, corteza cerebral, giro dentado y capas CA del hipocampo, varios núcleos talámicos e hipotalámicos, amígdala, núcleos motores del tronco encefálico y células de Purkinje y granulares de cerebelo. Por el contrario, el mRNA de la subunidad β2 no pudo ser detectado con las sondas diseñadas en ninguna de las dos especies.

Las subunidades α presentan una distribución de los mRNA similar en ambas especies, con pequeñas diferencias, siendo máximos los niveles de expresión en el sistema límbico y en el caudato-putamen. Las mayores diferencias entre las especies se observaron en la distribución laminar del mRNA de la subunidad α1. Mientras que en la rata la expresión es máxima en capas externas corticales, en mono, los niveles máximos se detectan en las capas internas. La subunidad α2 se encuentra homogéneamente distribuida en ambas especies en las capas cortiales. Por otro lado, también existe diferencia en cuanto a la abundancia relativa de cada subunidad. Mientras que en mono el mRNA de la subunidad α1 es más ubicuo, en la rata lo es el de la subunidad α2.

Una alta expresión de las tres subunidades estudiadas se observó en los ganglios basales, el sistema olfatorio, el hipocampo y el cortex cerebral mientras que en otras regiones fue posible detectar niveles elevados del mRNA de la subunidad β1 y sin embargo los mRNA de las subunidades α eran muy bajos o indetectables. Esta situación se puede apreciar en la rata en las islas de Calleja, la mayoría de los núcleos talámicos estudiados y en el colículo superior. En mono son los núcleos talámicos y el claustrum los lugares donde existen niveles elevados del mRNA de β1 y muy bajos o indetectables de las subunidades α.

En conclusión, hemos encontrado que los mensajeros de los dos heterodímeros de la GC_{NO} que ocurren naturalmente, el $\alpha1\beta1$ y el $\alpha2\beta1$, que poseen las mismas características cinéticas y farmacológicas, se encuentran ampliamente expresados en cerebro de mono y en

cerebro de rata. En regiones como los ganglios basales, el sistema olfatorio y el sistema límbico el patrón de distribución es similar entre ambas especies. Estas semejanzas sugieren que en primates, tal como ocurre en cerebro de roedores, el sistema de señalización NO-GMPc va a estar probablemente también involucrado en la regulación de importantes funciones cerebrales como son la plasticidad sináptica, el procesamiento sensorial y el comportamiento.

THE JOURNAL OF COMPARATIVE NEUROLOGY 500:942–957 (2007)

Species Differences in the Localization of Soluble Guanylyl Cyclase Subunits in Monkey and Rat Brain

P. PIFARRÉ,[1] A. GARCÍA,[1]* AND G. MENGOD[2]
[1]Institut de Biotecnologia i Biomedicina V. Villar Palasí and Departament de Bioquímica i Biologia Molecular, Universitat Autònoma de Barcelona, Spain
[2]Departament de Neuroquímica, Institut d'Investigacions Biomèdiques de Barcelona, CSIC-IDIBAPS, Barcelona, Spain

ABSTRACT

Nitric oxide (NO) exerts most of its physiological effects through activation of a predominantly soluble guanylyl cyclase (sGC). In mammalian cells sGC exists as a heterodimer of α and β subunits. Currently, four subunits (α1, α2, β1, and β2) have been characterized. We used in situ hybridization with subunit-specific ^{33}P-labeled oligonucleotide probes to compare the anatomical distribution of sGC subunit mRNAs in rat and monkey brains. Message for all subunits except β2 was detected in both species. The sGC subunit showing the highest expression and widest distribution was β1. High expression for all subunits was found in basal ganglia, olfactory system, hippocampus, cortex, and cerebellum. Minor species differences in the relative distribution of α subunits were observed. In general, the α1 message was more prominent in monkey brain and the α2 message in rat brain. This was more evident in limbic areas and cerebellar cortex. Some differences were also observed in subunit laminar distribution in cerebral cortex. The limited species differences in sGC subunit distribution suggest that in primates, as occurs in rodents, the NO-cGMP signaling pathway will be involved in important brain functions such as memory formation, sensory processing, and behavior. J. Comp. Neurol. 500:942–957, 2007.

Indexing terms: in situ hybridization; cGMP; NO; sGC subunits

The best-characterized target of NO is the predominantly soluble form of the enzyme guanylyl cyclase (sGC). Activation of this enzyme by NO results in the formation of cyclic GMP (cGMP), the mediator of the important physiological actions of NO in cardiovascular and nervous tissues (Moncada and Higgs, 1991; Garthwaite and Boulton, 1995). In rodent central nervous system (CNS), the NO-sGC-cGMP pathway has been implicated in short- and long-term modulation of synaptic efficacy (Haley and Schuman, 1994; Zhuo and Hawkins, 1995; Holscher, 1997) and appears to play a key role in specific forms of memory formation and behavior, visual and sensory processing, and neuroendocrine secretion (Garthwaite and Boulton, 1995; Zhang and Snyder, 1995; Cudeiro and Rivadulla, 1999; Prickaerts et al., 2004). The involvement of the NO-cGMP cascade in multiple aspects of neural development is also well documented (Bicker, 2001; Contestabile and Ciani, 2004).

In mammalian cells, sGC exists as an obligate heterodimer of one α and one β subunit with a prosthetic heme group that is the binding site for NO (Denninger and Marletta, 1999; Koesling et al., 2004). Two types of each subunit have been cloned (α1-2, β1-2). When coexpressed, all four possible combinations of α and β subunits exhibit NO-activated GC activity, but that of α1β1 and α2β1 is much higher than that of β2-containing heterodimers (Gibb et al., 2003). Furthermore, only the β1-containing isoforms have been shown to exist at the protein level (Russwurm et al., 1998). In rodents, sGC α1β1 is the most ubiquitous isoform; however, sGC α2β1 occurs predominantly in brain (Mergia et al., 2003). Recent evidence

Grant sponsor: Ministerio de Educación y Ciencia, Spain; Grant numbers: SAF2003-02083 (to G.M.) and SAF2004-01717 (to A.G.); Grant sponsor: Fellowship FPU 2000 to P. Pifarré.

*Correspondence to: Agustina García, Institut de Biotecnologia i Biomedicina V. Villar Palasí, Universitat Autònoma de Barcelona, 08193, Bellaterra, Spain. E-mail: agustina.garcia@uab.es

Received 22 February 2006; Revised 17 July 2006; Accepted 11 October 2006

DOI 10.1002/cne.21241

Published online in Wiley InterScience (www.interscience.wiley.com)..

indicates that the α2 subunit mediates the membrane association of the α2β1 isoform via interaction with a PDZ domain of the postsynaptic scaffold protein PSD-95 (Russwurm et al., 2001). Binding to PSD-95 may locate this isoform in close proximity to NO synthase 1 (NOS-1) and the NMDA receptor, suggesting a mechanism for the highly efficient stimulation of NO-dependent cGMP formation by glutamate in brain cells and the implication of the α2β1 heterodimer in NMDA receptor regulation of development and synaptic plasticity. In fact, expression of the α2 subunit in rat brain has been linked to cerebral development (Bidmon et al., 2004) and shown to be upregulated by NMDA-receptor activation during cerebellar granule cell maturation in vitro (Jurado et al., 2003).

The study of the anatomical distribution of the different sGC subunits in brain has been hampered by the lack of specific antibodies to perform immunocytochemical studies. Very early studies showed the presence of sGC immunoreactivity in neuronal populations and some glial cells in a few rat brain regions but did not provide information about sGC subunit distribution (Ariano et al., 1982; Nakane et al., 1983). A recent study by Ding et al. (2004), using a β1-specific antibody and an antibody that recognizes both α subunits, described the presence of cells strongly immunopositive in neostriatum, olfactory tubercle, and supraoptic nucleus. A high degree of cellular colocalization was shown by double-labeling experiments in most brain regions with the exception of the cerebellar cortex, where Purkinje cells and Bergmann glia were positive for both subunits, whereas granule cells and interneurons of the molecular layer stained strongly for β1 but weakly for α subunits.

Message for all four sGC subunits has been detected in rodent brain by reverse-transcriptase polymerase chain reaction (RT-PCR) (Gibb and Garthwaite, 2001; Mergia et al., 2003) but in situ hybridization studies have demonstrated expression of α1, α2, and β1, but not β2 (Gibb and Garthwaite, 2001). Matsuoka et al. (1992) first described the localization of β1 mRNA in discrete areas in the rat brain. Significant signals were shown in cerebral cortex, striatum, hippocampus, olfactory system, inferior and superior colliculus, locus coeruleus, and cerebellar Purkinje cells. Furuyama et al. (1993) confirmed the widespread distribution of β1 subunit mRNA in rat brain and described a distinct and more restricted localization of α1 mRNA. More recently, Gibb and Garthwaite (2001) compared the distribution of sGC α1, α2, and β1 message in parasagittal sections from 8-day-old rat brains and found notable differences in the distribution of α subunits, suggesting a differential distribution of α1β1 and α2β1 heterodimers. A detailed comparison of the localization of the three sGC subunit mRNAs in coronal sections from adult rodent brain is lacking.

Little information is available on the anatomical distribution of sGC subunits in primate brain. In humans, Budworth et al. (1999) showed by dot blot analysis higher β1 than α1 mRNA levels in all regions studied. Higher expression of β1 was also reported at the protein level but a good correlation was found in the regional distribution of these subunits (Ibarra et al., 2001). Message for the α2 subunit was detected in human brain (Budworth et al., 1999) but nothing is known about its regional distribution.

Given the important roles that the NO-cGMP signaling pathway has been shown to play in rodent brain and the

Abbreviations

3N	oculomotor nucleus
7N	facial nucleus
Acb	accumbens nucleus
Amy	amygdala
B	basal nucleus of Meynert
BL	basolateral amygdaloid nucleus
CA1	field CA1 of hippocampus
CA2	field CA2 of hippocampus
CA3	field CA3 of hippocampus
CA4	field CA4 of hippocampus
cal	calcarine sulcus
Cd	caudate
Cg	cingulate cortex
Cl	claustrum
CPu	caudate-putamen
DG	dentate gyrus
DPCx	dorsal parietal cortex
DR	dorsal raphe
ECx	entorhinal cortex
Gpl	globus pallidus pars lateralis
Gpm	globus pallidus pars medialis
GL	granular cell layer
hil	hilus of the dentate gyrus
Hp	hippocampus
IC	inferior colliculus
ICj	islands of Calleja
InsCx	insular cortex
IP	interpeduncular nucleus
La	lateral amygdaloid nucleus
Lat	lateral (dentate) cerebellar nucleus
LC	locus coeruleus
LL	lateral lemniscus
LSO	lateral superior olive
LTg	lateral tegmental area
MA3	medial accessory oculomotor nucleus
MD	mediodorsal thalamic nucleus
Med	medial (fastigial) cerebellar nucleus
MG	medial geniculate nucleus
MHb	medial habenular nucleus
MM	medial mammillary nucleus
Mo5	motor trigeminal nucleus
ML	molecular layer
opt	optic tract
PAG	periaqueductal gray
PCx	parietal cortex
Pi	pineal gland
Pir	piriform cortex
PK	Purkinje cell layer
Pn	pontine nuclei
Pr5	principal sensory trigeminal nucleus
Pul	pulvinar nucleus
PrS	presubiculum
Pu	putamen
Rt	reticular thalamic nucleus
SC	superior colliculus
SN	substantia nigra
SSCx	somatosensorial cortex
STh	subthalamic nucleus
SuG	superficial gray layer of the superior colliculus
TCx	temporal cortex
TT	taenia tecta
Tu	olfatory tubercle
VA	ventral anterior thalamic nucleus
VCx	visual cortex
V1Cx	visual cortex 1
V2Cx	visual cortex 2
V4Cx	visual cortex 4
VMH	ventromedial hypothalamic nucleus
VP	ventral posterior thalamic nucleus
VPTh	ventral posterior thalamic nucleus
wm	white matter
ZI	zona incerta

potentially different involvement of sGC α1β1 and α2β1 isoforms in these activities, we thought it of interest to compare the anatomical distribution of sGC subunits in primates and rodent brain. We report here the detailed distribution of sGC subunit mRNAs in monkey and rat brains determined by in situ hybridization using ^{33}P-labeled oligonucleotide probes. A preliminary account of this work has been published in abstract form (Pifarre et al., 2005).

MATERIALS AND METHODS

Animals and tissues preparation

Adult male Wistar rats (n = 4; 200–300 g) were purchased from Iffa Credo (Lyon, France). The animals were killed by decapitation, brains were removed quickly, frozen on dry ice, and kept at −20°C. Monkey brains (n = 5) (*Macaca fascicularis,* age 3–7 years old, weight range 2.4–2.7 kg, mean postmortem delay 1 hour) were used. The animals were sacrificed by administration of an overdose of sodium pentobarbital. All the procedures conformed to the European Communities Council directive of November 24, 1986 (86/609/EEC). Tissue sections, 20 μm thick, were cut using a microtome-cryostat (Microm HM500 OM, Walldorf, Germany), thaw-mounted onto APTS (3-aminopropyltriethoxysilane; Sigma, St Louis, MO)-coated slides, and kept at −20°C until use.

Hybridization probes

For the detection of sGC subunit mRNAs oligodeoxyribonucleotides were used that were complementary to bases 556–600 and bases 738–755 (α1 subunit, GenBank acc. no. M57405), bases 675–711 and 713–757 (α2 subunit, GenBank acc. no. NM_023956) bases 70–114 and 196–240 (β1 subunit, GenBank acc. no. M22562), and bases 2154–2198 and 306–350 (β2 subunit, GenBank acc. no. NM_012770) were used. These regions were chosen because they share no similarity with other subunits of guanylyl cyclases. Evaluation of the oligonucleotide sequences with the basic local alignment search tool of EMBL and GenBank databases indicated that the probes do not present any significant similarity with mRNAs other than their corresponding targets in the rat.

Oligonucleotides were synthesized and high-performance liquid chromatography (HPLC)-purified by Isogen Bioscience BV (Maarsden, The Netherlands). They were individually labeled at their 3′-end using [α-^{33}P]dATP (3000 Ci/mmol; New England Nuclear, Boston, MA) and terminal deoxynucleotidyltransferase (Oncogene Research Products, San Diego, CA), purified using QIAquick Nucleotide Removal Kit (Qiagen, Hilden, Germany).

In situ hybridization histochemistry procedure

The protocol used is based on a previously described procedure (Tomiyama et al., 1997). Briefly, frozen tissue sections were brought to room temperature, fixed for 20 minutes at 4°C in 4% paraformaldehyde in phosphate-buffered saline (PBS; 1× PBS: 8 mM Na_2HPO_4, 1.4 mM KH_2PO_4, 136 mM NaCl, 2.6 mM KCl), washed for 5 minutes in 3× PBS at room temperature, twice for 5 minutes each in 1× PBS, and incubated for 2 minutes at 21°C in a solution of predigested pronase (Calbiochem, San Diego, CA) at a final concentration of 24 U/mL in 50 mM Tris-HCl, pH 7.5, 5 mM EDTA. The enzymatic activity was stopped by immersion for 30 seconds in 2 mg/mL glycine in 1× PBS. Tissues were finally rinsed in 1× PBS and dehydrated through a graded series of ethanol. For hybridization, radioactively labeled and nonradioactively labeled probes were diluted in a solution containing 50% formamide, 4× SSC (1× SSC: 150 mM NaCl, 15 mM sodium citrate), 1× Denhardt's solution (0.02% Ficoll, 0.02% polyvinylpyrrolidone, 0.02% bovine serum albumin), 10% dextran sulfate, 1% sarkosyl, 20 mM phosphate buffer pH 7.0, 250 μg/mL yeast tRNA, and 500 μg/mL salmon sperm DNA. The final concentration of radioactive probes in the hybridization buffer was ≈1.5 nM. Tissue sections were covered with hybridization solution containing the labeled probes, overlaid with Nescofilm coverslips (Bando Chemical, Kobe, Japan), and incubated overnight at 42°C in humid boxes. Sections were washed four times (45 minutes each) in 0.6 M NaCl, 10 mM Tris-HCl pH 7.5 at 60°C. The sections were then dipped in 70% and 100% ethanol, air-dried, and exposed to Biomax-MR (Kodak, Rochester, NY) films for 3–5 weeks at –70°C with intensifying screens. For microscopic localization, hybridized sections were dipped into Ilford K5 (Mobberly, Chesire, UK) nuclear emulsion diluted 1:1 with distilled water. They were exposed in the dark at 4°C for 4–6 weeks, and finally developed in Kodak D19 for 5 minutes and fixed in Ilford Hypam fixer.

Analysis of results

Tissue sections were examined in bright- and darkfield in a Wild 420 macroscope (Leica, Heerbrugg, Germany) equipped with bright- and darkfield condensers for transmitted light and with epi-illumination. A Darklite illuminator (Micro Video Instruments, Avon, MA) was used to improve the visualization of autoradiographic silver grains and capture of darkfield images.

Preparation on figures

Hybridized tissue section images from film autoradiograms were digitalized with an Agfa Duoscan scanner (Agfa Gevaert, Mortsel, Belgium). Microphotography was performed using a Zeiss Axioplan microscope equipped with a digital camera (DXM1200 F, Nikon) and ACT-1 Nikon Software. Figures were prepared for publication using Adobe Photoshop software (San Jose, CA). Contrast and brightness of images were the only variables we adjusted digitally. For anatomical reference, sections close to those used were stained with cresyl violet or acetylcholinesterase (Karnovsky and Roots, 1964).

RESULTS

The data on the mRNA expression of sGC subunits was obtained from the examination of X-ray films and emulsion-dipped hybridized sections of four adult rat brains and five monkey brains by two independent observers. Table 1 summarizes the results for sGC α1, α2, and β1 mRNA expression levels observed in the rat brain and Table 2 those for monkey brain. Significant hybridization signal for the β2 subunit could not be detected.

Controls for specificity of the probes

The specificity of the autoradiographic signal obtained in the in situ hybridization histochemistry experiments was confirmed by performing a series of routine controls

TABLE 1. Estimated Densities of sGC Subunit mRNAs in Different Regions of the Rat Brain

Brain Area	sGC α1mRNA	sGC α2mRNA	sGC β1mRNA
Cortex			
Parietal cortex	+	+	++
Frontal cortex	+	+	++
Cingulate cortex	+	+	++
Retrosplenial cortex	+	+	++
Entorhinal cortex	+	+	++
Olfactory system			
Olfactory bulb	+	+/++	++
Anterior olfactory nucleus	+	+/++	++
Olfactory tubercle	+++	+++	+++
Piriform cortex	++	++	+++
Islands of Calleja	+	+	+++
Basal ganglia and related areas			
Caudat-putamen	+++	++	+++
Accumbens	+++	++	+++
Substantia nigra	+/−	+/−	++
Limbic areas			
Ammon's horn			
CA1 (pyramidal cell layer)	+/++	++	+++
CA2 (pyramidal cell layer)	++	++	+++
CA3 (pyramidal cell layer)	+/++	++	+++
Dentate gyrus	−	++	+++
Hilus	++	+++	+++
Subiculum	+	++	+++
Amygdala	+	+/++	++/+++
Taenia tecta	++	++	+++
Thalamus and Hypothalamus			
Subthalamic nu	+	+	++/+++
Medial habenular nu	+++	+++	+++
Lateral habenular nu	+	+	+/++
Ventroposterior thalamic nu	+	+	+/++
Mediodorsal thalamic nu	+	+	++/+++
Zona incerta	+	+	++/+++
Reticular thalamic nu	+	+	++/+++
Ventromedial hypothalamic nu	+/−	+/−	++
Dorsomedial hypothalamic nu	+/−	+/−	++
Arcuate nu	+/−	+/−	+/++
Periventricular hypothalamic nu	+/−	+/−	+/++
Medial geniculate nu	+	+	++
Interpeduncular nu	+	+	++
Midbrain and brainstem			
Red nucleus	+/−	+	++
Inferior colliculus	+	+	++
Superior colliculus	+/−	+/−	++/+++
Pontine nu	+	+	++
Facial nu	+/−	+/−	+
Spinal trigeminal nu, oral	+/++	+/++	++
Locus coeruleus	++/+++	+/−	+++
Motor trigeminal nu	+/−	+/−	++
Raphe nu	+/−	+/−	++
Lateral lemniscus	+	+	+
Cerebellum			
Molecular layer	+/−	+	+/−
Granule cells	++	+++	++
Purkinje cells	−	+++	+++
White matter	+	+/−	+/−
Circumventricular organs			
Choroid plexus	−	−	−
Pineal gland	+++	++	+/++
White matter tracts			
Corpus Callosum	+	+	+/−
Anterior commisure	+	+	+/−
Internal capsule	+	+	+/−
Cerebral peduncle	+	+	+/−
Fimbria of hippocampus	+	+	+/−

Relative intensity of each sGC subunit mRNAs labeling in the adult rat brain (n = 4) expressed as semiquantitative estimates of hybridization intensity. The levels of hybridization signals are indicated by "+++" very strong; "++" moderate; "+" low; "+/−" very low and "−" not detected.

TABLE 2. Estimated Densities of sGC mRNA in Different Regions of the Monkey Brain

Brain Area	sGCα1 mRNA	sGCα2 mRNA	sGCβ1 mRNA
Cortex			
Parietal cortex	+++	++	++
Frontal cortex	+++	++	++
Cingulate cortex	+++	++	++
Retrosplenial cortex	+++	++	++
Entorhinal cortex	+++	++	++
Olfactory system			
Anterior olfactory nucleus	+++	++	++
Basal ganglia and related areas			
Caudate	+++	+++	+++
Putamen	+++	+++	+++
Globus pallidus			
pars lateralis	+	++	++
pars medialis	+	+	++
Claustrum	+	+/−	+++
Nucleus basalis of Meynert	++	+	++
Substantia nigra	−	−	nd
Limbic areas			
Ammon's horn			
CA1 (pyramidal cell layer)	++	++	+++
CA2 (pyramidal cell layer)	++	++	+++
CA3 (pyramidal cell layer)	++	++	+++
Dentate gyrus	+++	+++	+++
Hilus	+	++	+++
Subiculum	+++	++	++
Pre, parasubiculum	+++	++	++
Lateral amygdaloid nucleus	++	+++	++
Thalamus and Hypothalamus			
Ventralis posterior thalamic nu	+	+/−	++
Ventralis anterior thalamic nu	+	+/−	++
Reticular thalamic nu	++	+/−	+
Pulvinar thalamic nu	+	+	+
Posterior hypothalamic nu	++	+/−	nd
Midbrain and Brainstem			
Superior colliculus	+	+/−	nd
Dorsal raphe nu	+	+	nd
Pontine nu	+++	++	nd
Lateral tegmental nu	+	+	nd
Facial nu	−	−	nd
Trigeminal nu	+	+	nd
Vestibular nu	++	+/−	nd
Hypoglossal nu	+++	−	nd
Oculomotor nu	+	+	nd
Cerebellum			
Molecular layer	−	−	+/−
Granule cells	++	+	+++
Purkinje cells	+/−	++	+++
Cerebellar nuclei	++	+	++
White matter tracts	+/−	+/−	+/−
Circumventricular organs			
Choroid plexus	−	−	−
Pineal gland	+	+	nd

Relative intensities of sGC subunit mRNAs labeling in the monkey brain (n = 5) expressed as semiquantitative estimates of hybridization intensity. The levels of hybridization signals are indicated by "+++" very strong; "++" moderate; "+" low; "+/−" very low and "−" not detected, "nd" not determined.

(Pompeiano et al., 1992). In Figure 1 we show an example of these controls performed for the β1 oligonucleotide probe. For each mRNA under study, at least two different oligonucleotide probes complementary to different regions of the same mRNA were used independently as hybridization probes in consecutive sections of the same animal showing identical patterns of hybridization. For a given oligonucleotide probe, addition in the hybridization solution of an excess of the same unlabeled oligonucleotide resulted in the complete abolition of the specific hybridization signal. The remaining autoradiographic signal was considered background. If the unlabeled oligonucleotide included in the hybridization was a different oligonucleotide, then the hybridization signal was not affected. The thermal stability of the hybrids was examined by washing at increasing temperatures: a sharp decrease in the hybridization signal was observed at a temperature consistent with the T_m of the hybrids.

In situ hybridization histochemistry provides reliable information concerning the relative abundance of a given mRNA species in different regions. However, caution must be taken in comparing the relative hybridization signals produced by different probes that detect different mRNAs. In addition to the actual abundance of the different mRNAs, the intensity of the hybridization signals observed, which is the parameter used in the present series of experiments for comparison between mRNAs, can be af-

fected by other factors, such as differences in the hybridization efficiency of the various probes or differences in the specific activities of the probes.

Regional distribution of sGC β1, α1, and α2 subunit mRNAs in rat brain

In situ hybridization with sGC subunit-specific ^{33}P-labeled probes performed at various coronal levels from adult rat brain confirmed that sGC β1 is the most abundant and ubiquitous subunit. Also in agreement with previous reports, we found a more restricted localization of α1 and α2 subunit mRNAs and notable differences in their distribution. Results are summarized in Table 1 and illustrated in Figures 2–5.

Cerebral cortex. The β1 subunit mRNA was widely distributed through all cortical areas and cell layers with higher intensity in layer V. In contrast, α2 mRNA was homogeneously distributed through all cortical layers and α1 expression was higher in layers II–III and V (Figs. 2, 3).

Olfactory system. Strong hybridization signals were observed in the olfactory tubercle for all subunit mRNAs (Fig. 2), where they were present in many intensely labeled cells, in both the pyramidal dense cell layer and in cells scattered in the multiform layer. In the olfactory bulb and anterior olfactory nucleus hybridization signal is high for β1 and moderate to low for both α subunits. The cells of the piriform cortex also showed high levels of expression for β1 mRNA and moderate for α1 and α2 mRNAs. The compact clusters of granule cells that make up the islands of Calleja were selectively labeled with the β1 probe.

Basal ganglia and related areas. The caudate-putamen and nucleus accumbens were among the most prominent labeled brain regions when hybridized with β1 ^{33}P-labeled probes. These were also the areas with highest levels of mRNA coding for α1 and α2 subunits. Moderate expression of β1 was observed in substantia nigra, where α subunits expression was very low.

Limbic areas. sGC α2 and β1 subunits were expressed strongly by dentate gyrus granule cells as well as CA1-CA3 pyramidal neurons (Fig. 4). In contrast, expression of α1 mRNA was high in CA2 pyramidal cells but low in the other CA subfields and dentate gyrus. In the hilus, large neurons contained significantly higher levels of the three subunits. The subiculum showed high expression of β1, moderate of α2, and low of α1. Some amygdaloid nuclei were labeled prominently for β1 and to a lesser extent for the other subunits.

Thalamus and hypothalamus. In the thalamus high levels of mRNA for the three subunits were observed in the medial habenula. In other thalamic nuclei mainly β1 mRNA was visualized (Fig. 2).

In the hypothalamus the expression of the β1 subunit was moderate in the ventromedial, dorsomedial, arcuate, and geniculate nuclei. In these hypothalamic nuclei the hybridization levels for the α subunits were low in general. All three subunits were found at moderate levels in the interpeduncular nucleus.

Midbrain and brainstem. Intense hybridization signal for β1 but low for α subunits was observed in superior colliculus (Fig. 2). The locus coeruleus presented high hybridization signal for β1 and α1 subunits. The ventral tegmental nucleus exhibited moderate levels of expression for the three sGC subunits

Cerebellum. A differential expression pattern was observed in the cerebellum (Fig. 5). Two subunits, α2 and β1, were abundant in Purkinje cells, whereas small cells close to Purkinje cells expressed high levels of α1 mRNA. In addition, α2 and β1 expression was very high and homogeneous in the granule cell layer.

White matter tracts. In general, moderate expression of α1 and α2 mRNAs could be observed in many white matter tracts of the rat brain, whereas β1 mRNA was very low (see Table 1, Fig. 2).

Regional distribution of sGC β1, α1, and α2 subunit mRNAs in monkey brain

The mRNAs coding for sGC β1, α1, and α2 subunits presented a widespread distribution in the monkey brain. Regions with the highest expression for the three subunits were caudate and putamen nuclei, hippocampal formation, cortical areas, and cerebellum. The results obtained are summarized on Table 2 and illustrated in Figs. 6–12.

Cerebral cortex. All different neocortical areas examined presented hybridization signal for the three subunits (Figs. 6–9). Expression for the three subunits was observed in all cortical layers, but the α1 subunit was found enriched in layer VI.

Basal ganglia and basal forebrain. In caudate and putamen nuclei the mRNAs coding for all subunits were high and homogeneously distributed (Figs. 6, 7). Moderate hybridization signal could be appreciated for β1 subunit in both parts of the globus pallidus, lateralis and medialis, where very low levels of α1 mRNA were observed. Transcripts of α2 were seen in the pars lateralis of the globus pallidus at moderate levels and at low levels in the pars medialis. No alpha subunits could be observed in the substantia nigra. Strong hybridization signal for α1 and β1 mRNAs were detected in the nucleus basalis of Meynert.

Amygdala and hippocampal formation. High levels of α2, and moderate for α1 and β1 were detected in the lateral amygdaloid nucleus (Figs. 6, 7). In the hippocampal formation the presence of α1 and α2 mRNA was higher in the dentate gyrus and in the presubiculum (Figs. 7, 10) and lower in the different CA subfields. β1 mRNA was particularly enriched in the hippocampal fields. In the hilus, large neurons contained significantly higher levels of β1 and α2.

Thalamus and hypothalamus. Many of the thalamic nuclei presented hybridization signals for the three subunits. α1 and β1 mRNA could be appreciated in both the anterior and posterior ventralis nuclei and in the pulvinar and reticular nuclei of the thalamus (Figs. 6, 7). The α2 subunit mRNA was present at low levels in the pulvinar nucleus and was barely detectable in other thalamic nuclei.

Midbrain and brainstem. The α1 subunit mRNA presents a restricted distribution in mesencephalic areas of the monkey brain. Moderate to high hybridization levels were found in the dorsal aspects of the periaqueductal gray, vestibular lateral and medial nuclei, and in prepositus hypoglossal nuclei (Fig. 11). Low α1 and α2 mRNA was found in the dorsal raphe nucleus, pedunculopontine tegmental nucleus, and oculomotor nuclei. Expression for α alpha subunits was pronounced in pontine nuclei.

Cerebellum. The mRNA coding for β1 and α2 subunits is high in Purkinje cells (Fig. 12). As in the rat, small cells located close to the Purkinje cells, probably Bergmann glia, contain high densities of α1 mRNA. The granule cell layer was enriched in β1 mRNA and showed mod-

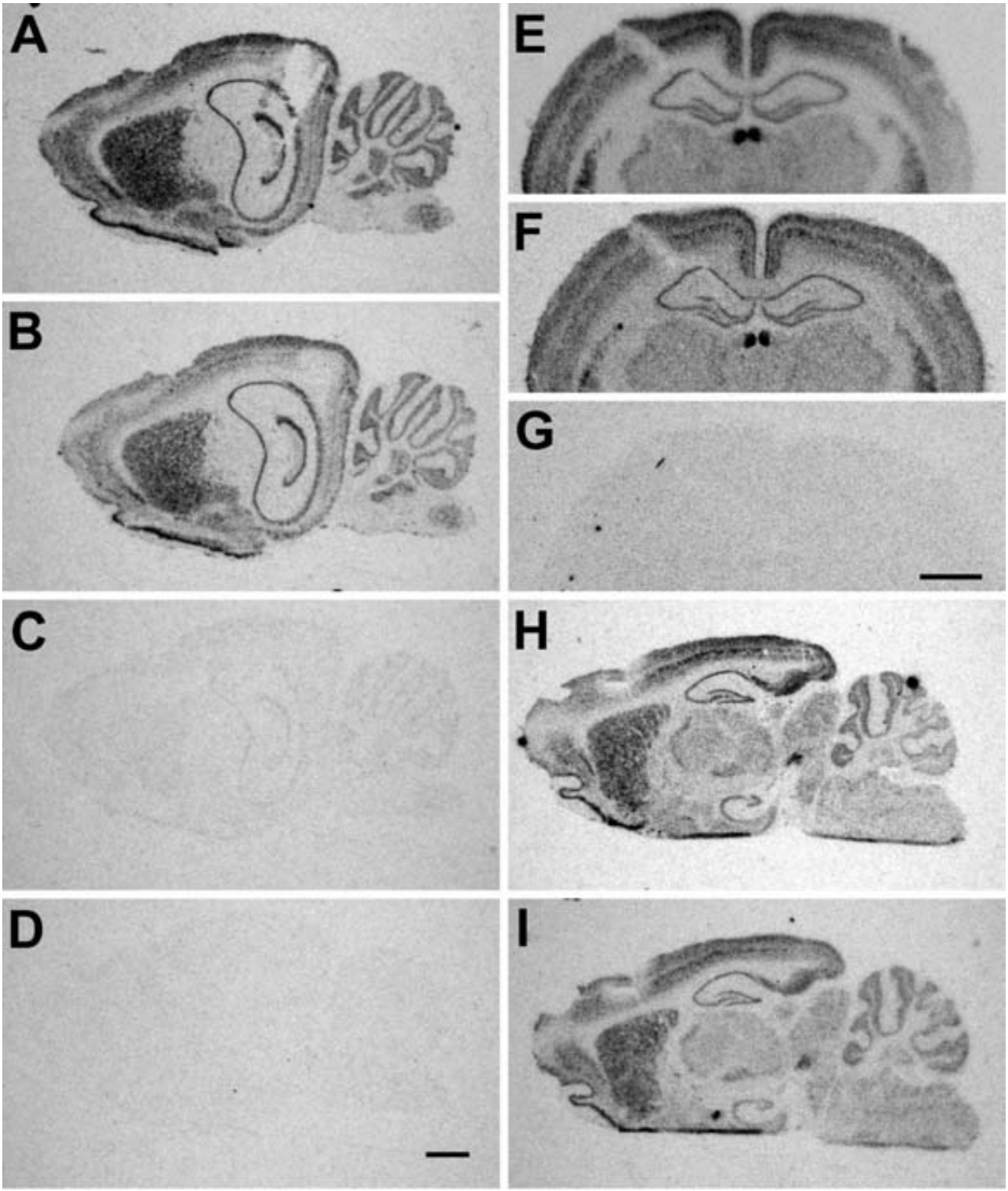

Fig. 1. Specificity controls of the hybridization signal with the β1 oligonucleotide probe. Rat sagittal and coronal consecutive sections were hybridized with the ^{33}P-labeled β1 probe. Hybridized sections were washed at increasing temperatures of 50°C (**A**), 60°C (**B**), 70°C (**C**), and 90°C (**D**). A large decrease in the hybridization signal could be observed between 70°C and 90°C. **E–G:** Cohybridization experiments. The signal obtained with the β1-labeled oligonucleotide (E) was completely blocked by competition with a 50-fold excess of the corresponding unlabeled probe (G) but not by an excess of a different unlabeled β1 oligonucleotide (F). The same hybridization pattern was obtained with the two different β1 probes (H,I). Scale bars = 2 mm.

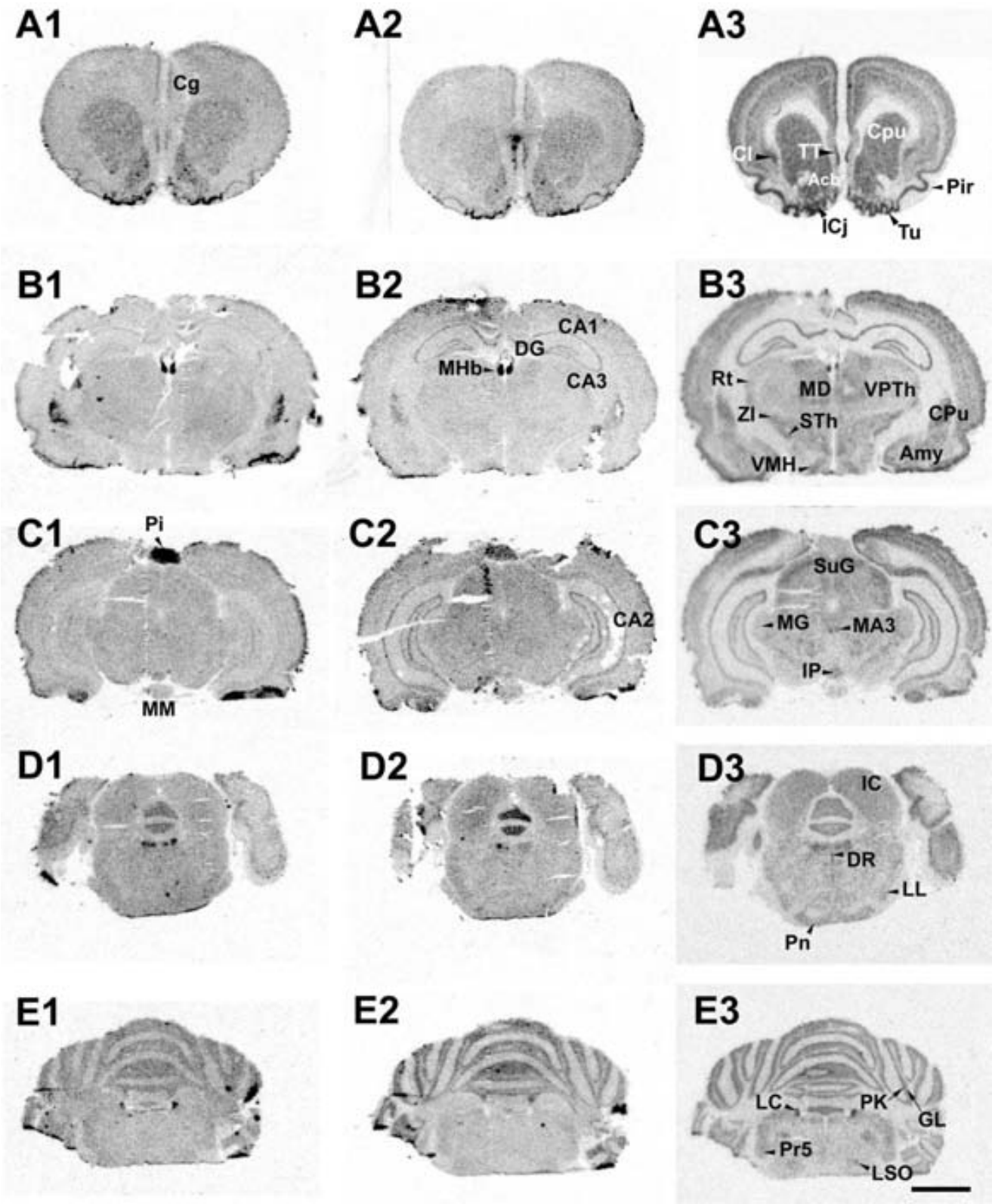

Fig. 2. Regional distribution of the different sGC subunit mRNAs in consecutive sections of the rat brain at different rostrocaudal levels. Autoradiographic images of α1 (**A1–E1**), α2 (**A2–E2**), and β1 (**A3–E3**) mRNAs visualized by in situ hybridization with the corresponding ^{33}P-labeled oligonucleotides. Pictures are digital scanners from film autoradiograms. For abbreviations, see list. Scale bar = 2 mm.

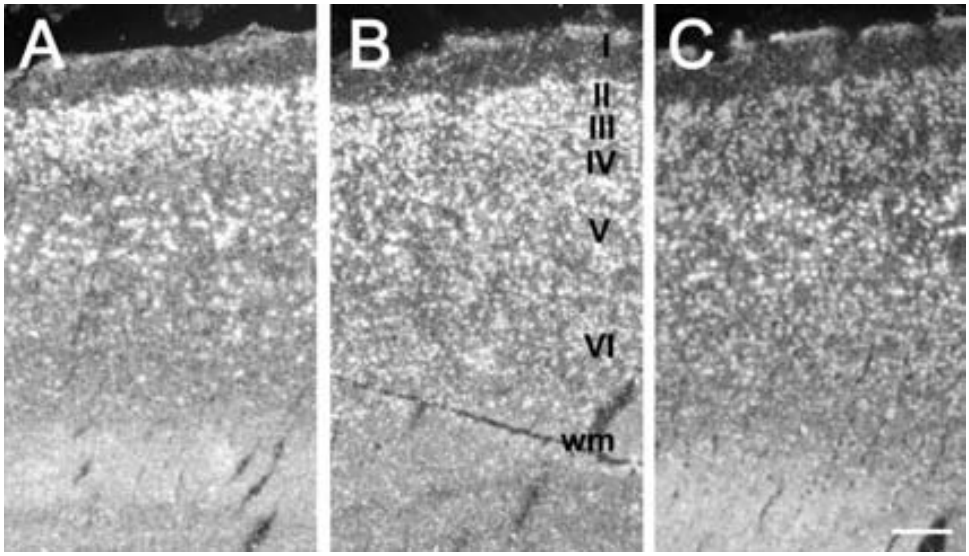

Fig. 3. Laminar distribution of sGC subunits in the rat motor cortex. Darkfield photomicrograph of sagittal sections through cortical layers indicated by roman numbers where α1 (**A**), α2 (**B**), and β1 (**C**) mRNA-containing cells (white silver grains) appear localized in the different layers. Scale bar = 0.1 mm.

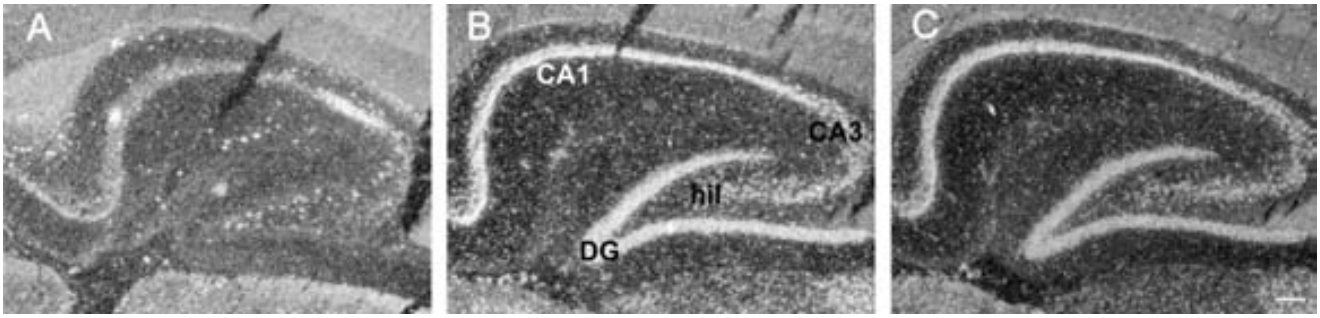

Fig. 4. Expression of sGC subunit mRNAs in rat hippocampus. Darkfield photomicrograph of sagittal sections through the hippocampal region showing the presence of mRNA coding for α1 (**A**), α2 (**B**), and β1 (**C**) subunits. Scale bar = 0.2 mm.

erate hybridization levels for α2 and low for α1 mRNA. The medial and lateral inferior olive nuclei exhibited intense hybridization for β1 (Fig. 6).

White matter tracts. In general, low expression of all subunit mRNAs could be observed in many of the white matter tracts of the monkey brain, possibly in astrocytes (see Table 2, Figs. 6–8).

DISCUSSION

In agreement with previous studies performed in rodent brain by in situ hybridization and RT-PCR (Matsuoka et al., 1992; Furuyama et al., 1993; Burgunder and Cheung, 1994; Gibb and Garthwaite, 2001; Mergia et al., 2003), our results show that the sGC β1, α1, and α2 subunits are expressed in different mammalian brain areas and that β1 is more abundant and widely distributed. In contrast, message for β2, previously detected in rat brain by RT-PCR, but not by in situ hybridization (Gibb and Garthwaite, 2001), was undetectable in our study in both rat and monkey brains. To our knowledge this is the first detailed report of the distribution of sGC β1, α1, and α2 subunits in primate brain and of the sGC α2 subunit in adult rat brain.

Localization of sGC β1, α1 and α2 subunit mRNAs in rat brain and comparison with the localization of protein

The distribution of β1 and α1 mRNAs in coronal sections of the adult rat brain and of the three subunits in parasagittal sections of the developing (8-day-old) rat brain was previously reported (Matsuoka et al., 1992; Furuyama et al., 1993; Burgunder and Cheung, 1994; Gibb and Garthwaite, 2001) and our results are in general agreement with those studies. We confirm here that high levels of expression of all subunits are found in caudate-putamen, nucleus accumbens, and olfactory tubercle, suggesting that both α1β1 and α2β1 sGC isoforms colocalize in these areas. However, a differential expression of sGC heterodimers may occur in cortical cell populations. The α2β1 isoform may be homogeneously distributed, while the α1β1 isoform will concentrate in layers

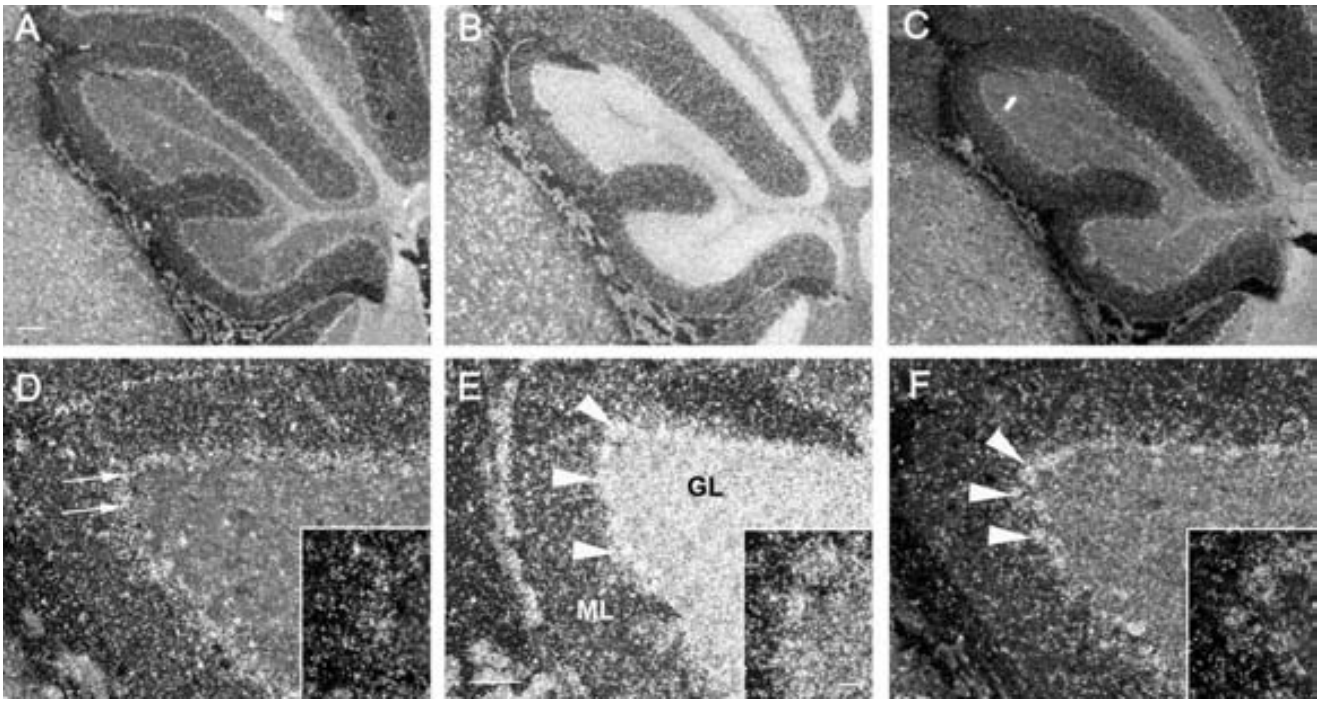

Fig. 5. Distribution of sGC subunit mRNAs in the rat cerebellum. Emulsion-dipped sections of α1 (**A,D**), α2 (**B,E**) and β1 (**C,F**) mRNAs. Arrowheads point to α2 and β1 positive Purkinje cells, and arrows in D point to small α1 hybridizing cells in the granule cell layer edge (see high magnification). Scale bars = 0.2 mm in A–C; 0.1 mm in D–F; 20 μm in high magnification.

II–III and V. Similarly, in the hippocampus the α2β1 heterodimer may be the predominant isoform in dentate gyrus granule cells and CA1-CA3 pyramidal cells, while the sGC α1β1 isoform may be confined to cells in the CA2 subfield. Our results differ from those of Gibb and Garthwaite (2001) in 8-day-old rats regarding the relative abundance of the α subunits in some brain areas, most notably in the cerebellar cortex. Those authors observed a similar level of message for β1 and α1, but an absence of α2 in the Purkinje cell layer and high signal for α2 in granule cells, whereas we found high expression of β1 and α2 in both Purkinje and granule cell layers. This discrepancy can be probably explained by differences in the developmental pattern of sGC subunits. A marked postnatal increase of sGC α2, but not of β1 and α1, has been recently demonstrated at the level of mRNA and immunoreactive protein in different rat brain areas, including cerebellar Purkinje and molecular layers (Bidmon et al., 2004). Interestingly, we found a moderate expression of α1 in the Purkinje cell layer that was predominantly located in small cells, most probably Bergmann glia. A similar observation was reported in young rats by Gibb and Garthwaite (2001). Thus, in the cerebellum α2β1 is probably the main sGC isoform in Purkinje and granule cells, while α1β1 may be more abundant in Bergmann glia.

The distribution of message for the sGC subunits observed in this study fits well with the distribution of immunoreactivity shown recently by using anti-β1 and anti-α1/α2 antibodies (Ding et al., 2004). A similar widespread staining with both antibodies was shown throughout the brain of adult rats that was more prominent in the same areas where we found high to moderate in situ hybridization signals for the three subunits. In double-labeling experiments cellular colocalization was observed in most brain regions. Discrepancies were observed in the cerebellar cortex, where granule cells were strongly immunopositive for sGC β1 but weakly for sGC α subunits. This was probably a reflection of the presumably lower affinity of the antibody for the α2 subunit (Ding et al., 2004) since according to results shown here and elsewhere (Gibb and Garthwaite, 2001; Bidmon et al., 2004) α2 is highly expressed in those cells. In agreement with our results, Ding et al. (2004) observed immunostaining with both antibodies in Bergmann glia, supporting the expression of the α1β1 isoform in these cells.

We have found a much higher expression of β1 than of α subunits in some areas, i.e., the Islands of Calleja, the substantia nigra, and many thalamic, hypothalamic, and brainstem nuclei. This is surprising because β1/β1 and α1/α1 homodimers appear to be catalytically inactive (Zabel et al., 1999). Mismatches of sGC subunits have been also observed during brain development and the possibility of single subunits serving functions other than sGC has been suggested (Bidmon et al., 2004).

sGC β1, α1, and α2 subunit mRNAs in monkey brain

As observed in the rat, the distribution of sGC β1, α1, and α2 subunit mRNAs is widespread in the monkey brain. The three subunits are highly expressed throughout the cortex, but α1 is stronger in layer VI, indicating a predominance of sGC α1/β1 in cells of this layer. High levels of mRNA for the three subunits was also observed in caudate and putamen nuclei and anterior olfactory nucleus, suggesting colocalization of both sGC isoforms.

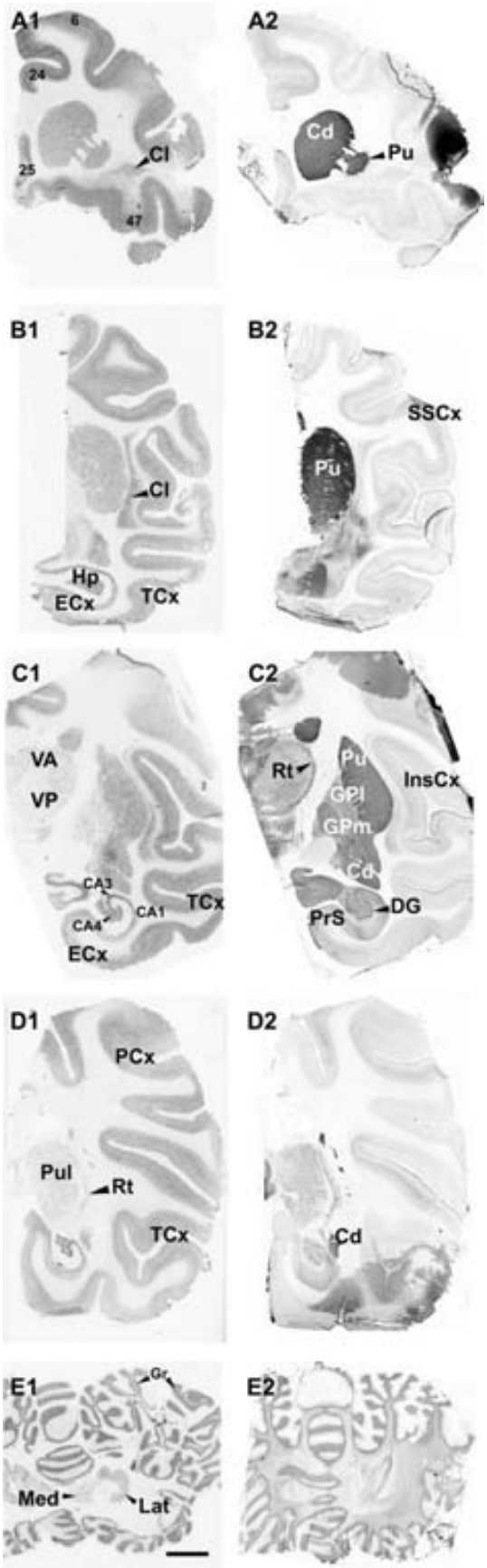

This may also occur in limbic areas, except in large neurons of the hilus, where sGC α2/β1 may be more abundant. sGC α2/β1 may also be the predominant isoform in cerebellar Purkinje cells, while sGC α1/β1 may be preferentially expressed in cerebellar granule cells and small cells in the Purkinje cell layer, presumably Bergmann glia. To our knowledge this is the only study showing the anatomical distribution of sGC subunit message in primate brain. Our results are in general agreement with previous reports on the relative abundance of β1 and α1 mRNA (dot blot) and protein (Western blot) in different human brain regions (Budworth et al., 1999; Ibarra et al., 2001).

Species differences in sGC β1, α1, and α2 subunit mRNA distribution

In the two species studied, β1 was the sGC subunit more highly expressed and widely distributed in brain structures. However, although both α subunits were also widely expressed, the α1 message was relatively more abundant in monkey brain and the α2 message in rat brain, particularly in the cerebral and cerebellar cortex, basal ganglia and related structures, and the limbic system. The most notable difference between species in the distribution of α subunit message was observed in granule cells of the cerebellum that are particularly rich in α2 message in rat but not in monkey. Differences were also observed in layer distribution in the cerebral cortex. Hybridization signal for α1 is higher in external layers in rat but is more enriched in internal layers in monkey. The physiological significance of differences in expression of sGC α1/β1 and sGC α2/β1 isoforms is difficult to ascertain at present. No major differences have been described in the kinetic and pharmacological characteristics of these naturally occurring heterodimers (Russwurm et al., 1998; Gibb et al., 2003). but their subcellular localization may differ. The α2/β1 isoform may be targeted to postsynaptic membranes by interaction with scaffold protein PSD-95 and be located close to NOS-1 and NMDA receptors, suggesting a particular relevance for synaptic NO signaling (Russwurm et al., 2001; Wykes and Garthwaite, 2004). Additionally, recent studies in rat CA1 pyramidal cells indicate that NOS-1 lies at excitatory synapses predominantly postsynaptic to sGC β1-positive axon terminals, supporting a role for NO as retrograde messenger (Burette et al., 2002). A calcium-dependent membrane association of the α1/β1 dimer has been also shown in different tissues (Zabel et al., 2002). In the rat brain, α2 immunoreactivity was shown as a neuropil stain in most regions (Bidmon et al., 2004), whereas sGC β1 and mixed α1/α2 immunostaining appeared also in neuronal somata and proximal dendrites (Ding et al., 2004).

In both rat and monkey the mRNA hybridization pattern observed is typically neuronal, but a close observation of hybridization signals in white matter indicates that sGC subunits are expressed in glial cells, although at

Fig. 6. Hybridization pattern of sGC β1 subunit mRNA in consecutive sections of the monkey brain in several regions. **A1–E1:** Film autoradiograms showing β1 mRNA containing regions. **A2–E2:** Consecutive sections to A1–E1 stained for acetylcholinesterase. Pictures are digital scanners from film autoradiograms. For abbreviations, see list. Scale bar = 2 mm.

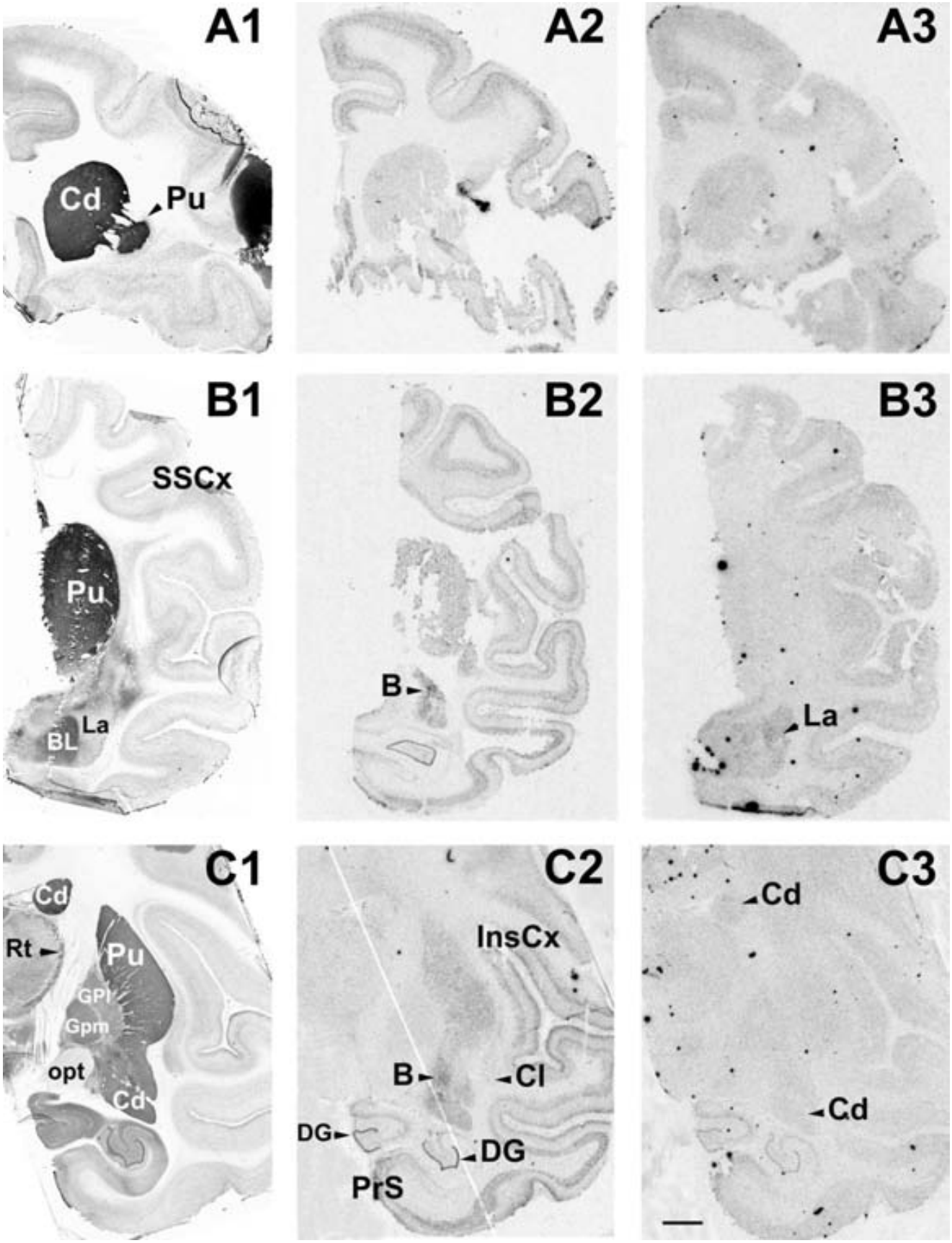

Fig. 7. Regional distribution of the different sGC α subunit mRNAs in consecutive sections of the monkey brain at different rostrocaudal levels. **A2–C2:** α1 mRNA. **A3–C3:** α2 mRNA. **A1–C1** are adjacent sections stained with acetylcholinesterase. For abbreviations, see list. Scale bar = 2 mm.

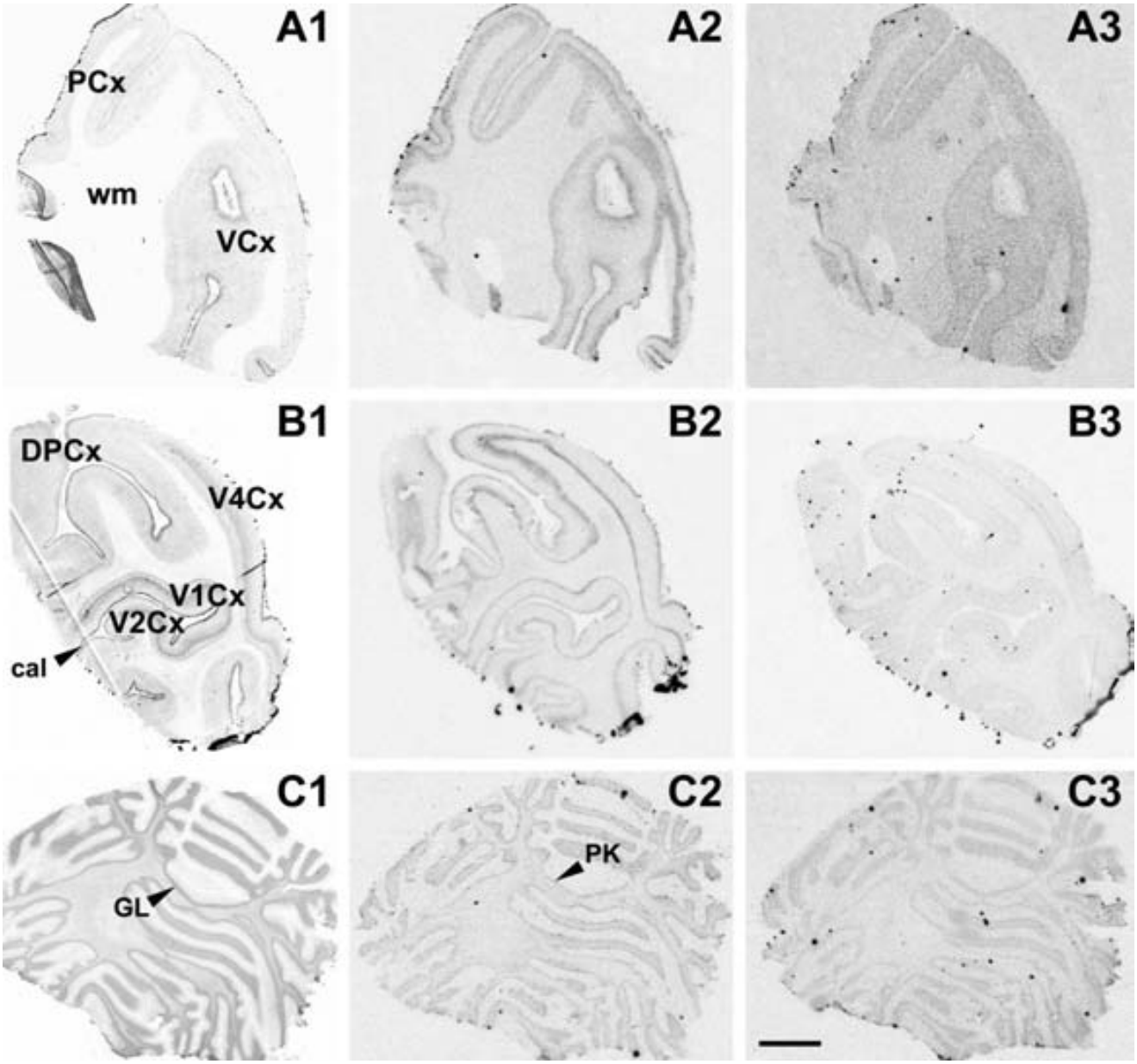

Fig. 8. Regional distribution of the different sGC α subunit mRNAs in coronal sections of two cortical areas (A1–B3) and cerebellum (C1–C3) of the monkey brain. **A2–C2:** α1 mRNA. **A3–C3:** α2 mRNA. **A1–C1:** Acetylcholinesterase-stained sections. For abbreviations, see list. Scale bar = 2 mm.

lower levels than in gray matter cells. Additionally, as mentioned above, labeling of small cells in the Purkinje cell layer in both rat and monkey is compatible with the expression of sGC α1/β1 in Bergmann glia. This is in agreement with studies demonstrating immunoreactivity for sGC β1 and α subunits and NO-stimulated cGMP formation in different astroglial populations in rodent brain (Chan-Palay and Palay, 1979; Nakane et al., 1983; Teunissen et al., 2001; Ding et al., 2004; van Staveren et al., 2004). A recent study from our laboratory also showed immunoreactivity for the β1 subunit in human subcortical white matter astrocytes (Baltrons et al., 2004).

NO/cGMP signaling

NO-stimulated cGMP formation has been mapped in rat brain by using cGMP immunocytochemistry and its distribution compared to that of NOS-1 (Southam and Garthwaite, 1993; de Vente et al., 1998). Results from those studies demonstrated that NOS-1 and NO-dependent cGMP formation are found in varicose fibers throughout the brain and most often occur in structures that are in very close proximity of each other, and rarely in the same structures, indicating that NO acts mainly in a paracrine manner. Similar studies have not been performed in pri-

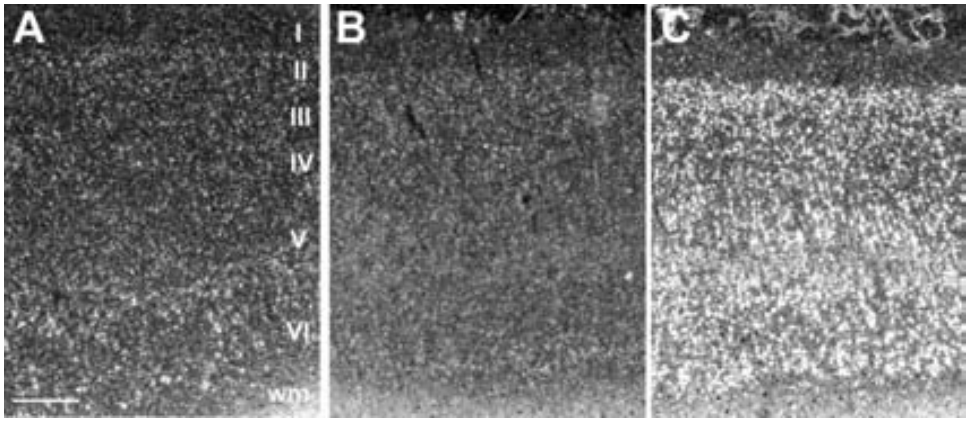

Fig. 9. Laminar distribution of sGC subunit mRNAs in monkey cortical layers. Darkfield photomicrograph of emulsion-dipped sections of α1 (**A**), α2 (**B**), and β1 (**C**) hybridization through cortical layers indicated by roman number. Scale bar = 0.1 mm

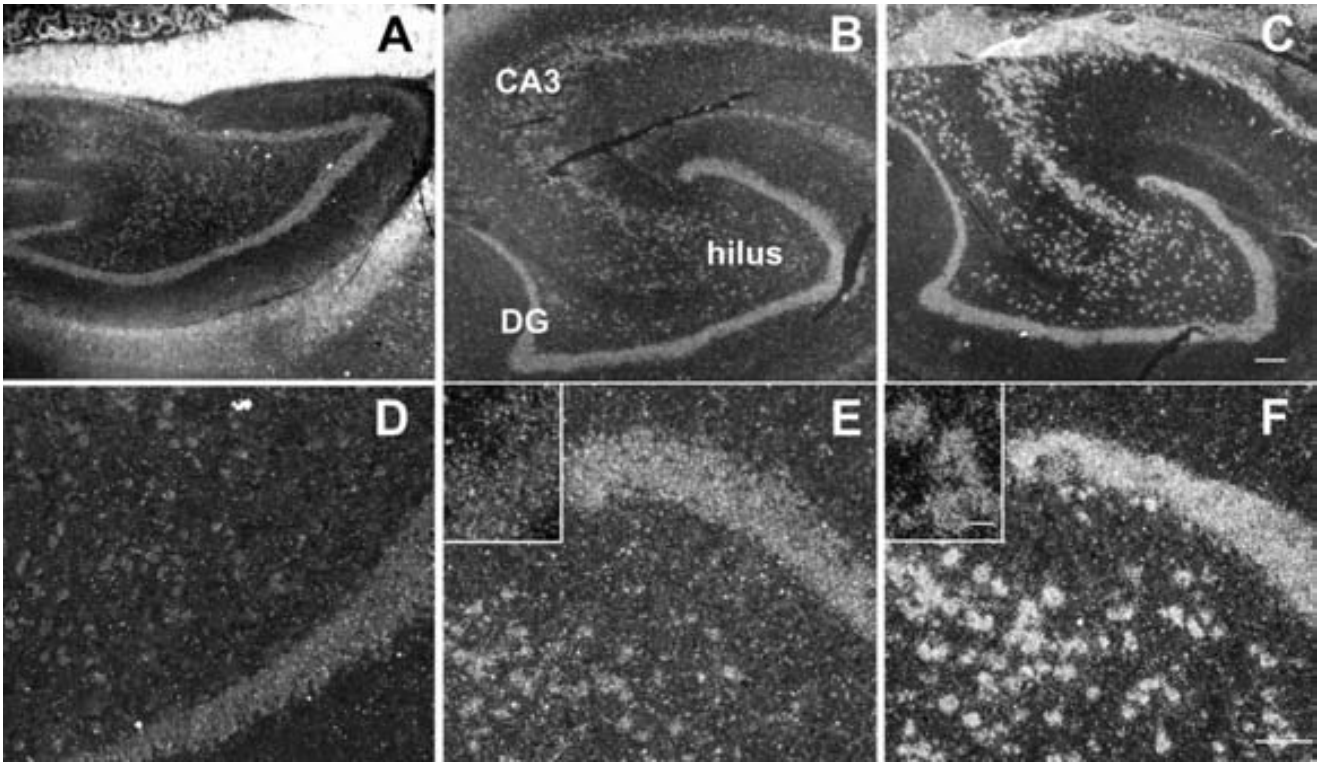

Fig. 10. Expression of sGC mRNA in monkey hippocampus. Darkfield photomicrograph of emulsion-dipped sections through the hippocampal region showing the presence of mRNA coding for α1 (**A,D**), α2 (**B,E**), and β1 (**C,F**) subunits. High magnification of a few large hybridizing neurons of the hilus are shown in the upper-left corner in E, and F. Scale bars = 0.2 mm in A–C; 0.1 mm in D–F; 20 μm in high magnification.

mate brain but the distribution of NOS-1 appears to be quite similar to the rat (Egberongbe et al., 1994; Hashikawa et al., 1994). In general, the areas that present strongest NO-dependent cGMP immunolabeling in rat brain coincide with areas where we and others have found the highest density of sGC subunit mRNA and protein, with some notable exceptions. cGMP immunostaining was not detected in pyramidal cells of the hippocampus and granule cells of the dentate gyrus and was very weak in cerebellar Purkinje cells, all cell populations with high expression of sGC subunits. Recent data on the properties and localization of cGMP hydrolyzing enzymes have shed some light into this apparent paradox. It has been reported that PDE 9, the specific cGMP phosphodiesterase

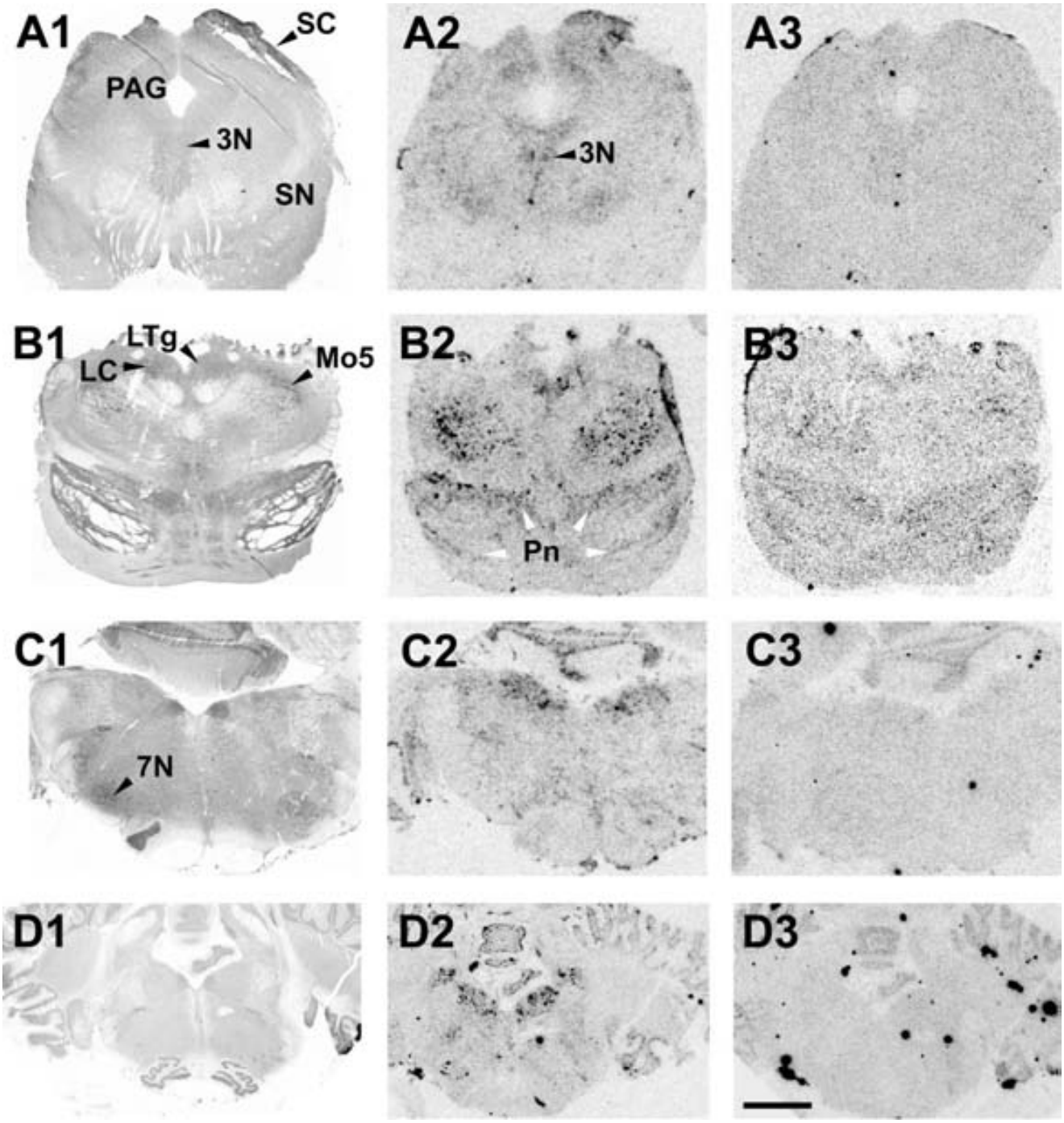

Fig. 11. Distribution of the different sGC α subunit mRNAs in different levels of monkey brainstem. **A2–D2:** α1 mRNA. **A3–D3:** α2 mRNA. **A1–D1:** acetylcholinesterase-stained sections. For abbreviations, see list. Scale bar = 2 mm.

with highest affinity for cGMP and strongly expressed in the above cell populations (Andreeva et al., 2001; van Staveren et al., 2002), is insensitive to the nonselective PDE inhibitor isobutylmethylxanthine commonly used in the cGMP immunolabeling studies in slices (Soderling et al., 1998). The importance of differences in PDE isoform expression in determining the cellular location and intensity of the cGMP response has been recently stressed (van Staveren et al., 2004). Compared to other PDEs, the distribution of PDE9 mRNA in the rat brain follows more closely that of the sGC subunits (van Staveren et al., 2003), supporting the concept that this high-affinity isoform functions to keep cGMP levels low in most brain cells. Additionally, factors such as sGC association to

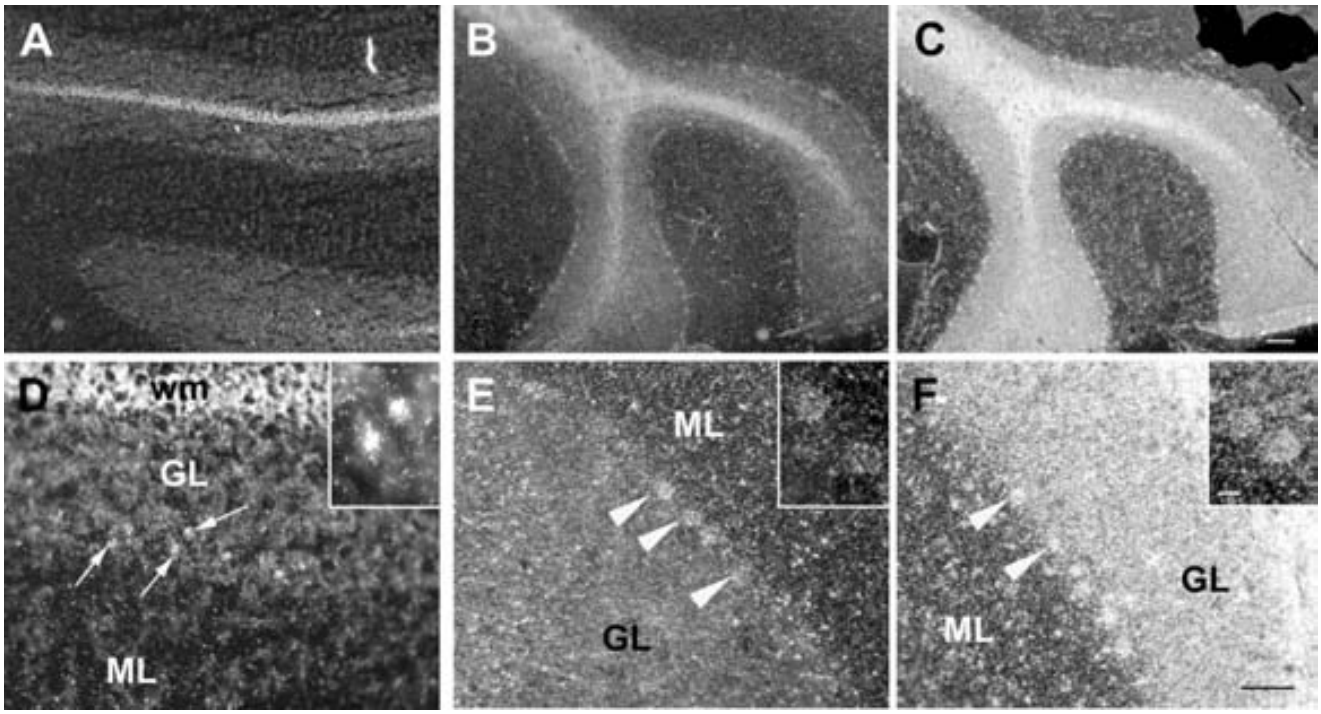

Fig. 12. Cellular distribution of sGC subunit mRNAs in monkey cerebellum. Emulsion-dipped sections of α1 (**A,D**), α2 (**B,E**), and β1 (**C,F**) mRNAs, where some Purkinje cells (arrowheads) showed hybridization signal for α2 and β1, whereas some small cells (arrows) hybridized for α1 (see high magnification). Scale bars = 0.2 mm in A–C; 0.1 mm in D–F; 20 μm in high magnification.

membranes or interaction with endogenous activators or inhibitors may determine the efficiency of NO stimulation of sGC in CNS cells, as appears to occur in other tissues (Burette et al., 2002; Zabel et al., 2002; Venema et al., 2003; Hanafy et al., 2004; Balashova et al., 2005).

In general, the actions of cGMP are mediated via activation of cGMP-dependent protein kinases (cGKs), regulation of cyclic nucleotide-gated channels (CNGs), and regulation of PDEs that preferentially hydrolyze cAMP (Lucas et al., 2000). All these targets are expressed in brain but cGKs have been more often implicated in NO-cGMP actions. The two mammalian cGK isoforms, cGKI and cGKII, are widely distributed in rodent brain (Lohmann et al., 1981; El-Husseini et al., 1999; Feil et al., 2005). Recent genetic studies have shown that genetic ablation of the cGKI gene in hippocampal pyramidal cells impairs protein synthesis-dependent LTP but not spatial learning in adult mice, while ablation in cerebellar Purkinje cells impairs cerebellar LTD and motor learning (Hofmann et al., 2006). Furthermore, cGKII-deficient mice exhibit increased anxiety and reduced sensitivity to the hypnotic effects of ethanol and altered clock gene expression (Hofmann et al., 2006). Knowledge about a similar differential involvement of sGC α1β1 and α2β1 isoforms in NO-cGMP functions awaits the availability of specific subunit-deficient mice.

In conclusion, we have shown that message for the three subunits that form the two naturally occurring sGC isoforms, α1β1 and α2β1, having similar kinetic and pharmacological properties, are widely expressed in monkey brain and present an anatomical distribution similar to that observed in rat brain with only minor differences in the relative abundance of α subunit mRNAs. This suggests that, as occurs in rodent brain, the NO-cGMP signaling pathway will be involved in primate brain in the regulation of important brain functions such as memory formation, sensory processing, and behavior.

LITERATURE CITED

Andreeva SG, Dikkes P, Epstein PM, Rosenberg PA. 2001. Expression of cGMP-specific phosphodiesterase 9A mRNA in the rat brain. J Neurosci 21:9068–9076.

Ariano MA, Lewicki JA, Brandwein HJ, Murad F. 1982. Immunohistochemical localization of guanylate cyclase within neurons of rat brain. Proc Natl Acad Sci U S A 79:1316–1320.

Balashova N, Chang FJ, Lamothe M, Sun Q, Beuve A. 2005. Characterization of a novel type of endogenous activator of soluble guanylyl cyclase. J Biol Chem 280:2186–2196.

Baltrons MA, Pifarre P, Ferrer I, Carot JM, Garcia A. 2004. Reduced expression of NO-sensitive guanylyl cyclase in reactive astrocytes of Alzheimer disease, Creutzfeldt-Jakob disease, and multiple sclerosis brains. Neurobiol Dis 17:462–472.

Bicker G. 2001. Nitric oxide: an unconventional messenger in the nervous system of an orthopteroid insect. Arch Insect Biochem Physiol 48:100–110.

Bidmon HJ, Starbatty J, Gorg B, Zilles K, Behrends S. 2004. Cerebral expression of the alpha2-subunit of soluble guanylyl cyclase is linked to cerebral maturation and sensory pathway refinement during postnatal development. Neurochem Int 45:821–832.

Budworth J, Meillerais S, Charles I, Powell K. 1999. Tissue distribution of the human soluble guanylate cyclases. Biochem Biophys Res Commun 263:696–701.

Burette A, Zabel U, Weinberg RJ, Schmidt HH, Valtschanoff JG. 2002. Synaptic localization of nitric oxide synthase and soluble guanylyl cyclase in the hippocampus. J Neurosci 22:8961–8970.

Burgunder JM, Cheung PT. 1994. Expression of soluble guanylyl cyclase gene in adult rat brain. Eur J Neurosci 6:211–217.

Chan-Palay V, Palay SL. 1979. Immunocytochemical localization of cyclic GMP: light and electron microscope evidence for involvement of neuroglia. Proc Natl Acad Sci U S A 76:1485–1488.

Contestabile A, Ciani E. 2004. Role of nitric oxide in the regulation of neuronal proliferation, survival and differentiation. Neurochem Int 45:903–914.

Cudeiro J, Rivadulla C. 1999. Sight and insight—on the physiological role of nitric oxide in the visual system. Trends Neurosci 22:109–116.

de Vente J, Hopkins DA, Markerink-van Ittersum M, Emson PC, Schmidt HHHW, Steinbusch HWM. 1998. Distribution of nitric oxide synthase and nitric oxide-receptive, cyclic GMP-producing structures in the rat brain. Neuroscience 87:207–241.

Denninger JW, Marletta MA. 1999. Guanylate cyclase and the NO/cGMP signaling pathway. Biochim Biophys Acta 1411:334–350.

Ding JD, Burette A, Nedvetsky PI, Schmidt HH, Weinberg RJ. 2004. Distribution of soluble guanylyl cyclase in the rat brain. J Comp Neurol 472:437–448.

Egberongbe YI, Gentleman SM, Falkai P, Bogerts B, Polak JM, Roberts GW. 1994. The distribution of nitric oxide synthase immunoreactivity in the human brain. Neuroscience 59:561–578.

El-Husseini AE, Williams J, Reiner PB, Pelech S, Vincent SR. 1999. Localization of the cGMP-dependent protein kinases in relation to nitric oxide synthase in the brain. J Chem Neuroanat 17:45–55.

Feil S, Zimmermann P, Knorn A, Brummer S, Schlossmann J, Hofmann F, Feil R. 2005. Distribution of cGMP-dependent protein kinase type I and its isoforms in the mouse brain and retina. Neuroscience 135:863–868.

Furuyama T, Inagaki S, Takagi H. 1993. Localizations of alpha 1 and beta 1 subunits of soluble guanylate cyclase in the rat brain. Brain Res Mol Brain Res 20:335–344.

Garthwaite J, Boulton CL. 1995. Nitric oxide signaling in the central nervous system. Annu Rev Physiol 57:683–706.

Gibb BJ, Garthwaite J. 2001. Subunits of the nitric oxide receptor, soluble guanylyl cyclase, expressed in rat brain. Eur J Neurosci 13:539–544.

Gibb BJ, Wykes V, Garthwaite J. 2003. Properties of NO-activated guanylyl cyclases expressed in cells. Br J Pharmacol 139:1032–1040.

Haley JE, Schuman EM. 1994. Involvement of nitric oxide in synaptic plasticity and learning. Semin Neurosci 6:11–20.

Hanafy KA, Martin E, Murad F. 2004. CCTeta, a novel soluble guanylyl cyclase-interacting protein. J Biol Chem 279:46946–46953.

Hashikawa T, Leggio MG, Hattori R, Yui Y. 1994. Nitric oxide synthase immunoreactivity colocalized with NADPH-diaphorase histochemistry in monkey cerebral cortex. Brain Res 641:341–349.

Hofmann F, Feil R, Kleppisch T, Schlossmann J. 2006. Function of cGMP-dependent protein kinases as revealed by gene deletion. Physiol Rev 86:1–23.

Holscher C. 1997. Nitric oxide, the enigmatic neuronal messenger: its role in synaptic plasticity. Trends Neurosci 20:298–303.

Ibarra C, Nedvetsky PI, Gerlach M, Riederer P, Schmidt HH. 2001. Regional and age-dependent expression of the nitric oxide receptor, soluble guanylyl cyclase, in the human brain. Brain Res 907:54–60.

Jurado S, Sanchez-Prieto J, Torres M. 2003. Differential expression of NO-sensitive guanylyl cyclase subunits during the development of rat cerebellar granule cells: regulation via N-methyl-D-aspartate receptors. J Cell Sci 116:3165–3175.

Karnovsky MJ, Roots L. 1964. A "direct-coloring" thiocholine method for cholinesterases. J Histochem Cytochem 12:219–221.

Koesling D, Russwurm M, Mergia E, Mullershausen F, Friebe A. 2004. Nitric oxide-sensitive guanylyl cyclase: structure and regulation. Neurochem Int 45:813–819.

Lohmann SM, Walter U, Miller PE, Greengard P, De Camilli P. 1981. Immunohistochemical localization of cyclic GMP-dependent protein kinase in mammalian brain. Proc Natl Acad Sci U S A 78:653–657.

Lucas KA, Pitari GM, Kazerounian S, Ruiz-Stewart I, Park J, Schulz S, Chepenik KP, Waldman SA. 2000. Guanylyl cyclases and signaling by cyclic GMP. Pharmacol Rev 52:375–414.

Matsuoka I, Giuili G, Poyard M, Stengel D, Parma J, Guellaen G, Hanoune J. 1992. Localization of adenylyl and guanylyl cyclase in rat brain by in situ hybridization: comparison with calmodulin mRNA distribution. J Neurosci 12:3350–3360.

Mergia E, Russwurm M, Zoidl G, Koesling D. 2003. Major occurrence of the new alpha2beta1 isoform of NO-sensitive guanylyl cyclase in brain. Cell Signal 15:189–195.

Moncada S, Higgs EA. 1991. Endogenous nitric oxide: physiology, pathology and clinical relevance. Eur J Clin Invest 21:361–374.

Nakane M, Ichikawa M, Deguchi T. 1983. Light and electron microscopic demonstration of guanylate cyclase in rat brain. Brain Res 273:9–15.

Pifarre P, Garcia A, Mengod G. 2005. Comparative anatomical distribution of soluble guanylyl cyclase subunit mRNAs in mammalian brain. J Neurochem 94:31.

Pompeiano M, Palacios JM, Mengod G. 1992. Distribution and cellular localization of mRNA coding for 5-HT1A receptor in the rat brain: correlation with receptor binding. J Neurosci 12:440–453.

Prickaerts J, Sik A, van Staveren WC, Koopmans G, Steinbusch HW, van der Staay FJ, de Vente J, Blokland A. 2004. Phosphodiesterase type 5 inhibition improves early memory consolidation of object information. Neurochem Int 45:915–928.

Russwurm M, Behrends S, Harteneck C, Koesling D. 1998. Functional properties of a naturally occurring isoform of soluble guanylyl cyclase. Biochem J 335(Pt 1):125–130.

Russwurm M, Wittau N, Koesling D. 2001. Guanylyl cyclase/PSD-95 interaction: targeting of the nitric oxide-sensitive alpha2beta1 guanylyl cyclase to synaptic membranes. J Biol Chem 276:44647–44652.

Soderling SH, Bayuga SJ, Beavo JA. 1998. Cloning and characterization of a cAMP-specific cyclic nucleotide phosphodiesterase. Proc Natl Acad Sci U S A 95:8991–8996.

Southam E, Garthwaite J. 1993. The nitric oxide-cyclic GMP signalling pathway in rat brain. Neuropharmacology 32:1267–1277.

Teunissen C, Steinbusch H, Markerink-van Ittersum M, Koesling D, de Vente J. 2001. Presence of soluble and particulate guanylyl cyclase in the same hippocampal astrocytes. Brain Res 891:206–212.

Tomiyama M, Palacios JM, Cortes R, Vilaro MT, Mengod G. 1997. Distribution of AMPA receptor subunit mRNAs in the human basal ganglia: an in situ hybridization study. Brain Res Mol Brain Res 46:281–289.

van Staveren WC, Glick J, Markerink-van Ittersum M, Shimizu M, Beavo JA, Steinbusch HW, de Vente J. 2002. Cloning and localization of the cGMP-specific phosphodiesterase type 9 in the rat brain. J Neurocytol 31:729–741.

van Staveren WC, Steinbusch HW, Markerink-van Ittersum M, Behrends S, de Vente J. 2004. Species differences in the localization of cGMP-producing and NO-responsive elements in the mouse and rat hippocampus using cGMP immunocytochemistry. Eur J Neurosci 19: 2155–2168.

Venema RC, Venema VJ, Ju H, Harris MB, Snead C, Jilling T, Dimitropoulou C, Maragoudakis ME, Catravas JD. 2003. Novel complexes of guanylate cyclase with heat shock protein 90 and nitric oxide synthase. Am J Physiol Heart Circ Physiol 285:H669–678.

Wykes V, Garthwaite J. 2004. Membrane-association and the sensitivity of guanylyl cyclase-coupled receptors to nitric oxide. Br J Pharmacol 141:1087–1090.

Zabel U, Hausler C, Weeger M, Schmidt HH. 1999. Homodimerization of soluble guanylyl cyclase subunits. Dimerization analysis using a glutathione s-transferase affinity tag. J Biol Chem 274:18149–18152.

Zabel U, Kleinschnitz C, Oh P, Nedvetsky P, Smolenski A, Muller H, Kronich P, Kugler P, Walter U, Schnitzer JE, Schmidt HH. 2002. Calcium-dependent membrane association sensitizes soluble guanylyl cyclase to nitric oxide. Nat Cell Biol 4:307–311.

Zhang J, Snyder SH. 1995. Nitric oxide in the nervous system. Annu Rev Pharmacol Toxicol 35:213–233.

Zhuo M, Hawkins RD. 1995. Long-term depression — a learning-related type of synaptic plasticity in the mammalian central-nervous-system. Rev Neurosci 6:259–277.

6 Resumen Trabajo 2

Numerosos estudios han demostrado la inducción de la NOS-2 en células gliales de cerebros de pacientes con enfermedades neurodegenerativas que llevan asociadas neuroinflamación como Alzheimer (AD) y Esclerosis múltiple (MS). Estudios previos del laboratorio habian demostrado que el tratamiento con agentes inflamatorios que inducen la NOS-2 en células gliales como péptidos β-amiloides, LPS o IL-1β, son capaces de disminuir los niveles de la actividad GC_{NO} y de la subunidad β1 en astrocitos de rata en cultivo, así como en cerebro de ratas adultas.

En el presente trabajo, hemos estudiado si la GC_{NO} se encuentra alterada en cerebro de pacientes en diferentes estadios de AD y en pacientes de Creutzfeldt-Jakob (CJ) y MS. No hemos encontrado diferencias significativas entre controles y enfermos de AD en la actividad GC_{NO} basal o estimulada por donadores de NO, ni en los niveles de expresión de las subunidades β1 y α1 en homogenados de corteza cerebral. Los estudios inmunohistoquímicos mostraron un marcaje intenso de la GC_{NO} β1 en las neuronas corticales y de hipocampo y en astrocitos fibrilares de la sustancia blanca, mientras que los astrocitos de la sustancia gris presentaban una débil inmunoreactividad, indicando bajos niveles de expresión para esta subunidad en este tipo de células. En pacientes con AD la inmunoreactividad en neuronas y en astrocitos fibrilares no se ve alterada mientras que el marcaje en astrocitos reactivos ubicados alrededor de las placas amiloides se encuentra muy reducido. El marcaje de la GC_{NO} β1 se ve también disminuido en astrocitos reactivos de la corteza y de la sustancia blanca subcortical en cerebro de pacientes con la enfermedad de CJ y en las lesiones crónicas y subagudas en cerebros de pacientes con MS. Así, la inducción de la reactividad glial está asociada a una disminución en la capacidad de generar GMPc en respuesta a NO tanto *in vitro* como *in vivo*.

El significado fisiológico de esta disminución es difícil de interpretar actualmente debido a lo poco que se ha estudiado el papel del GMPc en astrocitos. Se sabe por estudios inmunohistoquímicos en cortes de cerebro que el NO generado en las neuronas actúa sobre la GC_{NO} de astrocitos. La bajada en los niveles de la GC_{NO} en astrocitos podría ser un mecanismo adaptativo para prevenir el exceso de señalización mediada por el GMPc en condiciones de elevada formación de NO en células gliales durante la neuroinflamación. La falta de este mecanismo en neuronas podría ser la causa de la mayor vulnerabilidad de estas células a los excesos de NO. Se ha descrito que el GMPc regula la expresión de genes inflamatorios, como la NOS-2, COX-2 o el TNFα en diferentes tipos celulares. Si bien se han descrito efectos positivos y negativos, en macrófagos el papel del GMPc parece ser inhibitorio. Teniendo en cuenta estos resultados, es posible plantear la hipótesis de que la capacidad reducida de

generar GMPc en respuesta al NO de los astrocitos reactivos puede tener un efecto permisivo sobre la respuesta inflamatoria en estas células.

ELSEVIER

Neurobiology of Disease

www.elsevier.com/locate/ynbdi
Neurobiology of Disease 17 (2004) 462–472

Reduced expression of NO-sensitive guanylyl cyclase in reactive astrocytes of Alzheimer disease, Creutzfeldt–Jakob disease, and multiple sclerosis brains

María Antonia Baltrons,[a] Paula Pifarré,[a] Isidre Ferrer,[b] José Miguel Carot,[c] and Agustina García[a,*]

[a]*Departament de Bioquímica i Biologia Molecular, Institut de Biotecnologia i Biomedicina V. Villar Palasí, Universitat Autònoma de Barcelona, Spain*
[b]*Institut de Neuropatologia, Servei d'Anatomia Patològica, Hospital de Bellvitge, Barcelona, Spain*
[c]*Departament d'Estadística, Universitat Politècnica de Valencia, Spain*

Received 6 April 2004; revised 10 July 2004; accepted 30 July 2004
Available online 30 September 2004

In Alzheimer's disease (AD) brains increased NO synthase (NOS) expression is found in reactive astrocytes surrounding amyloid plaques. We have recently shown that treatment with β-amyloid peptides or IL-1β down-regulates NO-sensitive soluble guanylyl cyclase (sGC) in cultured astrocytes and in adult rat brain. In this work, we have examined sGC activity and expression in postmortem brain tissue of AD patients and matched controls. No significant alteration was observed in basal or NO-stimulated sGC activity, nor in sGC β1 and α1 subunit levels in cortical extracts of AD brains. Immunohistochemistry showed intense and widespread labeling of sGC β1 in cortical and hippocampal neurons and white matter fibrillar astrocytes, while grey matter astrocytes were faintly stained. In AD, expression of sGC in neurons and fibrillar astrocytes is not altered but is markedly reduced in reactive astrocytes surrounding amyloid plaques. Immunostaining for sGC β1 was also lacking in reactive astrocytes in cortex and subcortical white matter in Creutzfeldt–Jakob disease brains and in subacute and chronic plaques in multiple sclerosis (MS) brains. Thus, induction of astrocyte reactivity is associated with decreased capacity to generate cGMP in response to NO both in vitro and in vivo. This effect may be related to the development of the astroglial inflammatory response.

Keywords: Astroglia; Cyclic GMP; Soluble guanylyl cyclase; Nitric oxide; Alzheimer's disease; Creutzfeldt–Jakob disease; Multiple sclerosis

Introduction

Nitric oxide (NO) is an important physiological messenger in the central nervous system (CNS) involved in the modulation of development, synaptic plasticity, neuroendocrine secretion, sensory processing, and cerebral blood flow (Garthwaite and Boulton, 1995; Zhang and Snyder, 1995). NO has been also implicated in a number of neurological disorders including Alzheimer's disease (AD) and other neurodegenerative conditions. NO is synthesized from L-arginine by a highly regulated family of NO synthases (NOS) encoded by three distinct genes, neuronal NOS (nNOS or NOS1), inducible NOS (iNOS or NOS2), and endothelial NOS (eNOS or NOS3). In the healthy brain, moderate amounts of NO can be generated by neurotransmitter stimulation of the calcium-dependent NOS1 and NOS3 isoforms expressed in particular populations of neurons and astrocytes (review in Förstermann et al., 1998; García and Baltrons, 2003; Zhang and Snyder, 1995). In contrast, the NOS2 isoform is not expressed under normal conditions but is transcriptionally induced in glial cells and possibly also in neurons during neuroinflammation, giving rise to elevated NO levels (Heneka and Feinstein, 2001; Loihl and Murphy, 1998). Several evidences suggest that all three isoforms are aberrantly expressed in AD and that NO is involved in the pathogenesis of the disease (De la Monte and Bloch, 1997; Lüth et al., 2000, 2001; Simic et al., 2000; Wallace et al., 1997). In initial studies, NOS2 was found to be induced in reactive astrocytes associated with β-amyloid plaques and was suggested to be a major source of NO (Wallace et al., 1997). More recently, an increased expression of NOS1 and NOS3 in reactive astrocytes and neurons was reported in AD brains (De la Monte and Bloch, 1997; Lüth et al., 2000, 2001; Simic et al., 2000). Increased NOS isoforms colocalized with nitrotyrosine, an indicator of peroxynitrite formation, a result of concomitant local synthesis of superoxide and NO (Lüth et al., 2002). Thus, all three isoforms could contribute to nitrosative stress and altered intracellular signalling leading to neuronal dysfunction and/or cell death in AD.

* Corresponding author. Institut de Biotecnologia i Biomedicina V. Villar Palasí, Universitat Autònoma de Barcelona, 08193 Bellaterra (Cerdanyola del Vallés), Spain. Fax: +34 935812011.
E-mail address: agustina.garcia@uab.es (A. García).
Available online on ScienceDirect (www.sciencedirect.com.)

0969-9961/$ - see front matter © 2004 Elsevier Inc. All rights reserved.
doi:10.1016/j.nbd.2004.07.022

NO-stimulated guanylyl cyclase, also known as soluble guanylyl cyclase [sGC; GTP pyrophosphate-lyase (cyclizing), EC 4.6.1.2], is a major target for NO in the CNS and cyclic GMP (cGMP), the recognized mediator of most neuromodulatory actions of NO (Garthwaite and Boulton, 1995; Zhang and Snyder, 1995). Additionally, cGMP is emerging as a mediator of neuroprotective actions of NO (Ciani et al., 2002; Estevez et al., 1998; Kim et al., 1999). sGC largely exists as a heterodimer of α and β subunits that is activated by binding of NO to its heme prosthetic group. Two different α (α1-2) and β (β1-2) sGC subunits have been cloned and sequenced but only α1β1 and α2β1 have been isolated as functional heterodimers (Russwurm and Koesling, 2002). In the rat brain, in situ hybridization studies have demonstrated a wide distribution of the β1 isoform, whereas α subunits have a more restricted localization (Furuyama et al., 1993; Gibb and Garthwaite, 2001; Matsuoka et al., 1992). Immunocytochemical studies utilizing antibodies against sGC or cGMP have shown immunoreactivity in both neuronal and astroglial cells in the rat brain (Ariano et al., 1982; De Vente and Steinbusch, 1992; Nakane et al., 1983; Teunissen et al., 2001). In the human brain, mRNA expression of β1 is also higher than that of α1 in all regions studied, and α1 and α2 mRNAs present a different distribution (Budworth et al., 1999). Regional differences in α1 and β1 protein have been also reported (Zabel et al., 1998), but information about cellular localization of the enzyme in human brain is lacking.

Very little is known about the regulation of NO-dependent cGMP formation under neuropathological conditions associated with chronic inflammation and excess NO production. We have recently shown that inflammatory compounds known to induce astroglial reactivity and NOS2 expression, such as bacterial endotoxin, IL-1β, and β-amyloid peptides, down-regulate sGC at the protein and mRNA level in rat brain astroglial cell cultures and after intracerebral administration in adult rat brain (Baltrons and García, 1999; Baltrons et al., 2002; Pedraza et al., 2003). A decrease in sGC mRNA levels with age has been reported in rat (Gibb and Garthwaite, 2001) and human brain (Ibarra et al., 2001), which could be related to elevated proinflammatory cytokine levels (Cunningham et al., 2002). Reduced NO-stimulated sGC activity has been also reported in brain extracts from subjects with AD (Bonkale et al., 1995). The aim of this study was to investigate if sGC expression was altered in AD brains. We have found that sGC expression does not appear to be altered in neurons or white matter fibrillar astrocytes but is absent in reactive astrocytes surrounding amyloid plaques. Further evidence for down-regulation of sGC in reactive astrocytes was obtained in sporadic Creutzfeldt–Jakob (sCJD) and multiple sclerosis brains (MS).

Materials and methods

Human subjects

Human cases were obtained from the Institute of Neuropathology and Brain Bank of the Hospital Universitari de Bellvitge (Barcelona, Spain) following the guidelines of the local Ethic Committee. Control and diseased brains were processed in the same way. One hemisphere was cut on coronal sections, frozen on dry ice, and stored at −80°C until use for biochemical determinations. The other hemisphere was fixed in 10% buffered formalin. In addition, small blocks, 3 mm thick, of several brain regions were fixed in 4% paraformaldehyde for 24 h, cryoprotected in 30% saccharose, and frozen at −80°C until use for specific immunohistochemical methods.

Biochemical studies were carried out in the frontal cortex (area 8) of AD cases with increased β-amyloid burden, which were classified as A, B, and C following the nomenclature of Braak and Braak (1999). Cases with stage A show a few senile plaques in the basal regions of the brain but not in the convexity of the cerebral hemispheres, and therefore no senile plaques were present in the area 8; cases with stage B had moderate numbers of senile plaques in the convexity of the cerebral hemispheres, whereas cases with stage C had large numbers of senile plaques in the convexity and hence in the area 8 of the frontal cortex. Three cases were analyzed of groups A and B and six of group C and these were compared with six age-matched controls with no neurological disease and which were normal after neuropathological study.

For immunohistochemical studies, the following cases were analyzed: eight cases with AD stage C of senile plaque burden and stage V/VI of neurofibrillar degeneration (isocortical involvement), again according to the nomenclature of Braak and Braak (1999); six cases of sCJD, homozygous to methionine at codon 129 (Ferrer et al., 1999); three cases of MS with subacute and chronic plaques; and five age-matched controls.

The postmortem delay between death and processing of the brain was between 3 and 21 h in control and diseased brains. The proportion of male and female was similar in control and pathologic cases. The final diagnosis was based on well-established clinical and neuropathological findings.

The neuropathological examination was carried out in formalin-fixed tissue for no less than 3 weeks; the tissue was then embedded in paraffin. Dewaxed sections, 5 μm thick, were stained with hematoxylin and eosin and Klüver–Barrera Luxol fast blue or processed for immunohistochemistry following the streptavidin LSAB method (Dako). After incubation with methanol and normal serum, the sections were incubated with one of the primary antibodies at 4°C overnight. Antibodies to glial fibrillary acidic protein (GFAP, Dako) and βA4-amyloid (Boehringer-Mannheim) were used at dilutions of 1:5. Following incubation with the primary antibody, the sections were incubated with LSAB for 1 h at room temperature. The peroxidase reaction was visualized with 0.05% diaminobenzidine and 0.01% hydrogen peroxide. Sections were slightly counterstained with hematoxylin.

Measurement of sGC activity

Tissue blocks from the area 8 of the frontal cortex were homogenized in 10 volumes of ice-cold 50 mM Tris–HCl, pH 7.4, 0.32 M sucrose, 1 mM EDTA, antiprotease cocktail (Roche), and antiphosphatase cocktail (Sigma), with a glass-Teflon Potter-Elvehjeim homogenizer mechanically driven at 800 rpm. Homogenates were centrifuged at 1000 × *g* for 5 min and nuclear pellets discarded. The supernatants were centrifuged at 100,000 × *g* for 1 h. For sGC activity, soluble fractions (5 μg of protein) were incubated for 10 min at 37°C with 1 mM GTP, 1 mM DTT, 4 mM $MgCl_2$, 15 mM creatine phosphate, 200 mg/l creatine kinase, 1 mM 3-isobutyl-1-methylxanthine (IBMX), and 1 mM EGTA in 50 mM Tris–HCl, in the presence or absence of 2 μM diethylamine NONOate (DEA/NO). The cGMP product

was determined by radioimmunoassay as reported (Agulló and García, 1992) and protein concentration by the method of Lowry using bovine serum albumin as standard. The sGC activity was linear up to at least 10 min and 12 μg of protein.

Analysis of sGC β1 and α1 subunit protein by immunoblotting

Western blots were performed as described (Baltrons and García, 1999). Cytosolic fractions (10–15 μg of protein) were subjected to 10% sodium dodecyl sulfate–polyacrylamide gel electrophoresis (SDS-PAGE) followed by transfer to PDVF filters at 100 V for 1.5 h at 4°C. Membranes were blocked at 4°C overnight in phosphate-buffered saline (pH 7.4) containing 5% nonfat dry milk and then incubated at room temperature for 2 h with affinity purified rabbit polyclonal antibody against peptide 189–207 of the β1 subunit of sGC (1:4000; Sigma), rabbit polyclonal antibody against peptide 670–690 of the α1 subunit of sGC (1:4000; Sigma), and monoclonal anti-β-actin antibody (1:125,000; AC-74, Sigma). Bound antibodies were detected with alkaline phosphatase-linked anti-rabbit (Bio-Rad) and anti-mouse (Sigma) antibodies (1:3000) and revealed with nitroblue tetrazolium and 5-bromo-4-choro-3-indyl-phosphate (NBT-BCIP) (Sigma). Alternatively, bound antibodies were detected with a horseradish peroxidase conjugated anti-rabbit and anti-mouse IgGs (1:4000) visualized by chemiluminescence (Pierce Supersignal West-Pico kit). The intensity of the immunobands was quantified by densitometry with the program Molecular Analyst 1.3 (Bio-Rad). The sGC β1 and α1 protein levels were normalized against β-actin to control for variance in sample loading and transfer.

The specificity of the anti-sGC β1 and α1 subunit antibodies was verified using cytosolic protein (up to 30 μg) from normal human cortex. The sGC β1 antibody (1:4000) labeled a single 70-kDa protein and labeling was totally blocked when the antibody was preabsorbed with a 1000-fold excess concentration of the antigenic peptide (Cayman) (Fig. 1A). The α1 antibody labeled an 80-kDa band that was blocked when the antibody was preincubated with a 1000-fold excess concentration of the antigenic peptide (donated by Sigma) but also labeled numerous low molecular weight bands that were not blocked by preabsorbing the antibody (Fig 1B). The intensity of the specific β1 and α1 immunobands was

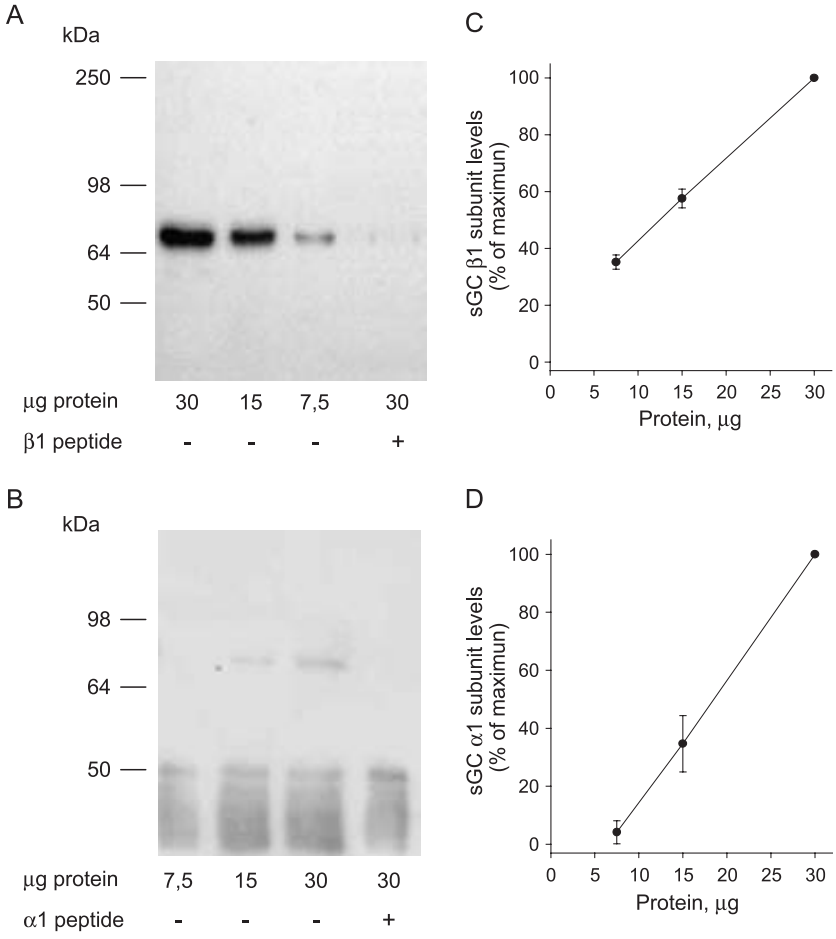

Fig. 1. Specificity of the antibodies against sGC β1 and α1 subunits. Western blot analysis was performed using cytosolic protein from frontal cortex of an 80-year-old control. Protein (7.5–30 μg) was fractionated by SDS-PAGE and transferred to PDVF membranes. Immunoreactive sGC β1 (70 kDa) and α1 (80 kDa) subunits were detected using a 1:4000 dilution of rabbit polyclonal antibodies (Sigma). The immunoreactive bands were not detected when the antibodies were preabsorbed with a 1000-fold excess concentration of the respective antigenic peptides. (A and B) Representative immunoblots; (C and D) immunoreactive bands were analyzed by densitometry and results plotted as a function of the amount of protein loaded. Results, expressed as percent of the highest amount of protein, are means ± SD of two different experiments.

proportional to the amount of protein loaded at least up to 30 μg of protein (Figs. 1C and D).

sGC β1 subunit immunohistochemistry

Serial sections, 30 μm thick, were processed free floating with the LSAB method (Dako LSAB + kit) following the instructions of the supplier. Samples of the frontal cortex (area 8) and underlying white matter and entorhinal cortex and hippocampus were obtained for AD, sCJD, and controls. Samples of the cerebral cortex, normal white matter, and plaques were obtained for MS cases. Briefly, after blocking endogenous peroxidases, the sections were incubated with normal serum for 2 h and then incubated overnight at 4°C with one of the primary antibodies. The anti-sGC β1 (Sigma) was used at a dilution of 1:1000. The anti-GFAP antibody was used at a dilution of 1:250. After washing, the sections were incubated with link solution (LSAB) and with streptavidin–peroxidase solution for 15 min each at room temperature. The peroxidase reaction was visualized, as a dark blue precipitate, with NH_4NiSO_4 (0.05 M) in phosphate buffer (0.1 M), 0.05% diaminobenzidine, NH_4Cl, and 0.01% hydrogen peroxide. Blank sections stained only with the secondary antibodies were used as negative controls. In addition, some sections were incubated with the antigenic peptide before sGC immunohistochemistry.

Double-labeling immunohistochemistry was conducted by incubating the sections following a two-step protocol. The sections were first incubated with anti-sGC β1 and the immunoreaction was visualized with 0.05% diaminobenzidine and 0.01% hydrogen peroxide. Subsequently, the sections were incubated with anti-GFAP antibodies (Dako, dilution 1:100). The immunoreaction was visualized with NH_4NiSO_4 (0.05 M) in phosphate buffer (0.1 M), diaminobenzidine, NH_4Cl, and 0.01% hydrogen peroxide. The first primary antibody was recognized as a brown homogeneous precipitate, whereas the second primary antibody was recognized as a dark blue precipitate. Other sections were first incubated with anti-GFAP (brown precipitate) and then with anti-βA4-amyloid antibodies (Boehringer-Mannheim, dilution 1:15) (dark blue precipitate).

Double-labeling immunofluorescence and confocal microscopy

Dewaxed sections were stained with a saturated solution of Sudan black B (Merck) for 30 min to block the autofluorescence of lipofuscin granules present in nerve cell bodies, rinsed in 70% ethanol, and washed in distilled water. The sections were incubated, at 4°C overnight, with the anti-sGC β1 antibody (Sigma) at a dilution of 1:1000 and monoclonal mouse anti-GFAP antibody at a dilution of 1:500 in a vehicle solution composed of Tris buffer, pH 7.2, containing 15 mmol/l NaN_3, and protein (Dako). After washing in PBS, the sections were incubated in the dark with the cocktail of secondary antibodies, diluted in the same vehicle solution as the primary antibodies, during 45 min at room temperature. Secondary antibodies were Alexa488 anti-rabbit and Alexa546 anti-mouse (both from Molecular Probes), and they were used at a dilution of 1:400. After washing in PBS, the sections were mounted in immuno-Fluore Mounting medium (ICN Biomedicals), sealed, and dried overnight. Sections were examined in a Leica TCS-SL confocal microscope.

Statistical analysis

Data were analyzed with the program SPSS v. 12.0 using least significant difference test (LSD). Level of significance $P < 0.05$.

Table 1
Characteristics of AD patients and age-matched controls

Stage	Subject	Sex	Age	Postmortem time (h)	sGC activity (pmol cGMP/min/mg protein)		
					Basal	NO stimulated	Fold stimulation
N	1	M	80	21	40 ± 4	1329 ± 59	33
N	2	M	79	7	78 ± 4	2575 ± 24	33
N	3	F	63	17	40 ± 2	974 ± 25	24
N	4	M	78	19	48 ± 1	1165 ± 60	24
N	5	F	73	5.3	96 ± 10	4265 ± 317	44
N	6	F	80	3.30	45 ± 6	1277 ± 49	28
Means ± SEM			75.5 ± 3	12 ± 4	58 ± 10	1931 ± 521	31 ± 3
A	13	F	80	13	42 ± 3	2042 ± 102	47
A	14	M	66	15	78 ± 8	3274 ± 39	42
A	15	M	79	18	60 ± 12	4847 ± 330	81
Means ± SEM			75 ± 5	15 ± 2	60 ± 10	3388 ± 812	57 ± 12
B	16	M	74	24	34 ± 2	861 ± 7	25
B	17	M	81	18	29 ± 3	1733 ± 14	60
B	18	F	85	15	73 ± 3	4354 ± 34	60
Means ± SEM			80 ± 3	19 ± 4	45 ± 14	2316 ± 1050	48 ± 12
C	7	F	82	10	52 ± 5	2165 ± 160	42
C	8	F	86	10	41 ± 3	1808 ± 216	44
C	9	M	64	6	39 ± 3	974 ± 25	25
C	10	F	78	19	65 ± 12	2360 ± 275	36
C	11	M	93	7.2	105 ± 10	3920 ± 305	37
C	12	F	84	2	130 ± 15	1890 ± 220	14
Means ± SEM			81 ± 4	9 ± 3	72 ± 15	2186 ± 397	33 ± 5

Basal and NO-stimulated sGC activities in soluble fraction from frontal cortex. Basal or DEA/NO (2 μM)-stimulated sGC activities were measured in cytosolic fractions of frontal cortex (area 8) from controls (N) and AD cases with variable stages of amyloid burden. A: no isocortical plaques; B: a few plaques; and C: large numbers of senile plaques. No statistical correlation was found between disease stage, age, sex, or postmortem delay time (LSD test).

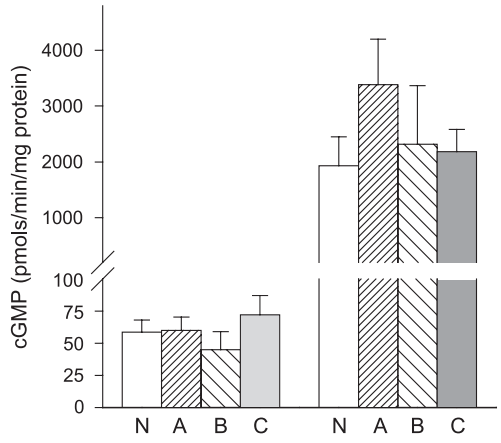

Fig. 2. Soluble guanylyl cyclase activity in frontal cortex of AD patients and age-matched controls. Mean ± SEM values of basal and DEA/NO-stimulated sGC activities of control subjects and AD disease groups presented in Table 1. Differences between group mean values did not reach statistical significance.

Results

Basal and NO-stimulated sGC activities are not altered in cortical soluble fractions from AD patients

Basal and DEA/NO-stimulated GC activity was measured in soluble fractions (100,000 × *g*) of the frontal cortex (area 8) from AD cases with variable amounts of amyloid and in age-matched controls. Results are shown in Table 1, together with the characteristics (age, sex, and postmortem delay time) of the subjects studied. Mean values for basal and DEA/NO-stimulated sGC activities of the different groups are summarized in Fig. 2. Statistical analysis indicated that there are no significant differences in sGC activities between the groups. Furthermore, no significant correlation was found between the individual sGC activities and disease stage, age, sex, or postmortem delay time.

sGC β1 and α1 subunit protein content is not altered in cortical soluble fractions from AD patients

The content of sGC β1 and α1 subunit protein was analyzed by immunoblotting in the same soluble extracts used for determination of sGC activity (Fig. 3). Representative immunoblots of β1 and α1

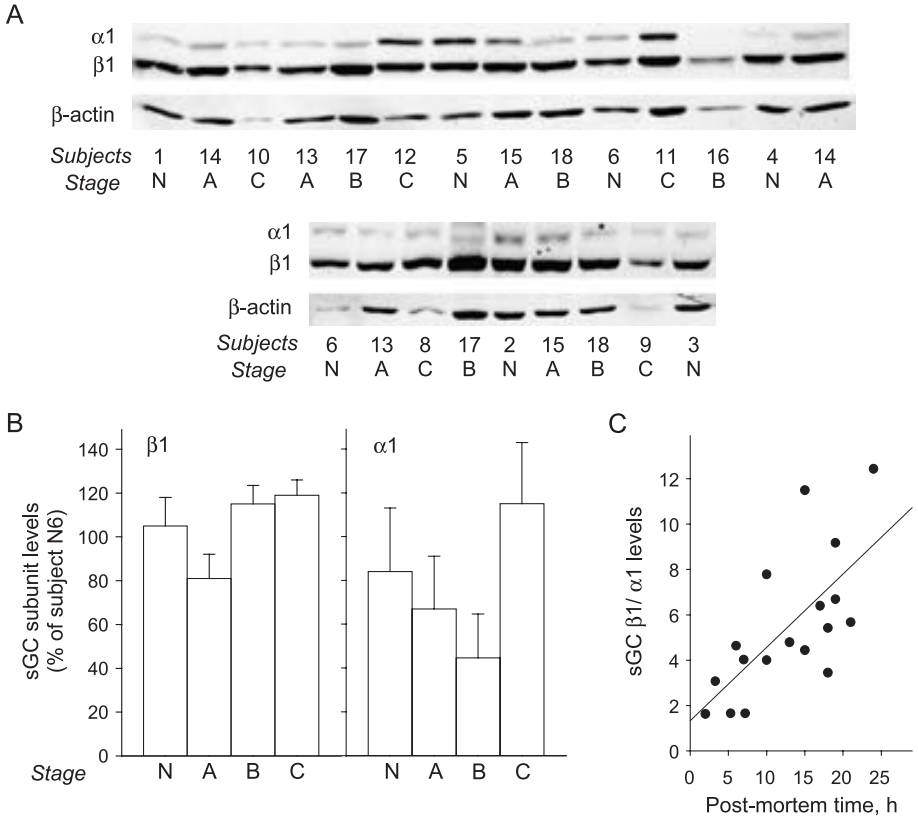

Fig. 3. Analysis of sGC β1 subunit protein in soluble fractions from frontal cortex of AD patients and matched controls. Equal amounts of protein (12 μg) from soluble fractions (100,000 × *g*) of frontal cortex (area 8) of controls (N, subjects 1–6) and AD patients in stages A (subjects 13–15), B (subjects 16–18), and C (subjects 7–12) were fractionated by SDS-PAGE and transferred to PDVF membranes. Immunoreactive sGC β1 (70 kDa) and α1 (80 kDa) subunits were detected using a 1:4000 dilution of the respective polyclonal antibodies. β-actin, used as loading control, was detected with a 125,000 dilution of a monoclonal antibody. (A) Immunoblots representative of three to six replications for β1 and two to four replications for α1. (B) Immunoreactive bands were analyzed by densitometry and following normalization to β-actin levels, the values were expressed relative to normal subject 6 (N6) that was included in all blots. Data shown are means ± SEM of six subjects in control and AD stage C groups and three subjects in AD stages A and B groups. Differences between groups were not statistically significant. (C) Plot of β1/α1 values vs. postmortem delay time for each subject (statistically significant correlation, $P < 0.02$). Line corresponds to the best fit by linear regression analysis (linear correlation coefficient: 0.68; slope: 0.32).

subunits, together with β-actin used as loading control, are shown in Fig. 3A. Results from the densitometric analysis of the bands performed in three to six replications per individual for β1 and two to four for α1 are shown in Fig. 3B. Levels of α1 were more variable than those of β1, but no significant differences were observed for either subunit between control and AD brains at different stages of the disease. However, a positive correlation was found between individual ratios β1/α1 and the postmortem delay time which may be an indication that the subunits differ in stability.

sGC β1 expression in cortical areas of human brain

There is no information available about the cellular localization of sGC in human brain cells. In order to investigate the possibility that alterations in sGC expression could occur only in particular cell populations, we first examined by immunohistochemistry the localization of the β1 subunit in cortical structures of normal brain. The β1 subunit is the obligate monomer in active sGC heterodimers and the only sGC subunit for which, at least in our hands, the commercially available antibody is suitable for immunohistochemistry. As shown in Figs. 4A–E, sGC β1 immunoreactivity was present in the majority of, if not all, neurons in the cerebral cortex, entorhinal cortex, subiculum, cellular layer of the hippocampus, and neurons of the dentate gyrus and hilus in control cases. sGC immunoreactivity decorated also fibrillar astrocytes of the subcortical white matter (Fig. 4F) but was barely detectable in protoplasmic astrocytes in the cerebral cortex. The immunostaining was specific as pretreatment with the immunogenic peptide abolished the immunoreaction (Fig. 4G). Double-labeling immunofluorescence for sGC β1 and the astrocytic marker

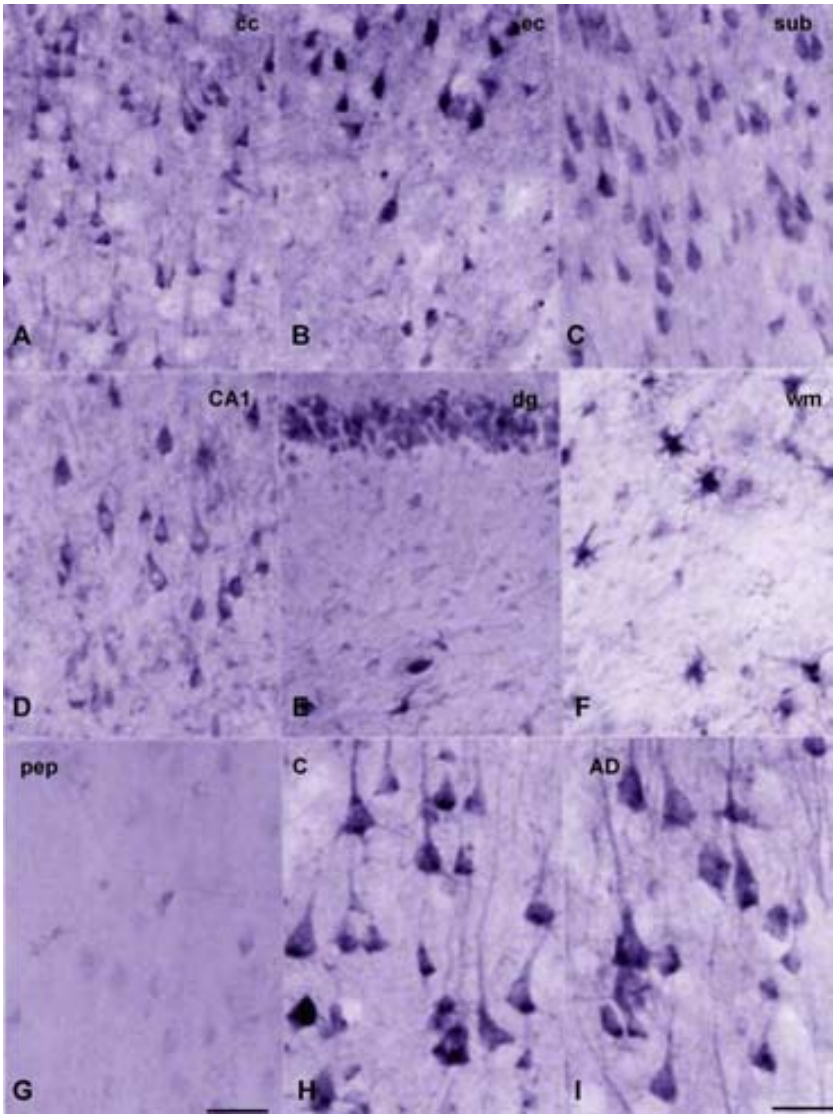

Fig. 4. sGC β1 subunit immunoreactivity in control and AD brains. Cryostat sections (30 μm thick) processed free floating were incubated with a 1:1000 dilution of rabbit polyclonal anti-β1 antibody. Representative sections of cerebral cortex, cc (A); entorhinal cortex, ec (B); subiculum, sub (C); cellular layers of the hippocampus, CA1 (D); dentate gyrus, dg and hilus (E); and subcortical white matter, wm (F) in the control human brain. sGC immunoreactivity is found in the majority of, if not all, neurons and in fibrillary astrocytes of the white matter. The immunoreaction is specific as preincubation with the antigenic peptide (pep) abolishes sGC immunoreactivity (G). Similar staining is observed in control: C (H) and AD (I) cases. A–G, scale bar in G = 25 μm; H and I, scale bar in I = 10 μm.

GFAP and confocal microscopy further supported the observation of sGC β1 immunoreactivity in fibrillar astrocytes in normal white matter (Figs. 7A–C).

sGC β1 expression is down-regulated in reactive astrocytes but not in neurons in AD cases

No apparent differences in sGC β1 staining were observed in cortical neurons of control and AD cases (Figs. 4H and I). Double-labeling immunohistochemistry for sGC β1 and GFAP also showed sGC β1 immunoreactivity in fibrillar astrocytes in AD white matter (Fig. 5A). Yet markedly reduced sGC β1 immunoreactivity was shown in reactive astrocytes characterized by enlarged cytoplasm strongly immunoreactive for GFAP, including those surrounding amyloid plaques, in the cerebral cortex, and immediate subcortical white matter in AD (Figs. 5B–D). This was further demonstrated in double-stained sections examined with confocal microscopy (Figs. 7D–F).

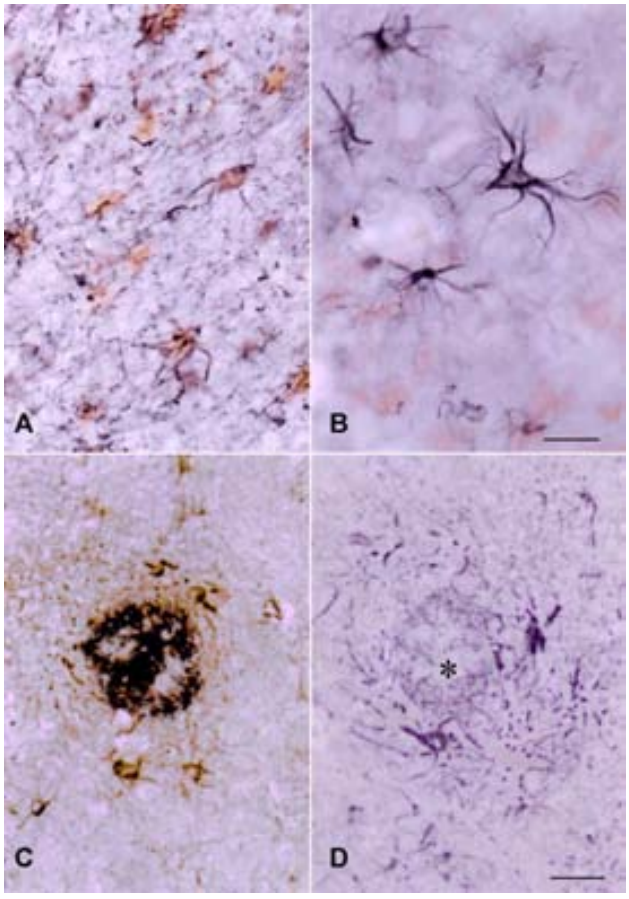

Fig. 5. sGC β1 immunohistochemistry of astrocytes. Double immunohistochemistry for GFAP and sGC β1 in the white matter (A) and cerebral cortex (B and D) in AD. In sections A, B, and D, GFAP is visualized as a dark blue precipitate whereas sGC β1 as a brown precipitate. Sections C and D are consecutive sections of a similar area focused on a senile (amyloid plaque) and separated about 50 μm. The amyloid core in C is recognized as a blue precipitate and astrocytes (visualized with anti-GFAP) are brown. Fibrillar astrocytes in the white matter show sGC immunoreactivity (A), whereas reactive astrocytes (B) are negative. This is further illustrated in C and D in which reactive astrocytes surrounding amyloid plaques are not stained with anti-sGC β1 antibodies. Cryostat sections processed free floating. A and B, scale bar in B = 10 μm; C and D, scale bar in D = 25 μm.

sGC β1 expression is down-regulated in reactive astrocytes in sCJD and MS cases

To obtain further evidence on the down-regulation of sGC β1 expression in reactive astrocytes, we examined brains of patients with sCJD and MS that present intense astroglial reactivity in the white matter. Immunohistochemistry disclosed sGC β1 immunoreactivity in remaining neurons in the cerebral cortex in sCJD but reduced sGC β1 immunostaining in cells in the white matter (Figs. 6A and C). This was in striking contrast with the large amount of reactive astrocytes in consecutive sections stained with anti-GFAP antibodies (Figs. 6B and D, respectively) as usually seen in sCJD. Similar observations were made in MS cases. Very few sGC-positive astrocytes were observed in subacute plaques, which were recognized by their positivity to GFAP in consecutive sections of the damaged white matter (Figs. 6E and F). Confocal microscopy studies further supported that sGC β1 immunoreactivity is almost absent in strongly GFAP-positive reactive astrocytes in the white matter in sCJD brains (Figs. 7G–I). No signal was observed in sections incubated only with the secondary antibodies (Figs. 7J–L).

Discussion

The neuronal NO/cGMP signaling pathway coupled to NMDA glutamate receptor stimulation has been implicated in the modulation of processes critical for normal CNS function, namely, brain development and synaptic plasticity (Garthwaite and Boulton, 1995; Zhang and Snyder, 1995). On the other hand, neuronal NO overproduction and subsequent formation of more reactive nitrogen oxides are believed to contribute to excitotoxic cell death (Gross and Wolin, 1995; Szabó, 1996), whereas cGMP appears to have neuroprotective actions (Ciani et al., 2002; Estevez et al., 1998; Kim et al., 1999). Enzymatic components of the NO/cGMP system are also constitutively expressed in astroglial cells, and regulation of astroglial function by NO and cGMP is likely to contribute to some of the neuromodulatory actions of NO since three important aspects of astroglial physiology relevant for neuronal function—calcium homeostasis, gene expression, and survival—are regulated by the NO–cGMP protein kinase G pathway (García and Baltrons, 2003). Additionally, activation of glial cells by infectious or inflammatory agents leads to induction of NOS2 and sustained production of NO that may contribute to neuronal damage (Loihl and Murphy, 1998). Increased expression of NOS2 in reactive astroglia has been reported in neurodegenerative diseases associated with chronic neuroinflammation in humans. In AD brains, expression of all NOS isoforms has been shown in reactive astrocytes surrounding β-amyloid plaques (Wallace et al., 1997). In contrast, NO-stimulated sGC activity was reported decreased in homogenates of the temporal lobe of AD patients (Bonkale et al., 1995). Our recent observation that aggregated β-amyloid peptides and other agents that induce astroglial reactivity (LPS, IL-1β) cause a decrease in sGC protein and mRNA in rat astrocytes (Baltrons et al., 2002; Pedraza et al., 2003), and that IL-1β lowers NO-dependent cGMP formation in human fetal astrocytes (García and Baltrons, 2003) prompted us to examine if the reported decrease in sGC in AD brains occurred in astrocytes.

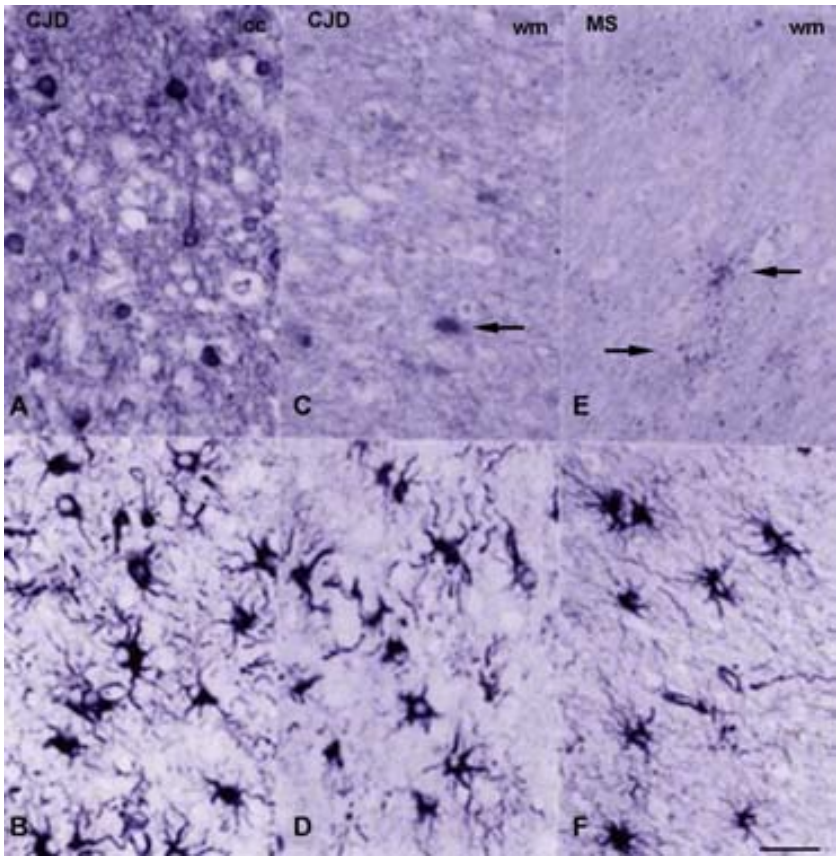

Fig. 6. Comparison between sGC β1 and GFAP immunostaining in sCJD and MS brains. sGC β1 (sGC; A, C, and E) and GFAP (B, D, and F) immunohistochemistry in consecutive corresponding sections of the cerebral cortex (cc; A and B) and white matter (wm; C–F) in sCJD (A–D) and in chronic plaques in MS (E and F) at the same magnification. sGC immunoreactivity is found in neurons (A) but only in a few cells (arrows) in the white matter (C and E), which are otherwise filled with reactive astrocytes (B, D, and F). Cryostat sections processed free floating. Scale bar = 25 μm.

In this study, we have not observed a significant difference in basal sGC activity in cortical cytosolic fractions from controls and AD patients in different stages of the disease. In agreement with this, no significant differences were detected in the levels of the sGC β1 and α1 subunit protein analyzed by Western blot in the same fractions. Levels of the α1 subunit showed more variability than those of the β1, and statistical analysis of the variation in the β1/α1 relationship showed a positive correlation with the postmortem delay time suggesting that the α1 subunit may be less stable. In contrast to the results of Bonkale et al. (1995), we have not observed significant differences in NO-stimulated sGC activity between normal and AD brains. We do not have a plausible explanation for the discrepancy. NO-stimulated sGC activity measured by us is much higher and shows more individual variability that could not be related to disease stage, age, sex, or postmortem delay time. Variations in NO-stimulated sGC activity could arise from differences in NO scavenging environments, for instance differences in superoxide generating systems or in the activity of endogenous NO inactivating mechanisms (Griffiths et al., 2002; Keynes et al., 2003).

Although our results on basal or NO-stimulated activity in cortical cytosolic fractions indicated that AD is not associated with a significant alteration in the level of sGC protein or the capacity of the enzyme to respond to NO, the possibility of local or cellular changes in sGC expression was investigated by immunocytochemical methods. The cellular expression of sGC protein in human brain had not been previously reported probably due to the unavailability of suitable antibodies. In this work, we have used a commercial antibody generated against a peptide of β1 that detects a single protein band on Western blots to assess the cellular distribution and possible alterations of the sGC subunit in cortex of human brain. The suitability of the antibody for immunohistochemistry was shown by the absence of labeling when the antibody was preabsorbed with the antigenic peptide. The β1 subunit is an obligate partner in the functional sGC heterodimers identified so far (Buechler et al., 1991; Harteneck et al., 1990). In humans, a single transcript for β1 has been identified and its expression reported to be higher than that of the α1 and α2 subunit mRNAs in all brain regions (Budworth et al., 1999). As occurs in the rat (Furuyama et al., 1993; Gibb and Garthwaite, 2001; Matsuoka et al., 1992), the β1 mRNA appears to have a wider distribution than the α1 and α2 mRNAs. Results from our immunocytochemical studies with the anti-sGC β1 antibody show a strong and widespread labeling of neurons in cortical and hippocampal structures both in normal as well as in AD brains. In contrast, sGC β1 immunostaining was strong in fibrillar astrocytes of subcortical white matter but low or undetectable in protoplasmic astrocytes. The pattern and intensity of staining was similar in normal and diseased brains, but double labeling for GFAP and sGC revealed that reactive astrocytes in the cerebral cortex and subcortical white matter, including those surrounding amyloid plaques, had markedly reduced sGC β1 immunoreactivity. This is

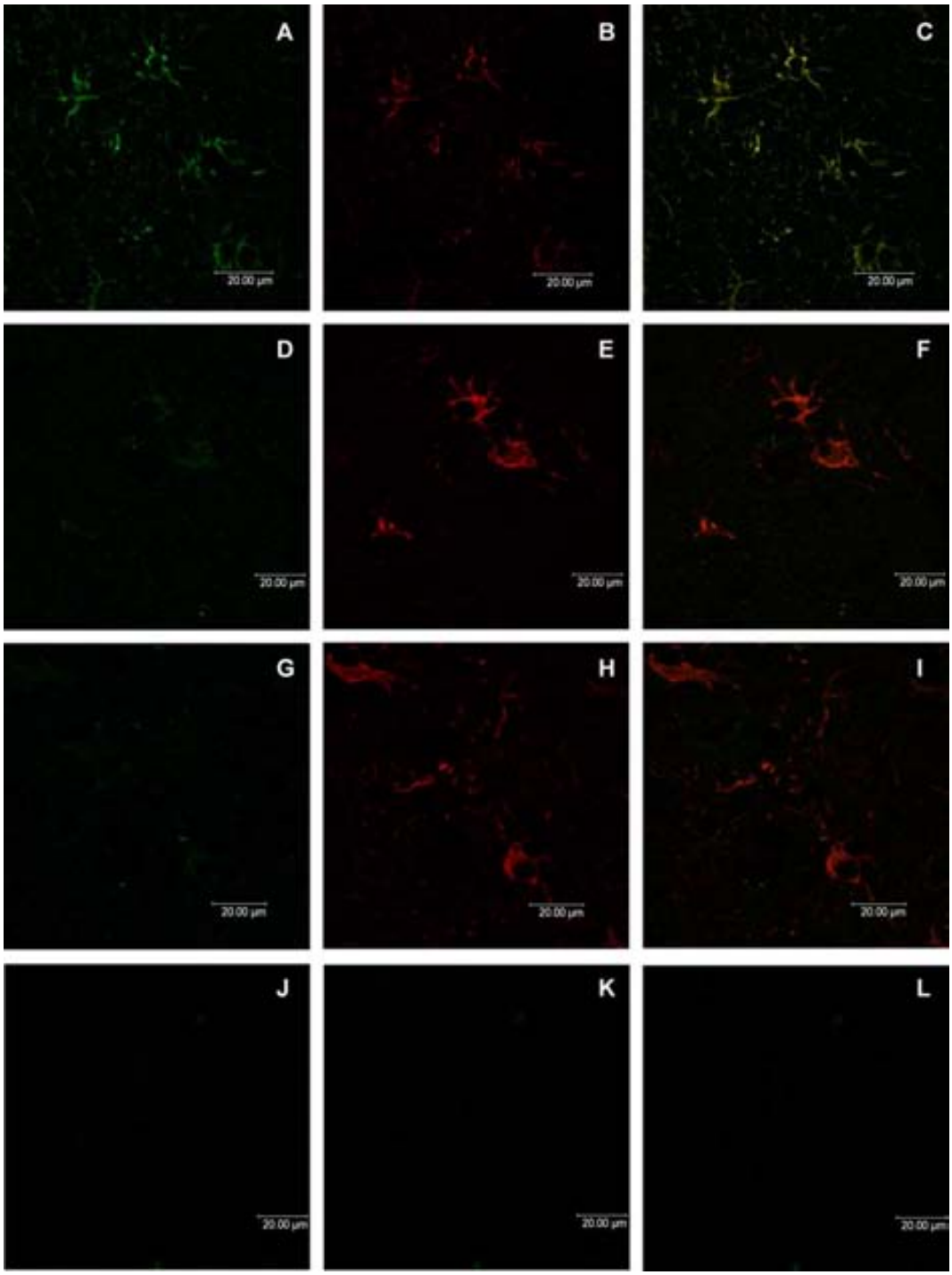

Fig. 7. Double-labeling immunofluorescence for GFAP and sGC β1 and confocal microscopy in normal, AD, and sCJD brains. sGC β1 immunoreactivity (green) colocalizes with GFAP (red) in fibrillar astrocytes in the subcortical white matter of control brains (merge, yellow), as seen in the upper panel (A–C). sGC β1 immunoreactivity is markedly reduced in reactive astrocytes (strong GFAP, red) surrounding amyloid cores in AD (D–F). Similarly, almost absent sGC immunoreactivity is found in reactive astrocytes in the white matter in sCJD (G–I). No signal is observed in samples incubated with the secondary antibodies alone (J–L).

in agreement with our in vitro observation that sGC is down-regulated in astrocytes exposed to aggregated β-amyloid peptides or the proinflammatory cytokine IL-1β whose levels are elevated in AD brains (Mrak and Griffin, 2001), whereas sGC is not altered in a neuronal population (cerebellar granule cells) treated with the same agents (Baltrons et al., 2002; Pedraza et al., 2003). Neurons have been shown to respond to proinflammatory cytokines with induction of NOS2 (Heneka and Feinstein, 2001), but they may lack components of the pathway involved in sGC down-regulation. Alternatively, differently regulated sGC isoforms may be expressed in neurons and astrocytes. Knowledge about cellular expression of the different sGC subunits is lacking. In cultured rat cerebellar

astrocytes, treatment with IL-1β can diminish sGC protein by two mechanisms (Pedraza et al., 2003). The cytokine first decreases the half-life of the β1 subunit protein in a transcription- and translation-dependent manner. The increase in the rate of sGC β1 degradation, which is independent of NOS induction and NO formation, is prevented by proteasome inhibitors (Baltrons and García, unpublished observations), but the mechanism determining the fate of sGC is unknown at present. Recent evidence has demonstrated the occurrence of the α2β1 isoform in rat brain synaptosomes and its association with the presynaptic density protein-95 (PSD-95) by direct interaction between the C-terminal amino acids of the α2 subunit and a PDZ domain of PSD-95 (Russwurm et al., 2001). The interaction with PSD-95 results in membrane association and may cause the formation of a 'transducisome' with NMDA receptors and NOS1 that also bind to PDZ domains of PSD-95 (Russwurm and Koesling, 2002). It is possible that formation of this complex protects the neuronal α2β1 isoform from degradation. IL-1β also decreases sGC subunit mRNA levels in astrocytes in an NO-dependent manner (Pedraza et al., 2003). Since sGC is a low turnover protein, this second mechanism will contribute to maintain sGC levels low for prolonged periods of time. Decreased sGC mRNA and protein levels have been reported in cells of neural and peripheral origin exposed for long periods of time to NO donors (Ferrero and Torres, 2002; Filippov et al., 1997; Sardón et al., 2004). Thus, increased NO production as demonstrated in the vicinity of amyloid plaques in AD may contribute to down-regulate sGC in reactive astrocytes.

Since sGC β1 immunoreactivity is more evident in white matter fibrillar astrocytes than in grey matter protoplasmic astrocytes to obtain stronger evidence for a diminished expression of sGC in reactive astrocytes, we examined sGC β1 immunoreactivity in the brains of patients affected by sCJD and MS, diseases that present strong glial reactivity in the white matter. In these cases, sGC β1 immunostaining was found in preserved cortical neurons but rarely in white matter where numerous and huge reactive astrocytes are present. We have previously observed a diminished NO-dependent cGMP formation in human fetal astrocytes exposed to IL-β1 and INF-ã (García and Baltrons, 2003). Thus, increased release of proinflammatory cytokines by infiltrating monocytes or activated microglia may be responsible for sGC down-regulation in the brains of sCJD and MS.

The functional significance of decreased sGC expression in reactive astrocytes is difficult to ascertain at present since little is know about the role of cGMP in normal astrocyte physiology or pathophysiology. As shown in rat brain slices immunostained with a cGMP antibody, astroglial sGC is a target of NO generated in neurons (De Vente and Steinbusch, 1992). Additionally, synaptically released neurotransmitters (norepinephrine, glutamate) can stimulate the NO/cGMP signaling pathway in neighboring astrocytes by increasing intracellular calcium (Agulló and García, 1992; Baltrons and García, 1997). An impairment of the astroglial NO/cGMP system may negatively affect neuronal function since this transduction pathway appears to be implicated in the control of neurotrophic factor release (Xiong et al., 1999) and in the generation of calcium waves (Willmott et al., 2000), a phenomenon relevant for the bidirectional communication between neurons and astrocytes (Araque et al., 2001). On the other hand, a decrease of sGC in reactive astrocytes may constitute an adaptive mechanism to prevent excess cGMP signaling in a situation of high NO production. The lack of such a mechanism in neurons may have some bearing on their higher vulnerability of these cells to the cytotoxic effects of excess NO.

Increasing evidence points to a role of cGMP in the regulation of inflammatory gene expression (Pilz and Casteel, 2003). Regulation by cGMP of the expression of NOS2, COX2, and TNF-α has been reported in different cell types. Although both positive and negative effects have been found depending on the cell type and the stimulus, in macrophages and glial cells, cGMP appears to be inhibitory (Kiemer and Vollmar, 1998; Kiemer et al., 2000; Paris et al., 1999). Thus, it is appealing to hypothesize that a decreased capacity to synthesize cGMP in response to NO in activated astrocytes may have a permissive effect on the inflammatory response of these cells. This possibility is presently under investigation.

Acknowledgments

This work was supported in part by SAF 2001-2540 and SGR2001-212 grants to A.G. and by UE contract BrainNet II and FIS grant G03-006 to I.F. P. Pifarré is the recipient of a predoctoral fellowship from MECD (Spain).

References

Agulló, L., García, A., 1992. Characterization of noradrenaline-stimulated cyclic GMP formation in brain astrocytes in culture. Biochem. J. 288, 619–624.

Araque, A., Carmignoto, G., Haydon, P.G., 2001. Dynamic signaling between astrocytes and neurons. Annu. Rev. Physiol. 63, 795–813.

Ariano, M.A., Lewicki, J.A., Brandwein, H.J., Murad, F., 1982. Immunohistochemical localization of guanylate cyclase within neurons of rat brain. Proc. Natl. Acad. Sci. U. S. A. 79, 1316–1320.

Baltrons, M.A., García, A., 1997. AMPA receptors are couple to the nitric oxide/cyclic GMP pathway in cerebellar astroglial cells. Eur. J. Neurosci. 9, 2497–2501.

Baltrons, M.A., García, A., 1999. Nitric oxide-independent down-regulation of soluble guanylyl cyclase by bacterial endotoxin in astroglial cells. J. Neurochem. 73, 2149–2157.

Baltrons, M.A., Pedraza, C.E., Heneka, M.T., García, A., 2002. β-Amyloid peptides decrease soluble guanylyl cyclase expression in astroglial cells. Neurobiol. Dis. 10, 139–149.

Bonkale, W.L., Winblad, B., Ravid, R., Cowburn, R.F., 1995. Reduced nitric oxide responsive soluble guanylyl cyclase activity in the superior temporal cortex of patients with Alzheimer's disease. Neurosci. Lett. 187, 5–8.

Braak, H., Braak, E., 1999. Temporal sequence of Alzheimer's disease related pathology. In: Peters, A., Morrison, J.H. (Eds.), Cerebral Cortex, Neurodegenerative and Age-Related Changes in Structure and Function of Cerebral Cortex vol. 14. Kluwer Academic/Plenum Publishers, pp. 475–512.

Budworth, J., Meillerais, S., Charles, I., Powell, K., 1999. Tissue distribution of the human soluble guanylate cyclases. Biochem. Biophys. Res. Commun. 263, 696–701.

Buechler, W.A., Nakane, M., Murad, F., 1991. Expression of soluble guanylate cyclase activity requires both enzyme subunits. Biochem. Biophys. Res. Commun. 174, 351–357.

Ciani, E., Virgili, M., Contestabile, A., 2002. Akt pathway mediates a cGMP-dependent survival role of nitric oxide in cerebellar granule neurones. J. Neurochem. 81, 218–228.

Cunningham, C., Konsman, J.P., Cartmell, T., 2002. Cytokines and the ageing brain. Trends Neurosci. 25, 546–547.

De la Monte, S.M., Bloch, K.D., 1997. Aberrant expression of the

constitutive endothelial nitric oxide synthase gene in Alzheimer disease. Mol. Chem. Neuropathol. 30, 139–159.

De Vente, J., Steinbusch, H.W.M., 1992. On the stimulation of soluble and particulate guanylate cyclase in the rat brain and the involvement of nitric oxide as studied by cGMP immuno-cytochemistry. Acta Histochem. 92, 13–38.

Estevez, A.G., Spear, N., Thompson, J.A., Cornwell, T.L., Radi, R., Barbeito, L., Beckman, J.S., 1998. Nitric oxide-dependent production of cGMP supports the survival of rat embryonic motor neurons cultured with brain-derived neurotrophic factor. J. Neurosci. 18, 3708–3714.

Ferrer, I., Ribera, R., Blanco, R., Martí, E., 1999. Expression of proteins linked with exocytosis and neurotransmission in patients with Creutzfeldt-Jakob disease. Neurobiol. Dis. 6, 92–100.

Ferrero, R., Torres, M., 2002. Prolonged exposure of chromaffin cells to nitric oxide down-regulates the activity of soluble guanylyl cyclase and corresponding mRNA and protein levels. BMC Biochem. 3, 1471–2091.

Filippov, G., Bloch, D.B., Bloch, K.D., 1997. Nitric oxide decreases stability of mRNAs encoding soluble guanylate cyclase subunits in rat pulmonary artery smooth muscle cells. J. Clin. Invest. 100, 942–948.

Förstermann, U., Boissel, J.-P., Kleinert, H., 1998. Expressional control of the 'constitutive' isoforms of nitric oxide synthase (NOS I and NOS III). FASEB J. 12, 773–790.

Furuyama, T., Inagaki, S., Takagi, H., 1993. Localizations of α1 and β1 subunits of soluble guanylate cyclase in the rat brain. Mol. Brain Res. 20, 335–344.

García, A., Baltrons, M.A., 2003. The nitric oxide/cyclic GMP signalling pathway in CNS glial cells. Adv. Mol. Cell Biol. 31, 575–594.

Garthwaite, J., Boulton, C.L., 1995. Nitric oxide signalling in the central nervous system. Annu. Rev. Physiol. 57, 683–706.

Gibb, B.J., Garthwaite, J., 2001. Subunits of the nitric oxide receptor, soluble guanylyl cyclase, expressed in rat brain. Eur. J. Neurosci. 13, 539–544.

Griffiths, C., Yamini, B., Hall, C., Garthwaite, J., 2002. Nitric oxide inactivation in brain by a novel O_2-dependent mechanism resulting in the formation of nitrate ions. Biochem. J. 362, 459–464.

Gross, St., Wolin, M.S., 1995. Nitric oxide: pathophysiological mechanisms. Annu. Rev. Physiol. 57, 237–269.

Harteneck, C., Koesling, D., Soling, A., Schultz, G., Bohme, E., 1990. Expression of soluble guanylyl cyclase. Catalytic activity requires two enzyme subunits. FEBS Lett. 272, 221–223.

Heneka, M.T., Feinstein, D.L., 2001. Expression and function of inducible nitric oxide synthase in neurons. J. Neuroimmunol. 114, 8–18.

Ibarra, C., Nedvetsky, P.I., Gerlach, M., Riederer, P., Schmidt, H.H.H., 2001. Regional and age-dependent expression of the nitric oxide receptor, soluble guanylyl cyclase, in the human brain. Brain Res. 907, 54–60.

Keynes, R.G., Griffiths, C., Garthwaite, J., 2003. Superoxide-dependent consumption of nitric oxide in biological media may confound in vitro experiments. Biochem. J. 369, 399–406.

Kiemer, A.K., Vollmar, A.M., 1998. Autocrine regulation of inducible nitric-oxide synthase in macrophages by atrial natriuretic peptide. J. Biol. Chem. 273, 13444–13551.

Kiemer, A.K., Hartung, T., Vollmar, A.M., 2000. cGMP-mediated inhibition of TNF-alpha production by the atrial natriuretic peptide in murine macrophages. J. Immunol. 165, 175–181.

Kim, Y.-M., Chung, H.-T., Kim, S.-S., Han, J.-A., Yoo, Y.-M., Kim, K.-M., Lee, G.-H., Yun, H.-Y., Green, A., Li, J., Simmons, R.L., Billiar, T.R., 1999. Nitric oxide protects PC12 cells from serum deprivation-induced apoptosis by cGMP-dependent inhibition of caspase signaling. J. Neurosci. 19, 6740–6747.

Loihl, A.K., Murphy, S., 1998. Expression of NOS-2 in glia associated with CNS pathology. Prog. Brain Res. 118, 253–267.

Lüth, H.J., Holzer, M., Gertz, H.J., Arendt, T., 2000. Aberrant expression of nNOS in pyramidal neurons in Alzheimer's disease is highly co-localized with p21ras and p16INK4a. Brain Res. 852, 45–55.

Lüth, H.J., Holzer, M., Gartner, U., Staufenbiel, M., Arendt, T., 2001. Expression of endothelial and inducible NOS-isoforms is increased in Alzheimer's disease, in APP23 transgenic mice and after experimental brain lesion in rat: evidence for an induction by amyloid pathology. Brain Res. 913, 57–67.

Lüth, H.J., Munch, G., Arendt, T., 2002. Aberrant expression of NOS isoforms in Alzheimer's disease is structurally related to nitrotyrosine formation. Brain Res. 953, 135–143.

Matsuoka, I., Giuli, D., Poyard, M., Stengel, D., Parma, J., Guellaen, G., Hanoune, J., 1992. Localization of adenylyl and guanylyl cyclase in rat brain by in situ hybridization: comparison with calmodulin mRNA distribution. J. Neurosci. 12, 3350–3360.

Mrak, R.E., Griffin, W.S., 2001. Interleukin-1, neuroinflammation, and Alzheimer's disease. Neurobiol. Aging 22, 903–908.

Nakane, M., Ichikawa, M., Deguchi, T., 1983. Light and electron microscopic demonstration of guanylate cyclase in rat brain. Brain Res. 273, 9–15.

Paris, D., Town, T., Parker, T.A., Tan, J., Humphrey, J., Crawford, F., Mullan, M., 1999. Inhibition of Alzheimer's beta-amyloid induced vasoactivity and proinflammatory response in microglia by a cGMP-dependent mechanism. Exp. Neurol. 157, 211–221.

Pedraza, C.E., Baltrons, M.A., Heneka, T.M., García, A., 2003. Interleukin-1β and lipopolysaccharide decrease soluble guanylyl cyclase in cells of the CNS: NO-independent destabilization of protein and NO-dependent decrease of mRNA. J. Neuroimmunol. 144, 80–90.

Pilz, R.B., Casteel, D.E., 2003. Regulation of gene expression by cyclic GMP. Circ. Res. 93, 1034–1046.

Russwurm, M., Koesling, D., 2002. Isoforms of NO-sensitive guanylyl cyclase. Mol. Cell. Biochem. 230, 159–164.

Russwurm, M., Wittau, N., Koesling, D., 2001. Guanylyl cyclase/PSD-95 interaction: targeting of the nitric oxide-sensitive α2/β1 guanylyl cyclase to synaptic membranes. J. Biol. Chem. 276, 44647–44652.

Sardón, T., Baltrons, M.A., García, A., 2004. Nitric oxide-dependent and independent down-regulation of NO-sensitive guanylyl cyclase in neural cells. Toxicol. Lett. 149, 75–83.

Simic, G., Lucassen, P.J., Krsnik, Z., Kruslin, B., Kostovic, I., Winblad, B., Bogdanovi, N., 2000. nNOS expression in reactive astrocytes correlates with increased cell death related DNA damage in the hippocampus and entorhinal cortex in Alzheimer's disease. Exp. Neurol. 165, 12–26.

Szabó, C., 1996. Physiological and pathological roles of nitric oxide in the central nervous system. Brain Res. Bull. 41, 131–141.

Teunissen, C., Steinbusch, H., Markerink-van Ittersum, M., Koesling, D., de Vente, J., 2001. Presence of soluble and particulate guanylyl cyclase in the same hippocampal astrocytes. Brain Res. 891, 206–212.

Wallace, M.N., Geddes, J.G., Farquhar, D.A., Masson, M.R., 1997. Nitric oxide synthase in reactive astrocytes adjacent to β-amyloid plaques. Exp. Neurol. 144, 266–272.

Willmott, N.J., Wong, K., Strong, A.J., 2000. A fundamental role for the nitric oxide-G-kinase signaling pathway in mediating intercellular Ca^{2+} waves in glia. J. Neurosci. 20, 1767–1779.

Xiong, H., Yamada, K., Jourdi, H., Kawamura, M., Takei, N., Han, D., Nabeshima, T., Nawa, H., 1999. Regulation of nerve growth factor release by nitric oxide through cyclic GMP pathway in cortical glial cells. Mol. Pharmacol. 56, 339–347.

Zabel, U., Weeger, M., LA, M., Schmidt, H.H.W., 1998. Human soluble guanylate cyclase: functional expression and revised isoenzyme family. Biochem. J. 335, 51–57.

Zhang, J., Snyder, S.H., 1995. Nitric oxide in the nervous system. Annu. Rev. Pharmacol. Toxicol. 35, 213–233.

7 Resumen Trabajo 3

En trabajos anteriores del laboratorio se estudió la regulación de la formación de GMPc por agentes inflamatorios (LPS, IL-1β, péptidos β-amiloides) que inducen reactividad glial y expresión de NOS-2. En estos estudios se demostró que estos agentes producían una disminución de la actividad enzimática de la GC_{NO}. El efecto era el resultado de una disminución de la vida media de subunidad β1, que es independiente de la inducción de la NOS-2 y de la generación de NO, pero que sin embargo requiere trascripción y síntesis de proteínas. En el presente trabajo demostramos que la disminución a nivel de proteína de la subunidad β1 inducida por el LPS en cultivos de astrocitos cerebelares de rata es prevenida por inhibidores específicos de la actividad del proteosoma (MG-132 y lactacistin) y no por inhibidores de otras proteasas lisosomales (leupeptin) o no lisosomales (inhibidor de la calpaína, inhibidor II ICE). La actividad del proteosoma es requerida para la activación del factor de transcripción NFκB, factor que media muchas de las acciones del LPS en células gliales. Para averiguar si el NFκB estaba implicado en el efecto del LPS sobre la β1 se examinó si inhibidores de la activación de este factor de transcripción (BAY-117082 y PDTC) eran capaces de impedir el efecto del LPS sobre la β1, pero se observó que mientras la actividad NOS era inhibida totalmente por estos inhibidores, la bajada de proteína β1 no se alteraba, lo que nos reforzaba la idea de que el proteosoma estaba directamente implicado en la degradación de esta proteína.

En otras células, la estabilidad de la GC_{NO} parece estar controlada por su interacción con la HSP90. Sin embargo, en este trabajo demostramos que en astrocitos la posible interacción HSP90 - GC_{NO} no tendría un papel en el mecanismo involucrado en la degradación acelerada de la subunidad β1, ya que ni el LPS alteraba los niveles de la HSP90 ni el tratamiento de las células durante 24 hs con inhibidores de la HSP90 afectaba a los niveles de la subunidad β1, contrariamente a lo que ocurre en otras células.

El análisis de los estudios inmunocitoquímicos y de microscopía confocal reveló que el LPS promueve la colocalización de la β1 en estructuras ricas en proteosoma 20S y ubiquitina en el núcleo celular con características de clastosomas, cuerpos nucleares implicados en la proteolisis vía ubiquitina-proteosoma. Sin embargo, en condiciones normales tanto la presencia de clastosomas como la colocalización β1 con los componentes de la vía ubiquitina-proteosoma resultó ser escasa. Por otro lado, también observamos que tanto inhibidores del proteosoma como de la síntesis de proteínas eran capaces de prevenir la formación de clastosomas y la colocalización en el núcleo de la subunidad β1 con la ubiquitina y el 20S

inducidas por el LPS. Estos resultados apoyarían el papel de estas estructuras nucleares en la degradación de la subunidad β1 en astrocitos durante la neuroinflamación.

LPS-INDUCED DOWN-REGULATION OF NO-SENSITIVE GUANYLYL CYCLASE IN ASTROCYTES OCCURS BY PROTEASOMAL DEGRADATION IN NUCLEAR BODIES

María Antonia Baltrons1, Paula Pifarré1, María Teresa Berciano2, Miguel Lafarga2, and Agustina García1

1Institute of Biotechnology and Biomedicine 'V. Villar Palasí' and Departament of Biochemistry and Molecular Biology, Autonomous University of Barcelona, 08193 Bellaterra, Spain and 2Department of Anatomy and Cell Biology and Biomedicine Unit, CSIC, University of Cantabria, Avd. Cardenal Herrera Oria, s/n, 39011 Santander, Spain.

To whom correspondence should be sent: María Antonia Baltrons:
Instituto de Biotecnología y Biomedicina V. Villar Palasí, Universidad Autónoma de Barcelona; 08193, Bellaterra, Spain.
e-mail: mariaantonia.baltrons@uab.es
Tel ++34-93 5811181
Tel Fax ++34 93 5812011

Submitted to Molecular and Cellular Neuroscience.

ABSTRACT

We previously showed that treatment with bacterial cell wall lipopolysaccharide (LPS) or pro-inflammatory cytokines decreases NO-sensitive guanylyl cyclase (GC_{NO}) activity in astrocytes by decreasing the half-life of the obligate GC_{NO} β1 subunit in a NO-independent but transcription- and translation-dependent process. Here we show that LPS-induced β1 degradation requires proteasome activity and is independent of NFκB activation or inhibition of β1 interaction with HSP90. Immunocytochemistry and confocal microscopy revealed that LPS promotes co-localization of the predominantly soluble β1 protein with ubiquitin and the 20S proteasome in nuclear aggregates that present characteristics of clastosomes, nucleoplasmic substructures involved in ubiquitin-proteasome-dependent nuclear proteolysis. Proteasome and protein synthesis inhibitors prevented LPS-induced clastosome assembly and nuclear co-localization of β1 with ubiquitin and 20S proteasome strongly supporting a role for these transient nuclear structures in GC_{NO} down-regulation during neuroinflammation.

INTRODUCTION

NO-sensitive guanylyl cyclase or soluble guanylyl cyclase (GC_{NO}; EC 4.6.1.2) is the best characterized target of NO and converts GTP into the second messenger cyclic GMP (cGMP), the recognized mediator of vasodilating and neuromodulatory actions of NO (Garthwaite and Boulton, 1995; Zhang and Snyder, 1995).

GC_{NO} largely exists as a heterodimer of α and β subunits that is activated by binding of NO to its heme prosthetic group. Two different α (α1-2) and β (β1-2) subunits have been cloned and sequenced but only $\alpha1\beta1$ and $\alpha2\beta1$ have been isolated as functional heterodimers (Russwurm and Koesling, 2002). In mammalian brain, immunocytochemical studies utilizing antibodies against GC_{NO} or cGMP have shown immunoreactivity in both neuronal and astroglial cells but not in microglia (Baltrons et al., 2004; Ding et al., 2004; Garcia and Baltrons, 2003; van Staveren et al., 2005).

GC_{NO} activity can be regulated by transcriptional, posttranscriptional and posttranslational mechanisms. Regulation by phosphorylation/dephosphorylation mechanisms have been reported with conflicting results (Ferrero et al., 2000; Meurer et al., 2005; Murthy, 2001; Murthy, 2004; Zwiller et al., 1985). Studies in vascular tissue in relation to the mechanism of development of tolerance to nitrovasodilators have revealed that an important regulator of GC_{NO} activity is its own activator NO. Subacute exposure to NO donors has been shown to desensitize GC_{NO} without altering GC_{NO} subunit expression in different cell types, apparently by means of a reversible oxidation, whereas more prolonged incubation with NO-generating agents reduces GC_{NO} subunit mRNA and protein (Davis et al., 1997; Papapetropoulos et al., 1996a; Sardon et al., 2004; Ujiie et al., 1994). In smooth muscle cells, the decrease in subunit mRNA appears to be due to loss of stability and occurs through a transcription- and translation-dependent process (Filippov et al., 1997). Recently, depletion of the mRNA binding protein HuR was implicated in the cGMP-dependent down-regulation of $\alpha1$ subunit mRNA (Kloss et al., 2003). In the same cells, GC_{NO} was also down-regulated by NO endogenously generated after induction of nitric oxide synthase type 2 (NOS-2) by treatment with bacterial wall lipopolysaccharide (LPS) or pro-inflammatory cytokines (Papapetropoulos et al., 1996a; Scott and Nakayama, 1998; Takata et al., 2001). Takata and colleagues showed that cytokines decreased GC_{NO} subunit protein by a NO- and transcription-dependent mechanism as well as by a NO-independent mechanism. NO-independent decrease in GC_{NO} levels has been also observed in pheochromocytoma PC12 cells treated with nerve growth factor (Liu et al., 1997a). In rat brain astroglial cultures we have shown a decrease in GC_{NO} after long-term treatment with LPS, pro-inflammatory cytokines or β-amyloid peptides, conditions that induce astroglial

reactivity and NOS-2 expression (Baltrons and Garcia, 1999; Baltrons et al., 2002; Pedraza et al., 2003). We demonstrated that the initial mechanism by which these agents decrease GC_{NO} activity involves a NO-independent but transcription- and translation-dependent decrease in the half-life of the β1 subunit protein although a NO-dependent decrease in subunit mRNA also occurs (Pedraza et al., 2003).

It has been recently reported that GC_{NO} protein stability can be regulated by interaction with chaperon proteins. In rat aortic smooth muscle cells Papapetropoulos et al., (2005) demonstrated that blockade of the interaction of GC_{NO} with heat shock protein 90 (HSP90) destabilizes the enzyme and promotes its proteosomal degradation. Down-regulation of GC_{NO} by C-type natriuretic peptide was also reported to involve proteasome activity (de Frutos et al., 2003).

The metabolic turnover of numerous proteins has been attributed to ubiquitylation and degradation by the 26S proteasome. The proteolytic core, the 20S proteasome. associates with two 19S regulatory complexes to form the 26S proteasome. Proteasomes are found both in the cytoplasm and the nucleus of eukaryotic cells. In the nucleus proteasomes are present throughout the nucleoplasm, concentrating in subnuclear structures such as splicing speckles (Chen et al., 2002; Rockel et al., 2005), promyelocytic leukemia protein bodies (PML) (Lallemand-Breitenbach et al., 2001; Rockel and von Mikecz, 2002) and clastosomes (Lafarga et al., 2002). Ubiquitin and the ubiquitin-attachment machinery are also found in cell nuclei (Anton et al., 1999; Lain et al., 1999; Plafker et al., 2004). In rat brain immunocytochemical studies utilizing antibodies against the 20S proteasome and ubiquitin have shown a prominent nuclear immunoreactivity in both neuronal and glial cells (Adori et al., 2005; Lafarga et al., 2002; Mengual et al., 1996).

The aim of this work was to investigated if the ubiquitin-proteasome-system (UPS) was implicated in LPS-induced GC_{NO} β1 degradation in astroglial cells. We show here that proteasome inhibitors prevent this LPS effect. We further demonstrate that while GC_{NO} β1 subunit protein is mainly cytoplasmic in untreated cells, LPS treatment promotes colocalization of β1 with ubiquitin and 20S proteasome in clastosomes, small transient nuclear structures involved in ubiquitin-proteasome-dependent proteolysis. Proteasome and protein synthesis inhibition prevents this effect. This report shows for the first time that LPS orchestrates the recruitment of GC_{NO} β1 protein and components of the UPS to clastosomes in astrocytes, suggesting a mechanism for inflammation-induced down-regulation of GC_{NO} in astrocytes.

RESULTS

LPS-induced down regulation of astroglial GC_{NO} is prevented by proteasome inhibitors.

We previously reported that exposure of rat cerebellum astroglial cells to LPS (10 ng/ml) produces a time–dependent decrease in GC_{NO} activity as a result of a reduction in the level of the GC_{NO} β1 subunit protein (Baltrons and Garcia, 1999). This reduction appeared to occur by a decrease in the half-life of the protein because GC_{NO} β1 decreased faster in LPS-treated than in cycloheximide-treated cells (Pedraza et al., 2003). In agreement with this, as shown by western blot in Fig. 1A, the reduction in the amount of GC_{NO} β1 induced by LPS is accompanied by the appearance of a lower molecular weight band that is recognized by an anti-β1 specific antibody suggesting that it is a degradation peptide. To provide evidence about the mechanism involved in GC_{NO} β1 degradation, we examined the ability of different protease inhibitors to prevent the LPS effect. As shown in Fig 1C, MG132 a proteasome inhibitor, known to prevent NFκB activation and hence NOS-2 induction, produced the expected inhibition of LPS-induced nitrite accumulation in rat cerebellum astrocyte-enriched cultures. Additionally, MG132 prevented the LPS-induced decrease in GC_{NO} activity (SNP - stimulated cGMP formation), although with different potency (maximal effect at 1 and 5 μM, respectively) (Fig. 1D). MG132 (5 μM) also prevented the LPS-induced decrease in the 70 KDa GC_{NO} β1 immunoreactive band as well as the appearance of the low molecular weight band on western blots (Fig. 1B). LPS-induced nitrite accumulation and the decrease in GC_{NO} activity were also abolished by other proteasome inhibitors (lactacystin at 10 μM; ABSF at 400 μM) (Table 1). However, inhibitors of other major non-lysosomal proteases such as calpain (25 μM) and ICE (100 μM) that were partially effective in inhibiting nitrite accumulation (50- 60 %) did not prevent the decrease in cGMP formation. The lysosomal protease inhibitor leupeptin (5 μM) was totally ineffective in preventing both LPS effects. These results strongly indicate that LPS-induced degradation of GC_{NO} β1 in astrocytes involves proteasome activity.

LPS-induced proteasome-dependent degradation of astroglial GC_{NO} does not involve NFκB activation or decreased interaction with HSP90

In our previous studies we demonstrated that the decrease in the half-life of GC_{NO} β1 protein induced by LPS is independent of NOS-2 induction but is dependent on transcription and protein synthesis (Pedraza et al., 2003). The transcription factor NFκB is activated by LPS in a proteasome-dependent manner and regulates expression of many inflammatory

genes (Magnani et al., 2000; Zhang and Ghosh, 2000). To investigate if inhibition of LPS-induced GC_{NO} β1 degradation by proteasome inhibitors involved inhibition of NFκB activation and thus NFκB-dependent induction of proteins potentially implicated in the down-regulation process, we examined if activation of NFκB was required for β1 degradation with the use of the NFκB inhibitors pyrrolidine dithiocarbamate (PDTC) and BAY-117082. These compounds prevent degradation of the inhibitory partner protein I kappa B (Henkel et al., 1993; Schreck et al., 1992). As expected, both compounds inhibited LPS-induced nitrite accumulation (Fig. 2A), however they did not prevent the decrease in β1 protein (Fig. 2B) suggesting a more direct involvement of the proteasome in β1 degradation.

In smooth muscle cells it has been recently demonstrated that GC_{NO} is stabilized by interaction with the heat shock protein HSP90 (Papapetropoulos et al., 2005). To investigate if this was also true in astrocytes and if the LPS-induced decrease in β1 stability was due to an alteration in HSP90 levels, we examined the effect on β1 protein levels of a 24 h treatment of the cells with the HSP90 inhibitors radicicol and 17-AGG. As shown in Fig. 3A and B, these two compounds prevented to a large extend the morphological change (soma retraction and filament elongation) induced by LPS in astrocytes and inhibited LPS-induced nitrite accumulation in a concentration dependent manner. However, maximally effective concentrations of these compounds (5 μM radicicol and 50 nM 17-AGG) did no alter GC_{NO} β1 protein levels (Fig. 3C). Furthermore, LPS treatment (10 ng/ml, 24 h) had no effect on the amount of HSP90 protein (Fig. 3D). These results rule out disruption of a potential stabilizing interaction with HSP90 as the cause for GC_{NO} β1-accelerated degradation in astrocytes.

LPS promotes the formation of nuclear GC_{NO} β1 protein aggregates that colocalize with UPS components

In order to investigate if treatment with LPS promoted a direct interaction of GC_{NO} with the proteasome, we examined by double-immunofluorescence the co-localization of GC_{NO} β1 with components of the UPS. We first examined the effect of LPS on the intracellular localization of β1 protein in astrocytes. As shown in Fig. 4A, in untreated cultures where GFAP-positive cells present a flat epithelial-like morphology, β1 immunoreactivity was observed throughout the cytoplasm presenting a granular appearance and often concentrated in perinuclear areas (Fig. 4Aa, asterisk). Staining was also detected in cell nuclei (Fig. 4Aa, arrowhead). In contrast, in cultures treated with LPS (10 ng/ml, 24h), cytoplasmic staining was reduced while β1 immunoreactivity was strong in nuclei where it concentrated in nuclear dots or aggregates over

a diffuse nucleoplasmic signal (Fig. 4Ac, arrowhead). Both cytoplasmic and nuclear immunostaining were abolished by pre-absorbing the antibody with the antigenic peptide (Fig. 4Abd). The LPS-induced relocalization of β1 into nuclear dots was significant after 12 h of treatment indicating that it is a long-term effect and practically all cells presented aggregates by 24 h (Fig 4B). The presence of nuclear aggregates of β1 in LPS-treated cells was confirmed by immunogold electron microscopy (Fig. 4C). In agreement with the immunocytochemical studies, β1 protein was detected in nuclear extracts from LPS-treated and untreated cells by western blot and both cytosolic and nuclear β1 levels were decreased by LPS treatment (Fig 4D).

To investigate if GC_{NO} β1 co-localizes with 20S proteasome in the nuclei, we performed double-immunostaining experiments. Under control conditions, the monoclonal 20S proteasome antibody showed a diffuse nucleoplasmic staining, excluding nucleoli, and a weak cytoplasmic labeling (Fig. 5B) in agreement with other studies (Chen et al., 2002; Lafarga et al., 2002; Mengual et al., 1996). In LPS-treated cells, however, in addition to the diffuse nucleoplasmic signal, 20S proteasome was concentrated in numerous nuclear aggregates (Fig 5E). Merged images showed that β1 co-localized with the 20S proteasome in many of these nucleoplasmic aggregates (Fig. 5D-F). Similar results were obtained when double immunostaining with anti-β1 and anti-ubiquitin antibodies was performed (Fig. 6A-H). In untreated cells, ubiquitin staining was mostly nuclear and diffuse and presented little overlapping with the β1 signal (Fig. 6A-D). In LPS-treated cells ubiquitin immunoreactivity appeared concentrated in numerous nuclear domains/foci upon a diffuse nucleoplasmic staining (Fig. 6, F). Co-localization of ubiquitin and GC_{NO} β1 immunoreactivities was evident in many of these aggregates (Fig. 6E-H). A staining pattern similar to that of ubiquitin was observed with a polyclonal anti-ubiquitin antibody that recognizes ubiquitin-protein complexes and these complexes co-localized with the 20S proteasome (Fig.7A-C). These results suggest that in astrocytes LPS promotes the recruitment of ubiquitylated GC_{NO} β1 to the 20S proteasome in nuclear subdomains to promote its degradation.

Recent reports have shown that different nuclear structures of the interchromatin region, such as splicing speckles (Rockel et al., 2005), promyelocytic leukaemia (PML) protein bodies (Fabunmi et al., 2001; Lallemand-Breitenbach et al., 2001; Rockel et al., 2005) and clastosomes (Janer et al., 2006; Lafarga et al., 2002) recruit components of the UPS and might represent proteolytic centers under certain conditions. To define the nuclear subdomain targeted by GC_{NO} β1 in LPS-treated cells we double-stained cells for β1 and anti-pan-histone as a chromatin marker, 2,2,7-trimethylguanosine cap (TMG-CAP) as a marker of

nuclear speckles of splicing factors (Lamond and Spector, 2003) and small ubiquitin-like modifier protein 1 (SUMO-1) that concentrates in PML bodies (Ching et al., 2005). As shown in Fig. 8, β1 did not co-localize with any of these markers suggesting that its degradation may take place in clastosomes, nuclear bodies highly enriched in components of the UPS but devoid of splicing factors and SUMO-1 (Lafarga et al., 2002).

LPS-induced recruitment of GC_{NO} β1 to ubiquitin-proteasome-enriched nuclear bodies is prevented by proteasome and protein synthesis inhibitors

The proteasome inhibitor MG132, at a concentration that totally abolished LPS-induced GC_{NO} β1 degradation (5 μM, added 1 h before LPS; Fig. 1), prevented LPS-induced recruitment of β1 to the 20S proteosome/ubiquitin-enriched nuclear bodies as shown by double-immunofluorescence (Fig. 5J-L and Fig. 6M-P), supporting the notion that these structures are the sites of β1 degradation. Furthermore, MG132 prevented the LPS-promoted assembly of 20S proteosome and ubiquitin-protein-complexes in nuclear bodies. (Fig.7D-I), further supporting the identity of these sites as clastosomes (Lafarga et al., 2002). Notably, in MG132-treated cells the 20S proteasome immunostainig remained mostly nuclear (Fig. 5H,K) but ubiquitin immunoreactivity decreased in the nuclei and presented a pronounced accumulation in small and big aggregates throughout the cytoplasm showing some co-localization with β1 particularly in perinuclear areas (Fig. 6I-L). Identical results have been obtained using the proteasome inhibitors PSI (2 μM) and epoxomycin (5 μM) (not shown), ruling out that inhibition of nuclear translocation of ubiquitinated-proteins was a non-specific effect of MG132.

We previously showed that the protein synthesis inhibitor cycloheximide (CHX) was able to prevent the decrease in GC_{NO} β1 levels induced by LPS in astroglial cells (Pedraza et al., 2003). To investigate if the targeting of β1 to clastosomes induced by LPS was also dependent on protein synthesis we examined the effect of CHX (10 μM, 24 h) on the co-localization of β1 with the 20S proteasome and ubiquitin. As shown in Fig. 5 and Fig. 6, in CHX-treated cells β1 immunoreactivity presented a diffuse staining in the cytoplasm and the nucleus similar to that shown in control cells and this pattern was not altered by co-treatment with LPS (Fig. 5M,P and Fig. 6 Q,U). On the other hand, while the distribution of 20S immunoreactivity in CHX-treated cells was similar to that in untreated cells (Fig 5N), nuclear co-localization of 20S with β1 was abolished (Fig 5R). Additionally, CHX treatment greatly diminished ubiquitin immunostaining throughout the cell (Fig 6 R, V). These results

demonstrate that CHX inhibits clastosome formation and suggest that this effect may result from depletion of ubiquitin pools.

DISCUSSION

We previously demonstrated that LPS-treatment decreases the half-life of the GC_{NO} β1 subunit protein in astrocytes (Baltrons and Garcia, 1999). In this work with the use of a different and more specific anti-β1 antibody we show by western blot analysis of glial cytosolic fractions that the LPS-induced decrease in the specific anti-β1 immunoreactive band is accompanied by the appearance of a lower molecular weight band, also recognized by the anti-β1 antibody, suggesting that it is a degradation peptide. Inhibition of proteasome activity with MG132 blocked the LPS-induced decrease in the 70 KDa β1 immunoreactive band as well as the appearance of the low molecular weight band and this was accompanied by a restoration of NO-stimulated cGMP formation to control levels. Lactacystin, another proteasome inhibitor with a structure different from MG132 (Fenteany and Schreiber, 1998) was also able to prevent LPS-induced GC_{NO} down-regulation but inhibitors of major lysosomal and non-lysosomal proteases were without effect pointing to a specific implication of proteasome activity in the degradation of GC_{NO}. In control cells, proteasome inhibition by MG132 (5 μM, 24 h) did not produce a significant increase in β1 protein levels (Fig. 1) in agreement with the reported low turnover rate of this protein (Ferrero and Torres, 2002; Papapetropoulos et al., 1995; Shimouchi et al., 1993). Recently, Papapetropoulos et al., 2005 demonstrated that in rat aortic smooth muscle cells the interaction of the β1 subunit with HSP90 stabilizes the protein and that disruption of this interaction by long-term treatment (24-48 h) with HSP90 inhibitors (geldanamycin or radicicol) leads to β1 proteasome-dependent degradation. In this work, we explored the possibility that the effect of LPS on β1 stability was due to an impaired HSP90/β1 interaction with negative results. First, we did not observe a significant decrease in β1 after treating the cells for 24 h with the HSP90 inhibitors radicicol or 17 AGG at a concentration effective in blocking LPS-induced NOS activity (Dello Russo et al., 2006; Jeon et al., 2000) and LPS-induced astrocyte stellation (Fig. 3A). Second, we show that an LPS treatment (10 ng/ml, 24 h) that significantly reduces β1 protein does not alter HSP90 levels in astrocytes. These results rule out a major role of HSP90 in β1 stabilization and in the LPS-induced proteasome-dependent degradation of β1 in astrocytes. The difference in the effect of HSP90 inhibitors on β1 levels between this work and that of Papetropoulos et al. (2005) may be attributed to differences in cell type or in the inhibitor concentration used. These authors used a four-time higher concentration of radicicol (20 μM) that could no be used in astrocytes because it was toxic.

We showed in our previous works that the LPS-induced degradation of GC_{NO} was transcription- and translation-dependent (Pedraza et al., 2003). It is well documented that activation of the transcription factor NFκB is involved in induction of gene expression by LPS and that proteasome inhibitors prevent NFκB activation by inhibiting degradation of IκB (Magnani et al., 2000; Zhang and Ghosh, 2000). The possibility that the proteasome activity was involved in the activation of this transcription factor rather than more directly in β1 degradation was ruled out by the inability of NFκB inhibitors (PDTC and BAY-1182) to prevent LPS-induced β1 degradation at concentrations that completely blocked nitrite accumulation due to NOS-2 induction. These data further supports the independence from NO of the LPS effect on β1 protein.

In this work, we show for the first time with the used of immunofluorescence and confocal microsocopy that LPS-induces the co-localization of GC_{NO} β1 with components of the UPS (20S proteasoma and ubiquitin) in nuclear bodies with the characteristics of clastosomes (Lafarga et al., 2002). In contrast to untreated cells where β1-specific immunostaining is present mainly in the cytoplasm and only a weak and homogeneous staining is observed in nuclei, in LPS-treated cells a strong β1 immunostaining was observed in nuclear aggregates by confocal microscopy and by immunoelectron microscopy. The nuclear presence of the protein both in untreated and LPS-treated cells was confirmed by western blot analysis of nuclear proteins. The percentage of cells showing nuclear β1 aggregates was significant after 12 h exposure to LPS and by 24 h aggregates were observed all cells. This time-course is consistent with a process requiring mRNA and protein synthesis (Baltrons and Garcia, 1999). Double-labeling experiments showed that in control cells β1 did not co-localize with components of the UPS system, however in the nuclei of LPS-treated cells β1 co-localized with both 20S proteasome and ubiquitin. Nuclear localization of GC_{NO} β1 is not unprecedented although the protein lacks a classical nuclear localization signal (NLS) in the primary amino acid sequence. It has been previously observed in hepatocytes (Earp et al., 1977; Gobeil et al., 2006), hair cells of guinea pig cochlea (Heinrich et al., 2000) and embryonic stem cell-derived cardiomyocytes (Krumenacker and Murad, 2006), but was never reported in brain cells. We have also observed nuclear localization of β1 but not of α subunits after transient transfection in C6 glioma cells (Pifarré et al., submitted). The mechanism by which GC_{NO} β1 enters the nucleus is unknown at present. Recently, Balashova et al.(2005) suggested that interaction with HSP70 mediates β1 intracellular translocation but we found no evidence of co-localization of HSP70 with β1 in our cells (not shown).

Nuclear targeting and formation of subnuclear structures are among the biological consequences of SUMO protein modification (Dohmen, 2004). SUMO-1 protein is concentrated

in PML bodies (Ching et al., 2005) that recruit components of the UPS and might represent proteolytic centers. Bioinformatical analysis with SUMOplot™ software (www.abgent.com/doc/sumoplot) identified several possible SUMOylation sites in the β1 sequence. However, we did not detect overlapping of SUMO-1 and β1 immunostaining in double-label experiments. The nuclear bodies enriched in β1 in LPS-treated cells were also devoid of TMG-CAP, a marker of nuclear speckles (Lamond and Spector, 2003). On the other hand, we show that the LPS-induced assembly of β1 with 20S proteasome and ubiquitin in nuclear dots is largely prevented by proteasome inhibitors. We previously reported that inhibition of proteosomal function produced the disappearance of clastosomes, another type of nucleoplasmic substructures involved in ubiquitin-proteasome-dependent nuclear proteolysis (Lafarga et al., 2002), but this has not been described for splicing speckles or PML bodies. Taken together these results indicate that LPS orchestrates the recruitment of GC_{NO} β1 to clastosomes together with components of the UPS system and suggest a mechanism for inflammation-induced down-regulation of GC_{NO} in astrocytes.

Interestingly, we show here that upon proteasome inhibition ubiquitin localization in astrocytes is significantly altered. In untreated cells ubiquitin immunoreactivity concentrates in the nuclei and only a weak and homogeneous staining is observed in the cytoplasm. However, in MG1232-treated cells ubiquitin immunoreactivity is seeing in small and big aggregates throughout the cytoplasm presenting some co-localization with GC_{NO} β1 particularly in perinuclear areas. These data suggest that ubiquitylation of proteins, including β1, occurs mainly in the cytoplasm and that upon proteasome inhibition accumulated ubiquitylated proteins probably exceed the capacity of the citoplasmic/nucleoplasmic translocation systems. Accumulation of ubiquitin in the cytoplasm and formation of aggresomes in the perinuclear region together with depletion of the nuclear pool upon proteasome inhibition has been also reported recently in living cells transfected with GFP-ubiquitin (Dantuma et al., 2006). These authors suggest that the increase in the amount of polyubiquitylated proteins as well as the increased size of polyubiquitin complexes in MG132-treated cells are likely responsible for reduced diffusion velocity through the nuclear pore.

The finding that cycloheximide prevents recruitment of GC_{NO} β1 to clastosomes in LPS-treated cells is in accordance with our previous results demonstrating that this protein synthesis inhibitor prevents β1 degradation induced by inflammatory compounds (Baltrons and Garcia, 1999; Baltrons et al., 2002; Pedraza et al., 2003) and supports that clastosomes are the degradation site. Inhibition of ubiquitin/proteasomal degradation by CHX has been also observed for other substrates (Adeli, 1994; Ravid et al., 2000; Shenkman et al., 2007; Wikstrom

and Lodish, 1991). It has also been reported that a protein not requiring ubiquitylation for its proteasomal degradation, such ornithine decarboxylase, is still degraded in the presence of CHX (Li et al., 1998). Interestingly, we show here that CHX greatly diminishes ubiquitin immunoreactivity in LPS-treated or untreated cells. It was reported that that CHX does not inhibit degradation of ubiquitin conjugates (Hershko *et al.*, 1982). Furthermore, it has been shown that free ubiquitin is rapidly depleted upon inhibition of protein synthesis in S.cerevisae (Hanna et al., 2003). Our results agree with ubiquitin depletion as the reason for CHX inhibition of LPS-induced β1 proteasomal degradation. Another possibility is depletion of E3 ubiquitin ligases These proteins also have a short half-life and can be depleted fast upon inhibition of protein synthesis abrogating ubiquitinization of their substrates (Joazeiro and Weissman, 2000). Interestingly, in endothelial cells LPS has been shown to induce the synthesis of E3 ubiquitin ligase HERC5 (Kroismayr et al., 2004). On the other hand, LPS has been reported to induce expression of immunoproteasome subunits that replace constitutively expressed subunits and change the enzymatic properties of the 20S proteasome (Stohwasser et al., 2000), a possibility that we cannot exclude with our present results.

In summary, we report here the novel finding that GC_{NO} β1 down-regulation by bacterial cell wall LPS in astroglial cells involves recruitment to nuclear bodies enriched in components of the UPS system with the characteristics of clastosomes. We also show that proteasome inhibitors prevent clastosome assembly as well as β1 degradation, strongly supporting a role of these transient nuclear structures in GC_{NO} regulation during neuroinflammation. Down-regulation of GC_{NO} β1 protein has been shown in reactive astrocytes in human postmortem brain tissue of patients with neurodegenerative conditions associated with neuroinflammation such as Alzheimer, Multiple Sclerosis and Creutzfeld-Jacob disease (Baltrons et al., 2004). Whether astroglial GC_{NO} down-regulation occurs by a similar mechanism in human cells and the functional implications of a decrease in NO-dependent cGMP formation in reactive astrocytes needs further investigation.

Experimental Methods

Reagents. Dulbecco's modified Eagle's medium (DMEM) was obtained from Flow Laboratories and foetal calf serum (FCS) from Biowhittaker; [^{3}H]cGMP (34.5 Ci/mmol) from New England Nuclear. Proteasome inhibitor I (PSI), lactacystin, MG132, calpain inhibitor II, ICE inhibitor II from Calbiochem; antigenic peptide of GC_{NO} β1 from Cayman; Supersignal Ultra Chemilumininescent Substrate from Pierce; Fluoroprep from BioMerieux; all other reagents

were purchased from Sigma Química. 17- AGG was kindly provided by Conforma Therapeutics Corporation.

Antibodies. Purified rabbit polyclonal antibody against peptide 189-207 of the β1 subunit of GC_{NO} and mouse anti-actin were from Sigma; Proteasome 20S was detected using a monoclonal antibody (Biomol International) that reacts with the six different α-type subunits; mouse anti-ubiquitin (P4D1) was from Santa Cruz Biotechnology; rabbit polyclonal anti-ubiquitin-conjugates from Biomol, International; mouse monoclonal anti-GFAP from DAKO; mouse monoclonal anti-SUMO-1 and anti-lamin from Zymed; mouse monoclonal anti-2,2,7-trimethylguanosine cap from Oncogene, mouse monoclonal anti-pan-histone from Roche and mouse anti-HSP90 from Transduction Laboratories. Anti-cGMP antiserum was prepared in our laboratory as described by Brooker et al. (1979). As secondary antibodies, we used goat anti-mouse and goat anti-rabbit antibodies conjugated with Alexa 488 or Alexa 555 (Molecular Probes).

Cell cultures. Primary cultures enriched in astrocytes were prepared from cerebellum of 7 day-old Sprague-Dawley rats as previously described (Agullo et al., 1995). Tissue was mechanically dissociated by successive passages through nylon cloths of 211 µm and 135 µm mesh openings. To obtain astrocyte-enriched cultures cells were suspended in DMEM-10 % FCS, 20 U/ml penicillin and 20 µg/ml streptomycin, seeded in plastic Petri dishes ($1.25x10^5$ cells/cm^2) and maintained in a humidified atmosphere of 90 % air-10 % CO_2. Medium was changed once a week and cells were used after 14 days in culture. Cells were incubated for the indicated times with LPS in DMEN -10% FCS. Inhibitors were added 1 h before LPS treatment.

Immunocytochemistry. For immunofluorescence cells were grown on glass coverslips, rinsed in phosphate-buffered saline (PBS) and fixed with 4% paraformaldehyde for 30 min at room temperature. Before immunostaining, the samples were sequentially incubated with 0,5% Triton X-100 in PBS for 10 min and 0,1 M glycine in PBS for 30 min at room temperature, washed and incubated overnight at 4ºC with primary antibodies diluted in PBS. After washing the cells with PBS containing 0,05% Twin-20 for 20 min, cultures were incubated for 1 h at room temperature with the appropriate secondary antibodies (Alexa 555 or 488 anti-rabbit IgG or anti-mouse IgG from goat) at 1:1000 dilution in PBS. The primary antibody was omitted in controls. In addition, some sections were incubated with the antigenic peptide before GC_{NO} -β1 immunocitochemistry. Finally, the coverslips were mounted in fluoroprep. Double stained samples were analyzed with a laser confocal microscope (Zeiss LSM 510 or Leica TCS SP2 AOBS). Each channel was recorded independently and pseudocolor images were generated and superimposed. TIFF images were transferred to Adobe Photoshop 7.0 software (Adobe Systems Inc.) for presentation.

For electron microscopy immunocytochemistry, cell monolayers were rinsed in PBS and fixed with 4% paraformaldehyde for 10 min at room temperature scraped from the plates and centrifugated. The pellet was rinsed in PBS before were dehydrated in increasing concentration of methanol, and embedded in Lowicryl K4M at -20ºC. Ultrathin sections were sequentially incubated with 0.1 M glycine in PBS (15 min), normal goat serum diluted 1:100 in PBS (3 min), and the primary antibody diluted in PBS containing 0.1 M glycine and 1% BSA (1h at room temperature). After washing, the sections were incubated with the secondary antibody conjugated to 15 nm gold-particles (BioCell, UK) diluted 1:25 in 1% BSA in PBS (45 min at room temperature). After washing, the sections were stained with uranyl acetate and lead citrate and examined with an electron microscope (Philips EM208). As controls, sections were treated as described but omitting the primary antibody.

cGMP and nitrite accumulation. For determination of cGMP, cell monolayers pretreated with different agents, were washed and preincubated for 10 min in Hepes-buffered saline (118 mM NaCl, 4.7 mM KCl, 2.5 mM $CaCl_2$, 1.2 mM $MgSO_4$, 1.2 mM KH_2PO_4, 10 mM glucose and 20 mM Hepes, pH 7.4) before adding 1 mM IBMX alone or with sodium nitroprusside (SNP, 100 μM). After 3 min incubation, reactions were terminated by aspirating the medium and adding ice-cold ethanol. Ethanol extracts were evaporated, resuspended in acetate buffer and cGMP quantified by radioimmunoassay using acetylated [^{3}H]cGMP as described previously (Agullo and Garcia, 1992). Nitrite accumulation was assayed in the media by the Greiss reaction as described (Baltrons and Garcia, 1999).

Western blotting. Western blots were performed in cytosolic or nuclear fractions as described (Baltrons and Garcia, 1999). To obtain cytosolic fractions cell monolayers were washed twice with cold Hepes-buffered saline Ca^{2+} and Mg^{2+} free and scraped from the plates. Cells were homogenized with a glass-Teflon Potter-Elvehjeim homogenizer (800 rpm) in ice-cold 50 mM Tris/HCl buffer (pH 7.4 at 37°C), containing 1 mM DTT, 1 mM EDTA, anti-protease (Roche) and anti-phosphatase cocktail (Sigma). Homogenates were centrifuged at 100,000 x g for 1 h at 4°C and supernatants were stored at -80°C until use. To prepare nuclear extracts cells were scraped from the dishes in ice-cold PBS, centrifuged and pellets resuspended in low salt buffer (10 mM Hepes, pH 7.9, 1.5 mM $MgCl_2$, 10 mM KCl, supplemented with 1 mM DTT and anti-protease and anti-phosphatase cocktails). Samples were allowed to sit on ice for 10 min before addition of 10% Nonidet P-40, vortexed 10 sec and centrifuged 30 sec at high speed at 4°C. Supernatants were centrifuged at 100,000 x g for 1 h at 4°C and used as a soluble fraction. Nuclear pellets were resuspended in high salt buffer (20 mM Hepes, pH 7.9, 25% glycerol, 420 mM NaCl, 0.5 mM EDTA, supplemented with 1 mM DTT and anti-protease and anti-phosphatase cocktails) and rocked gently at 4°C for 30 min. Samples were then centrifuged for

15 min at high speed at 4°C. The supernatant was quantitated for protein concentration and stored at −80 °C until use. Cytosolic and nuclear fractions (15-20µg of protein) were subjected to 8 % sodium dodecyl sulfate-polyacrylamide gel electrophoresis (SDS-PAGE) followed by transfer to PDVF filters at 100 V for 1.5 h at 4°C. Membranes were blocked at 4°C overnight in phosphate-buffered saline (pH 7.4) containing 5 % non-fat dry milk, and then incubated at room temperature for 2 h with affinity purified rabbit polyclonal antibody against peptide 189-207 of the β1 subunit of GC_{NO} (1:2,000), or with antibody against HSP90 (1:4,000) or actin (1:100,000). Immunoreactive bands were detected with a horseradish peroxidase conjugated anti-rabbit and anti-mouse IgGs (1:4,000; Amersham Life Science) visualized by chemiluminescence using a luminol–based commercial kit (Pierce Supersignal West-Pico) and exposed X-OMAT AR films were developed and scanned. The GC_{NO} β1 immunoreactivity was totally blocked when the antibody was pre-absorbed with a 1,000-fold excess concentration of the antigenic peptide (Cayman).

Protein was determined by the method of Lowry or with the Bradford reagent using bovine serum albumin as standard. Experiments were always performed in triplicate plates and were replicated the indicated number of times in different culture preparations.

ACKNOWLEDGEMENTS

This work was supported by grants from Ministerio de Educación y Ciencia, Spain (SAF2004-01717) and Direcció General de Recerca (DGR), Generalitat de Catalunya (SGR2001-212). P. Pifarré was a recipient of a FPU fellowship from the Ministry of Science and Education, Spain.

REFERENCES

Adeli, K., 1994. Regulated intracellular degradation of apolipoprotein B in semipermeable HepG2 cells. J Biol Chem 269, 9166-9175.

Adori, C., Kovacs, G.G., Low, P., Molnar, K., Gorbea, C., Fellinger, E., Budka, H., Mayer, R.J., Laszlo, L., 2005. The ubiquitin-proteasome system in Creutzfeldt-Jakob and Alzheimer disease: intracellular redistribution of components correlates with neuronal vulnerability. Neurobiol Dis 19, 427-435.

Agullo, L., Baltrons, M.A., Garcia, A., 1995. Calcium-dependent nitric oxide formation in glial cells. Brain Res 686, 160-168.

Agullo, L., Garcia, A., 1992. Characterization of noradrenaline-stimulated cyclic GMP formation in brain astrocytes in culture. Biochem J 288 (Pt 2), 619-624.

Anton, L.C., Schubert, U., Bacik, I., Princiotta, M.F., Wearsch, P.A., Gibbs, J., Day, P.M., Realini, C., Rechsteiner, M.C., Bennink, J.R., Yewdell, J.W., 1999. Intracellular localization of proteasomal degradation of a viral antigen. J Cell Biol 146, 113-124.

Balashova, N., Chang, F.J., Lamothe, M., Sun, Q., Beuve, A., 2005. Characterization of a novel type of endogenous activator of soluble guanylyl cyclase. J Biol Chem 280, 2186-2196.

Baltrons, M.A., Garcia, A., 1999. Nitric oxide-independent down-regulation of soluble guanylyl cyclase by bacterial endotoxin in astroglial cells. J Neurochem 73, 2149-2157.

Baltrons, M.A., Pedraza, C.E., Heneka, M.T., Garcia, A., 2002. Beta-amyloid peptides decrease soluble guanylyl cyclase expression in astroglial cells. Neurobiol Dis 10, 139-149.

Baltrons, M.A., Pifarre, P., Ferrer, I., Carot, J.M., Garcia, A., 2004. Reduced expression of NO-sensitive guanylyl cyclase in reactive astrocytes of Alzheimer disease, Creutzfeldt-Jakob disease, and multiple sclerosis brains. Neurobiol Dis 17, 462-472.

Brooker, G., Harper, J.F., Terasaki, W.L., Moylan, R.D., 1979. Radioimmunoassay of cyclic AMP and cyclic GMP. Adv Cyclic Nucleotide Res 10, 1-33.

Chen, M., Rockel, T., Steinweger, G., Hemmerich, P., Risch, J., von Mikecz, A., 2002. Subcellular recruitment of fibrillarin to nucleoplasmic proteasomes: implications for processing of a nucleolar autoantigen. Mol Biol Cell 13, 3576-3587.

Ching, R.W., Dellaire, G., Eskiw, C.H., Bazett-Jones, D.P., 2005. PML bodies: a meeting place for genomic loci? J Cell Sci 118, 847-854.

Dantuma, N.P., Groothuis, T.A., Salomons, F.A., Neefjes, J., 2006. A dynamic ubiquitin equilibrium couples proteasomal activity to chromatin remodeling. J Cell Biol 173, 19-26.

Davis, J.P., Vo, X.T., Sulakhe, P.V., 1997. Altered responsiveness of guanylyl cyclase to nitric oxide following treatment of cardiomyocytes with S-nitroso-D,L-acetylpenicillamine and sodium nitroprusside. Biochem Biophys Res Commun 238, 351-356.

de Frutos, S., Saura, M., Rivero-Vilches, F.J., Rodriguez-Puyol, D., Rodriguez-Puyol, M., 2003. C-type natriuretic peptide decreases soluble guanylate cyclase levels by activating the proteasome pathway. Biochim Biophys Acta 1643, 105-112.

Dello Russo, C., Polak, P.E., Mercado, P.R., Spagnolo, A., Sharp, A., Murphy, P., Kamal, A., Burrows, F.J., Fritz, L.C., Feinstein, D.L., 2006. The heat-shock protein 90 inhibitor 17-allylamino-17-demethoxygeldanamycin suppresses glial inflammatory responses and ameliorates experimental autoimmune encephalomyelitis. J Neurochem 99, 1351-1362.

Ding, J.D., Burette, A., Nedvetsky, P.I., Schmidt, H.H., Weinberg, R.J., 2004. Distribution of soluble guanylyl cyclase in the rat brain. J Comp Neurol 472, 437-448.

Dohmen, R.J., 2004. SUMO protein modification. Biochim Biophys Acta 1695, 113-131.

Earp, H.S., Smith, P., Huang Ong, S.H., Steiner, A.L., 1977. Regulation of hepatic nuclear guanylate cyclase. Proc Natl Acad Sci U S A 74, 946-950.

Fabunmi, R.P., Wigley, W.C., Thomas, P.J., DeMartino, G.N., 2001. Interferon gamma regulates accumulation of the proteasome activator PA28 and immunoproteasomes at nuclear PML bodies. J Cell Sci 114, 29-36.

Fenteany, G., Schreiber, S.L., 1998. Lactacystin, proteasome function, and cell fate. J Biol Chem 273, 8545-8548.

Ferrero, R., Rodriguez-Pascual, F., Miras-Portugal, M.T., Torres, M., 2000. Nitric oxide-sensitive guanylyl cyclase activity inhibition through cyclic GMP-dependent dephosphorylation. J Neurochem 75, 2029-2039.

Ferrero, R., Torres, M., 2002. Prolonged exposure of chromaffin cells to nitric oxide down-regulates the activity of soluble guanylyl cyclase and corresponding mRNA and protein levels. BMC Biochem 3, 26.

Filippov, G., Bloch, D.B., Bloch, K.D., 1997. Nitric oxide decreases stability of mRNAs encoding soluble guanylate cyclase subunits in rat pulmonary artery smooth muscle cells. J Clin Invest 100, 942-948.

Garcia, A., Baltrons, M.A., 2003. The nitric oxide/cyclic GMP signalling pathway in CNS glial cells. In: E.E. Bittar, E. (Ed.), Advances in Molecular and Cell Biology Vol. 31, pp. 575-594.

Garthwaite, J., Boulton, C.L., 1995. Nitric oxide signaling in the central nervous system. Annu Rev Physiol 57, 683-706.

Gobeil, F., Jr., Zhu, T., Brault, S., Geha, A., Vazquez-Tello, A., Fortier, A., Barbaz, D., Checchin, D., Hou, X., Nader, M., Bkaily, G., Gratton, J.P., Heveker, N., Ribeiro-da-Silva, A., Peri, K., Bard, H., Chorvatova, A., D'Orleans-Juste, P., Goetzl, E.J., Chemtob, S., 2006. Nitric oxide signaling via nuclearized endothelial nitric-oxide synthase

modulates expression of the immediate early genes iNOS and mPGES-1. J Biol Chem 281, 16058-16067.

Hanna, J., Leggett, D.S., Finley, D., 2003. Ubiquitin depletion as a key mediator of toxicity by translational inhibitors. Mol Cell Biol 23, 9251-9261.

Heinrich, U., Maurer, J., Koesling, D., Mann, W., Forstermann, U., 2000. Immuno-electron microscopic localization of the alpha(1) and beta(1)-subunits of soluble guanylyl cyclase in the guinea pig organ of corti. Brain Res 885, 6-13.

Henkel, T., Machleidt, T., Alkalay, I., Kronke, M., Ben-Neriah, Y., Baeuerle, P.A., 1993. Rapid proteolysis of I kappa B-alpha is necessary for activation of transcription factor NF-kappa B. Nature 365, 182-185.

Hershko, A., Eytan, E., Ciechanover, A., Haas, A.L., 1982. Immunochemical analysis of the turnover of ubiquitin-protein conjugates in intact cells. Relationship to the breakdown of abnormal proteins. J Biol Chem 257, 13964-13970.

Janer, A., Martin, E., Muriel, M.P., Latouche, M., Fujigasaki, H., Ruberg, M., Brice, A., Trottier, Y., Sittler, A., 2006. PML clastosomes prevent nuclear accumulation of mutant ataxin-7 and other polyglutamine proteins. J Cell Biol 174, 65-76.

Jeon, Y.J., Kim, Y.K., Lee, M., Park, S.M., Han, S.B., Kim, H.M., 2000. Radicicol suppresses expression of inducible nitric-oxide synthase by blocking p38 kinase and nuclear factor-kappaB/Rel in lipopolysaccharide-stimulated macrophages. J Pharmacol Exp Ther 294, 548-554.

Joazeiro, C.A., Weissman, A.M., 2000. RING finger proteins: mediators of ubiquitin ligase activity. Cell 102, 549-552.

Kloss, S., Furneaux, H., Mulsch, A., 2003. Post-transcriptional regulation of soluble guanylyl cyclase expression in rat aorta. J Biol Chem 278, 2377-2383.

Kroismayr, R., Baranyi, U., Stehlik, C., Dorfleutner, A., Binder, B.R., Lipp, J., 2004. HERC5, a HECT E3 ubiquitin ligase tightly regulated in LPS activated endothelial cells. J Cell Sci 117, 4749-4756.

Krumenacker, J.S., Murad, F., 2006. NO-cGMP signaling in development and stem cells. Mol Genet Metab 87, 311-314.

Lafarga, M., Berciano, M.T., Pena, E., Mayo, I., Castano, J.G., Bohmann, D., Rodrigues, J.P., Tavanez, J.P., Carmo-Fonseca, M., 2002. Clastosome: a subtype of nuclear body enriched in 19S and 20S proteasomes, ubiquitin, and protein substrates of proteasome. Mol Biol Cell 13, 2771-2782.

Lain, S., Midgley, C., Sparks, A., Lane, E.B., Lane, D.P., 1999. An inhibitor of nuclear export activates the p53 response and induces the localization of HDM2 and p53 to U1A-positive nuclear bodies associated with the PODs. Exp Cell Res 248, 457-472.

Lallemand-Breitenbach, V., Zhu, J., Puvion, F., Koken, M., Honore, N., Doubeikovsky, A., Duprez, E., Pandolfi, P.P., Puvion, E., Freemont, P., de The, H., 2001. Role of promyelocytic leukemia (PML) sumolation in nuclear body formation, 11S proteasome recruitment, and As2O3-induced PML or PML/retinoic acid receptor alpha degradation. J Exp Med 193, 1361-1371.

Lamond, A.I., Spector, D.L., 2003. Nuclear speckles: a model for nuclear organelles. Nat Rev Mol Cell Biol 4, 605-612.

Li, X., Zhao, X., Fang, Y., Jiang, X., Duong, T., Fan, C., Huang, C.C., Kain, S.R., 1998. Generation of destabilized green fluorescent protein as a transcription reporter. J Biol Chem 273, 34970-34975.

Liu, H., Force, T., Bloch, K.D., 1997. Nerve growth factor decreases soluble guanylate cyclase in rat pheochromocytoma PC12 cells. J Biol Chem 272, 6038-6043.

Magnani, M., Crinelli, R., Bianchi, M., Antonelli, A., 2000. The ubiquitin-dependent proteolytic system and other potential targets for the modulation of nuclear factor-kB (NF-kB). Curr Drug Targets 1, 387-399.

Mengual, E., Arizti, P., Rodrigo, J., Gimenez-Amaya, J.M., Castano, J.G., 1996. Immunohistochemical distribution and electron microscopic subcellular localization of the proteasome in the rat CNS. J Neurosci 16, 6331-6341.

Meurer, S., Pioch, S., Gross, S., Muller-Esterl, W., 2005. Reactive oxygen species induce tyrosine phosphorylation of and Src kinase recruitment to NO-sensitive guanylyl cyclase. J Biol Chem 280, 33149-33156.

Murthy, K.S., 2001. Activation of phosphodiesterase 5 and inhibition of guanylate cyclase by cGMP-dependent protein kinase in smooth muscle. Biochem J 360, 199-208.

Murthy, K.S., 2004. Modulation of soluble guanylate cyclase activity by phosphorylation. Neurochem Int 45, 845-851.

Papapetropoulos, A., Abou-Mohamed, G., Marczin, N., Murad, F., Caldwell, R.W., Catravas, J.D., 1996. Downregulation of nitrovasodilator-induced cyclic GMP accumulation in cells exposed to endotoxin or interleukin-1 beta. Br J Pharmacol 118, 1359-1366.

Papapetropoulos, A., Marczin, N., Mora, G., Milici, A., Murad, F., Catravas, J.D., 1995. Regulation of vascular smooth muscle soluble guanylate cyclase activity, mRNA, and protein levels by cAMP-elevating agents. Hypertension 26, 696-704.

Papapetropoulos, A., Zhou, Z., Gerassimou, C., Yetik, G., Venema, R.C., Roussos, C., Sessa, W.C., Catravas, J.D., 2005. Interaction between the 90-kDa heat shock protein and soluble guanylyl cyclase: physiological significance and mapping of the domains mediating binding. Mol Pharmacol 68, 1133-1141.

Pedraza, C.E., Baltrons, M.A., Heneka, M.T., Garcia, A., 2003. Interleukin-1 beta and lipopolysaccharide decrease soluble guanylyl cyclase in brain cells: NO-independent destabilization of protein and NO-dependent decrease of mRNA. J Neuroimmunol 144, 80-90.

Plafker, S.M., Plafker, K.S., Weissman, A.M., Macara, I.G., 2004. Ubiquitin charging of human class III ubiquitin-conjugating enzymes triggers their nuclear import. J Cell Biol 167, 649-659.

Ravid, T., Doolman, R., Avner, R., Harats, D., Roitelman, J., 2000. The ubiquitin-proteasome pathway mediates the regulated degradation of mammalian 3-hydroxy-3-methylglutaryl-coenzyme A reductase. J Biol Chem 275, 35840-35847.

Rockel, T.D., Stuhlmann, D., von Mikecz, A., 2005. Proteasomes degrade proteins in focal subdomains of the human cell nucleus. J Cell Sci 118, 5231-5242.

Rockel, T.D., von Mikecz, A., 2002. Proteasome-dependent processing of nuclear proteins is correlated withh their subnuclear localization. J Struct Biol 140, 189-199.

Russwurm, M., Koesling, D., 2002. Isoforms of NO-sensitive guanylyl cyclase. Mol Cell Biochem 230, 159-164.

Sardon, T., Baltrons, M.A., Garcia, A., 2004. Nitric oxide-dependent and independent down-regulation of NO-sensitive guanylyl cyclase in neural cells. Toxicol Lett 149, 75-83.

Schreck, R., Meier, B., Mannel, D.N., Droge, W., Baeuerle, P.A., 1992. Dithiocarbamates as potent inhibitors of nuclear factor kappa B activation in intact cells. J Exp Med 175, 1181-1194.

Scott, W.S., Nakayama, D.K., 1998. Escherichia coli lipopolysaccharide downregulates soluble guanylate cyclase in pulmonary artery smooth muscle. J Surg Res 80, 309-314.

Shenkman, M., Tolchinsky, S., Kondratyev, M., Lederkremer, G.Z., 2007. Transient arrest in proteasomal degradation during inhibition of translation in the unfolded protein response. Biochem J.

Shimouchi, A., Janssens, S.P., Bloch, D.B., Zapol, W.M., Bloch, K.D., 1993. cAMP regulates soluble guanylate cyclase beta 1-subunit gene expression in RFL-6 rat fetal lung fibroblasts. Am J Physiol 265, L456-461.

Stohwasser, R., Giesebrecht, J., Kraft, R., Muller, E.C., Hausler, K.G., Kettenmann, H., Hanisch, U.K., Kloetzel, P.M., 2000. Biochemical analysis of proteasomes from mouse

microglia: induction of immunoproteasomes by interferon-gamma and lipopolysaccharide. Glia 29, 355-365.

Takata, M., Filippov, G., Liu, H., Ichinose, F., Janssens, S., Bloch, D.B., Bloch, K.D., 2001. Cytokines decrease sGC in pulmonary artery smooth muscle cells via NO-dependent and NO-independent mechanisms. Am J Physiol Lung Cell Mol Physiol 280, L272-278.

Ujiie, K., Hogarth, L., Danziger, R., Drewett, J.G., Yuen, P.S., Pang, I.H., Star, R.A., 1994. Homologous and heterologous desensitization of a guanylyl cyclase-linked nitric oxide receptor in cultured rat medullary interstitial cells. J Pharmacol Exp Ther 270, 761-767.

van Staveren, W.C., Markerink-van Ittersum, M., Steinbusch, H.W., Behrends, S., de Vente, J., 2005. Localization and characterization of cGMP-immunoreactive structures in rat brain slices after NO-dependent and NO-independent stimulation of soluble guanylyl cyclase. Brain Res 1036, 77-89.

Wikstrom, L., Lodish, H.F., 1991. Nonlysosomal, pre-Golgi degradation of unassembled asialoglycoprotein receptor subunits: a TLCK- and TPCK-sensitive cleavage within the ER. J Cell Biol 113, 997-1007.

Zhang, G., Ghosh, S., 2000. Molecular mechanisms of NF-kappaB activation induced by bacterial lipopolysaccharide through Toll-like receptors. J Endotoxin Res 6, 453-457.

Zhang, J., Snyder, S.H., 1995. Nitric oxide in the nervous system. Annu Rev Pharmacol Toxicol 35, 213-233.

Zwiller, J., Revel, M.O., Malviya, A.N., 1985. Protein kinase C catalyzes phosphorylation of guanylate cyclase in vitro. J Biol Chem 260, 1350-1353.

FIGURES

Fig. 1. LPS-induced degradation the GC_{NO} β1 subunit in astrocytes is prevented by the proteasome inhibitor MG-132. Rat cerebellar astrocyte-enriched cultures were treated or not with 10 ng/ml LPS for 24 h in the absence or presence of MG-132 at 5 μM (B) or at the indicated concentrations (C,D) added 1 h before LPS. (A, B) Cytosolic fractions (15-20 μg protein) were subjected to SDS-PAGE and transferred to PDVF membranes. GC_{NO} β1 subunit (70 kDa) was detected using a 1:2,000 dilution of an affinity-purified rabbit polyclonal antibody. Immunoreactive bands were not detected when the antibody was pre-absorbed with a 1,000-fold excess concentration of antigenic peptide (A). Blots shown are representative of two similar experiments; (C) Nitrite levels in the culture media determined with the Greiss reagent; (D) Intracellular cGMP measured by radioimmunoassay in cell monolayers washed and stimulated with 100 μM SNP for 3 min in the presence of 1 mM IBMX. Results are means ± range of 2 experiments.

Fig. 2. LPS-induced degradation of GC_{NO} β1 is independent of NFkB activation. Cultures were treated or not with 10 ng/ml LPS for 24 h in the absence or presence of the NFkB inhibitors PDTC (100 μM) or BAY-117082 (10 μM) added one hour before. (A) Nitrite levels in the culture media were determined with the Greiss reagent. Results are means ± SEM of 3 experiments; (B) Immunodetection of GC_{NO} β1 in cytosolic fractions (15-20 μg protein). Blots shown are representative of two experiments.

Fig. 3. LPS-induced degradation of GC_{NO} β1 does not involve decreased interaction with HSP90. Cultures were treated or not with 10 ng/ml LPS for 24 h in the absence or presence of the HSP90 inhibitors radicicol (5 μM) or 17-AGG (50 nM) (A, C) or at the indicated concentrations (B) added 1 h before LPS. (A) Inhibition of LPS-induced morphological change by HSP90 inhibitors. Phase-contrast images representative of three (radicicol) and two (17-AGG) independent experiments. (B) Nitrite levels in the culture media, means ± SEM, n=3; (C, D) Immunodetection of GC_{NO} β1 and HSP90 in cytosolic fractions (15-20 μg protein). Blots shown are representative of two experiments.

Fig. 4. LPS induces the formation of GC_{NO} β1 protein aggregates in astrocyte nuclei. Cell cultures were treated or not with 10 ng/ml LPS for 24h (A,C,D) or the indicate times (B). (A) Cells were fixed and double-stained for GC_{NO} β1 (red) and GFAP (green) as described in Material and Methods. GC_{NO} β1 immunostaining was abolished by pre-absorption of the antibody with the antigenic peptide (Ab,d). Note the diffuse nuclear (arrowhead) and

cytoplasmic (astherisc) staining in untreated cells (Aa) compared with the punctuated nuclear staining (arrohead) in LPS-treated cells (Ac). Representative images of 8 independent experiments; (B) Percentage of astrocytes presenting GC_{NO} β1 immunostaining with diffuse or aggregated pattern as a function of LPS-treatment time; results are means ± range of 150-200 cells counted per assayed time in each of two independent experiments; (C) Immunogold electron microscopy with anti-β1 antibody in LPS-treated cells; (D) Soluble (Fs) and nuclear (N) proteins (10 µg) were subjected to SDS-PAGE and transferred to PDVF membranes for immunodetection of GC_{NO} β1 and the cytosolic and nuclear markers GAPDH and lamin B, respectively. The blot shown is representative of two experiments

Fig.5. GC_{NO} β1 co-localizes with the 20S proteasome in the nuclei of LPS-treated cells. Inhibition by MG-132 and cicloheximide. Cell cultures were treated or not with 10 ng/ml LPS for 24h in the absence o presence of 5 μM MG-132 and 10 μM cicloheximide (CHX) added 1 h before LPS. Then, cells were fixed and GC_{NO} β1 (red) and 20S proteasome (green) double-staining was performed as described in Materials and Methods and visualized with confocal microscope Zeiss LSM 510. Figures are representative of three independent experiments.

Fig.6. GC_{NO} β1 co-localizes with ubiquitin in the nuclei of LPS-treated cells. Inhibition by MG132 and cicloheximide. Cell cultures were treated or not with 10 ng/ml LPS for 24 h in the absence o presence of 5 μM MG132 or 10 μM cicloheximide (CHX) added 1 h before LPS. Then, cells were fixed and GC_{NO} β1 (red) and ubiquitin (green) double-staining was performed and visualized with confocal microscope Leica TCS SP2 AOBS. The mask (right column) represents colocalization of the two fluorophores. Figures are representative of three independent experiments.

Fig.7. Ubiquitin-protein conjugates co-localize with 20S proteasome in the nuclei of LPS-treated cells. Inhibition by MG132. Cell cultures were treated or not with 10 ng/ml LPS for 24 h in the absence o presence of 5 μM MG132 added 1 h before LPS. Then, cells were fixed and 20S proteasome (green) and ubiquitin-protein conjugates (red) double-staining was performed and visualized with confocal microscope Zeiss LSM 510. Figures are representative of two independent experiments.

Fig.8. GC_{NO} β1 protein does not co-localize with histones (A), SUMO-1 (B) and TMG-CAP (C) in the nuclei of LPS-treated cells. Cell cultures were treated with 10 ng/ml LPS for 24h. Then, cells were fixed and double-stained for GC_{NO} β1 (red) and pan-histone (green) (A), SUMO-1 (green) (B) or TMG-CAP (green) (C). Cells were visualized with confocal microscope Zeiss LSM 510. Figures are representative of two independent experiments.

Table 1. Effect of protease inhibitors on LPS-induced accumulation of nitrites and SNP-stimulated cGMP formation in cerebellar astrocyte cultures.

Compounds	Nitrites, μM (% of LPS)	SNP-stimulated cGMP (% of control)
-	100	40 ± 6
Lactacystin [1 μM] [10 μM]	 86 ± 1 4 ± 1	 43 ± 6 89 ± 10
AEBSF [500 μM]	7 ± 1	87 ± 3
Calpain inhibitor [25 μM]	55 ± 3	17 ± 5
ICE inhibitor II [100 μM]	66 ± 10	20 ± 5
Leupeptin [5 μM]	93 ± 9	45 ± 5

Cell cultures were treated or not with 10 ng/ml LPS for 24 h, in the absence or presence of proteases inhibitors at the indicated concentrations, added 1 h before LPS. Nitrite levels were determined with the Greiss reagent in the culture media. Cell monolayers were washed, stimulated with 100 μM SNP for 3 min in the presence of 1 mM IBMX and intracellular cGMP measured by RIA. Results are means ± range of 2 experiments.

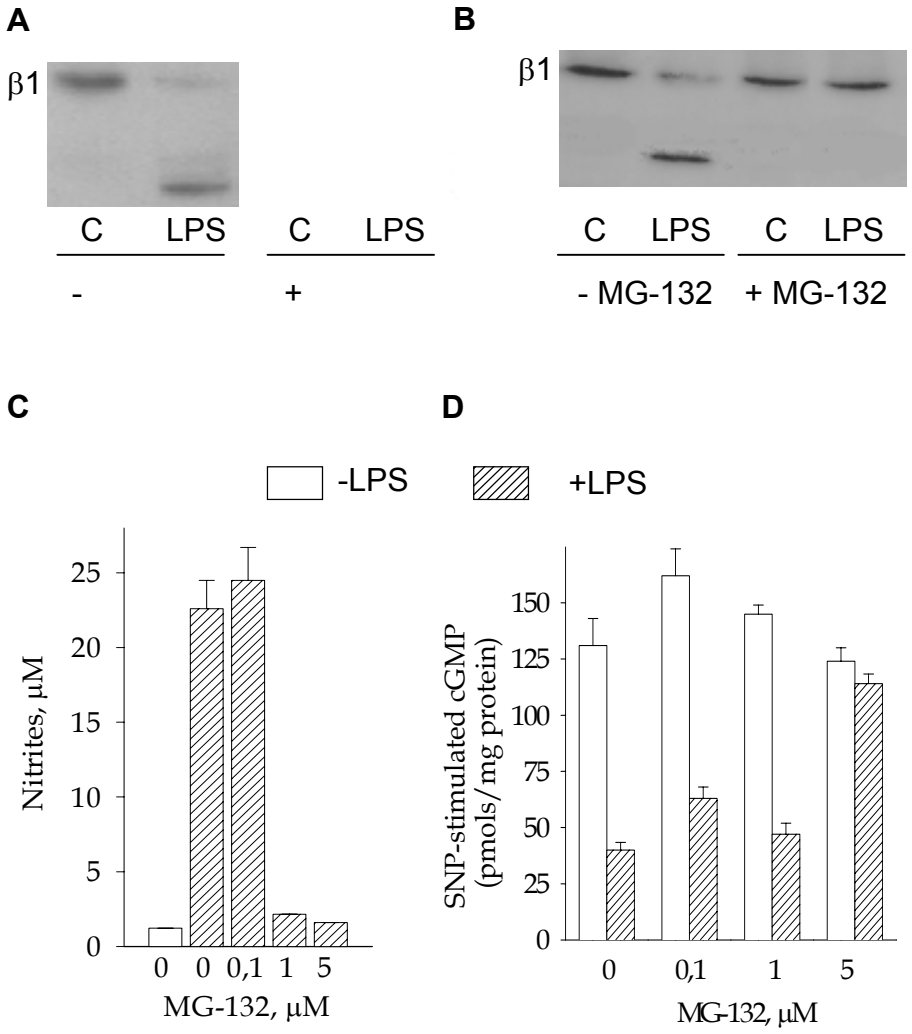
A
β1
C
LPS
C
LPS
-
+
B
β1
C
LPS
C
LPS
- MG-132
+ MG-132
C
-LPS
+LPS
Nitrites, μM
25
20
15
10
5
0
0
0
0,1
1
5
MG-132, μM
D
SNP-stimulated cGMP (pmols/mg protein)
150
125
100
75
50
25
0
0
0,1
1
5
MG-132, μM

Figure 1

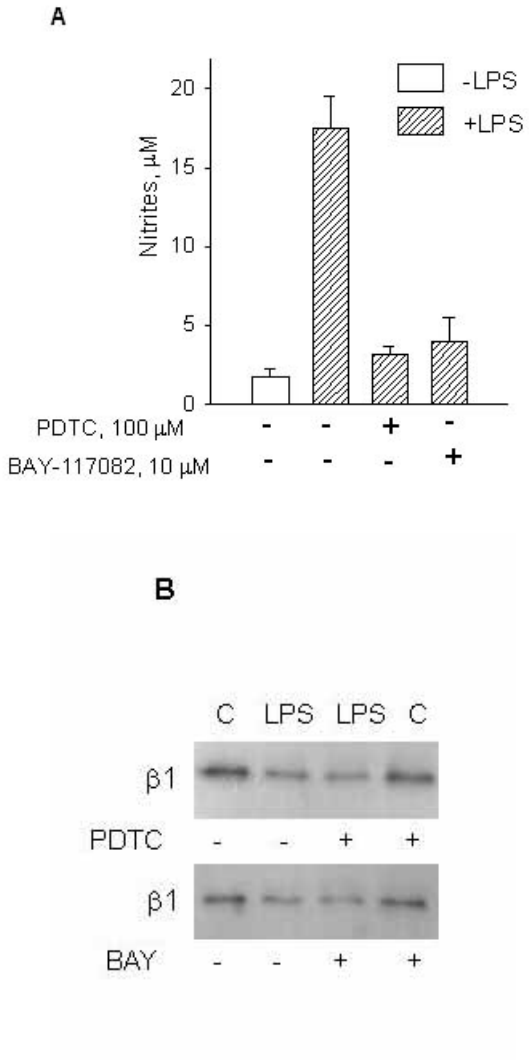
A
-LPS
+LPS
Nitrites, μM
20
15
10
5
0
PDTC, 100 μM
BAY-117082, 10 μM
B
C
LPS
LPS
C
β1
PDTC
β1
BAY

Figure 2

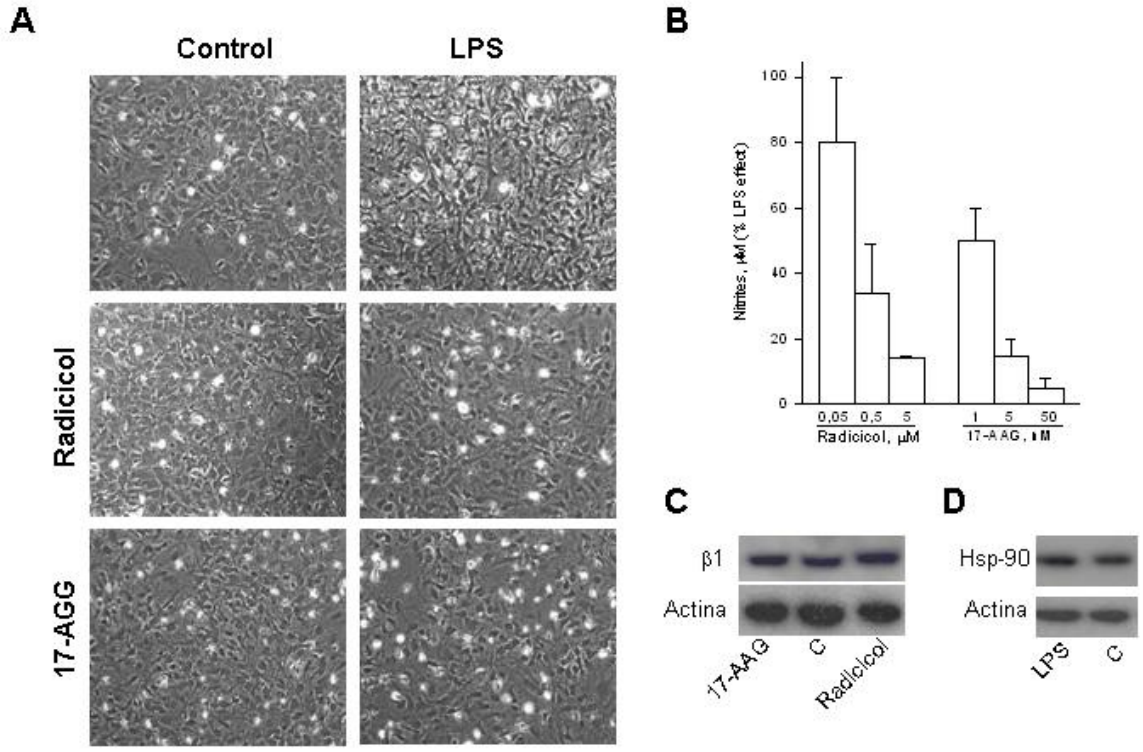
A
Control
LPS
Radicicol
17-AGG
B
Nitrites, µM (% LPS effect)
100
80
60
40
20
0
0,05 0,5 5
Radicicol, µM
1 5 50
17-AAG, nM
C
β1
Actina
17-AAG
C
Radicicol
D
Hsp-90
Actina
LPS
C

Figure 3

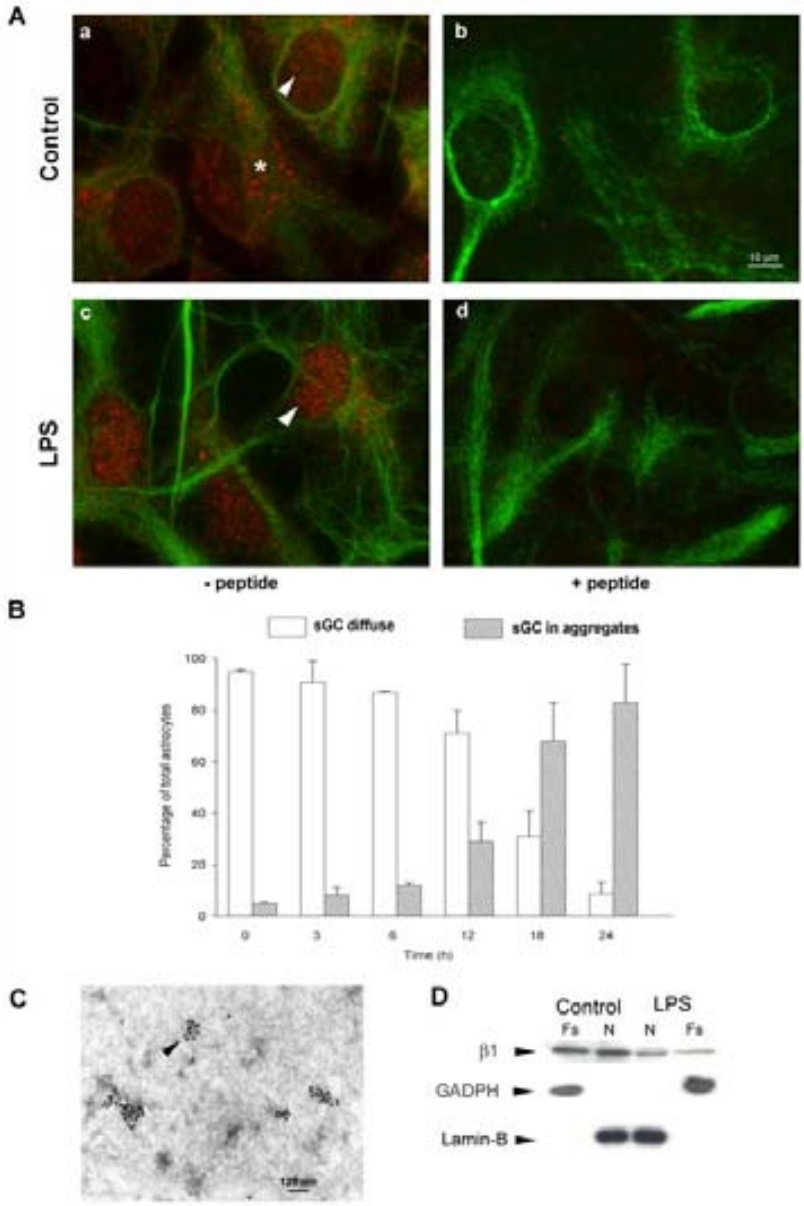
A
a
b
c
d
Control
LPS
- peptide
+ peptide
B
sGC diffuse
sGC in aggregates
Percentage of total astrocytes
Time (h)
C
D
Control
LPS
Fs
N
N
Fs
β1
GADPH
Lamin-B

Figure 4

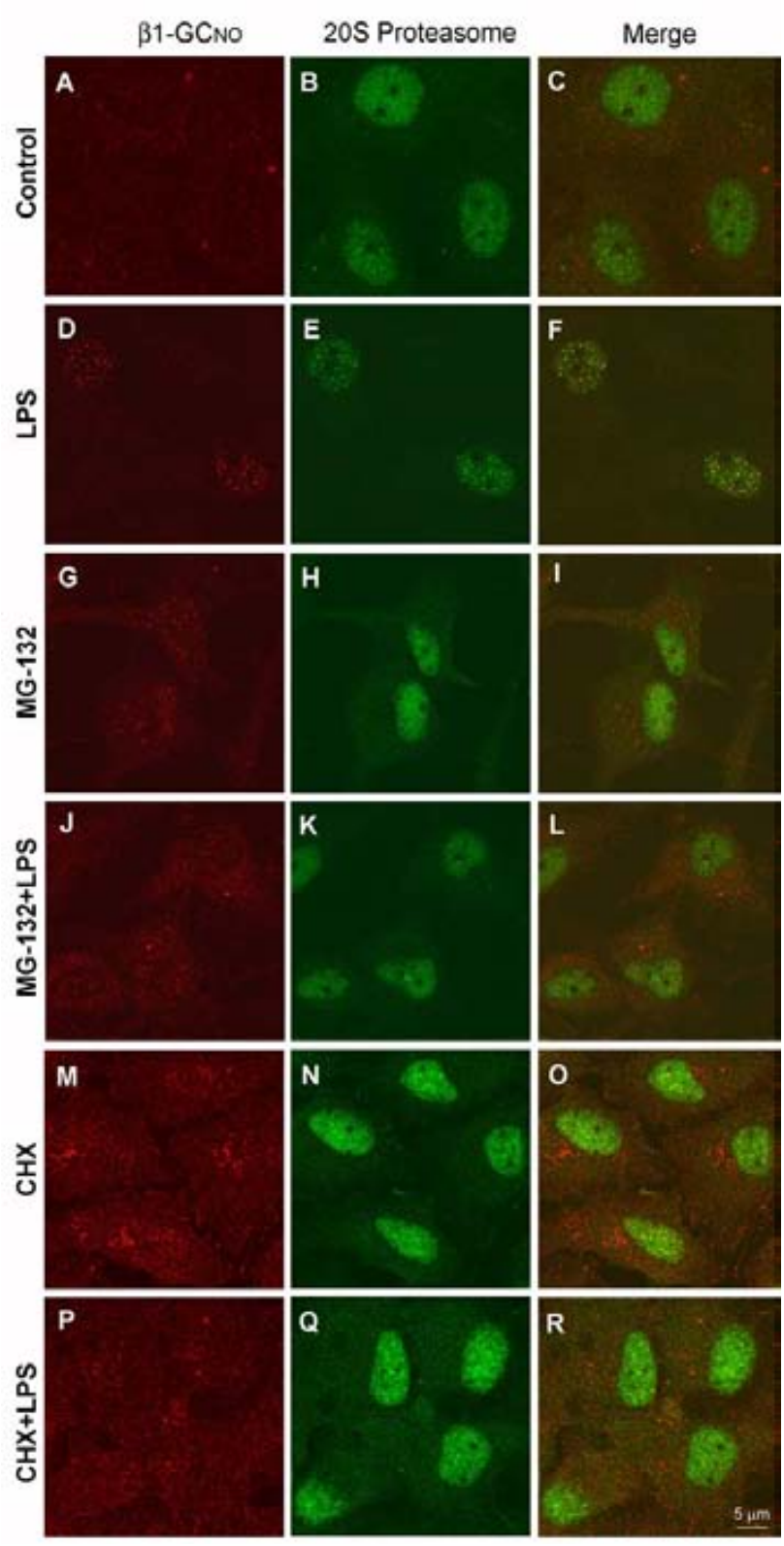
β1-GCNO
20S Proteasome
Merge
Control
LPS
MG-132
MG-132+LPS
CHX
CHX+LPS
A
B
C
D
E
F
G
H
I
J
K
L
M
N
O
P
Q
R
5 μm

Figure 5

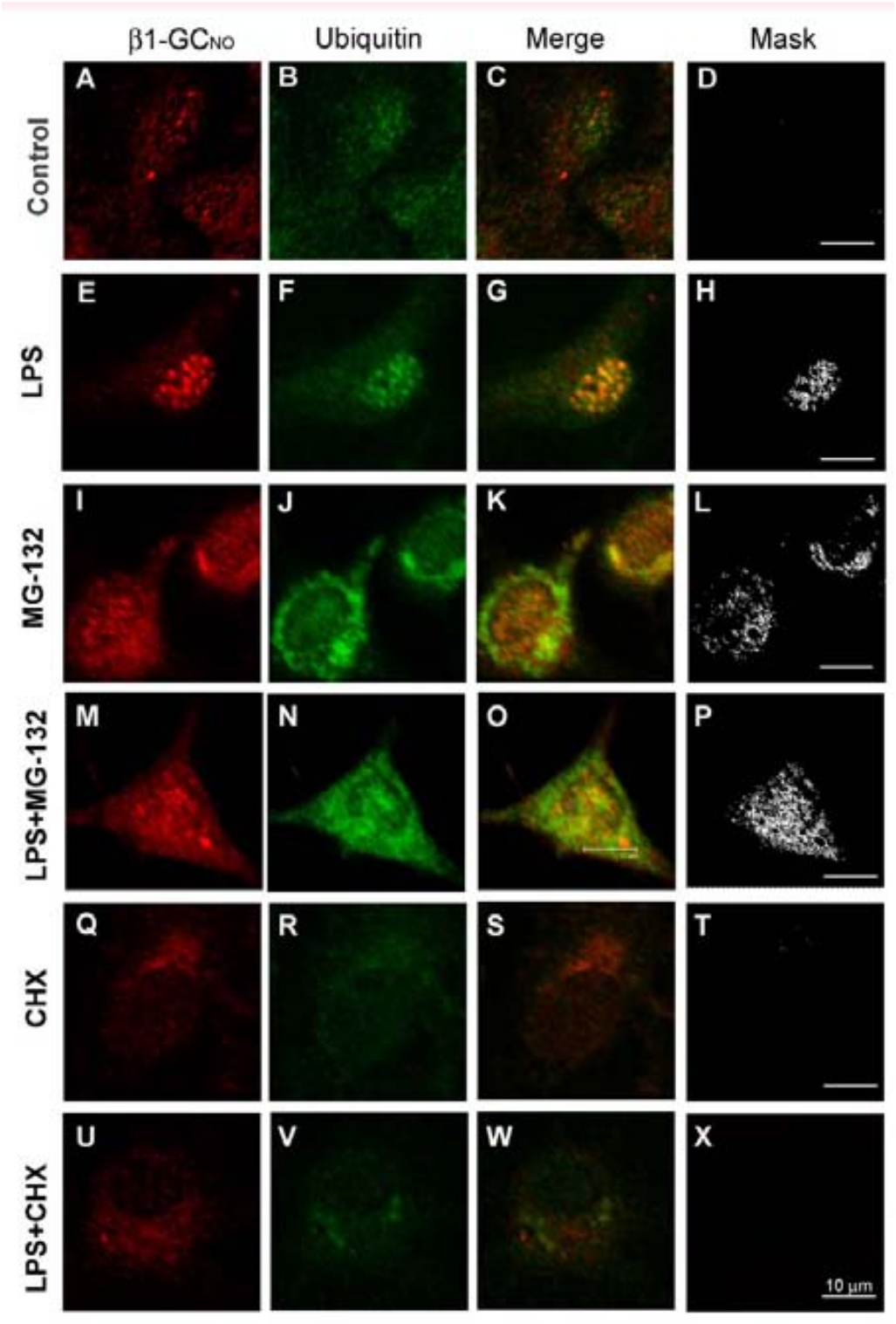
β1-GCNO
Ubiquitin
Merge
Mask
Control
LPS
MG-132
LPS+MG-132
CHX
LPS+CHX
A
B
C
D
E
F
G
H
I
J
K
L
M
N
O
P
Q
R
S
T
U
V
W
X
10 μm

Figure 6

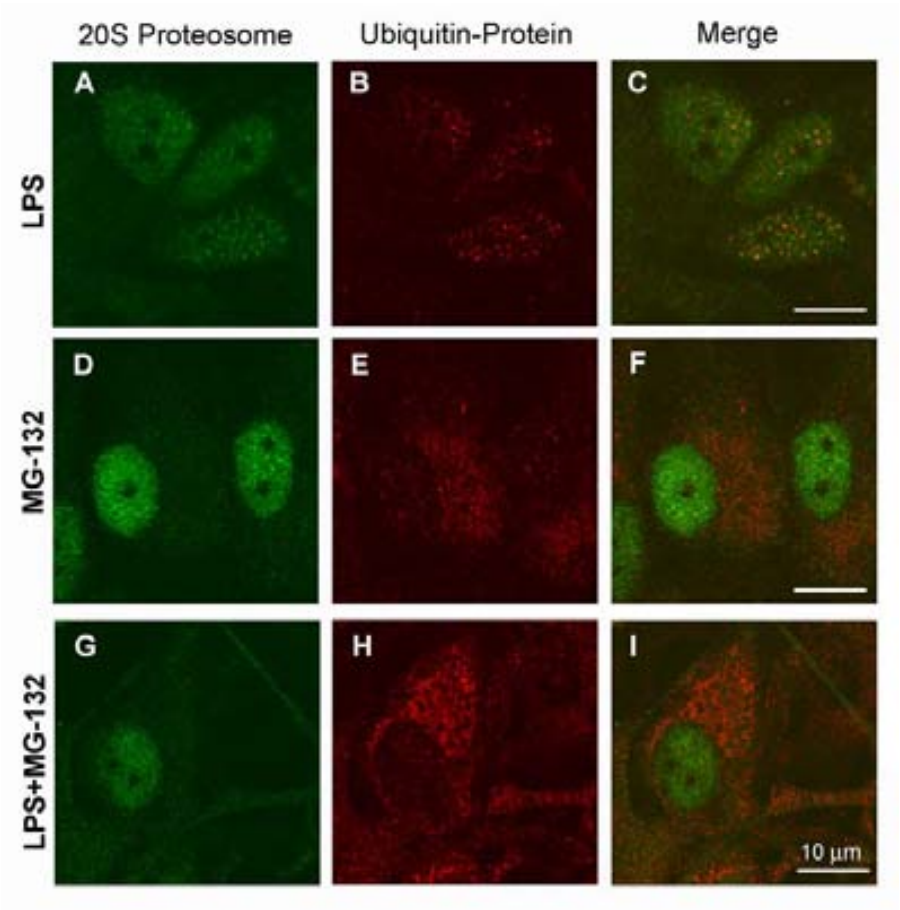

Figure 7

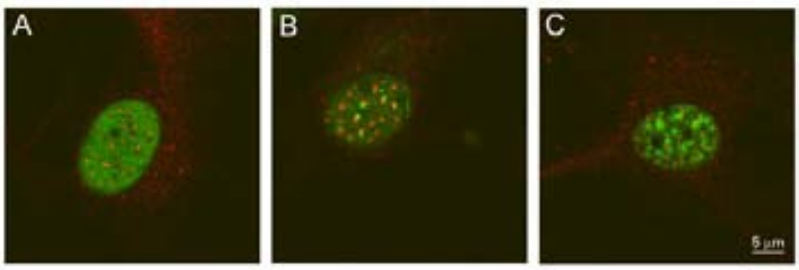

Figure 8

8 Resumen Trabajo 4

Estudios previos de nuestro grupo (trabajo 1) y de otros autores sobre la localización en el cerebro de las subunidades de la GC_{NO} demuestran que la subunidad β1 es más abundante y se encuentra más ampliamente distribuida que las subunidades α en el SNC. Además, según lo que hemos descrito en el primer trabajo, existen varias regiones donde los niveles de la subunidad β1 son elevados y los de las α son muy bajos o indetectables. Teniendo en cuenta que el homodímero β1/β1 es catalíticamente inactivo estos datos sugieren que esta subunidad pueda tener otra función independiente de la actividad enzimática. La localización intracelular de la GC_{NO} y de su producto GMPc es predominantemente citoplasmática, sin embargo estudios recientes publicados en el transcurso de este trabajo sugieren que la GC_{NO} es capaz de traslocarse a las membranas y a otras estructuras intracelulares. Durante el transcurso de nuestros estudios sobre la distribución celular y subcelular de las subunidades de la GC_{NO} en el SNC hemos detectado la expresión de la subunidad β1 en células con actividad enzimática GC_{NO} (neuronas y astroglía), así como en células incapaces de generar GMPc en respuesta a NO (microglía). En ambos casos, la β1 presentaba una localización mayoritariamente citoplasmática pero también se observó en el núcleo de células en interfase. Además, estudios de inmunocitoquímica en células tratadas con agentes mitogénicos como el éster de forbol PMA presentaban mayor intensidad de marcaje para la subunidad β1. Estudios a mayor resolución permitieron demostrar que la GC_{NO} β1 se encontraba asociada periféricamente a los cromosomas durante todas las fases de la mitosis. Al analizar las posibles funciones de esta asociación con los cromosomas observamos que la inmunodepleción del pool citoplasmático y nuclear de la proteína producían un aumento de la condensación de la cromatina, y que este aumento era independiente del GMPc ya que el tratamiento con un inhibidor específico de la GC_{NO} (ODQ) no producía los mismos efectos. Paralelamente, mediante técnicas de silenciamiento del mRNA (siRNA) observamos que la inhibición de la subunidad β1 produce un aumento del número de células que entran en ciclo celular (fase S, G_2 y M) y un aumento en la proliferación celular. Estos efectos tampoco eran mimetizados por el ODQ. Estos resultados indican que la subunidad β1 es una proteína multifuncional que puede tener un efecto regulador de la condensación de la cromatina y del ciclo celular independiente de la actividad GC_{NO}.

NO-sensitive guanylyl cyclase β1 subunit interacts with chromosomes during mitosis. Novel role in chromatin condensation and cell cycle progression.

Paula Pifarré*[1], María Antonia Baltrons*[1], Verónica Davalos[2], Simón Schwartz Jr.[2] and Agustina García[1]

[1]Institute of Biotechnology and Biomedicine and Department of Biochemistry and Molecular Biology, Autonomous University of Barcelona, Spain
[2]Molecular Oncology and Aging Group, Biochemistry and Molecular Biology Research Center (CIBBIM), Vall d'Hebron University Hospital Research Institute, Barcelona
* These authors have equally contributed to the work

Author for correspondence:

María Antonia Baltrons,
Instituto de Biotecnología y Biomedicina, V. Villar Palasí
Universidad Autónoma de Barcelona
Tel: +34 93 581 11 81
Fax:+34 93 581 20 11
e-mail: mariaantonia.baltrons@uab.es

Submitted to Journal Cell Science

SUMMARY

NO-sensitive guanylyl cyclase (GC_{NO}) is the best characterized target of NO and its product cGMP the mediator of most of the important physiological functions of NO in the cardiovascular and central nervous system (CNS). Functional GC_{NO} exists as $\alpha1/\beta1$ and $\alpha2/\beta1$ heterodimers and is predominantly cytosolic, although recent studies indicate that it can associate to membranes and other intracellular structures including nuclei. In the CNS, in situ hybridization studies evidenced that $\beta1$ is more widespread than α subunits and that in some areas is almost the only GC_{NO} subunit expressed, suggesting that it may have functions other than GC_{NO} activity. In the course of our studies on the cellular and sub-cellular distribution of GC_{NO} subunits in rat CNS glial cells we found that the $\beta1$ subunit is localized in the cytoplasm and the nucleus of cells expressing α subunits and GC_{NO} activity (astrocytes, C6 glioma), as well as in cells devoid of α subunits and GC_{NO} activity (microglia). In both cell types GC_{NO} $\beta1$ associates peripherally to chromosomes during all phases of mitosis. In C6 glioma cells, immunodepletion of $\beta1$ enhances chromatin condensation in an *in vitro* assay. Moreover, silencing $\beta1$ by siRNA increases the percentage of cells that enter the cell cycle and the proliferation rate. These actions are not mimicked by treatment with a specific GC_{NO} inhibitor (ODQ). We postulate that the $\beta1$ subunit is a multifunctional protein that, in addition to its role as an obligate monomer in active GC_{NO}, associates to chromosomes during mitosis and regulates chromatin condensation and cell cycle progression.

INTRODUCTION

Nitric oxide (NO) is an intra- and intercellular signalling molecule that exerts important regulatory functions in many cells and tissues particularly in the cardiovascular, immune and central nervous system (SNC) (Moncada et al., 1991). Additionally, a large body of evidence indicates that NO is a physiological modulator of cell proliferation able to promote in most cases cell cycle arrest (Villalobo, 2006). Special attention has been paid to the role of cGMP in all these effects because the predominantly soluble guanylyl cyclase is the major NO target.

In mammalian cells, NO-sensitive GC (GC_{NO}) exists as an obligate heterodimer of one α and one β subunit with a prosthetic heme group that is the binding site for NO (Denninger and Marletta, 1999; Koesling et al., 2004). Two types of each subunit have been cloned (α1-2, β1-2), but only the β1-containing isoforms have been shown to exist at the protein level (Russwurm et al., 1998). GC_{NO} $\alpha1\beta1$ is the most ubiquitous heterodimer specially in the cardiovascular system and lung whereas GC_{NO} $\alpha2\beta1$ is predominantly expressed in brain (Mergia et al., 2003). In general, expression of β1 has been found more widespread than that of α subunits and detailed tissue localization studies have in some instances shown mismatches in the mRNA expression of GC_{NO} subunits. For instance, in structures of the rat olfactory system, a strong expression of GC_{NO} β1 mRNA does not appear to be matched by a high expression of either of the α subunits (Mergia et al., 2003). Expression of GC_{NO} β1 mRNA and protein but not of the α subunits was recently observed in undifferentiated murine embryonic stem cells (Krumenacker et al., 2006). Bidmon et al (2004) described a mismatched in the levels of α2 subunit expressions during development in some regions of the CNS, where the increase of expression of these subunit was not compensated by an increase of α1 or β1 subunits. Since homodimers appear to be catalytically inactive (Zabel et al., 1999), these data suggested the possibility of single subunits serving functions other than GC_{NO} activity.

Although immunocytochemical and biochemical methods have localized GC_{NO} and NO-dependent cGMP formation predominantly in the cytosol, recent studies suggest that GC_{NO} translocates to membranes and other intracellular structures. The $\alpha2\beta1$ isoform has been found associated to neuronal membranes through interaction with postsynaptic density proteins (Bidmon et al., 2004; Russwurm et al., 2001). A Ca^{2+}-dependent targeting of the $\alpha1\beta1$ heterodimer to membranes has been shown in myocardial tissue, endothelial cells and platelets (Agullo et al., 2005; Zabel et al., 2002) and interaction with the chaperone Hsp70 has been suggested as a mechanism for GC_{NO} translocation to membranes in smooth muscle cells (Balashova et al., 2005). Moreover, nuclear localization of GC_{NO} and cGMP has been described

in liver (Earp et al., 1977; Gobeil et al., 2006), the organ of Corti (Earp et al., 1977; Heinrich et al., 2000) and embryonic stem cell-derived cardiomyocytes (Krumenacker et al., 2006).

In the course of our recent studies on the cellular and sub-cellular distribution of GC_{NO} subunits in CNS cells we have found that the β1 subunit is expressed in cells devoid of α subunits and GC_{NO} activity and that in these cells as well as in cells that express an active GC_{NO} the β1 subunit localizes both in the cytoplasm and the nucleus. We have also observed that GC_{NO} β1 associates peripherally to chromosomes during all phases of mitosis and appears to regulate chromatin condensation and cell cycle progression independent of cGMP formation.

RESULTS

Nuclear localization of the GC_{NO} β1 subunit and peripheral association to chromosomes during mitosis

As expected, immunocytochemical labeling of confluent primary astrocyte-enriched cultures from rat cerebellum with an affinity-purified polyclonal antibody against the β1 subunit of GC_{NO} and observation by confocal microscopy showed β1-immunoreactivity predominantly in the cytoplasm (Fig 1A). However, label appeared more concentrated in perinuclear structures and was also observed in the nuclei (Fig 1A, 2A). Nuclear β1 staining was much stronger in astrocytes treated with mitogenic agents. As shown in Fig 1B, in cultures treated with the phorbol ester PMA (100 nM, 24 hours) cells positive for the astroglial marker GFAP present the reported change in morphology with soma retraction and process elongation (Harrison and Mobley, 1990; Harrison et al., 1991) and β1-immunoreactivity is observed in the cytoplasm and along the elongated processes, but is particularly intense in nuclei where chromatin condensation is evidenced by DAPI counterstain. Similar nuclear staining was observed with other astrocyte mitogenic agents like IL-1β (10 ng/ml, 24 hours) or endothelin-1 (20 nM, 24 hours) (not shown). Observation of mitotic cells at higher magnification showed that β1-immunoreactivity was associated to chromatin at all stages of mitosis (Fig 2A). During prophase, metaphase and anaphase, β1-immunoreactivity associates peripherally with chromosomes. Even at telophase, strong immunoreactivity is still associated with decondensing chromosomes. This staining was absent when the primary antibody was omitted (not shown) or was pre-adsorbed with 1,000-fold excess of the β1-antigenic peptide (Fig 2B).

Nuclear as well as cytoplasmic β1-staining was also observed in GFAP- negative cells resembling microglia, the main contaminants of astrocyte-enriched cultures (insert in Fig 1B). This was confirmed in microglial cultures obtained from the astrocyte-enriched cultures by lifting the astrocyte monolayer by mild trypsinization (Saura et al., 2003). In cells double-stained with anti-β1 antibody and the microglial marker DIL-Ac-LDL, β1-immunoreactivity was observed in the cytoplasm and nuclei of all DIL-Ac-LDL-positive cells and staining was stronger in the few cells showing condensed chromatin (Fig 1C, arrowhead and insert).

GC_{NO} β1 subunit association with chromosomes during mitosis was also observed in the C6 glioma cell line and in the immortalized rat microglia cell line HAPI (Fig 3A, B) and in other cells types (human astrocytoma SW1088, human neuroblastoma SK-N-SH, murine microglia BV2, rat mesencephalic astroglia D1TNC1, primary cultures of fibroblasts from rat meninges and rat

smooth muscle cell line A7r5, not shown). In addition, similar immunoreactiviy was obteined when cells were fixed with PFA or methanol.

The peripheral association of β1-immunoreactivity was maintained in methaphase chromosome spreads obtained from C6 and HAPI cells after hypotonic swelling, cytocentrifugation and fixation with 4% PFA (Fig 3C).

Subcellular fractionation and western blot confirmed the presence of the β1 subunit in the cytosol and the nucleus in C6 cells but no association with membranes was evidenced (Fig 4D). No difference between quiescent and mitotic cells was observed in the amount of β1 protein in homogenates suggesting that the increased fluorescence labelling observed in mitotic cells is not due to increased expression of β1 protein (Fig 4F).

GC_{NO} β1 subunit is expressed in cells lacking GC_{NO} enzymatic activity

The observation of β1 immunoreactivity in microglia was surprising because rat brain microglia has been reported to be devoid of GC_{NO} activity (Agullo et al., 1995; Teunissen et al., 2000). This is confirmed here by the absence of cGMP-immunostaining in cultured microglia exposed to the NO donor SNP (100 μM, 3 min, in the presence of 1 mM IBMX) while a general staining is observed in astrocytes (Fig. 4A). In these later cells, in contrast to β1-immunoreactivity, cGMP-immunostaining was observed in the cytoplasm and along the processes but not in nuclei. Cyclic GMP formation in response to SNP was also measured by RIA in C6 glioma cells, although at a lower level than in primary astrocytes, but was not detected in HAPI cells (Fig 4B), in agreement with results in primary microglia.

When expression of GC_{NO} subunits was analyzed by RT-PCR (Fig 4C), primary astrocytes were shown to express mRNA for GC_{NO} α1 and α2 subunits in addition to β1, while C6 cells only expressed β1 and α2, suggesting that both β1α1 and β1α2 heterodimers contribute to GC_{NO} activity in astrocytes but only β1α2 is responsible for the activity in C6 cells. In contrast, only the mRNA for the β1 subunit was expressed in HAPI cells. Expression of the β1 subunit at the protein level was also shown in HAPI cells by immunoblot. Two β1-immunoreactive bands showing almost the same electrophoretic mobility between them (MW ≈ 70 kDa) and with the one in primary astrocytes and C6 cells were detected in cytosolic fractions and to a lower extend in nuclear fractions (Fig 4E). The expression of the GC_{NO} β1 subunit in cells lacking α subunits and GC_{NO} activity suggested that this protein could be playing additional functions.

Nuclear localization of β1 but not of α subunits in transiently transfected C6 cells

In order to discard the possibility that the immunodetection of the β1 subunit in cell nuclei was due to a non-specific binding of the anti-β1 antibody, we transiently transfected C6 cells with plasmids containing β1-GFP. Given the lack of anti-α1 and anti-α2 antibodies appropriate for immunocytochemistry, we also transfected cells with α1-YFP or α2-YFP constructs to examine if these subunits also had a nuclear localization. After 24 hours cells were fixed and fluorescence analysed by confocal microscopy. Cells transfected with β1-GFP presented fluorescence in both the cytoplasm and the nucleus, whereas in cells transfected with α1-YFP or α2-YFP fluorescence was detected in the cytoplasm (Fig 5A). However, when C6 cells were co-transfected with β1-GFP and α1-YFP or α2-YFP, β1 was never observed in the nuclei (Fig 5B) suggesting that interaction with α subunits may prevent β1 translocation to the nucleus. Time-lapse examination of β1-GFP transfected cells confirmed the nuclear localization in living cells (supplementary material, Movie 1).

Immunodepletion of GC_{NO} β1 increases chromatin condensation

Proteins that associate peripherally to mitotic chromosomes have been shown to regulate chromatin condensation (Van Hooser et al., 2005). To investigate if this was also a function of perichromosomal GC_{NO} β1 we used the in vitro chromatin condensation assay described by Collas et al. (1999). Nuclei from unsynchronized C6 cells were incubated with cytosolic extract from mitotic cells (synchronized and treated 18 hours with colcemid) for 90 minutes and chromatin condensation was assessed after staining with Hoechst 33342. Chromatin was considered to condense when it acquired an irregular and compact morphology sometimes with distinct chromosomes or chromosome fragments. In order to block the function of nuclear β1, nuclei were loaded with anti-β1 antibody (or IgG as control) as described in Material and Methods. Antibody-loaded nuclei were exposed to normal mitotic extracts or extracts pre-incubated for 1 hr with anti-β1 antibody. Results from the quantification of condensed (Fig 6B,B') and decondensed nuclei (Fig 6A) in different experiments are presented in Fig 6C and show that the anti-β1 antibody, but not pre-immune IgGs, significantly increased the ratio of condensed to decondensed nuclei from 57% to 74% when the antibody was present in both nuclei and mitotic extract. However, no significant effect on chromatin condensation was observed when the antibody was present only in the nuclei or the mitotic extract, indicating that total immunodepletion of β1 is necessary to alter chromatin condensation. Since C6 cells express an active GC_{NO} we examined the possibility that this activity rather than the β1 protein itself was responsible for the regulation of chromatin condensation by pre-treating both the interphase nuclei and the mitotic extract with the GC_{NO} specific inhibitor ODQ (100 μM). As

shown in Fig 6C, the presence of this inhibitor did not mimic the effect of the anti-β1 antibody in chromatin condensation thus ruling out the implication of basal GC_{NO} and supporting a functional role of β1 protein independent of cGMP generation.

Silencing GC_{NO} β1 with siRNA increases cell proliferation

Based on the effect of β1-immunodepletion on chromatin condensation we hypothesized that knock down of this protein would also affect cell cycle progression and hence proliferation. In order to suppress the β1 mRNA we transfected C6 cells with a specific siRNA. Real-time PCR analysis showed that 48 hours after transfection β1 mRNA levels were down to around 35% of those in control cells or cells transfected with scrambled siRNA (Fig 7A). Silencing of β1 mRNA lead to an increase of around 50% in cell proliferation as determined by the EZ4U assay in subcultured cells (Fig 7B). In agreement with this, when cell cycle progression was analysed by flow-cytometry we observed that the percentage of cells that had entered the cell cycle ($S\text{-}G_2\text{-}M$) increased from 22.1 ± 5.5 in control to 46.2 ± 9.0 in cells transfected with siRNA for 48 hours (means ± s.e.m., n=4; Fig 7C, D). These effects are specific for β1 siRNA because transfection with scrambled siRNA did not significantly affect cell proliferation or cell cycle progression (Fig 7). Treatment of cells with the GC_{NO} inhibitor ODQ (100 μM, 24 hours) did not mimic the effects of β1 mRNA disruption on cell proliferation (Fig 7A) indicating that basal cGMP formation is not involved.

DISCUSSION

The predominantly cytoplasmic GC_{NO} is the best characterized target of NO and its product cGMP the mediator of most of the important physiological functions of NO in the cardiovascular and central nervous system. Functional GC_{NO} exists as heterodimers of $\alpha1/\beta1$ and $\alpha2/\beta1$ subunits. In this study we provide evidence that the $\beta1$ subunit is a multivalent protein that, besides its role as an obligate monomer in functional GC_{NO} heterodimers, interacts with chromosomes during mitosis and regulates cell cycle progression in a cGMP-independent manner.

We confirm here in CNS cells previous reports showing a nuclear localization of the GC_{NO} $\beta1$ subunit in hepatocytes (Earp et al., 1977; Gobeil et al., 2006) and embryonic stem (ES) cell-derived cardiomyocytes (Krumenacker et al., 2006). In those studies, nuclear cGMP production was also shown. In contrast, in the present work we have detected $\beta1$ protein in the nuclei of cells that have a functional GC_{NO} such as rat astrocytes but cGMP immunostaining after stimulation with a NO donor (SNP) was observed only in the cytoplasm. Moreover, we have observed $\beta1$-immunoreactivity in the cytoplasm and the nucleus of cells where GC_{NO} activity is undetectable like rat microglia in primary culture and the rat microglial cell line HAPI. In these later cells we could detect by RT-PCR the mRNA for the $\beta1$ subunit but not that for $\alpha1$ and $\alpha2$ subunits in agreement with the lack of GC_{NO} activity. These findings lead us to investigate if GC_{NO} $\beta1$ had a function independent of GC_{NO} activity. The observation that $\beta1$ immunostaining was stronger in astrocytes treated with mitogenic agents (PMA, IL-1β, ET-1) and that it appeared associated peripherally to chromosomes during all phases of mitosis suggested that it could play a role in chromatin condensation and hence in cell division. Several evidences support this hypothesis. First, results obtained in C6 cells using an in vitro chromatin condensation assay previously described (Collas et al., 1999), demonstrated that when $\beta1$-immunodepleted interphase nuclei were incubated with $\beta1$-immunodepleted mitotic cytoplasmic extracts the percentage of nuclei showing chromatin condensation was significantly higher than when non-immunodepleted fractions were put together. Second, silencing $\beta1$ mRNA by siRNA increased the percentage of C6 cells entering the cell cycle as determined by flow cytometry. In agreement with this, mRNA silencing lead to enhanced cell proliferation as determined by an MTT assay. Since the C6 cells used in this study express $\alpha2$ subunits and present GC_{NO} activity, and previous evidences indicated that cGMP could mediate the inhibitory actions of NO on cell proliferation (Feil et al., 2005), we examined the possible implication of cGMP formation in the above effects with the use of the specific GC_{NO} inhibitor ODQ. Treatment with this compound (100 μM, 24 h) did not reproduce any of the effects observed after $\beta1$

immunodepletion or mRNA silencing, thus ruling out the participation of a basal RIA undetectable cGMP formation.

GC_{NO} β1-immunoreactivity in mitotic cells is stronger than in quiescent cells but when we analyzed by western blot the amount of protein in homogenates we did not find significant differences, indicating that the increased immunofluorescence is not due to increased de novo protein synthesis and suggesting that it results from the intracellular re-localization that takes place when the cell enters mitosis. The observation that immunodepletion of both the nuclear and the cytoplasmic pools is necessary to significantly stimulate chromatin condensation suggests that cytoplasmic β1 must be recruited to chromosomes after nuclear envelop breakdown. Thus, it is possible that the intense β1 immmunofluorescence associated with mitotic chromosomes is the result of a higher local concentration of β1 or that binding to chromosomes favors epitope recognition.

In metaphase chromosome spreads GC_{NO} β1-immunoreactivity was shown to be distributed peripherally along the entire length of chromosomes suggesting that it may form part of the specialized domain called perichromosomal layer that contains proteins know to be required for different cellular processes (mRNA synthesis, repair of DNA double-strand breaks, apoptosis, etc.) as well as proteins of unknown function (Van Hooser et al., 2005). During interphase, perichromosomal proteins localize in different intracellular compartments including the cytoplasm and targeting to the chromosomes occurs primarily during prophase. Peripheral sheaths begin to break down as the chromosomes begin to decondense at telophase. Because of the temporal link between perichromosomal layer formation and chromosome condensation a role in maintaining chromosome structure and in the progression of cells through mitosis has been suggested (Hernandez-Verdun and Gautier, 1994). Results shown here agree with a role of β1 in the regulation of both chromosome condensation and cell cycle progression. Chromosome condensation is a mechanism that involves a large number of protein families (Belmont, 2006). Whether a direct interaction of β1 with DNA or with chromosome scaffold proteins such as topoisomerasa II or members of the condensing complex is necessary for the regulation of chromatin condensation by β1 will have to be investigated. The presence in the GC_{NO} β1 sequence of phosphorylation motives for ataxia telengectasia mutated kinase (ATM) and DNA phospho kinase (DNA PK) (tyrosines 366 and 203, respectively), both implicated in early steps of DNA repair (Tomimatsu et al., 2007), suggests that β1 could additionally be involved in DNA repair processes. On the other hand, some authors have hypothesized that association to the chromosomal sheath could serve as an efficient mechanism to equally distribute proteins to daughter cells (Hernandez-Verdun and Roussel, 2003). This could be

particularly relevant in the case of GC_{NO} β1 whose essential role has been evidenced by the reported lethality of its knockout (Friebe et al., 2007; Hobbs, 1997).

Differences in the level of expression of GC_{NO} subunits have been described in the literature. Studies by in situ hybridization and RT-PCR in rat, monkey and human brain revealed that GC_{NO} β1 is more abundant and widely distributed than the α subunits (Bidmon et al., 2004; Gibb and Garthwaite, 2001; Mergia et al., 2003; Pifarre et al., 2007). Furthermore, a maximal expression of β1 in areas where α subunit expression is very low or undetectable has been observed in rat (Islands of Calleja, many thalamic and hypothalamic nuclei), and monkey brain (claustrum) (Pifarre et al., 2007). Mismatches in GC_{NO} subunit expression were also observed during brain development (Bidmon et al., 2004). Recently, Krumenacker et al (2006) reported that the β1 subunit is expressed at the mRNA and protein level in undifferentiated murine ES cells while α subunits are absent and the cells lack GC_{NO} activity. When ES cells were subjected to differentiation to cardiomyocytes expression of GC_{NO} α1 and β1 subunits increased over a several day time course and cells acquired GC_{NO} activity. However, levels of GC_{NO} β1 mRNA were still twice those of α1 mRNA. All these data supports the hypothesis of single subunits serving functions other than GC_{NO}. Because of the lack of α subunit-specific antibodies to perform immunolocalization studies, we examined the possible targeting of these subunits to the nuclei in cells transfected with pGFP-β1, pYFG-α1 or pYFP-α2 constructions. In C6 cells transfected with pGFP-β1 we could detect nuclear localization of this subunit in agreement with the immunofluorescence experiments, however pYFP-α1 and pYFP-α2 transfected cells presented expression in the cytoplasm but not in the nucleus. Furthermore, when β1 was co-transfected with α1 or α2, we could not detect any of the subunits in C6 nuclei, suggesting that when expressed at similar levels α subunits may bound β1 in heterodimers and sequester it in the cytoplasm. This observation and its possible significance regarding the function of β1 as an obligate monomer of active GC_{NO} heterodimers or independently as a regulator of chromatin condensation and cell cycle progression deserves further investigation.

MATERIALS AND METHODS.

Materials. Dulbecco's modified Eagle's medium (DMEM), penicillin, streptomycin, Triton X-100, methanol, bovine serum albumin (BSA), 4',6-diamidino-2-phenylindole (DAPI), affinity purified rabbit polyclonal GC_{NO} anti- β1 subunit and mouse anti-GFAP antibodies were obtained from Sigma. Rabbit anti-glial-fibrillar-acidic-protein (GFAP) antibody from DAKO; the antigenic peptide of the GC_{NO} β1 subunit from Cayman; anti-cGMP antiserum for RIA was prepared in our laboratory as described by Brooker et al. (1979); anti-cGMP-para-formaldehyde-tiroglobuline polyclonal antibody was a gift of Dr. J. de Vente (Maastricht University, Netherlands); colcemid from Gibco, acetylated low density lipoprotein labelled with 1,1´ dioctadecyl-3,3,3´,3´ tetramethylindocarbocyanine perchlorate (DIL-Ac-LDL) was from Biomedical Technologies; propidium iodide (PI) and phorbol 12-myristate 13-acetate (PMA) from Sigma, Alexa 488 or Alexa 555 coupled to anti-IgG antibodies were from Molecular Probes; FITC conjugated to rabbit IgG from DAKO; horseradish peroxidase conjugated to rabbit or mouse IgG from Amersham Life Science. Fetal-calf serum (FCS) from Ingelheim Diagnóstica; colcemid from GIBCO; [^{3}H]cGMP (34.5 Ci/mmol) from New England Nuclear; plasmid pEGFP-C1 from Clonotech; plasmid containing GC_{NO} β1 sequence and plasmids pEYFP-C1 containing GC_{NO} α1 and α2 sequences were a gift from Dr. J. Garthwaite (Wolfson Inst. Biomed. Res, UCL, UK). Trizol reagent, Superscript-II reverse transcriptase, oligofectamine and RT-PCR reactive were from Invitrogen, real-time PCR reactive, restriction enzymes MroI and XbaI, ligase, dNTPs and Taq polymerase were from Roche. 25 KDa lineal polyethylamide (PEI) was for Polyscience.

Cell cultures. Primary cultures enriched in astrocytes were prepared from cerebellum of 7 day-old Sprague-Dawley rats as previously described (Agullo et al., 1995). Tissue was mechanically dissociated by successive passages through nylon cloths of 211 µm and 135 µm mesh openings. To obtain astrocyte-enriched cultures cells were suspended in DMEM-10 % FCS, 20 U/ml penicillin and 20 µg/ml streptomycin, seeded in plastic Petri dishes ($1.25x10^5$ cells/cm^2) and maintained in a humidified atmosphere of 90 % air-10 % CO_2. Medium was changed once a week and cells were used after 14 days in culture.

Microglial cultures were prepared by mild trypsinization of actrocytes enriched cultures as described by Saura et al. (2003). Briefly, cultures in 35 mm diameter Petri dishes were treated with a trypsin solution (0.06% trypsin, 1 mM EDTA) diluted in DMEM for at least 30 minutes. This resulted in the detachment of the upper layer of astrocytes, whereas microglia remained attached to de dish.

The rat C6 glioma cell line was obtained from the American Type Culture Collection and the rat HAPI microglia cell line was a generous gift of Dr. James R. Connor (Hershey Medical Center, Hershey, PA, USA). Cells were grown in DMEM supplemented with 2 mM L-glutamine and 10% FCS or 5 % FCS, for C6 and HAPI cells respectively. Cells were maintained in a humidified atmosphere of 90 % air-10 % CO_2 at 37°C. Cells were passaged every 3–4 days and seeded at a density of 1.10^5 cells/cm^2. In some experiments cells were arrested in metaphase by treatment of nonconfluent cultures with colcemid (0.1 µg/ml) for 24 hours.

Cells stainings. Cells were grown on glass coverslips, rinsed in phosphate-buffered saline (PBS) and fixed with 4% paraformaldehyde (PFA) for 30 minutes at room temperature, or fixed in methanol for 2 minutes at –20°C, before 30 minutes permeabilitation step in PBS containing 0.1% Triton. After, cells were incubated with primary antibodies (GFAP 1:600, GC_{NO} β1 1:300 and GMPc 1:4,000) in PBS containing 1% BSA overnight at 4ºC. After washing, cultures were incubated for 1 hour at room temperature with secondary antibodies (Alexa 555 or 488 anti-rabbit IgG or anti-mouse IgG from goat) at 1:1,000 in PBS containing 0.1% BSA. The primary antibody was omitted in controls. In addition, some samples were incubated with the antigenic peptide before GC_{NO} immunocitochemistry. To label microglía, cultures were incubated with DIL-Ac-LDL (10 µg/ml) for 4 hours at 37ºC and after several washes were fixed with 4% PFA for 30 minutes at room temperature and incubated with antibody anti-GC_{NO} and GMPc. The cells were counterstained with DAPI (0.5 µg/ml in PBS). After washing in PBS, cells were mounted in Fluoprep (Biomérieux SA, France). Images were recorded using a confocal laser scanning microscope Leica TCS SP2 AOBS equipped with argon (488 nm) and He ne (561 nm) lasers or a fluorescence microscope Eclipse 600 Nikon. Double-label fluorescence images were acquired in sequential mode.

Immunofluorescence labeling of metaphase chromosome spreads. Methaphase chromosome spreads were obtained from C6 and HAPI cells treated for 1 hour with 0.2 µg/ml colcemid. Cells were recovered by mitotic shake off and sedimented by centrifugation (450 x g for 3 minutes), washed in PBS, and the pellet resuspended and incubated in 75 mM KCl for 20 minutes at 37ºC for hypotonic swelling. After, the cell suspension was sedimented onto superfrost glass microscope slides by cytocentrifugation (2000 rpm, 10 minutes). Immediately, spread chromosomes were fixed with 4% paraformaldehyde for 30 minutes at room temperature in Tris-EDTA buffer (120 mM KCl, 20 mM NaCl, 0,5 mM EDTA, 10 mM Tris-HCl pH 8, and 0,1% Triton X-100), then cell membranes were solubilized by immersion in Tris-EDTA buffer for 10 minutes at room temperature. The slides were blocked in Tris-EDTA containing 1% BSA and

incubated 1hour at room temperature with anti-β1 antibody in PBS containing 1% BSA. After washing, slides were incubated for 30 minutes at room temperature with FITC –conjugated donkey anti-rabbit IgG at 1:50 in Tris-EDTA containing 1% BSA. Finally, after three washes, slides were mounted in anti-fade medium containing DAPI and observed under a fluorescence microscope (Eclipse 600, Nikon).

Plasmid constructs. The plasmid pEYFP containing the GC_{NO} β1 sequence was used as template to PCR-amplify the cDNA. The primers GC_{NO} β1-foward (5′-TCCGGAAT GTACGGTTTTGTG-3′) and GC_{NO} β1-reverse (5′-TCTAGACATTCAGTTTCACTG-3′) were designed to include the restriction sites *Mro*I and *Xba*I, respectively. The PCR reaction mixture contained 5 µl of reaction buffer (Roche), 4 µl of dNTP mixture (2.5 mM, Roche), 1 µl of each primer (50 µM), 5 µl of DNA template and 1.5 units of high expand Taq polymerase (Roche) and was adjusted to a final volume of 50 µl with sterile water. The PCR was performed in a Minicycler ^{tm} PCR machine according to the following schedule: a pre-denature step at 94°C for 3 minutes, followed by 35 cycles at 94°C for 30 seconds, 50°C for 30 seconds, and 68°C for 2 minutes and finally one step at 68°C for 7 minutes. The PCR products were recovered by agarose gel separation and gel extraction (Qiagen) and cloned into the *Mro*I and *Xba*I digested pEGFP-C1 vector. This plasmid contains a cytomegalovirus promoter for protein expression and a neomycin/kanamycin resistance gene to select transfected cells. After ligation, several clones were selected from each transformation, amplified, and analyzed by DNA sequencing to confirm the correct insertion and orientation of the internal fragments. Plasmids pEYFP-C1 containing GC_{NO} α1 and α2 sequences were used for co-transfection experiments.

Transient transfections. To examine GC_{NO} subunit localization C6 cells were grown on 24x24 mm coverslips placed in 35 mm culture plates and were transiently transfected with 1 µg DNA of pEGFP-β1 or pEGFP as control of transfection or with 1 µg DNA of pEYFP-α1 and pEYFP-α2 using the transfection reagent PEI. On the day of transfection, medium of cells between 50-80% confluence were changed to 900 µl of fresh DMEN-10% FCS. One µg of plasmidic DNA was diluted in serum-free DMEN in a volume equivalent to one-tenth of that in the culture (final volume 1 ml for 35 mm dish), after that, PEI was added to this suspention in a 1:10 relation ratio between DNA and PEI (1 µg DNA: 10 µl PEI). The mixture (100 µl) was immediately vortexed for 5 seconds, incubated for 10 minutes at room temperature and added drop-wise to the cells. Cells were incubated for 24 hours at 37°C in a humidified atmosphere of 90 % air-10 % CO_2. Efficiency of transfection was 25-40%.

Reverse transcription-polymerase chain reaction (RT-PCR) analysis. Total RNA from astrocyte primary cultures and cell lines were extracted with TRIzol reagent and quantified spectrophotometrically. Integrity of RNAs was checked by ethidium bromide staining in agarose gels (1% agarose). 1 μg of total RNA was reverse transcribed (RT) into cDNA using 1 U of Superscipt-II reverse transcriptase and 3 μg of random hexamer primers in a final reaction volume of 20 μl. Amplification was performed in a 50 μl reaction volume containing 10 mM Tris-HCl pH 8.3, 50 mM KCl, 1.75 mM $MgCl_2$, 200 μM each dNTPs, 0.5 U of Taq DNA polymerase, 0.4 μM of each primer and 5 μl of RT product. Primer sequences for GC_{NO} α_1 subunit were: foward, 5'-ATACGGGTGAGGAGATGGGATAACT-3'; reverse, 5'-CCTCATTGAACTTCT TGGCTTGC-3'; PCR reaction performed at 36 cycles of amplification (95ºC for 30 seconds; 59ºC for 25 seconds, 72ºC for 25 seconds). Primer sequences for GC_{NO} β_1 subunit were: foward, 5'-GCCAAAAGATACGACAATGTGACCA-3' and reverse, 5'-TTGCCATCTACTTGAAC TTGACCAG-3'; PCR was performed at 34 cycles of amplification (95ºC for 30 seconds; 61ºC for 25 seconds, 72ºC for 25 seconds). Primers sequences for GC_{NO} α2 subunit were: forward, 5'- ACTGCAAATGTACTCGGACTG AAG-3'; reverse 5'-CAGCT CGAAGGACTCGCTCATTCT-3'; PCR was performed at 30 cycles of amplification (95ºC for 30 seconds, 60ºC for 30 seconds, 72ºC for 30 seconds). Amplification of GAPDH was used to control for differences in cDNA synthesis efficiency between samples. Primers for GAPDH were: forward, 5'-GCCAA GTATGATGACATCAAGAAG-3' and reverse, 5'-TCCAGGGGTTTCTTAC TCCTTGGA-3'; PCR was performed at 24 cycles of amplification (95ºC for 30 seconds; at 61ºC for 25 seconds, 72ºC for 25 seconds). PCR products were analyzed by electrophoresis through 2% agarose gels containing 0.5 μg/ml ethidium bromide. The amplification was found to be linear between 33 and 37 cycles for GC_{NO} α_1, 28 and 34 cycles for α2, 30 and 36 cycles for GC_{NO} β_1 and 20 to 30 cycles for GAPDH.

Quantitative Real-time PCR: Real-time PCR was performed using the Roche Light Cycler (Roche, Indianapolis, IN, USA) using Roche LightCycler FastStart DNA Master Plus SYBR Green I under conditions described by the manufacturer with specific primers. Briefly, the final 10 μl PCR reaction contained 2.4 μl cDNA, 1 μl custom primers (50 mM each), 2 μl of Kit master mix and 4.6 μl of MilliQ H_2O. The optimal PCR amplification conditions for the individual primer pairs were determined experimentally. Two negative and one positive control (astrocytes cDNA) were incorporated in each PCR run. Negative controls included a PCR reaction in which water was substituted for the template and an RT reaction in which the Superscript II RT enzyme was omitted. Quantitative differences in mRNA of β1 subunit were normalised with the constitutive

gene GAPDH. The primers used to identify the expression were the same as in RT-PCR (see above). Fold differences were determined using crossing point analysis, as described by Pasuit et al (2004).

cGMP accumulation. For determination of cGMP, cell monolayers were washed and preincubated for 10 minutes at 37°C in Hepes-buffered saline (118 mM NaCl, 4.7 mM KCl, 2.5 mM $CaCl_2$, 1.2 mM $MgSO_4$, 1.2 mM KH_2PO_4, 10 mM glucose and 20 mM Hepes, pH 7.4) before adding 1 mM 3-isobutyl-1-methylxanthine (IBMX) alone or with sodium nitroprusside (SNP, 100 μM). After 3 minutes incubation, reactions were terminated by aspirating the medium and adding ice-cold ethanol. Ethanol extracts were evaporated, resuspended in 5 mM sodium acetate pH 4.8 and cGMP quantified by radioimmunoassay using acetylated [^{3}H]cGMP as described previously (Agullo and Garcia, 1992).

Chromatin condensation assay.

The chromatin condensation assay was performed as described by Collas et al. (1999) with some modifications.

Mitotic cell extracts. C6 glioma cells were synchronized and treated with colcemid for 18 hours for mitotic arrest. Mitotic C6 cells were washed once in ice-cold PBS, once in 20 volume of ice-cold lysis buffer (20 mM Hepes, pH 8.2, 5 mM $MgCl_2$, 10 mM EDTA, 1 mM DTT and 20 µg/ml cytocalasin B and protease inhibitors (Roche) and packed at 800 x g for 10 minutes. The cell pellet was resuspended in 1 volume of lysis buffer and incubated for 30 minutes on ice. Cells were homogenized by 2x2 minutes sonication on ice and the lysate was centrifuged at 10,000 x g for 15 minutes at 4ºC. The supernatant was cleared at 100,000 x g for 1 hour at 4ºC. The clear supernatant (mitotic cytosolic extract) was aliquoted and stored at -80ºC

Preparation of nuclei. Confluent un-synchronized C6 glioma cells were harvested, washed in PBS, sedimented at 400 x g, and resuspended in 20 volumes of ice-cold buffer N (10 mM Hepes, pH 7.5, 2 mM $MgCl_2$, 250 mM sucrose, 25 mM KCl, 1 mM DTT and protease inhibitors) containing 10 μg/ml cytocalasin B. After 30 minutes incubation on ice, cells were homogenized by 140-170 strokes of a tight fitting glass pestle in a 5 ml-homogenizer. Nuclei were sedimented at 400 x g for 10 minutes at 4ºC and washed twice by resuspending in buffer N and centrifuging as above. All nuclei recovered were morphologically intact, as judged by phase-contrast microscopy and DAPI stain. Nuclei were stored frozen at -80ºC in buffer N containing 70% glycerol

Loading of nuclei with anti-GC_{NO} β1 antibody. Purified C6 cell nuclei (2,000 nuclei/μl) were permeabilized in 500 μl buffer N containing 0.75 μg/ml L-A-lysophosphatidylcholine type I

(Sigma) for 15 minutes at room temperature. Excess lysophosphatidylcholine was quenched by adding 1 ml of 3% BSA made in buffer N and incubating for 5 minutes on ice, before sedimenting the nuclei and washing once in buffer N. Nuclei were resuspended at 2,000 nuclei/μl in 100 μl buffer N containing 2.5 μg of anti-GC_{NO} β1 antibodies or 2.5 μg of pre-immune rabbit IgGs. After 1 hour incubation on ice with gentle agitation, nuclei were sedimented at 500 x g through 1 M sucrose for 20 minutes and held in buffer N on ice until use. Antibody loading of nuclei was verified by immunofluorescence.

Nuclear disassembly and chromatin condensation assay. As describe Collas et al. (1999), a nuclear disassembly/chromatin condensation reaction consisted of 25 μl of mitotic extract, 5 μl of nuclear suspension (~2,000 nuclei), and 2 μl of an ATP-generating system (1 mM ATP, 10 mM creatine phosphate, 25 μg/ml creatine kinase). The reaction was started by addition of the ATP generating system and allowed to proceed at 30ºC for up to 1.5 hours. Chromatin condensation was monitored by adding 0.1 μg/ml Hoechst 33342. Chromatin was considered to condense when it acquired an irregular and compact morphology sometimes with distinct chromosomes or chromosome fragments. In some instances, the mitotic extract was pre-incubated with antibody for 1 hour before adding the nuclei and the ATP generating system or treated with the inhibitor of NO sensitive-GC_{NO}, ODQ 100 μM (Sigma). Percent chromatin condensation was calculated as the ratio of condensed chromatin masses per number of nuclei examined (100 nuclei per treatment).

GC_{NO} genetic disruption with siRNA. Complementary siRNA against the rat GC_{NO} β1 cDNA and scrambled siRNA were designed using Dharmacon software (Meister and Tuschl, 2004), and synthesized by Invitrogen. Both siRNA were labeled with fluorescein to evaluate the efficiency of transfection (40-60%, 24 and 48 hours post tansfection respectably) and to identified the C6 transfected-cells by flow cytometry. After annealing the complementary specific single strand siRNAs, 20 mM of the double strand (DS) siRNAs were transfected in C6 cells grown in 12-well plates (50-70% confluency) with oligofectamine for 24 or 48 hours.

Analysis of GC_{NO} β1 protein by immunobloting. Subcellular factions were prepared from C6 interphase cells as described above. Briefly, after isolation of nuclei, the supernatant was centrifuged at 100,000 g for 1 hour to obtain the soluble fraction (S1). The pellet was washed ones by centrifugation at 100,000 g in buffer N to obtain the membrane fraction (M). Supernatant was considered the second soluble fraction (S2). Isolated nuclei were homogenized mechanically with a glass-teflon Petter-Elvehjeim in buffer N supplemented with NaOH 5M to extract DNA associated proteins and centrifuge 10 minutes at 14,000 g to obtain

the nuclear fraction (N). Western blots were performed as described previously (Baltrons and García, 1999). Fractions (15-20 µg of protein) were subjected to 10% sodium dodecyl sulfate-polyacrylamide gel electrophoresis (SDS-PAGE) followed by transfer to PDVF membranes at 100 V for 1.5 hours at 4°C. Membranes were blocked at 4°C overnight in phosphate-buffered saline (pH 7.4) containing 5 % non-fat dry milk, and then incubated at room temperature for 2 hours with anti- GC_{NO} β1 polyclonal antibody (1:2,000), polyclonal lamin-B antibody (1:2,000) or monoclonal anti-GAPDH antibody (1:10,000). Bound antibodies were detected with a horseradish peroxidase conjugated anti-rabbit IgG or anti-mouse IgG (1:4,000) and visualized by chemiluminescence (EZ-ECL kit, biological industries). Metaphase and interphase C6 homogenates were obtained from cells treatment or not with colcemid for 24 hours respectable. After this period cells were homogenate with a glass-teflon Petter-Elvehjeim homogenizer mechanically driven at 800 rpm and stored at -20ºC. For all experiments protein was determined as described by Lowry (1951) or Bradford (1976) using BSA as a protein standard.

Other methods:

Nonradioactive cell proliferation assay. Cell proliferation was measured in C6 cells after 48 hours of transfection with siRNA using the commercial kit EZ4U (Biomedica Gruppe). Absorbance measurements were made every 30 minutes during 2 hours at 450 nm. Absorbance at 620 nm was used to correct for non-specific background.

Cell cycle analysis by flow cytometry. For cell cycle analysis, 2 x 10^6 cells were fixed with 70% (v/v) ice-cold ethanol (-20 °C). After the ethanol fixation, 1 ml of PBS was added, and the cells were centrifuged (4,000 rpm, 5 minutes at room temperature) and resuspended in 0.3 ml of PBS. Propidium iodide (PI) was added to this suspension at a final concentration of 0.003%. After vortexing, cells were kept at 4ºC for approximately 30 minutes and then analyzed in a flow cytometer FACSCalibur-Beckton Dickinson. Results were analysed with ModFit LT and CellQUEST-Pro software.

Statistic analysis*:* Experiments were always performed in triplicate and were replicated the indicated number of times in different preparations (see figures legends). Statistical analysis of the date was performed using one-way ANOVA followed by Turkey's comparison test or using T-Student's test.

Acknowledgements

This work was supported by grants from Ministerio de Educación y Ciencia (MEC), Spain (SAF2004-01717) and Direcció General de Recerca (DGR), Generalitat de Catalunya (SGR2001-212) to A. García and Universidad Autónoma de Barcelona grant (EME 2006-31) to MA. Baltrons. P. Pifarré is a recipient of a predoctoral fellowship from MEC, Spain. We thank Ignasi Roca (Universidad Autónoma de Barcelona, Barcelona, Spain) for β1 cloning and plasmid construction assistance and Annie Beuve (New Jersey Medical School, NY, USA) for her helpful advice in the siRNA experiments.

REFERENCES

Agullo, L., Baltrons, M. A. and Garcia, A. (1995). Calcium-dependent nitric oxide formation in glial cells. *Brain Res* **686**, 160-8.

Agullo, L. and Garcia, A. (1992). Characterization of noradrenaline-stimulated cyclic GMP formation in brain astrocytes in culture. *Biochem J* **288 (Pt 2)**, 619-24.

Agullo, L., Garcia-Dorado, D., Escalona, N., Ruiz-Meana, M., Mirabet, M., Inserte, J. and Soler-Soler, J. (2005). Membrane association of nitric oxide-sensitive guanylyl cyclase in cardiomyocytes. *Cardiovasc Res* **68**, 65-74.

Balashova, N., Chang, F. J., Lamothe, M., Sun, Q. and Beuve, A. (2005). Characterization of a novel type of endogenous activator of soluble guanylyl cyclase. *J Biol Chem* **280**, 2186-96.

Belmont, A. S. (2006). Mitotic chromosome structure and condensation. *Curr Opin Cell Biol* **18**, 632-8.

Bidmon, H. J., Starbatty, J., Gorg, B., Zilles, K. and Behrends, S. (2004). Cerebral expression of the alpha2-subunit of soluble guanylyl cyclase is linked to cerebral maturation and sensory pathway refinement during postnatal development. *Neurochem Int* **45**, 821-32.

Bradford, M. M. (1976). A rapid and sensitive method for the quantitation of microgram quantities of protein utilizing the principle of protein-dye binding. *Anal Biochem* **72**, 248-54.

Brooker, G., Harper, J. F., Terasaki, W. L. and Moylan, R. D. (1979). Radioimmunoassay of cyclic AMP and cyclic GMP. *Adv Cyclic Nucleotide Res* **10**, 1-33.

Collas, P., Le Guellec, K. and Tasken, K. (1999). The A-kinase-anchoring protein AKAP95 is a multivalent protein with a key role in chromatin condensation at mitosis. *J Cell Biol* **147**, 1167-80.

Denninger, J. W. and Marletta, M. A. (1999). Guanylate cyclase and the .NO/cGMP signaling pathway. *Biochim Biophys Acta* **1411**, 334-50.

Earp, H. S., Smith, P., Huang Ong, S. H. and Steiner, A. L. (1977). Regulation of hepatic nuclear guanylate cyclase. *Proc Natl Acad Sci U S A* **74**, 946-50.

Feil, R., Feil, S. and Hofmann, F. (2005). A heretical view on the role of NO and cGMP in vascular proliferative diseases. *Trends Mol Med* **11**, 71-5.

Friebe, A., Mergia, E., Dangel, O., Lange, A. and Koesling, D. (2007). Fatal gastrointestinal obstruction and hypertension in mice lacking nitric oxide-sensitive guanylyl cyclase. *Proc Natl Acad Sci U S A* **104**, 7699-704.

Gibb, B. J. and Garthwaite, J. (2001). Subunits of the nitric oxide receptor, soluble guanylyl cyclase, expressed in rat brain. *Eur J Neurosci* **13**, 539-44.

Gobeil, F., Jr., Zhu, T., Brault, S., Geha, A., Vazquez-Tello, A., Fortier, A., Barbaz, D., Checchin, D., Hou, X., Nader, M. et al. (2006). Nitric oxide signaling via nuclearized endothelial nitric-oxide synthase modulates expression of the immediate early genes iNOS and mPGES-1. *J Biol Chem* **281**, 16058-67.

Harrison, B. C. and Mobley, P. L. (1990). Phorbol ester-induced change in astrocyte morphology: correlation with protein kinase C activation and protein phosphorylation. *J Neurosci Res* **25**, 71-80.

Harrison, B. C., Staskavage, D. L. and Mobley, P. L. (1991). Effects of sphingosine on phorbol ester-mediated changes in astrocyte morphology and protein phosphorylation. *J Neurosci Res* **29**, 181-9.

Heinrich, U., Maurer, J., Koesling, D., Mann, W. and Forstermann, U. (2000). Immuno-electron microscopic localization of the alpha(1) and beta(1)-subunits of soluble guanylyl cyclase in the guinea pig organ of corti. *Brain Res* **885**, 6-13.

Hernandez-Verdun, D. and Gautier, T. (1994). The chromosome periphery during mitosis. *Bioessays* **16**, 179-85.

Hernandez-Verdun, D. and Roussel, P. (2003). Regulators of nucleolar functions. *Prog Cell Cycle Res* **5**, 301-8.

Hobbs, A. J. (1997). Soluble guanylate cyclase: the forgotten sibling. *Trends Pharmacol Sci* **18**, 484-91.
Koesling, D., Russwurm, M., Mergia, E., Mullershausen, F. and Friebe, A. (2004). Nitric oxide-sensitive guanylyl cyclase: structure and regulation. *Neurochem Int* **45**, 813-9.
Krumenacker, J. S., Katsuki, S., Kots, A. and Murad, F. (2006). Differential expression of genes involved in cGMP-dependent nitric oxide signaling in murine embryonic stem (ES) cells and ES cell-derived cardiomyocytes. *Nitric Oxide* **14**, 1-11.
Lowry, O. H., Rosebrough, N. J., Farr, A. L. and Randall, R. J. (1951). Protein measurement with the Folin phenol reagent. *J Biol Chem* **193**, 265-75.
Meister, G. and Tuschl, T. (2004). Mechanisms of gene silencing by double-stranded RNA. *Nature* **431**, 343-9.
Mergia, E., Russwurm, M., Zoidl, G. and Koesling, D. (2003). Major occurrence of the new alpha2beta1 isoform of NO-sensitive guanylyl cyclase in brain. *Cell Signal* **15**, 189-95.
Moncada, S., Palmer, R. M. and Higgs, E. A. (1991). Nitric oxide: physiology, pathophysiology, and pharmacology. *Pharmacol Rev* **43**, 109-42.
Pasuit, J. B., Li, Z. and Kuzhikandathil, E. V. (2004). Multi-modal regulation of endogenous D1 dopamine receptor expression and function in the CAD catecholaminergic cell line. *J Neurochem* **89**, 1508-19.
Pifarre, P., Garcia, A. and Mengod, G. (2007). Species differences in the localization of soluble guanylyl cyclase subunits in monkey and rat brain. *J Comp Neurol* **500**, 942-57.
Russwurm, M., Behrends, S., Harteneck, C. and Koesling, D. (1998). Functional properties of a naturally occurring isoform of soluble guanylyl cyclase. *Biochem J* **335 (Pt 1)**, 125-30.
Russwurm, M., Wittau, N. and Koesling, D. (2001). Guanylyl cyclase/PSD-95 interaction: targeting of the nitric oxide-sensitive alpha2beta1 guanylyl cyclase to synaptic membranes. *J Biol Chem* **276**, 44647-52.
Saura, J., Tusell, J. M. and Serratosa, J. (2003). High-yield isolation of murine microglia by mild trypsinization. *Glia* **44**, 183-9.
Teunissen, C. E., Steinbusch, H. W., Markerink-van Ittersum, M., De Bruijn, C., Axer, H. and De Vente, J. (2000). Whole brain spheroid cultures as a model to study the development of nitric oxide synthase-guanylate cyclase signal transduction. *Brain Res Dev Brain Res* **125**, 99-115.
Tomimatsu, N., Tahimic, C. G., Otsuki, A., Burma, S., Fukuhara, A., Sato, K., Shiota, G., Oshimura, M., Chen, D. J. and Kurimasa, A. (2007). Ku70/80 modulates ATM and ATR signaling pathways in response to DNA double-strand breaks. *J Biol Chem*.
Van Hooser, A. A., Yuh, P. and Heald, R. (2005). The perichromosomal layer. *Chromosoma* **114**, 377-88.
Villalobo, A. (2006). Nitric oxide and cell proliferation. *Febs J* **273**, 2329-44.
Zabel, U., Hausler, C., Weeger, M. and Schmidt, H. H. (1999). Homodimerization of soluble guanylyl cyclase subunits. Dimerization analysis using a glutathione s-transferase affinity tag. *J Biol Chem* **274**, 18149-52.
Zabel, U., Kleinschnitz, C., Oh, P., Nedvetsky, P., Smolenski, A., Muller, H., Kronich, P., Kugler, P., Walter, U., Schnitzer, J. E. et al. (2002). Calcium-dependent membrane association sensitizes soluble guanylyl cyclase to nitric oxide. *Nat Cell Biol* **4**, 307-11.

Figure 1: Intracellular distribution of GC_{NO} β1 immunoreactivity in primary glial cultures. Confluent rat cerebellar astrocyte-enriched cultures were incubated in the absence (A) or presence (B) of the mitogen PMA (100 nM, 24 hours). Cells were fixed and double-immunostained with affinity-purified polyclonal anti-GC_{NO} β1 antibody (1:500) and GFAP (1:500). (C) Primary microglial cultures obtained by lifting the astrocyte monolayer by mild trypsinitation (see Material and Methods) and double-stained for the microglial marker DIL-Ac-LDL and for GC_{NO} β1. Cells were counterstained for DNA with DAPI and observed by confocal fluorescence microscopy. Arrowhead in B points to a GFAP-negative cell presenting nuclear β1-immunoreactivity and shown at higher magnification in the insert. Arrowhead in C indicates point to a mitotic microglia shown at higher magnification in the insert. Figures are representative of three independent experiments.

Figure 2: GC_{NO} β1 associates with chromosomes during mitosis. Asynchronous astrocyte-enriched cultures were fixed with 4% PFA and immunostained with anti-β1 antibody (1:500), counterstained with DAPI and observed by fluorescence microscopy Images representative of the different phases of mitosis are shown (A). Anti-β1 antibody pre-incubation with 1,000-fold excess of the antigenic peptide totally abolished β1 staining (B).

Figure 3: Intracellular distribution of GC_{NO} β1 immunoreactivity in C6 and HAPI cells. (A) C6 glioma and microglia HAPI cell cultures were incubated in the absence or presence of the mitotic arresting agent colcemid for 18 hours, fixed and immunostained with anti-β1 antibody (1:300) Cells were counterstained with DAPI and observed by confocal microscopy. (B) Higher magnification showing chromosomal association of GC_{NO} β1 with C6 and HAPI chromosomes during different phases of mitosis. (C) Anti-β1 and DAPI staining of metaphase chromosome spreads of C6 (left) and HAPI cells (rigth) showing peripheral association of β1 immunoreactivity. Figures are representative of three independent experiments. Bar 10 μm.

Figure 4: GC_{NO} activity and GC_{NO} subunit mRNA and protein expression in astrocytes and microglia. Cells were washed and stimulated for 3 minutes with SNP 100 μM in the presence of 1 mM IBMX, washed and immediately fixed with 4% PFA before immunostaining for cGMP (1:3,000, red) (A) or extracted with ethanol for determination of cGMP levels by RIA (B) as described in Material and Methods. (C) RT-PCR analysis of GC_{NO} subunit mRNA expression. (D) C6 subcellular fractions were analyzed by western blot with polyclonal anti GC_{NO} β1 (1:2,000), monoclonal anti-GAPDH (1:10,000) or polyclonal anti-lamin-B (1:2,000).

Homogenate (H), soluble (S1, S2), membrane (M), and nuclear (N) proteins. Western blot analysis of GC_{NO} β1 (1:2,000) in soluble (S1) and nuclear (N) fractions of HAPI cells (E) and in interphase and mitotic C6 cells (F). Cb, cerebellar homogenate. Results are representative of three independent experiments.

Figure 5: Localization of GC_{NO} subunits in transiently transfected C6 cells. C6 cells were transiently transfected using PEI with pGPF-β1, pYFP-α1 or pYFP-α2 (A) or co-tranfected with pGPF-β1 and pYFP-α1 or pYFP-α2. The efficiencies of transfections oscillated between 25-40% (n=5). Cells were fixed and examined by confocal microscopy after 24 hours of transfection. Bar 10 μm.

Figure 6: Effect of GC_{NO} β1 immunodepletion on chromatin condensation. Purified interphase C6 cell nuclei were loaded with anti-β1 antibody or with preimmune IgG, and incubated with mitotic cell extract pretreated or not with anti-β1 antibody, for 90 minutes, as described in Materials and Methods. The specific GC_{NO} inhibitor ODQ (100 μM) was added before starting the condensation assay. DNA was stained with Hoechst 33342 and condensed and decondensed chromatin masses quantified. Representative images of condensed (A) and decondensed (B,B') chromatin. (C) Percentage of cells showing condensed or decondensed chromatin masses. Results are means ± s.e.m. of four independent experiment (100 nuclei per condition were counted in each experiment). Data were analyzed using two-way ANOVA followed by Turkey's test. #,* Statistically significant difference versus respective control ($p < 0.01$).

Figure 7: Effect of silencing GC_{NO} β1 with siRNA on cell proliferation and cell cycle progression. C6 cells were transfected with specific GC_{NO} β1 siRNA or scrambled siRNA using oligofectamine as described by the manufacturer in triplicate plates. (A) After 48 hours GC_{NO} β1 mRNA levels were determined by real-time PCR. The percent decrease in β1 mRNA was 75 ± 3.8%, mean. ± s.e.m of four independent experiments (B) Cell proliferation was assayed with EZ4U kit into sub-cultured transfected cells (# Statistically significant difference vs scrambled siRNA, $p< 0.001$). (C) Cell cycle progression was analyzed by flow cytometry, a representative experiment is shown in C. R1 represents the untransfected cell population and R2 the cells transfected with GC_{NO} β1 siRNA. (D) Percent of cells in G_0-G_1 or in S-G_2-M phases of the cell cycle. Results are means ± s.e.m. of four independent experiments (* statistically significant differences vs controls using student-t test $p < 0.001$).

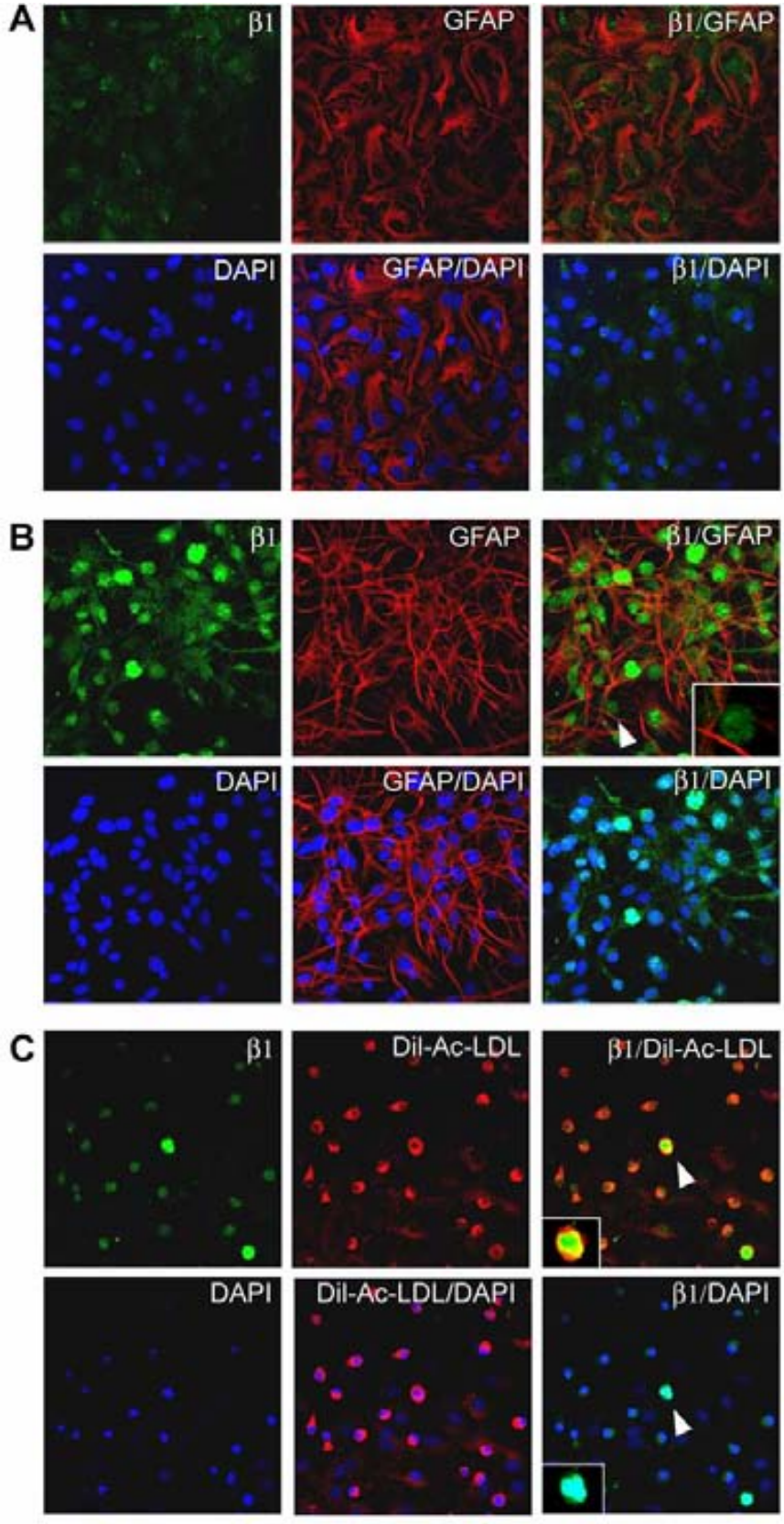
A
β1
GFAP
β1/GFAP
DAPI
GFAP/DAPI
β1/DAPI
B
β1
GFAP
β1/GFAP
DAPI
GFAP/DAPI
β1/DAPI
C
β1
DiI-Ac-LDL
β1/DiI-Ac-LDL
DAPI
DiI-Ac-LDL/DAPI
β1/DAPI

Figure 1

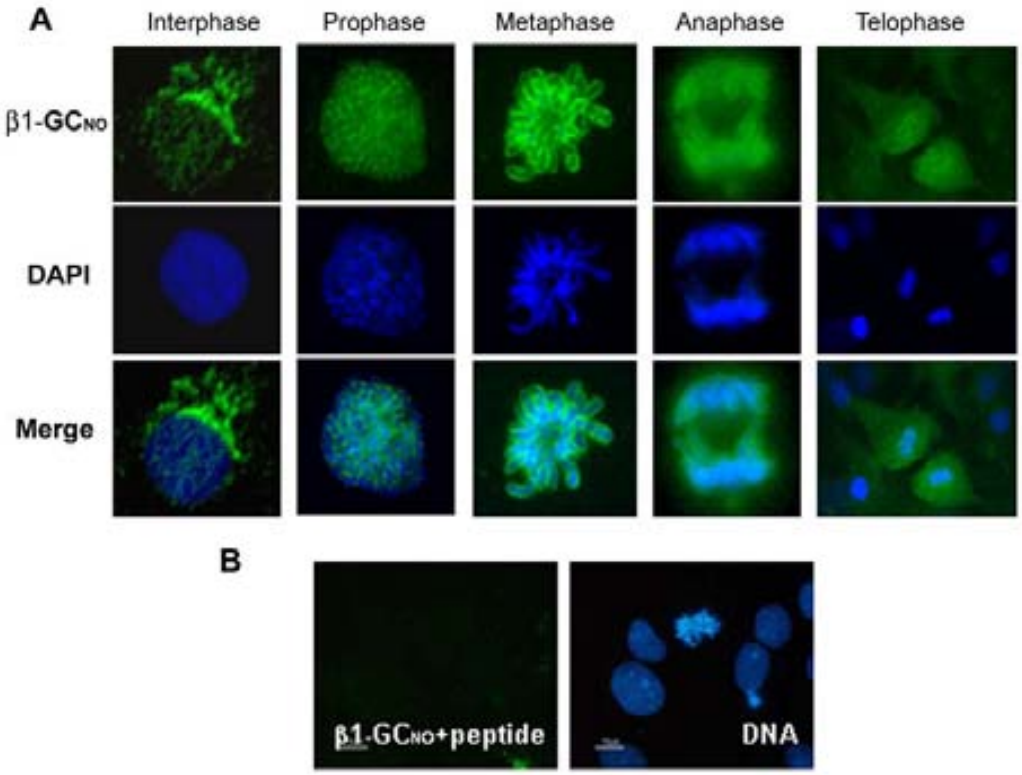
A
Interphase
Prophase
Metaphase
Anaphase
Telophase
β1-GCNO
DAPI
Merge
B
β1-GCNO+peptide
DNA

Figure 2

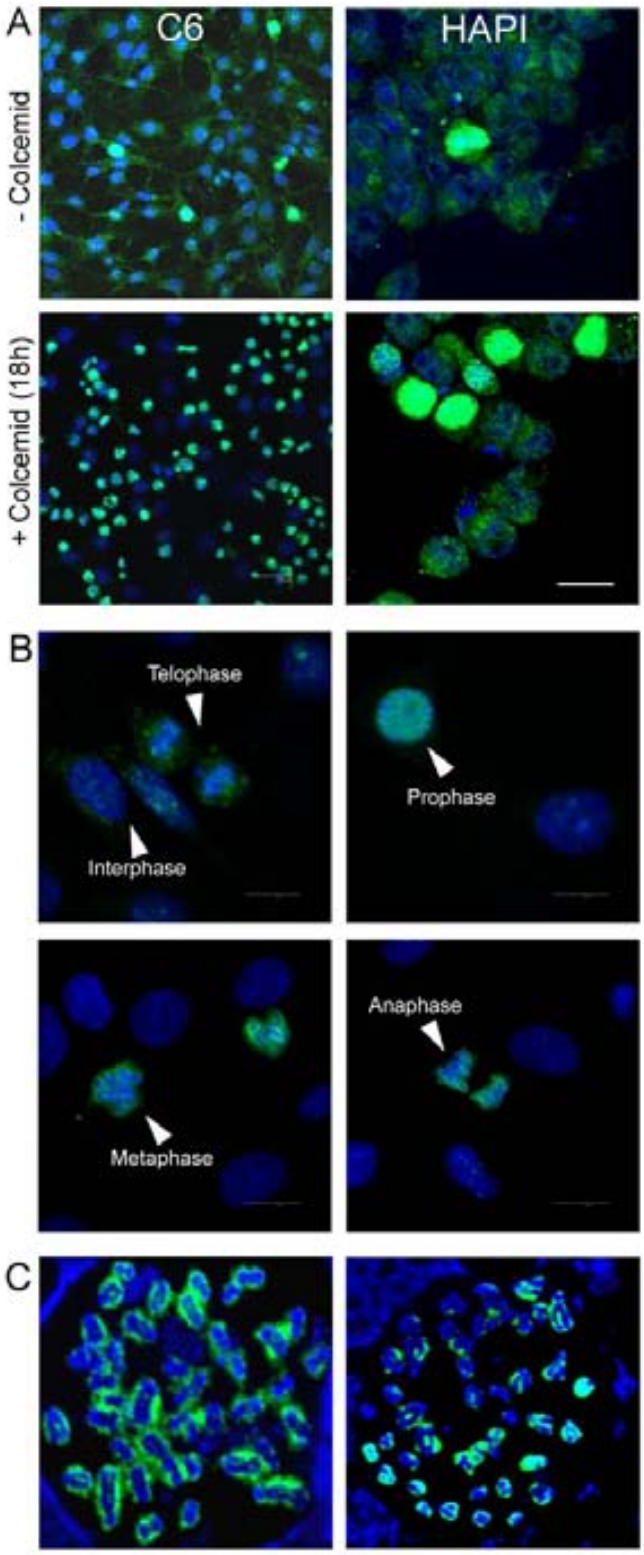
A
C6
HAPI
- Colcemid
+ Colcemid (18h)
B
Telophase
Interphase
Prophase
Metaphase
Anaphase
C

Figure 3

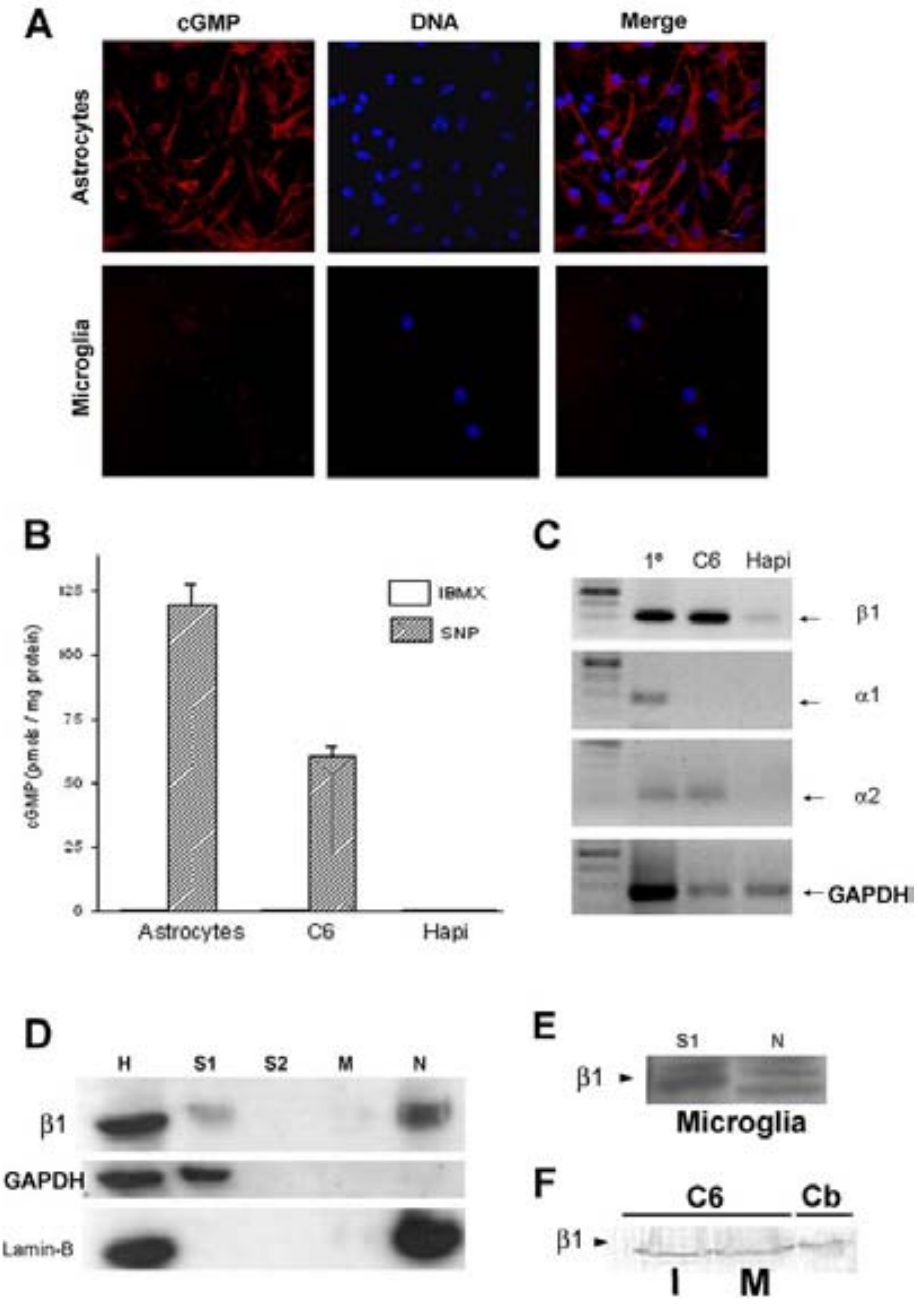
A
cGMP
DNA
Merge
Astrocytes
Microglia
B
IBMX
SNP
cGMP (pmole / mg protein)
Astrocytes
C6
Hapi
C
1°
C6
Hapi
β1
α1
α2
GAPDH
D
H
S1
S2
M
N
β1
GAPDH
Lamin-B
E
S1
N
β1
Microglia
F
C6
Cb
β1
I
M

Figure 4

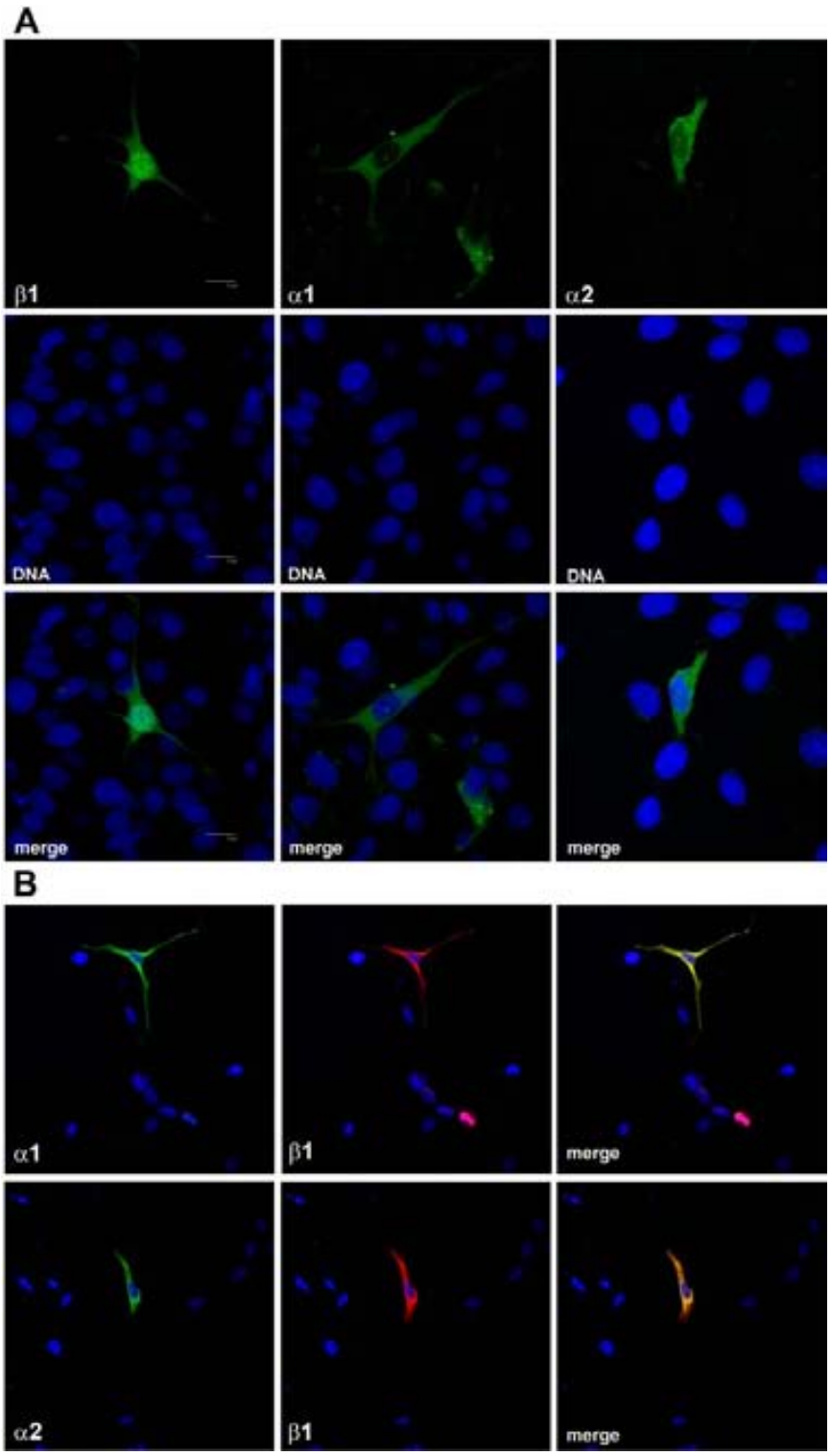
A
β1
α1
α2
DNA
DNA
DNA
merge
merge
merge
B
α1
β1
merge
α2
β1
merge

Figure 5

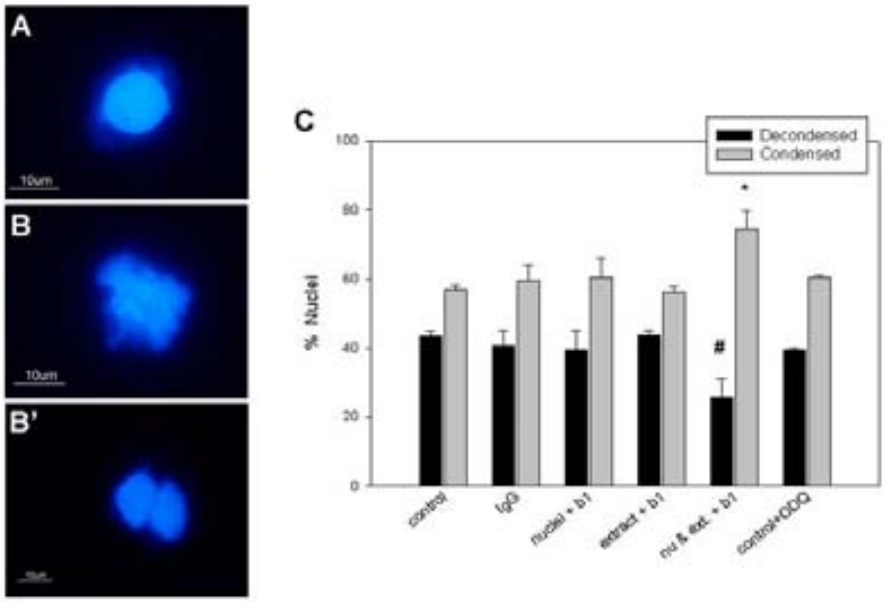
A
10um
B
10um
B'
C
Decondensed
Condensed
% Nuclei
100
80
60
40
20
0
*
#
control
IgG
nuclei + b1
extract + b1
nu & ext. + b1
control+ODQ

Figure 6

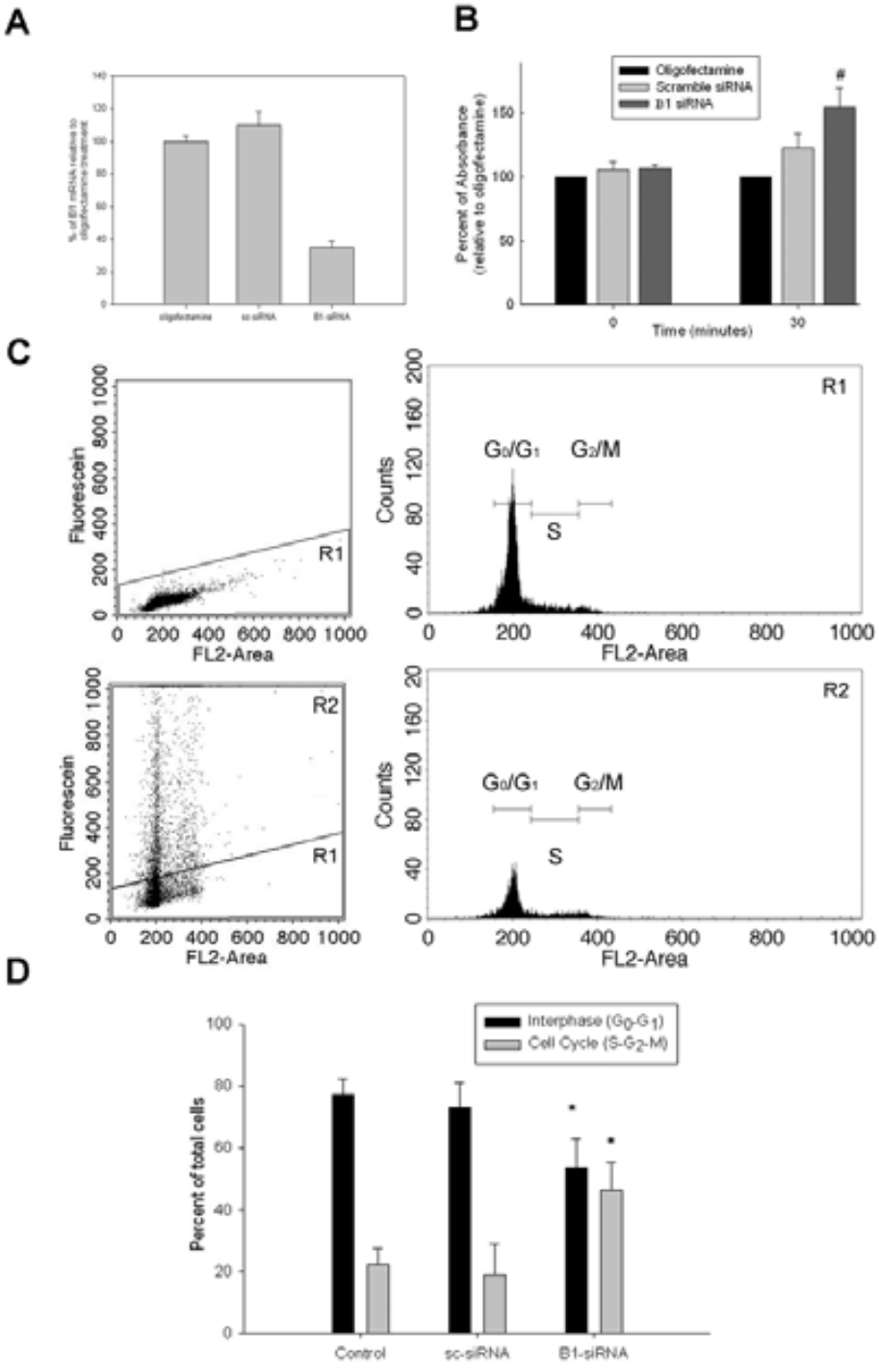
A
B
Oligofectamine
Scramble siRNA
B1 siRNA
Percent of Absorbance (relative to oligofectamine)
Time (minutes)
C
Fluorescein
FL2-Area
R1
R2
Counts
G0/G1
G2/M
S
D
Interphase (G0-G1)
Cell Cycle (S-G2-M)
Percent of total cells
Control
sc-siRNA
B1-siRNA

Figure 7

9 DISCUSION GENERAL

La GC_{NO} se expresa en prácticamente todas las células de mamífero y participa en un gran número de procesos fisiológicos en el SNC. Así, la vía de señalización NO-GC_{NO}-GMPc ha sido implicada en la regulación del desarrollo cerebral, la plasticidad sináptica, la secreción neuroendocrina, el procesamiento sensorial y el control del flujo sanguíneo cerebral (Garthwaite and Boulton, 1995; Zhang and Snyder, 1995). La estructura proteica funcional de la GC_{NO} es un heterodímero compuesto por una subunidad α1 o α2 y una subunidad β1. Además se ha clonado una subunidad β2 cuya función no está clara. Como primer objetivo de esta tesis se ha realizado un estudio comparativo de la localización de las distintas subunidades de la GC_{NO} en el cerebro de rata en comparación con el de mono para aportar datos sobre la posible distribución de los heterodímeros en las distintas estructuras cerebrales y su relación con las funciones en las que se ha implicado al sistema NO-GC_{NO}-GMPc.

Existen en la literatura trabajos referidos a la localización cerebral del mRNA de las subunidades de la GC_{NO} en los que se destaca que es la β1 la isoforma más ubicua en cerebro de rata (Furuyama et al, 1993; Gibb and Garthwaite, 2001). Sin embargo, nunca se había realizado un mapeo de las tres subunidades en secciones coronales de cerebro de rata. También describimos por primera vez la localización del mRNA de las distintas subunidades de la GC_{NO} en el cerebro de mono. En general, hemos observado que el mensajero de la subunidad β1 tiene un patrón regional de hibridación muy similar en los cerebros de estas dos especies. Por el contrario, la isoforma β2 no pudo ser detectada con ninguna de las tres sondas utilizadas individualmente o añadidas simultáneamente en el tampón de hibridación en ninguna de las zonas del cerebro estudiadas en rata o en mono. Aunque en la literatura se ha descrito la presencia de esta subunidad en cerebro de rata mediante la técnica de RT-PCR (Gibb y Garthwaite, 2001; Mergia et al., 2003), hasta el momento, ningún grupo ha sido capaz de detectar la presencia del mRNA de la subunidad β2 utilizando técnicas de Northern Blot, o de hibridación *in situ*, sugiriendo que los niveles de expresión de esta subunidad son demasiado bajos para ser detectados por estos métodos. Esta subunidad fue clonada y caracterizada a partir de placenta humana, y su papel fisiológico en cerebro continúa siendo cuestionado (Hobbs et al, 1997; Behrends et al, 2000).

Nuestros resultados demuestran que la máxima expresión de las tres subunidades estudiadas se observa en los ganglios basales, el sistema olfatorio, el hipocampo, el cortex y el cerebelo. Para las subunidades α se han encontrado diferencias en la localización de los mRNAs entre las dos isoformas y entre las dos especies estudiadas. Si bien la información disponible en la bibliografía no es muy abundante, los resultados obtenidos para la subunidad

α1 en cerebro de rata coinciden con los descritos previamente (Matsuoka et al, 1992; Furuyama et al, 1993; Gibb and Garthwaite, 2001). En este trabajo hemos observado que es más ubicuo el mRNA de α1 en mono mientras que en la rata lo es el de la subunidad α2. Estas diferencias fueron mayores en el sistema límbico y en el cortex cerebral. También fue posible detectar diferencias en la distribución laminar dentro del cortex cerebral. En la rata, la subunidad α1 es más intensa en capas externas corticales mientras que en el mono en las capas internas. La subunidad α2 se encuentra homogéneamente distribuida en ambas especies en las capas corticales.

En general, el patrón de distribución de las tres subunidades estudiadas se corresponde con un patrón de distribución típicamente neuronal. Existen trabajos en la literatura donde se describe la expresión de la GC_{NO} no sólo en neuronas sino también en células astrogliales, aunque los niveles de expresión en estas últimas son inferiores (Teunissen et al, 2001). En cerebelo, se observa un marcaje en substancia blanca que nos permite sugerir que las tres subunidades se encuentran expresadas en células gliales. Por otro lado, también es posible detectar los mensajeros para las subunidades α1 y β1 en la glía de Bergmann. Estos resultados deberían ser confirmados mediante dobles marcajes que permitan identificar el tipo celular.

Al estudiar la localización de las subunidades de la GC_{NO} en el cerebro es interesante comparar su distribución con la de otros componentes de la vía de señalización que involucran al NO y al GMPc, como son la NOS-1 o NOS neuronal (nNOS) y las PDEs específicas de GMPc (Garthwaite, 1995; García and Baltrons, 2004). Uno de los sistemas con mayor capacidad para generar GMPc es el que involucra a los receptores ionotrópicos del glutamato de tipo NMDA, la nNOS y la GC_{NO}. Como se comentó en la introducción de esta tesis, se ha descrito que la subunidad α2 es capaz de asociarse a través de un dominio PDZ con el receptor NMDA. Analizando la distribución de esta subunidad y comparándola con la localización del receptor, encontramos una gran coincidencia en las regiones de máxima expresión de ambos (Bredt, 1996; Cornil et al., 2000) como son las capas internas corticales, el núcleo anterior olfatorio, amígdala, hipocampo, núcleo reticular del tálamo, caudado-putamen, y cerebelo, lo cual indicaría que en estas regiones la entrada de calcio producida por la estimulación del receptor NMDA podría generar altos niveles de NO al existir en estas células una gran disponibilidad de los componentes de la vía de señalización NO-GC_{NO}-GMPc.

Diversos estudios electrofisiológicos han demostrado la implicación del sistema NO-GMPc-PKG en la regulación de procesos de plasticidad sináptica relacionados con el aprendizaje y la memoria en el hipocampo (LTP, potenciación a largo plazo) y con mecanismos de memoria motora en cerebelo (LTD, depresión a largo plazo). En el hipocampo, los niveles

de GMPc juegan un papel importante en los estadíos tempranos de consolidación de la memoria. Para que se genere LTP en el hipocampo es necesario que se produzca la síntesis de GMPc en las células piramidales (Wang et al., 2005). La presencia de los mRNAs de las tres subunidades en las células piramidales del hipocampo sugiere que ambos heterodímeros de la GC_{NO} se expresan en estas células. Sin embargo, la abundancia relativa de las subunidades sugiere que en el mono ambos heterodímeros se expresan de manera semejante en esta región mientras que en la rata el heterodímero $\alpha2\beta1$ parece ser el más abundante. Por otra parte, en células de Purkinje del cerebelo, la formación de GMPc podría deberse mayoritariamente al heterodímero $\alpha2\beta1$ en la rata mientras que en el mono también podría estar involucrado aunque en menor medida el heterodímero $\alpha1\beta1$. En las regiones del cerebro de rata que tienen relación con el comportamiento como son bulbo olfatorio, cerebelo, hipocampo y ganglios basales, se ha descrito que la vía de señalización NO-GMPc juega un papel fundamental en la regulación de los ciclos sueño-vigilia y en la conducta (Golombek et al, 2004). Nuestros resultados indican que, en estas regiones, no parece haber diferencias en cuanto al heterodímero predominante entre ambas especies, pudiendo detectarse la presencia de ambos y por lo tanto, esto podría indicar que tanto en roedores como en primates no existe un heterodímero asociado a la regulación de los ciclos seño-vigilia o de la conducta.

En nuestros estudios de localización por hibridación *in situ*, pudimos detectar regiones del cerebro tanto de mono como de rata donde se observaba un nivel elevado de la subunidad $\beta1$ y sin embargo los niveles de las subunidades α eran mínimos o indetectables. Gibb y Garthwaite (2001) describieron diferencias en el patrón de expresión de las diferentes subunidades y por consiguiente en los heterodímeros en cerebro de rata de 7 días. En nuestro trabajo sin embargo, en regiones como por ejemplo las islas de Calleja en rata o el claustrum del mono existen niveles de expresión máximos de la subunidad $\beta1$, a pesar de que los niveles de las subunidades α son muy bajos o nulos. También ocurre en el colículo superior y los núcleos hipotalámicos y talámicos de la rata donde los niveles de expresión de la $\beta1$ son muy elevados mientras que ambas subunidades α son prácticamente indetectables. Por otra parte, para la subunidad $\alpha1$ estas diferencias se observan en el núcleo reticular del tálamo en el mono y en menor medida en la sustancia blanca del cerebelo de la rata y en la glándula pineal. Teniendo en cuenta que los homodímeros $\alpha1\alpha1$ y $\beta1\beta1$ son catalíticamente inactivos (Zabel et al., 1999), estos resultados sugieren una posible función independiente la actividad GC_{NO} de estas subunidades.

En el transcurso de los estudios de la degradación de la subunidad $\beta1$ pudimos observar que ésta se localizaba en el núcleo. Otros autores han detectado mediante inmunocitoquímica

la presencia de la subunidad β1 en el núcleo (Krumenacker and Murad, 2006). Sin embargo, en nuestro trabajo no sólo detectamos la β1 en el núcleo de células que tienene actividad GC_{NO} (neuronas y astrocitos), sino que ante nuestra sorpresa y por primera vez también la detectamos en células incapaces de generar GMPc en respuesta al NO como es la microglía en cultivo. Estudios a mayor resolución permitieron demostrar que la GC_{NO} β1 se encontraba asociada periféricamente a los cromosomas en todas las fases de la mitosis. Sin embargo, las subunidades α no solo no se encontraban en el núcleo, sino que cuando se sobreexpresaban secuestraban a la subunidad β1 en el citoplasma.

Al analizar las posibles funciones de la asociación con los cromosomas de la subunidad β1 observamos que la inmunodepleción del pool citoplasmático y nuclear de la proteína producían un aumento de la condensación de la cromatina, y que este aumento era independiente la actividad GC_{NO} ya que el tratamiento con un inhibidor específico (ODQ) no producía los mismos efectos. En el mismo sentido, mediante técnicas de silenciamiento del mRNA (siRNA) observamos que la inhibición de la subunidad β1 producía un aumento del número de células que entraban en ciclo celular (fase S, G_2 y M) y un aumento en la proliferación celular determinada mediante la cuantificación de la actividad mitocondrial (MTT-EZ4U). Estos resultados no eran mimetizados por el ODQ sugiriendo que este efecto también era independiente de la síntesis de GMPc.

Teniendo en cuenta estos resultados y los resultados sobre localización que demostraban que existían regiones donde solo se expresa el mRNA de la subunidad β1, en esta tesis proponemos que la subunidad β1 posee una función independiente de la actividad GC_{NO} y de las subunidades α, o por lo menos de las subunidades α clonadas hasta la fecha.

Al inicio de este trabajo nos planteamos como objetivo general estudiar las diferencias en la localización y en la expresión de las diferentes subunidades de la GC_{NO}. Para ello eligimos la técnica de hibridación *in situ* ya que en ese momento no disponiamos de anticuerpos para las diferentes subunidades adecuados para realizar estudios inmunohistoquímicos además de inmunoblots. La aparición en el mercado de un anticuerpo para la subunidad β1, componente obligatorio del heterodímero funcional de la GC_{NO}, que tras su caracterización en el contexto de este trabajo resultó apto para estudios de inmunohistoquímica, nos permitió abordar un estudio para averiguar si en tejido humano también se ve afectada la expresión de la GC_{NO} en un proceso inflamatorio tal y como habíamos observado en la rata. Para ello se utilizaron muestras de cerebro de humanos con enfermedades neurodegenerativas con un componente inflamatorio como AD, CJ y MS. Nuestros resultados en muestras de corteza cerebral de humanos con AD indican que la subunidad β1 presenta un marcaje intenso en neuronas

corticales y neuronas de hipocampo mientras que el marcaje en la astroglía de la sustancia gris es muy bajo. En homogenados de corteza de cerebros de pacientes con AD no se veían alterado los niveles de expresión de la subunidad β1 ni de la subunidad α1 por inmunoblot ni se veían cambios en la actividad GC basal o estimulada por donadores de NO. Por inmunohistoquímica se corroboró que no existían diferencias en la inmunoreactividad de la β1 en neuronas y astrocitos fibrilares en controles y en AD. Sin embargo, se observó una disminución en la inmunoreactividad de la β1 en los astrocitos reactivos ubicados alrededor de las placas amiloides. Estos resultados están de acuerdo con los resultados obtenidos en células de rata en cultivo que indican una diferente sensibilidad de la actividad GC_{NO} de neuronas y astrocitos a los agentes inflamatorios. Además, el hecho de que no se afecte la actividad en neuronas probablemente impida detectar cambios en los niveles de actividad o en los niveles de la proteína en las muestras de tejido tomadas aleatoriamente. Sin embargo, parece confirmar que en la glía reactiva, donde se induce la NOS-2, se produce una respuesta adaptativa de disminución de la GC_{NO} (Baltrons et al., 2002; Pedraza et al., 2003). El hecho de que en neuronas no se detecte una regulación de la GC_{NO} podría indicar que en estas células falte alguno de los componentes implicados en la vía de la regulación de la GC_{NO}, o tal vez que, las isoformas expresadas en neuronas y astrocitos no sean iguales. Como se describe en la introducción, el heterodímero α2β1 tiene la capacidad de interaccionar con la proteína PSD-95, el receptor NMDA y la NOS-1 en neuronas. Esta interacción resulta en la asociación a la membrana del heterodímero α2β1. Probablemente esta asociación podría ser un mecanismo por el cual la enzima esté protegida en neuronas evitando así su degradación en condiciones de neuroinflamación. Por lo tanto, podríamos concluir que en los enfermos de AD no existe una asociación entre los niveles de expresión ni en la actividad de la GC_{NO} en células neuronales, pero sí en astrocitos reactivos incluidos los que se encuentran alrededor de las placas amiloides.

Por otro lado, como en astrocitos de la sustancia blanca se detectaron niveles altos de inmunoreactividad para la subunidad β1 en muestras de cerebros normales, nos propusimos estudiar las posibles alteraciones en enfermedades neurodegenerativas que afectaran principalmente a la sustancia blanca, como la MS. Por inmunohistoquímica observamos que los niveles de expresión de la subunidad β1 disminuían en los astrocitos reactivos de sustancia blanca en cerebro de MS. En CJ, enfermedad en la que se ve alterada tanto la sustancia blanca como la sustancia gris, la inmunoreactividad de la subunidad β1 se ve disminuida tanto en los astrocitos reactivos de la corteza como en los de la sustancia blanca subcortical. Todos estos datos parecen indicar que la reactividad glial podría estar asociada a una disminución en la capacidad de generar GMPc en respuesta a NO tanto *in vivo* como *in vitro.* Este mecanismo

podría constituir una adaptación de las células astrogliales para prevenir la señalización mediada por GMPc en condiciones de elevada formación de NO.

Trabajos previos de nuestro grupo demostraron que agentes inflamatorios como el LPS provocaban una disminución en la vida media de la subunidad β1. (Baltrons y col., 1999; Baltrons y col., 2002; Pedraza y col 2003). En este trabajo, demostramos que el efecto del LPS sobre la disminución de la proteína es prevenida por inhibidores del proteosoma, aunque no producen un aumento significativo en los niveles de proteína, debido probablemente a que se trata de una proteína de vida media larga (Ferrero and Torres, 2002, papetropoulos et al., 1995). Recientemente, se ha descrito que la desestabilización de la interacción entre la subunidad β1 y la HSP90 provocada con inhibidores de la HSP90 conduce a la degradación vía proteosoma de la β1 en células de músculo liso de aorta de rata (Papapetropoulos et al., 2005). En este trabajo demostramos por un lado, que el tratamiento con LPS no altera los niveles de la HSP90, y por otro, que los inhibidores de la HSP90 no alteran los niveles de β1, indicando que en astrocitos la HSP90 no tendría un papel estabilizador sobre la β1 y que tampoco estaría implicada en el mecanismo por el cual el LPS induce su degradación.

En los trabajos anteriores demostramos que el efecto del LPS sobre la β1 es independiente del NO generado endógenamente por este agente y es dependiente de transcripción y síntesis de proteínas. Está ampliamente documentado que el LPS induce la expresión de genes inflamatorios vía el factor de transcripción NFκB, cuya activación es además dependiente de la actividad del proteosoma. Para averiguar si el efecto de los inhibidores del proteosoma que observamos era dependiente de la acción de estos sobre el NFκB, en este trabajo estudiamos también la inhibición de la activación de este factor de transcripción y observamos que esta activación no impide la disminución de la β1 producida por el LPS pero sí impide la inducción de la NOS-2 como era de esperar. Estos datos refuerzan nuestros resultados de que el efecto del LPS no se debe al NO generado endógenamente y sugieren que el proteosoma está directamente implicado en la degradación de la subunidad β1.

El análisis de los estudios inmunocitoquímicos y de microscopía confocal reveló que el LPS induce la acumulación de la β1 en el núcleo donde colocaliza con la subunidad 20S del proteosoma y con la ubiquitina en unos cuerpos nucleares con características de clastosomas y no en otros cuerpos ricos también en proteosoma como son los cuerpos PML o los compartimentos nucleares de factores de splicing. En contraste, en células no tratadas, la β1 presenta principalmente inmunoreactividad citosólica y no se observa colocalización con los componentes del sistema UPS. Además, los inhibidores del proteosoma previenen la colocalización nuclear de la β1 con la ubiquitina y el 20 S, así como la formación de los

clastosomas. Estos datos nos permiten considerar claramente el papel de estas estructuras transitorias, los clastosomas, en la degradación de la β1 astroglial durante procesos inflamatorios. Averiguar si un mecanismo similar está involucrado en la degradación de la subunidad β1 en células humanas y conocer las implicaciones funcionales de la disminución en la capacidad de generar GMPc dependiente de NO en los astrocitos reactivos conlleva realizar nuevos estudios.

10 CONCLUSIONES

- Tanto en cerebro de rata como en primates, β1 es la subunidad de la GC_{NO} más abundante y ubicua, y su expresión es máxima en los ganglios basales, sistema olfatorio, corteza cerebral, sistema límbico, núcleos talámicos e hipotalámicos y células de Purkinje y granulares del cerebelo.
- En ambas especies, los niveles de expresión del mRNA de la subunidad β2 son indetectables por hibridación *in situ*.
- La expresión de las subunidades α en ambas especies es máxima en los ganglios basales y el sistema límbico.
- Existen diferencias en la distribución laminar de las subunidad α1 en la corteza cerebral entre ambas especies. Mientras en rata es mayor en capas externas corticales, en mono, la máxima expresión del mRNA de esta subunidad se encuentra en las capas internas corticales.
- La subunidad α1 parece expresarse más abundantemente que la subunidad α2 en mono mientras que en la rata ocurre lo contrario.
- Ambos heterodímeros α1β1 y α2β1 estan presentes en el SNC de las dos especies estudiadas.
- Existen regiones como las islas de Calleja, colículo superior y varios núcleos talámicos en rata o el claustrum y algunos núcleos talámicos en mono donde solo es posible detectar la presencia de la subunidad β1.
- En humanos, en corteza cerebral la inmunoreactividad para la subunidad β1 es elevada en neuronas y en astrocitos de la sustancia blanca, mientras que los astrocitos de la sustancia gris presentan un marcaje débil para esta subunidad.
- En enfermedades neurodegenerativas con un alto componente inflamatorio como son AD, CJ y MS disminuyen los niveles de la subunidad β1 en astrocitos reactivos situados alrededor de las placas amiloides en cerebro de AD o en astrocitos reactivos de sustancia blanca en MS, mientras que en CJ los niveles se ven alterados en astrocitos reactivos de la corteza y de la sustancia blanca subcortical. Sin embargo, los niveles proteícos en homogenados de cerebros AD medidos por inmunoblot y la actividad enzimática no se ven alterados, probablemente porque no se altera la expresión en neuronas.
- La degradación de la subunidad β1 de la GC_{NO} inducida por el tratamiento con LPS en astrocitos requiere la actividad del proteosoma y es independiente de la activación del factor de transcripción NFκB o de la inhibición de la interacción con la HSP90.

- Por inmunohistoquímica se ve que el LPS induce la colocalización de la subunidad β1 con la subunidad 20S del proteosoma y la ubiquitina en agregados nucleares con características de clastosomas.
- La subunidad β1 no se encuentra asociada a otras estructuras nucleares ricas en proteosomas como los cuerpos PML o los compartimientos donde se acumulan factores de splicing.
- Inhibidores del proteosoma y de la síntesis de proteínas previenen la colocalización nuclear de la subunidad β1 con los componentes de la vía de degradación ubiquitina-proteosoma y la formación de los clastosomas.
- En todas las células del sistema nervioso estudiadas, es posible detectar la presencia de la subunidad β1 no solo en el citoplasma sino también en el núcleo. Además, durante todas las fases de la mitosis se encuentra asociada periféricamente a los cromosomas.
- La subunidad β1 regula la condensación de la cromatina y la proliferación celular ya que la inmunodepleción de la proteína citoplasmática y nuclear genera un aumento de la condensación de la cromatina in vitro y su inhibición por siRNA incrementa el número de células que se encuentran dentro de las fases S, G_2 y M del ciclo celular produciendo un aumento en la proliferación.
- Todos los efectos de la unión de la subunidad β1 a los cromosomas y sus funciones sobre el control del ciclo celular son independientes de la síntesis de GMPc ya que el tratamiento con un inhibidor específico de la actividad GC_{NO} no mimetiza los efectos de la inmunodepleción ni del silenciamiento de la proteína.
- Por otro lado, hemos demostrado que células que son incapaces de generar GMPc como la microglía también expresan esta subunidad de la GC_{NO}, y en estas céluas también se encuentra asociada periféricamente a los cromosomas durante la mitosis.
- Teniendo en cuenta todos estos resultados, proponemos que la subunidad β1 posee una función independiente de las subunidades α y de la síntesis de GMPc.

11 BIBLIOGRAFíA

Adeli, K. (1994). Regulated intracellular degradation of apolipoprotein B in semipermeable HepG2 cells. J Biol Chem 269, 9166-75.

Adori, C., Kovacs, G. G., Low, P., Molnar, K., Gorbea, C., Fellinger, E., Budka, H., Mayer, R. J. and Laszlo, L. (2005). The ubiquitin-proteasome system in Creutzfeldt-Jakob and Alzheimer disease: intracellular redistribution of components correlates with neuronal vulnerability. Neurobiol Dis 19, 427-35.

Agullo, L., Baltrons, M. A. and Garcia, A. (1995). Calcium-dependent nitric oxide formation in glial cells. Brain Res 686, 160-8.

Agullo, L. and Garcia, A. (1992). Characterization of noradrenaline-stimulated cyclic GMP formation in brain astrocytes in culture. Biochem J 288 (Pt 2), 619-24.

Agullo, L., Garcia-Dorado, D., Escalona, N., Ruiz-Meana, M., Mirabet, M., Inserte, J. and Soler-Soler, J. (2005). Membrane association of nitric oxide-sensitive guanylyl cyclase in cardiomyocytes. Cardiovasc Res 68, 65-74.

Almer, G., Vukosavic, S., Romero, N. and Przedborski, S. (1999). Inducible nitric oxide synthase up-regulation in a transgenic mouse model of familial amyotrophic lateral sclerosis. J Neurochem 72, 2415-25.

Andreeva, S. G., Dikkes, P., Epstein, P. M. and Rosenberg, P. A. (2001). Expression of cGMP-specific phosphodiesterase 9A mRNA in the rat brain. J Neurosci 21, 9068-76.

Anton, L. C., Schubert, U., Bacik, I., Princiotta, M. F., Wearsch, P. A., Gibbs, J., Day, P. M., Realini, C., Rechsteiner, M. C., Bennink, J. R. et al. (1999). Intracellular localization of proteasomal degradation of a viral antigen. J Cell Biol 146, 113-24.

Ariano, M. A., Lewicki, J. A., Brandwein, H. J. and Murad, F. (1982). Immunohistochemical localization of guanylate cyclase within neurons of rat brain. Proc Natl Acad Sci U S A 79, 1316-20.

Balashova, N., Chang, F. J., Lamothe, M., Sun, Q. and Beuve, A. (2005). Characterization of a novel type of endogenous activator of soluble guanylyl cyclase. J Biol Chem 280, 2186-96.

Baltrons, M. A. and Garcia, A. (1999). Nitric oxide-independent down-regulation of soluble guanylyl cyclase by bacterial endotoxin in astroglial cells. J Neurochem 73, 2149-57.

Baltrons, M. A., Pedraza, C., Sardon, T., Navarra, M. and Garcia, A. (2003). Regulation of NO-dependent cyclic GMP formation by inflammatory agents in neural cells. Toxicol Lett 139, 191-8.

Baltrons, M. A., Pedraza, C. E., Heneka, M. T. and Garcia, A. (2002). Beta-amyloid peptides decrease soluble guanylyl cyclase expression in astroglial cells. Neurobiol Dis 10, 139-49.

Baltrons, M. A., Pifarre, P., Ferrer, I., Carot, J. M. and Garcia, A. (2004). Reduced expression of NO-sensitive guanylyl cyclase in reactive astrocytes of Alzheimer disease, Creutzfeldt-Jakob disease, and multiple sclerosis brains. Neurobiol Dis 17, 462-72.

Bellamy, T. C., Wood, J., Goodwin, D. A. and Garthwaite, J. (2000). Rapid desensitization of the nitric oxide receptor, soluble guanylyl cyclase, underlies diversity of cellular cGMP responses. Proc Natl Acad Sci U S A 97, 2928-33.

Belmont, A. S. (2006). Mitotic chromosome structure and condensation. Curr Opin Cell Biol 18, 632-8.

Bender, A. T. and Beavo, J. A. (2006). Cyclic nucleotide phosphodiesterases: molecular regulation to clinical use. Pharmacol Rev 58, 488-520.

Bidmon, H. J., Starbatty, J., Gorg, B., Zilles, K. and Behrends, S. (2004). Cerebral expression of the alpha2-subunit of soluble guanylyl cyclase is linked to cerebral maturation and sensory pathway refinement during postnatal development. Neurochem Int 45, 821-32.

Bo, L., Dawson, T. M., Wesselingh, S., Mork, S., Choi, S., Kong, P. A., Hanley, D. and Trapp, B. D. (1994). Induction of nitric oxide synthase in demyelinating regions of multiple sclerosis brains. Ann Neurol 36, 778-86.

Boran, M. and Garcia, A. (2005). Cyclic GMP regulates cytoeskeleton dynamics in glial cells. In J Neurochem, vol. 94, pp. 107.

Bradford, M. M. (1976). A rapid and sensitive method for the quantitation of microgram quantities of protein utilizing the principle of protein-dye binding. Anal Biochem 72, 248-54.

Bredt, D. S. (1996). NO NMDA receptor activity. Nat Biotechnol 14, 944.

Bredt, D. S. (1999). Endogenous nitric oxide synthesis: biological functions and pathophysiology. Free Radic Res 31, 577-96.

Bredt, D. S., Glatt, C. E., Hwang, P. M., Fotuhi, M., Dawson, T. M. and Snyder, S. H. (1991). Nitric oxide synthase protein and mRNA are discretely localized in neuronal populations of the mammalian CNS together with NADPH diaphorase. Neuron 7, 615-24.

Bredt, D. S., Hwang, P. M. and Snyder, S. H. (1990). Localization of nitric oxide synthase indicating a neural role for nitric oxide. Nature 347, 768-70.

Brenman, J. E., Chao, D. S., Gee, S. H., McGee, A. W., Craven, S. E., Santillano, D. R., Wu, Z., Huang, F., Xia, H., Peters, M. F. et al. (1996a). Interaction of nitric oxide synthase with the postsynaptic density protein PSD-95 and alpha1-syntrophin mediated by PDZ domains. Cell 84, 757-67.

Brenman, J. E., Christopherson, K. S., Craven, S. E., McGee, A. W. and Bredt, D. S. (1996b). Cloning and characterization of postsynaptic density 93, a nitric oxide synthase interacting protein. J Neurosci 16, 7407-15.

Brooker, G., Harper, J. F., Terasaki, W. L. and Moylan, R. D. (1979). Radioimmunoassay of cyclic AMP and cyclic GMP. Adv Cyclic Nucleotide Res 10, 1-33.

Budworth, J., Meillerais, S., Charles, I. and Powell, K. (1999). Tissue distribution of the human soluble guanylate cyclases. Biochem Biophys Res Commun 263, 696-701.

Bukrinsky, M. I., Nottet, H. S., Schmidtmayerova, H., Dubrovsky, L., Flanagan, C. R., Mullins, M. E., Lipton, S. A. and Gendelman, H. E. (1995). Regulation of nitric oxide synthase activity in human immunodeficiency virus type 1 (HIV-1)-infected monocytes: implications for HIV-associated neurological disease. J Exp Med 181, 735-45.

Chen, M., Rockel, T., Steinweger, G., Hemmerich, P., Risch, J. and von Mikecz, A. (2002). Subcellular recruitment of fibrillarin to nucleoplasmic proteasomes: implications for processing of a nucleolar autoantigen. Mol Biol Cell 13, 3576-87.

Ching, R. W., Dellaire, G., Eskiw, C. H. and Bazett-Jones, D. P. (2005). PML bodies: a meeting place for genomic loci? J Cell Sci 118, 847-54.

Colasanti, M., Persichini, T., Di Pucchio, T., Gremo, F. and Lauro, G. M. (1995). Human ramified microglial cells produce nitric oxide upon Escherichia coli lipopolysaccharide and tumor necrosis factor alpha stimulation. Neurosci Lett 200, 144-6.

Collas, P., Le Guellec, K. and Tasken, K. (1999). The A-kinase-anchoring protein AKAP95 is a multivalent protein with a key role in chromatin condensation at mitosis. J Cell Biol 147, 1167-80.

Cornil, C., Foidart, A., Minet, A. and Balthazart, J. (2000). Immunocytochemical localization of ionotropic glutamate receptors subunits in the adult quail forebrain. J Comp Neurol 428, 577-608.

Currie, M. G., Fok, K. F., Kato, J., Moore, R. J., Hamra, F. K., Duffin, K. L. and Smith, C. E. (1992). Guanylin: an endogenous activator of intestinal guanylate cyclase. Proc Natl Acad Sci U S A 89, 947-51.

Dantuma, N. P., Groothuis, T. A., Salomons, F. A. and Neefjes, J. (2006). A dynamic ubiquitin equilibrium couples proteasomal activity to chromatin remodeling. J Cell Biol 173, 19-26.

Davis, J. P., Vo, X. T. and Sulakhe, P. V. (1997). Altered responsiveness of guanylyl cyclase to nitric oxide following treatment of cardiomyocytes with S-nitroso-D,L-acetylpenicillamine and sodium nitroprusside. Biochem Biophys Res Commun 238, 351-6.

Dawson, V. L. and Dawson, T. M. (1996). Nitric oxide neurotoxicity. J Chem Neuroanat 10, 179-90.

de Frutos, S., Saura, M., Rivero-Vilches, F. J., Rodriguez-Puyol, D. and Rodriguez-Puyol, M. (2003). C-type natriuretic peptide decreases soluble guanylate cyclase levels by activating the proteasome pathway. Biochim Biophys Acta 1643, 105-12.

de Vente, J., Bol, J. G. and Steinbusch, H. W. (1989). Localization of cGMP in the cerebellum of the adult rat: an immunohistochemical study. Brain Res 18, 332-7.

de Vente, J. and Steinbusch, H. W. (1992). On the stimulation of soluble and particulate guanylate cyclase in the rat brain and the involvement of nitric oxide as studied by cGMP immunocytochemistry. Acta Histochem 92, 13-38.

Dello Russo, C., Polak, P. E., Mercado, P. R., Spagnolo, A., Sharp, A., Murphy, P., Kamal, A., Burrows, F. J., Fritz, L. C. and Feinstein, D. L. (2006). The heat-shock protein 90 inhibitor 17-allylamino-17-demethoxygeldanamycin suppresses glial inflammatory responses and ameliorates experimental autoimmune encephalomyelitis. J Neurochem 99, 1351-62.

Denninger, J. W. and Marletta, M. A. (1999). Guanylate cyclase and the .NO/cGMP signaling pathway. Biochim Biophys Acta 1411, 334-50.

Dinerman, J. L., Dawson, T. M., Schell, M. J., Snowman, A. and Snyder, S. H. (1994). Endothelial nitric oxide synthase localized to hippocampal pyramidal cells: implications for synaptic plasticity. Proc Natl Acad Sci U S A 91, 4214-8.

Ding, J. D., Burette, A., Nedvetsky, P. I., Schmidt, H. H. and Weinberg, R. J. (2004). Distribution of soluble guanylyl cyclase in the rat brain. J Comp Neurol 472, 437-48.

Ding, M., St Pierre, B. A., Parkinson, J. F., Medberry, P., Wong, J. L., Rogers, N. E., Ignarro, L. J. and Merrill, J. E. (1997). Inducible nitric-oxide synthase and nitric oxide production in human fetal astrocytes and microglia. A kinetic analysis. J Biol Chem 272, 11327-35.

Dohmen, R. J. (2004). SUMO protein modification. Biochim Biophys Acta 1695, 113-31.

Earp, H. S., Smith, P., Huang Ong, S. H. and Steiner, A. L. (1977). Regulation of hepatic nuclear guanylate cyclase. Proc Natl Acad Sci U S A 74, 946-50.

Endoh, M., Maiese, K. and Wagner, J. A. (1994). Expression of the neural form of nitric oxide synthase by CA1 hippocampal neurons and other central nervous system neurons. Neuroscience 63, 679-89.

Fabunmi, R. P., Wigley, W. C., Thomas, P. J. and DeMartino, G. N. (2001). Interferon gamma regulates accumulation of the proteasome activator PA28 and immunoproteasomes at nuclear PML bodies. J Cell Sci 114, 29-36.

Fan, B., Gupta, G., Danziger, R. S., Friedman, J. M. and Rousseau, D. L. (1998). Resonance Raman characterization of soluble guanylate cyclase expressed from baculovirus. Biochemistry 37, 1178-84.

Feil, R., Feil, S. and Hofmann, F. (2005). A heretical view on the role of NO and cGMP in vascular proliferative diseases. Trends Mol Med 11, 71-5.

Fenteany, G. and Schreiber, S. L. (1998). Lactacystin, proteasome function, and cell fate. J Biol Chem 273, 8545-8.

Ferrero, R., Rodriguez-Pascual, F., Miras-Portugal, M. T. and Torres, M. (2000). Nitric oxide-sensitive guanylyl cyclase activity inhibition through cyclic GMP-dependent dephosphorylation. J Neurochem 75, 2029-39.

Ferrero, R. and Torres, M. (2002). Prolonged exposure of chromaffin cells to nitric oxide down-regulates the activity of soluble guanylyl cyclase and corresponding mRNA and protein levels. BMC Biochem 3, 26.

Feussner, M., Richter, H., Baum, O. and Gossrau, R. (2001). Association of soluble guanylate cyclase with the sarcolemma of mammalian skeletal muscle fibers. Acta Histochem 103, 265-77.

Filippov, G., Bloch, D. B. and Bloch, K. D. (1997). Nitric oxide decreases stability of mRNAs encoding soluble guanylate cyclase subunits in rat pulmonary artery smooth muscle cells. J Clin Invest 100, 942-8.

Foerster, J., Harteneck, C., Malkewitz, J., Schultz, G. and Koesling, D. (1996). A functional heme-binding site of soluble guanylyl cyclase requires intact N-termini of alpha 1 and beta 1 subunits. Eur J Biochem 240, 380-6.

Forstermann, U., Closs, E. I., Pollock, J. S., Nakane, M., Schwarz, P., Gath, I. and Kleinert, H. (1994). Nitric oxide synthase isozymes. Characterization, purification, molecular cloning, and functions. Hypertension 23, 1121-31.

Forstermann, U., Pollock, J. S., Schmidt, H. H., Heller, M. and Murad, F. (1991). Calmodulin-dependent endothelium-derived relaxing factor/nitric oxide synthase activity is present in the particulate and cytosolic fractions of bovine aortic endothelial cells. Proc Natl Acad Sci U S A 88, 1788-92.

Forte, L. R., Eber, S. L., Fan, X., London, R. M., Wang, Y., Rowland, L. M., Chin, D. T., Freeman, R. H. and Krause, W. J. (1999a). Lymphoguanylin: cloning and characterization of a unique member of the guanylin peptide family. Endocrinology 140, 1800-6.

Forte, L. R., Freeman, R. H., Krause, W. J. and London, R. M. (1999b). Guanylin peptides: cyclic GMP signaling mechanisms. Braz J Med Biol Res 32, 1329-36.

Foster, D. C., Wedel, B. J., Robinson, S. W. and Garbers, D. L. (1999). Mechanisms of regulation and functions of guanylyl cyclases. Rev Physiol Biochem Pharmacol 135, 1-39.

Friebe, A., Mergia, E., Dangel, O., Lange, A. and Koesling, D. (2007). Fatal gastrointestinal obstruction and hypertension in mice lacking nitric oxide-sensitive guanylyl cyclase. Proc Natl Acad Sci U S A 104, 7699-704.

Furchgott, R. F. (1999). Endothelium-derived relaxing factor: discovery, early studies, and identification as nitric oxide. Biosci Rep 19, 235-51.

Furchgott, R. F. and Zawadzki, J. V. (1980). The obligatory role of endothelial cells in the relaxation of arterial smooth muscle by acetylcholine. Nature 288, 373-6.

Furuyama, T., Inagaki, S. and Takagi, H. (1993). Localizations of alpha 1 and beta 1 subunits of soluble guanylate cyclase in the rat brain. Brain Res Mol Brain Res 20, 335-44.

Garcia, A. and Baltrons, M. A. (2003). The nitric oxide/cyclic GMP signalling pathway in CNS glial cells. In Advances in Molecular and Cell Biology, vol. 31 (ed. E. E.E. Bittar), pp. 575-594.

Garthwaite, G. and Garthwaite, J. (1988). Electron microscopic autoradiography of D-[3H]aspartate uptake sites in mouse cerebellar slices shows poor labelling of mossy fibre terminals. Brain Res 440, 162-6.

Garthwaite, J. and Boulton, C. L. (1995). Nitric oxide signaling in the central nervous system. Annu Rev Physiol 57, 683-706.

Gibb, B. J. and Garthwaite, J. (2001). Subunits of the nitric oxide receptor, soluble guanylyl cyclase, expressed in rat brain. Eur J Neurosci 13, 539-44.

Gobeil, F., Jr., Zhu, T., Brault, S., Geha, A., Vazquez-Tello, A., Fortier, A., Barbaz, D., Checchin, D., Hou, X., Nader, M. et al. (2006). Nitric oxide signaling via nuclearized endothelial nitric-oxide synthase modulates expression of the immediate early genes iNOS and mPGES-1. J Biol Chem 281, 16058-67.

Gruetter, C. A., Barry, B. K., McNamara, D. B., Gruetter, D. Y., Kadowitz, P. J. and Ignarro, L. (1979). Relaxation of bovine coronary artery and activation of coronary arterial guanylate cyclase by nitric oxide, nitroprusside and a carcinogenic nitrosoamine. J Cyclic Nucleotide Res 5, 211-24.

Grzybicki, D., Moore, S. A., Schelper, R., Glabinski, A. R., Ransohoff, R. M. and Murphy, S. (1998). Expression of monocyte chemoattractant protein (MCP-1) and nitric oxide synthase-2 following cerebral trauma. Acta Neuropathol (Berl) 95, 98-103.

Hanna, J., Leggett, D. S. and Finley, D. (2003). Ubiquitin depletion as a key mediator of toxicity by translational inhibitors. Mol Cell Biol 23, 9251-61.

Harrison, B. C. and Mobley, P. L. (1990). Phorbol ester-induced change in astrocyte morphology: correlation with protein kinase C activation and protein phosphorylation. J Neurosci Res 25, 71-80.

Harrison, B. C., Staskavage, D. L. and Mobley, P. L. (1991). Effects of sphingosine on phorbol ester-mediated changes in astrocyte morphology and protein phosphorylation. J Neurosci Res 29, 181-9.

Heinrich, U., Maurer, J., Koesling, D., Mann, W. and Forstermann, U. (2000). Immuno-electron microscopic localization of the alpha(1) and beta(1)-subunits of soluble guanylyl cyclase in the guinea pig organ of corti. Brain Res 885, 6-13.

Henkel, T., Machleidt, T., Alkalay, I., Kronke, M., Ben-Neriah, Y. and Baeuerle, P. A. (1993). Rapid proteolysis of I kappa B-alpha is necessary for activation of transcription factor NF-kappa B. Nature 365, 182-5.

Hernandez-Verdun, D. and Gautier, T. (1994). The chromosome periphery during mitosis. Bioessays 16, 179-85.

Hernandez-Verdun, D. and Roussel, P. (2003). Regulators of nucleolar functions. Prog Cell Cycle Res 5, 301-8.

Hershko, A., Eytan, E., Ciechanover, A. and Haas, A. L. (1982). Immunochemical analysis of the turnover of ubiquitin-protein conjugates in intact cells. Relationship to the breakdown of abnormal proteins. J Biol Chem 257, 13964-70.

Hobbs, A. J. (1997). Soluble guanylate cyclase: the forgotten sibling. Trends Pharmacol Sci 18, 484-91.

Hunot, S., Boissiere, F., Faucheux, B., Brugg, B., Mouatt-Prigent, A., Agid, Y. and Hirsch, E. C. (1996). Nitric oxide synthase and neuronal vulnerability in Parkinson's disease. Neuroscience 72, 355-63.

Ibarra, C., Nedvetsky, P. I., Gerlach, M., Riederer, P. and Schmidt, H. H. (2001). Regional and age-dependent expression of the nitric oxide receptor, soluble guanylyl cyclase, in the human brain. Brain Res 907, 54-60.

Ignarro, L. J., Buga, G. M., Wood, K. S., Byrns, R. E. and Chaudhuri, G. (1987). Endothelium-derived relaxing factor produced and released from artery and vein is nitric oxide. Proc Natl Acad Sci U S A 84, 9265-9.

Janer, A., Martin, E., Muriel, M. P., Latouche, M., Fujigasaki, H., Ruberg, M., Brice, A., Trottier, Y. and Sittler, A. (2006). PML clastosomes prevent nuclear accumulation of mutant ataxin-7 and other polyglutamine proteins. J Cell Biol 174, 65-76.

Jeon, Y. J., Kim, Y. K., Lee, M., Park, S. M., Han, S. B. and Kim, H. M. (2000). Radicicol suppresses expression of inducible nitric-oxide synthase by blocking p38 kinase and nuclear factor-kappaB/Rel in lipopolysaccharide-stimulated macrophages. J Pharmacol Exp Ther 294, 548-54.

Joazeiro, C. A. and Weissman, A. M. (2000). RING finger proteins: mediators of ubiquitin ligase activity. Cell 102, 549-52.

Jurado, S., Sanchez-Prieto, J. and Torres, M. (2003). Differential expression of NO-sensitive guanylyl cyclase subunits during the development of rat cerebellar granule cells: regulation via N-methyl-D-aspartate receptors. J Cell Sci 116, 3165-75.

Kloss, S., Furneaux, H. and Mulsch, A. (2003). Post-transcriptional regulation of soluble guanylyl cyclase expression in rat aorta. J Biol Chem 278, 2377-83.

Koesling, D., Bohme, E. and Schultz, G. (1991). Guanylyl cyclases, a growing family of signal-transducing enzymes. Faseb J 5, 2785-91.

Koesling, D. and Friebe, A. (1999). Soluble guanylyl cyclase: structure and regulation. Rev Physiol Biochem Pharmacol 135, 41-65.

Koesling, D., Harteneck, C., Humbert, P., Bosserhoff, A., Frank, R., Schultz, G. and Bohme, E. (1990). The primary structure of the larger subunit of soluble guanylyl cyclase from bovine lung. Homology between the two subunits of the enzyme. FEBS Lett 266, 128-32.

Koesling, D., Russwurm, M., Mergia, E., Mullershausen, F. and Friebe, A. (2004). Nitric oxide-sensitive guanylyl cyclase: structure and regulation. Neurochem Int 45, 813-9.

Kostic, T. S., Andric, S. A. and Stojilkovic, S. S. (2004). Receptor-controlled phosphorylation of alpha 1 soluble guanylyl cyclase enhances nitric oxide-dependent cyclic guanosine 5'-monophosphate production in pituitary cells. Mol Endocrinol 18, 458-70.

Kroismayr, R., Baranyi, U., Stehlik, C., Dorfleutner, A., Binder, B. R. and Lipp, J. (2004). HERC5, a HECT E3 ubiquitin ligase tightly regulated in LPS activated endothelial cells. J Cell Sci 117, 4749-56.

Krumenacker, J. S., Katsuki, S., Kots, A. and Murad, F. (2006). Differential expression of genes involved in cGMP-dependent nitric oxide signaling in murine embryonic stem (ES) cells and ES cell-derived cardiomyocytes. Nitric Oxide 14, 1-11.

Krumenacker, J. S. and Murad, F. (2006). NO-cGMP signaling in development and stem cells. Mol Genet Metab 87, 311-4.

Labrecque, J., Mc Nicoll, N., Marquis, M. and De Lean, A. (1999). A disulfide-bridged mutant of natriuretic peptide receptor-A displays constitutive activity. Role of receptor dimerization in signal transduction. J Biol Chem 274, 9752-9.

Lafarga, M., Berciano, M. T., Pena, E., Mayo, I., Castano, J. G., Bohmann, D., Rodrigues, J. P., Tavanez, J. P. and Carmo-Fonseca, M. (2002). Clastosome: a subtype of nuclear body enriched in 19S and 20S proteasomes, ubiquitin, and protein substrates of proteasome. Mol Biol Cell 13, 2771-82.

Lain, S., Midgley, C., Sparks, A., Lane, E. B. and Lane, D. P. (1999). An inhibitor of nuclear export activates the p53 response and induces the localization of HDM2 and p53 to U1A-positive nuclear bodies associated with the PODs. Exp Cell Res 248, 457-72.

Lallemand-Breitenbach, V., Zhu, J., Puvion, F., Koken, M., Honore, N., Doubeikovsky, A., Duprez, E., Pandolfi, P. P., Puvion, E., Freemont, P. et al. (2001). Role of promyelocytic leukemia (PML) sumolation in nuclear body formation, 11S proteasome recruitment, and As2O3-induced PML or PML/retinoic acid receptor alpha degradation. J Exp Med 193, 1361-71.

Lamond, A. I. and Spector, D. L. (2003). Nuclear speckles: a model for nuclear organelles. Nat Rev Mol Cell Biol 4, 605-12.

Lefebvre, R. A. (1995). Nitric oxide in the peripheral nervous system. Ann Med 27, 379-88.

Li, X., Zhao, X., Fang, Y., Jiang, X., Duong, T., Fan, C., Huang, C. C. and Kain, S. R. (1998). Generation of destabilized green fluorescent protein as a transcription reporter. J Biol Chem 273, 34970-5.

Liu, H., Force, T. and Bloch, K. D. (1997a). Nerve growth factor decreases soluble guanylate cyclase in rat pheochromocytoma PC12 cells. J Biol Chem 272, 6038-43.

Liu, J., Zhao, M. L., Brosnan, C. F. and Lee, S. C. (1996). Expression of type II nitric oxide synthase in primary human astrocytes and microglia: role of IL-1beta and IL-1 receptor antagonist. J Immunol 157, 3569-76.

Liu, Y., Ruoho, A. E., Rao, V. D. and Hurley, J. H. (1997b). Catalytic mechanism of the adenylyl and guanylyl cyclases: modeling and mutational analysis. Proc Natl Acad Sci U S A 94, 13414-9.

Llansola, M., Minana, M. D., Montoliu, C., Saez, R., Corbalan, R., Manzo, L. and Felipo, V. (1999). Prenatal exposure to aluminum reduces expression of neuronal nitric oxide synthase and of soluble guanylate cyclase and impairs glutamatergic neurotransmission in rat cerebellum. J Neurochem 73, 712-8.

Lowry, O. H., Rosebrough, N. J., Farr, A. L. and Randall, R. J. (1951). Protein measurement with the Folin phenol reagent. J Biol Chem 193, 265-75.

Lucas, K. A., Pitari, G. M., Kazerounian, S., Ruiz-Stewart, I., Park, J., Schulz, S., Chepenik, K. P. and Waldman, S. A. (2000). Guanylyl cyclases and signaling by cyclic GMP. Pharmacol Rev 52, 375-414.

Magnani, M., Crinelli, R., Bianchi, M. and Antonelli, A. (2000). The ubiquitin-dependent proteolytic system and other potential targets for the modulation of nuclear factor-kB (NF-kB). Curr Drug Targets 1, 387-99.

Matsuoka, I., Giuili, G., Poyard, M., Stengel, D., Parma, J., Guellaen, G. and Hanoune, J. (1992). Localization of adenylyl and guanylyl cyclase in rat brain by in situ hybridization: comparison with calmodulin mRNA distribution. J Neurosci 12, 3350-60.

Meister, G. and Tuschl, T. (2004). Mechanisms of gene silencing by double-stranded RNA. Nature 431, 343-9.

Mengual, E., Arizti, P., Rodrigo, J., Gimenez-Amaya, J. M. and Castano, J. G. (1996). Immunohistochemical distribution and electron microscopic subcellular localization of the proteasome in the rat CNS. J Neurosci 16, 6331-41.

Mergia, E., Russwurm, M., Zoidl, G. and Koesling, D. (2003). Major occurrence of the new alpha2beta1 isoform of NO-sensitive guanylyl cyclase in brain. Cell Signal 15, 189-95.

Merrill, J. E., Murphy, S. P., Mitrovic, B., Mackenzie-Graham, A., Dopp, J. C., Ding, M., Griscavage, J., Ignarro, L. J. and Lowenstein, C. J. (1997). Inducible nitric oxide synthase and nitric oxide production by oligodendrocytes. J Neurosci Res 48, 372-84.

Meurer, S., Pioch, S., Gross, S. and Muller-Esterl, W. (2005). Reactive oxygen species induce tyrosine phosphorylation of and Src kinase recruitment to NO-sensitive guanylyl cyclase. J Biol Chem 280, 33149-56.

Minana, M. D., Corbalan, R., Montoliu, C., Teng, C. M. and Felipo, V. (1999). Chronic hyperammonemia in rats impairs activation of soluble guanylate cyclase in neurons and in lymphocytes: a putative peripheral marker for neurological alterations. Biochem Biophys Res Commun 257, 405-9.

Mittal, C. K. and Murad, F. (1977). Properties and oxidative regulation of guanylate cyclase. J Cyclic Nucleotide Res 3, 381-91.

Molina-Holgado, E., Vela, J. M., Arevalo-Martin, A. and Guaza, C. (2001). LPS/IFN-gamma cytotoxicity in oligodendroglial cells: role of nitric oxide and protection by the anti-inflammatory cytokine IL-10. Eur J Neurosci 13, 493-502.

Moncada, S., Palmer, R. M. and Higgs, E. A. (1991). Nitric oxide: physiology, pathophysiology, and pharmacology. Pharmacol Rev 43, 109-42.

Mrak, R. E. and Griffin, W. S. (2001). Interleukin-1, neuroinflammation, and Alzheimer's disease. Neurobiol Aging 22, 903-8.

Mujoo, K., Krumenacker, J. S., Wada, Y. and Murad, F. (2006). Differential expression of nitric oxide signaling components in undifferentiated and differentiated human embryonic stem cells. Stem Cells Dev 15, 779-87.

Murad, F., Mittal, C. K., Arnold, W. P., Katsuki, S. and Kimura, H. (1978). Guanylate cyclase: activation by azide, nitro compounds, nitric oxide, and hydroxyl radical and inhibition by hemoglobin and myoglobin. Adv Cyclic Nucleotide Res 9, 145-58.

Murphy, G. M., Jr., Jia, X. C., Song, Y., Ong, E., Shrivastava, R., Bocchini, V., Lee, Y. L. and Eng, L. F. (1995). Macrophage inflammatory protein 1-alpha mRNA expression in an immortalized microglial cell line and cortical astrocyte cultures. J Neurosci Res 40, 755-63.

Murphy, S., Simmons, M. L., Agullo, L., Garcia, A., Feinstein, D. L., Galea, E., Reis, D. J., Minc-Golomb, D. and Schwartz, J. P. (1993). Synthesis of nitric oxide in CNS glial cells. Trends Neurosci 16, 323-8.

Murthy, K. S. (2001). Activation of phosphodiesterase 5 and inhibition of guanylate cyclase by cGMP-dependent protein kinase in smooth muscle. Biochem J 360, 199-208.

Murthy, K. S. (2004). Modulation of soluble guanylate cyclase activity by phosphorylation. Neurochem Int 45, 845-51.

Nakane, M., Arai, K., Saheki, S., Kuno, T., Buechler, W. and Murad, F. (1990). Molecular cloning and expression of cDNAs coding for soluble guanylate cyclase from rat lung. J Biol Chem 265, 16841-5.

Nakane, M., Ichikawa, M. and Deguchi, T. (1983). Light and electron microscopic demonstration of guanylate cyclase in rat brain. Brain Res 273, 9-15.

Okuda, Y., Sakoda, S., Fujimura, H. and Yanagihara, T. (1997). Nitric oxide via an inducible isoform of nitric oxide synthase is a possible factor to eliminate inflammatory cells from the central nervous system of mice with experimental allergic encephalomyelitis. J Neuroimmunol 73, 107-16.

Palmer, R. M., Ferrige, A. G. and Moncada, S. (1987). Nitric oxide release accounts for the biological activity of endothelium-derived relaxing factor. Nature 327, 524-6.

Papapetropoulos, A., Abou-Mohamed, G., Marczin, N., Murad, F., Caldwell, R. W. and Catravas, J. D. (1996a). Downregulation of nitrovasodilator-induced cyclic GMP accumulation in cells exposed to endotoxin or interleukin-1 beta. Br J Pharmacol 118, 1359-66.

Papapetropoulos, A., Go, C. Y., Murad, F. and Catravas, J. D. (1996b). Mechanisms of tolerance to sodium nitroprusside in rat cultured aortic smooth muscle cells. Br J Pharmacol 117, 147-55.

Papapetropoulos, A., Marczin, N., Mora, G., Milici, A., Murad, F. and Catravas, J. D. (1995). Regulation of vascular smooth muscle soluble guanylate cyclase activity, mRNA, and protein levels by cAMP-elevating agents. Hypertension 26, 696-704.

Papapetropoulos, A., Zhou, Z., Gerassimou, C., Yetik, G., Venema, R. C., Roussos, C., Sessa, W. C. and Catravas, J. D. (2005). Interaction between the 90-kDa heat shock protein and soluble guanylyl cyclase: physiological significance and mapping of the domains mediating binding. Mol Pharmacol 68, 1133-41.

Parkinson, S. J., Jovanovic, A., Jovanovic, S., Wagner, F., Terzic, A. and Waldman, S. A. (1999). Regulation of nitric oxide-responsive recombinant soluble guanylyl cyclase by calcium. Biochemistry 38, 6441-8.

Pasuit, J. B., Li, Z. and Kuzhikandathil, E. V. (2004). Multi-modal regulation of endogenous D1 dopamine receptor expression and function in the CAD catecholaminergic cell line. J Neurochem 89, 1508-19.

Pedraza, C. E., Baltrons, M. A., Heneka, M. T. and Garcia, A. (2003). Interleukin-1 beta and lipopolysaccharide decrease soluble guanylyl cyclase in brain cells: NO-independent destabilization of protein and NO-dependent decrease of mRNA. J Neuroimmunol 144, 80-90.

Pifarre, P., Garcia, A. and Mengod, G. (2007). Species differences in the localization of soluble guanylyl cyclase subunits in monkey and rat brain. J Comp Neurol 500, 942-57.

Plafker, S. M., Plafker, K. S., Weissman, A. M. and Macara, I. G. (2004). Ubiquitin charging of human class III ubiquitin-conjugating enzymes triggers their nuclear import. J Cell Biol 167, 649-59.

Ravid, T., Doolman, R., Avner, R., Harats, D. and Roitelman, J. (2000). The ubiquitin-proteasome pathway mediates the regulated degradation of mammalian 3-hydroxy-3-methylglutaryl-coenzyme A reductase. J Biol Chem 275, 35840-7.

Rockel, T. D., Stuhlmann, D. and von Mikecz, A. (2005). Proteasomes degrade proteins in focal subdomains of the human cell nucleus. J Cell Sci 118, 5231-42.

Rockel, T. D. and von Mikecz, A. (2002). Proteasome-dependent processing of nuclear proteins is correlated withh their subnuclear localization. J Struct Biol 140, 189-199.

Russwurm, M., Behrends, S., Harteneck, C. and Koesling, D. (1998). Functional properties of a naturally occurring isoform of soluble guanylyl cyclase. Biochem J 335 (Pt 1), 125-30.

Russwurm, M. and Koesling, D. (2002). Isoforms of NO-sensitive guanylyl cyclase. Mol Cell Biochem 230, 159-64.

Russwurm, M., Wittau, N. and Koesling, D. (2001). Guanylyl cyclase/PSD-95 interaction: targeting of the nitric oxide-sensitive alpha2beta1 guanylyl cyclase to synaptic membranes. J Biol Chem 276, 44647-52.

Sardon, T., Baltrons, M. A. and Garcia, A. (2004). Nitric oxide-dependent and independent down-regulation of NO-sensitive guanylyl cyclase in neural cells. Toxicol Lett 149, 75-83.

Saura, J., Tusell, J. M. and Serratosa, J. (2003). High-yield isolation of murine microglia by mild trypsinization. Glia 44, 183-9.

Schmidt, H. H., Pollock, J. S., Nakane, M., Forstermann, U. and Murad, F. (1992). Ca2+/calmodulin-regulated nitric oxide synthases. Cell Calcium 13, 427-34.

Schmidt, R. E., Dorsey, D. A., McDaniel, M. L. and Corbett, J. A. (1993). Characterization of NADPH diaphorase activity in rat sympathetic autonomic ganglia--effect of diabetes and aging. Brain Res 617, 343-8.

Schreck, R., Meier, B., Mannel, D. N., Droge, W. and Baeuerle, P. A. (1992). Dithiocarbamates as potent inhibitors of nuclear factor kappa B activation in intact cells. J Exp Med 175, 1181-94.

Schulz, S., Yuen, P. S. and Garbers, D. L. (1991). The expanding family of guanylyl cyclases. Trends Pharmacol Sci 12, 116-20.

Scott, W. S. and Nakayama, D. K. (1998). Escherichia coli lipopolysaccharide downregulates soluble guanylate cyclase in pulmonary artery smooth muscle. J Surg Res 80, 309-14.

Serfass, L., Carr, H. S., Aschenbrenner, L. M. and Burstyn, J. N. (2001). Calcium ion downregulates soluble guanylyl cyclase activity: evidence for a two-metal ion catalytic mechanism. Arch Biochem Biophys 387, 47-56.

Shenkman, M., Tolchinsky, S., Kondratyev, M. and Lederkremer, G. Z. (2007). Transient arrest in proteasomal degradation during inhibition of translation in the unfolded protein response. Biochem J.

Shimouchi, A., Janssens, S. P., Bloch, D. B., Zapol, W. M. and Bloch, K. D. (1993). cAMP regulates soluble guanylate cyclase beta 1-subunit gene expression in RFL-6 rat fetal lung fibroblasts. Am J Physiol 265, L456-61.

Stohwasser, R., Giesebrecht, J., Kraft, R., Muller, E. C., Hausler, K. G., Kettenmann, H., Hanisch, U. K. and Kloetzel, P. M. (2000). Biochemical analysis of proteasomes from mouse microglia: induction of immunoproteasomes by interferon-gamma and lipopolysaccharide. Glia 29, 355-65.

Szabo, C. (1996). Physiological and pathophysiological roles of nitric oxide in the central nervous system. Brain Res Bull 41, 131-41.

Takata, M., Filippov, G., Liu, H., Ichinose, F., Janssens, S., Bloch, D. B. and Bloch, K. D. (2001). Cytokines decrease sGC in pulmonary artery smooth muscle cells via NO-dependent and NO-independent mechanisms. Am J Physiol Lung Cell Mol Physiol 280, L272-8.

Teunissen, C. E., Steinbusch, H. W., Markerink-van Ittersum, M., De Bruijn, C., Axer, H. and De Vente, J. (2000). Whole brain spheroid cultures as a model to study the development of nitric oxide synthase-guanylate cyclase signal transduction. Brain Res Dev Brain Res 125, 99-115.

Tomimatsu, N., Tahimic, C. G., Otsuki, A., Burma, S., Fukuhara, A., Sato, K., Shiota, G., Oshimura, M., Chen, D. J. and Kurimasa, A. (2007). Ku70/80 modulates ATM and ATR signaling pathways in response to DNA double-strand breaks. J Biol Chem.

Tomita, S., Nicoll, R. A. and Bredt, D. S. (2001). PDZ protein interactions regulating glutamate receptor function and plasticity. J Cell Biol 153, F19-24.

Tremblay, J., Desjardins, R., Hum, D., Gutkowska, J. and Hamet, P. (2002). Biochemistry and physiology of the natriuretic peptide receptor guanylyl cyclases. Mol Cell Biochem 230, 31-47.

Ujiie, K., Hogarth, L., Danziger, R., Drewett, J. G., Yuen, P. S., Pang, I. H. and Star, R. A. (1994). Homologous and heterologous desensitization of a guanylyl cyclase-linked nitric oxide receptor in cultured rat medullary interstitial cells. J Pharmacol Exp Ther 270, 761-7.

Van Hooser, A. A., Yuh, P. and Heald, R. (2005). The perichromosomal layer. Chromosoma 114, 377-88.

van Staveren, W. C., Glick, J., Markerink-van Ittersum, M., Shimizu, M., Beavo, J. A., Steinbusch, H. W. and de Vente, J. (2002). Cloning and localization of the cGMP-specific phosphodiesterase type 9 in the rat brain. J Neurocytol 31, 729-41.

van Staveren, W. C., Markerink-van Ittersum, M., Steinbusch, H. W., Behrends, S. and de Vente, J. (2005). Localization and characterization of cGMP-immunoreactive structures in rat brain slices after NO-dependent and NO-independent stimulation of soluble guanylyl cyclase. Brain Res 1036, 77-89.

Venema, R. C., Venema, V. J., Ju, H., Harris, M. B., Snead, C., Jilling, T., Dimitropoulou, C., Maragoudakis, M. E. and Catravas, J. D. (2003). Novel complexes of guanylate cyclase with heat shock protein 90 and nitric oxide synthase. Am J Physiol Heart Circ Physiol 285, H669-78.

Vickers, T. A., Koo, S., Bennett, C. F., Crooke, S. T., Dean, N. M. and Baker, B. F. (2003). Efficient reduction of target RNAs by small interfering RNA and RNase H-dependent antisense agents. A comparative analysis. J Biol Chem 278, 7108-18.

Villalobo, A. (2006). Nitric oxide and cell proliferation. Febs J 273, 2329-44.

Waldman, S. A. and Murad, F. (1987). Cyclic GMP synthesis and function. Pharmacol Rev 39, 163-96.

Wallace, M. N. and Bisland, S. K. (1994). NADPH-diaphorase activity in activated astrocytes represents inducible nitric oxide synthase. Neuroscience 59, 905-19.

Wallace, M. N., Geddes, J. G., Farquhar, D. A. and Masson, M. R. (1997). Nitric oxide synthase in reactive astrocytes adjacent to beta-amyloid plaques. Exp Neurol 144, 266-72.

Wang, H. G., Lu, F. M., Jin, I., Udo, H., Kandel, E. R., de Vente, J., Walter, U., Lohmann, S. M., Hawkins, R. D. and Antonova, I. (2005). Presynaptic and postsynaptic roles of NO, cGK, and RhoA in long-lasting potentiation and aggregation of synaptic proteins. Neuron 45, 389-403.

Wang, X. and Robinson, P. J. (1995). Cyclic GMP-dependent protein kinase substrates in rat brain. J Neurochem 65, 595-604.

Wedel, B. and Garbers, D. (2001). The guanylyl cyclase family at Y2K. Annu Rev Physiol 63, 215-33.

Wedel, B., Harteneck, C., Foerster, J., Friebe, A., Schultz, G. and Koesling, D. (1995). Functional domains of soluble guanylyl cyclase. J Biol Chem 270, 24871-5.

Wiencken, A. E. and Casagrande, V. A. (1999). Endothelial nitric oxide synthetase (eNOS) in astrocytes: another source of nitric oxide in neocortex. Glia 26, 280-90.

Wikstrom, L. and Lodish, H. F. (1991). Nonlysosomal, pre-Golgi degradation of unassembled asialoglycoprotein receptor subunits: a TLCK- and TPCK-sensitive cleavage within the ER. J Cell Biol 113, 997-1007.

Yuen, P. S., Potter, L. R. and Garbers, D. L. (1990). A new form of guanylyl cyclase is preferentially expressed in rat kidney. Biochemistry 29, 10872-8.

Zabel, U., Hausler, C., Weeger, M. and Schmidt, H. H. (1999). Homodimerization of soluble guanylyl cyclase subunits. Dimerization analysis using a glutathione s-transferase affinity tag. J Biol Chem 274, 18149-52.

Zabel, U., Kleinschnitz, C., Oh, P., Nedvetsky, P., Smolenski, A., Muller, H., Kronich, P., Kugler, P., Walter, U., Schnitzer, J. E. et al. (2002). Calcium-dependent membrane association sensitizes soluble guanylyl cyclase to nitric oxide. Nat Cell Biol 4, 307-11.

Zhang, G. and Ghosh, S. (2000). Molecular mechanisms of NF-kappaB activation induced by bacterial lipopolysaccharide through Toll-like receptors. J Endotoxin Res 6, 453-7.

Zhang, J. and Snyder, S. H. (1995). Nitric oxide in the nervous system. Annu Rev Pharmacol Toxicol 35, 213-33.

Zwiller, J., Revel, M. O. and Basset, P. (1981). Evidence for phosphorylation of rat brain guanylate cyclase by cyclic AMP-dependent protein kinase. Biochem Biophys Res Commun 101, 1381-7.

Zwiller, J., Revel, M. O. and Malviya, A. N. (1985). Protein kinase C catalyzes phosphorylation of guanylate cyclase in vitro. J Biol Chem 260, 1350-3.

12 ABREVIATURAS

AD	Alzheimer desease
AMPc	adenosina monofosfato
ANP	peptido natriuretico tipo A
ATP	adenosina trifosfato
BNP	peptido natriuretico tipo B
BSA	seroalbunina bovina
CA	cornu ammonis del hipocampo
CHX	cicloheximida
CJ	Creutzfeldt-Jakob
CNP	peptido natriurético tipo C
DAPI	4',6-diamidino-2-phenylindol
Db-GMPc	dibutiril GMPc
cDNA	DNA complementario
ds-siRNA	doble cadena siRNA
EDRF	factor derivado de endotelio
FCS	suero fetal bovino
GCp	guanilil ciclasa particulada
GC_{NO}	guanilil ciclasa sensible a NO
GMPc	guanosina 3´,5´-monofosfato cíclico
GTP	guanosina trifosfato
HSP70	heat shock protein 70
HSP90	heat shock protein 90
IBMX	isobutil-metilxantina
IL-1β	interleuquina 1 beta
INF-γ	interferon gamma
LPS	lipopolisacarido bacteriano
mRNA	RNA mensajero
MS	esclerosis múltiple
NGF	factor de crecimiento neuronal
NMDA	receptor ionotrópico de glutamato
NO	óxido nítrico
NOS	sintasa del óxido nítrico
ODQ	1H-[1,2,4]oxadiazolo[4,3-a]quinoxalin-1-one
ON	over night (toda la noche)

PBS	tampon salino fosfato
PCR	reacción en cadena de la polimerasa
PDZ	dominio de interacción de proteínas
PDE	fosfodiesterasa
PFA	paraformaldehído
PKA	proteína quinasa A
PKC	proteína quinasa C
PKG	proteína quinasa G
PMA	analogo de esteres de forbol
PML	cuerpos promielociticos
PSD-95	proteína de densidad post-sináptica 95
RIA	radioinmunoensayo
RT-PCR	PCR con transcripción reversa
SDS	dodecilsulfato sodico
SIDA	síndrome de inmunodeficiencia humana
siRNA	small interferense RNA
SNC	sistema nervioso central
SNP	sistema nervioso periférico
TNFα	tumor necrosis factor
UPS	sistema ubiquitina-proteosoma
WB	western blot

En primer lugar me gustaria agradecerle a la Dra. García por haberme aceptado en su laboratorio y por haber confiado en mí para realizar este trabajo. También me gustaria agraderle por corregirme esta tesis, porque a pesar de mis enojos se que finalmente quedo mejor que al principio, y que en definitiva, el español es más correcto que el argentino a la hora de escribir. Además me gustaria darle las gracias por las tardes interminables de discusión, el planteamiento de experimentos imposbles, y por darme la libertad de escribirle a todo el mundo para que me dieran consejos y protocolos, técnicas y sugerencia, etc. etc. etc.

Me gustaria agradecer también a la Dra. Baltrons, Marian, por su enorme generosidad, por ser la persona siempre dispuesta a darme una mano, por transmitirme todos sus conocimientos, por trabajar codo a codo conmigo, pero sobre todo por su amistad.

Quisiera agradecerle a la Dra. Mengod y a los chicos de su laboratorio ya que buena parte de este trabajo se ha realizado gracias a ellos. Por todo lo que me enseñaron y por los momentos dedicados a mi trabajo. Muchas Gracias.

No puedo dejar de nombrar a las chicas del laboratorio. Judith que con una sonrisa le da alegria a ese espacio en el que pasamos tanto tiempo, su ayuda incondicional para todo y su buena predispisicion y a Mariela, el toque argentino necesario para sobrellevar la nostalgia. Y las que ya no estan, pero se hicieron sentir en su momento, Laura y Agata. Tambien quisiera incluir a Mateu, “el chico del labo”, por sus concejos con las PCR y el real time.

Quisiera agradecer a los buenos amigos que hice durante estos años en el IBB, a Sebas1 y Sebas 2, Silvia, Anais, Nuria, la otra Nuria de abajo, Montse, Roger, Susanna, Arais la otra cubanita, Iñaki, Marta, Laia, Anabel, Almudena. Y por que no a los compañeros de comidas, Pepe, Julia, Toni y Paqui. Y a los que ya no estan pero estuvieron como Anna Rovira y Oscar Yanes. Asi como a todos los miembros del IBB que de alguna forma u otra colaboraron con esto.

Un lugar muy especial ocupan un grupo de gente que fue mi sosten afectivo en esta ciudad, y sin las cuales no hubiera podido aguantar los años que llevo en esta tesis. Monica, mi amiguita cubana del alma, que además de estar todos los días de mi estancia en catalunya presente, también lo esta en mis vacaciones, en las suyas, en mis experimentos yo en los suyos, en mis alegrias y tristezas. Marta, mi amiguita catalana, que con su toque de humor y su “justicia” nos ha “acogido” a todas las inmigranes que pasamos por el IBB y nos hace sentir como en casa. Maday, que a pesar de sus breves estancias deja huella para rato. Kari, mi hermana adoptiva, mi refugio en momentos dificiles en catalunya. Fatima, la locura del grupo, por su espontaneidad y por su energia incansable, por acompañarme en todas mis locura en los buenos y malos momentos. A todas las chicas de las “cenas de chicas”, incluidas las que

ya no estan en catalunya como Ire, queria darles las gracias desde lo más profundo de mi corazón.

A los amigos que me fui haciendo en mi estancia en catalunya y que me ayudaron a mantenerme entera, Fede, Javi y Hugo, Martín, Eva, Julie y Ela, Carmeta y a los que me dejo en el camino.

A mis amigos de alla, a Sol y Guille Ire, Many, Juli y Coco, Juan y Elena, Tincho, Dario, Lau Asseo, las chicas de la Facu y Maty. Porque siempre que vuelvo ellos estan alli para mi, para que les cuente mi vida, mis momentos felices y mis momentos tristes, mis exitos y mis fracasos. Por estar siempre, por ser mis amigos de toda la vida.

A mi familia, que a pesar de la distancia nunca me hicieron sentir lejos, porque siempre me apoyaron en mis proyectos aun cuando les suponia un esfuerzo entenderlos. Por su respeto incondicional y por su amor. A las nuevas integrantes, Tatu y Lola, para que sepan que las quiero mucho.

A Ignasi, por ayudarme con esta tesis, pero sobre todo por aguantarme todos estos años.